EVLA Memo # 227

VLA Calibrator List Revisited: 2018 X-band Astrometry and Alternative Phase-reference Sources

Loránt O. Sjouwerman[1]

[1] *National Radio Astronomy Observatory, Socorro NM*

(Dated: October 13, 2024)

ABSTRACT

Sources from the VLA calibrator list with potentially questionable positions were observed in X-band (8-12 GHz) using the BnA and BnA to A (move) array configurations for improved astrometry in February 2018. Promising calibrator or phase-reference sources from other surveys were included for potential inclusion in an updated VLA calibrator list. Presented here are 122 positions for existing calibrators and a list of at least 399 alternative sources, mostly at southern Declinations, that probably should be included in a future version of the VLA calibrator list, at least for X-band in the extended array configurations.

With additional resources the quality of the here presented results could be improved further, but the data contains sufficient valuable information already to not significantly further delay current findings. These new potential calibrator sources can already now be used after inspection and using the information presented here. The best-effort results of this work are available in the public and evolving "*VLA Alternatives*" source catalog of NRAO's VLA Observation Preparation Tool but should only be used with caution after consulting this memo. Practical guidelines for how to safely use the sources in the "*VLA Alternatives*" catalog as VLA calibrators are provided.

Keywords: catalogs – surveys – radio emission – radio interferometry

1. INTRODUCTION

The NSF's Karl G. Jansky Very Large Array (VLA) typically observes target fields interspersed with "calibrator" source observations to maintain a temporal sampling of the instrumental gains and atmospheric phase fluctuations. Phase-referencing of target fields using calibrators yields the relative angular frame in which radio sources in a target field are tied to the calibrator position and its positional accuracy. It is therefore important to reduce (or effectively eliminate) systematic positional errors in any calibrator position as much as possible to obtain an absolute target position referenced to such calibrators accurately.

The current (pre-2024) VLA calibrator source list[1] is a compilation of previous efforts, since the first short baseline and decimeter wavelength observations in the late 1970-ies. These efforts are not well documented or preserved[2]. Examples of expansion of the initial list are the additions of a spin-off of a gravitational lens search (CJ2 and JVAS sources) and a dedicated high-frequency campaign on VLBI sources in the late 1990-ies. However, apart from the fact that many sources are variable in flux density, the current list contains sources that are not sufficiently compact in the more extended configurations and/or at higher frequencies where the improved angular resolution should allow for much higher precision. Similarly, the sources observed during the VLA high-frequency campaign were not followed-up for suitability at lower frequencies[3]. Some sources are remnants of the early days, i.e. only suitable at low frequency using short baselines with low positional accuracy. Furthermore, the calibrator sky density is very coarse for high-frequency observations that generally need close-

[1] `http://go.nrao.edu/vla-callist`

[2] When available, a month-year label reference is given in Section 3 of the link in the first footnote.

[3] TCAL0008 is a long-term VLA filler program aimed for this.

Table 1. VLA Calibrator Source Density

Region	Area	All	Dens.	cm	Dens.	mm	Dens.
All-sky	35 955	1864	0.052	271	0.008	1593	0.044
North	20 626	1487	0.072	166	0.008	1321	0.064
South	15 329	377	0.025	105	0.007	272	0.018

Area: number of square degrees accessible to the VLA in that Region using a southern Declination limit of −48°.
cm: number of sources without high-frequency (K-band through Q-band) information.
mm: number of sources with high-frequency information (of which 668 have only Q-band information, 649 in the North, 19 in the South).
Dens.: the calibrator density per square degree; for example, ignoring suitability, a listed mm-calibrator in the South serves on average 56 square degrees (i.e. 1/0.018).

by calibrators, in particular south of the celestial equator. Apart from a careful cleanup[4] for typo's, duplicates, omissions and parsing errors of the *VLA* catalog in the Source Catalog Tool[5] (SCT) of the VLA Observation Preparation Tool in 2016, the current VLA calibrator list has not been updated nor supplemented since well before the first observations with the expanded VLA in 2010 and wideband observing capabilities (i.e. well before ingestion in the SCT around 2008), and even not until after the publication of this work.

With the execution of the VLA Sky Survey (VLASS; Lacy et al. 2020) starting in 2017, and with a handful of user reports over the years it became apparent that the current list not only has an insufficient sky coverage but also contains positional errors and inadequate positional accuracy for sources that would otherwise be excellent phase-referencing calibrators. The work presented in this memo is an astrometry campaign to amend and expand the list with more (potentially high-frequency) alternative calibrator sources, with an emphasis on southern Declinations.

2. THE CURRENT CALIBRATOR SOURCE LIST

The current VLA calibrator source list consist of 1864[6] sources and Table 1 provides and overview of the sky density for different uses by coarsely grouping them into regions of the sky and observing bands. Out of 1864 calibrators, 668 contain only Q-band (40-50 GHz) information, and 271 contain no high-frequency (20 GHz and above) information. Note that even though there may be information contained in the list, it does not guarantee that the source is a suitable calibrator. Using a southern Declination limit of −48° (covering 87.16% of the entire sky), the average listed calibrator density regardless of observing frequency (0.052, Table 1) is one per 19 square degrees regardless whether they are good calibrators or not.

Each source in the VLA calibrator list is given a *Position Error Code* of A, B, C or T. These codes are presumed to indicate an accuracy (i.e., absolute positional error) of a calibrator as documented in Table 2. The most accurate (better than 2 milli-arcseconds; 2 mas) are likely taken from VLBI observations and the least accurate are typical FRII or CSO sources (and the planetary nebula NGC 7027) that are only unresolved in the more compact arrays at low frequency where lower positional accuracy is acceptable due to the low angular resolution. The sky density should be as high as possible for positional code A and as low as possible for positional code T to achieve the highest accuracy anywhere on the visible sky.

Interferometers like the VLA (and VLBI) resolve radio sources to various degrees depending on observing frequency and projected baseline length (i.e., in units of wavelength). What is a good point-like calibrator in one array configuration at one frequency may not hold for the same source at another frequency and/or in another array configuration. Typical cases would be FRII sources that are dominated by their extended lobes at low frequency and by their central core at high frequency making them typically unsuitable at low frequencies in the extended array configurations. On the other hand, the more compact arrays may not resolve the source and observe the combined radiation of the lobes as a point-like calibrator but resolve them at the higher frequencies, yielding the opposite conclusion. It should also be said that a short (calibration) scan on a core-jet source may not yield enough sensitivity to actually be sensitive to the weaker extended structure; if a source is dominated by a point-like structure it may very well be suitable for phase and/or gain calibration regardless the fainter extended structure, provided that the position given is the position of the core, and not a weighted or fitted position of the sum of all emission.

For the four principal VLA array configurations (**A, B, C** and **D**) and for as many observing bands as available, the VLA calibrator list therefore also indicates the potential usefulness for that combination of array configuration and observing band with a *Calibrator Closure Code*. These more widely used "calcodes" address the amount of closure errors in phase ("closure phase") that

[4] See the "Notes" at the end of the calibrator list in Section 6 of the link in the first footnote.
[5] http://obs.vla.nrao.edu/sct – requires account registration.
[6] Ignoring an empty entry for 1118-465/J1118-4634 in the list.

Table 2. VLA Calibrator Positional Accuracy Codes

Code	Positional Accuracy	#	Dens. ($^{-1}$)
A	<0.002″ (better than 2 mas)	802	0.022 (45)
B	0.002 to 0.01″ (2-10 mas)	761	0.021 (47)
C	0.01 to 0.15″ (10-150 mas)	143	0.004 (251)
T	>0.15″ (worse than 150 mas)	158	0.004 (228)

Table 3. VLA Closure Phase Calibrator Codes (calcodes)

Code	Meaning for a point source model
P	<3% amplitude closure errors expected. Use it.
S	3-10% closure errors expected. Gain calibrator.
W	10-?% closure errors expected. Phase calibrator.
C	Confused source, avoid for calibration.
X	Do not use. Too resolved/weak or undetectable.
?	Source structure unknown.

can be expected when the observation is self-calibrated with a point-source model. For properly calibrated data, closure phase is an observation-independent measure and indicative of source structure; large errors warn about deviations from the (point-source) model. These calcodes are listed with their meaning in Table 3.

Note that in principle any source can be used as a calibrator if a reasonably decent source model is available, specifying the flux density, source structure and reference position. Models for the standard VLA flux density calibrators like 3C286 and 3C48 are distributed with the common radio interferometry data reduction packages CASA and AIPS.

2.1. Anchors: *calibrator sources used for calibration*

Not surprisingly, the calibrator list (and real life) contains many ambiguous sources and the choice of the main positional calibrators in this X-band (8-12 GHz) BnA/A-array astrometry experiment has to be done carefully. For a calibrator to be used as a positional calibrator it must have a good a-priori position and be point-like at X-band.

In order to judge the a-priori positions of sources in the calibrator list, the positions were compared to the latest VLBI positions from the ICRF and RFC (as defined prior to expansion updates in 2018; Charlot et al. (2020) and `http://astrogeo.org/rfc/`). If the ICRF and/or RFC positions agree with the VLA position within 50 mas (the approximate angular resolution using A-array configuration in Q-band), the VLA position is assumed to be correct[7], and these sources are acceptable as position (phase-referencing) calibrators in this experiment. It is reassuring to note that of the 1864 sources in the current calibrator list 1468 match this criteria[8]; the remaining ∼400 sources are candidates for an astrometric check-up using the VLA. For the rest of this document sources matching the VLBI position within 50 mas at the time of selecting the sample, the genuine VLA calibrators, are here referred to as "VLA *Anchors*", the other sources in the VLA calibrator list without this position accuracy match will be referred to as "VLA targets".

One caveat is that the listed VLA position may have originated from VLBI measurements and that an independently measured position using the VLA may differ from the ones obtained using the longer baselines from VLBI. On the other hand, VLBI calibrators as in the ICRF and RFC are likely dominated by a point-like static (extragalactic core) component and assumed here to unlikely have extended structure at VLA BnA/A-array configuration baselines in X-band. That is, for this experiment the calibrator positions matching the VLBI positions are used, regardless the "official" positional accuracy code they have in the current VLA calibrator list (i.e. ignoring the information described in Table 2).

It should also be pointed out that many VLA calibrator positions have been taken from VLBI source lists and were followed-up with the VLA in Q-band only. As many of them will not have been observed here due to a matching position (within 50 mas) with the VLBI position (obviously), there is no guarantee that these high-frequency VLA calibrators will still be point-like, with the emission centroid at the postulated position, at X-band in A-array configuration. Including them in these observations was, however, beyond the scope of this experiment.

3. ALTERNATIVE POTENTIAL CALIBRATORS

In an attempt to improve the (high-frequency) calibrator density, in particular in the southern hemisphere, the observations were extended to include sources from other compilations (See Fig. 1 and Table 7). In particular, using the ALMA calibrator list[9] (as known in December 2016, before any long baseline campaign), compact sources in the AT20G survey (Murphy et al.

[7] It is not uncommon for positions to differ in individual VLBI catalogs, with changes in the order of milli-arcseconds (mas).

[8] Of the 668 "Q-band only"-sources 547 passed this criteria.

[9] `https://almascience.nrao.edu/alma-data/calibrator-catalogue`

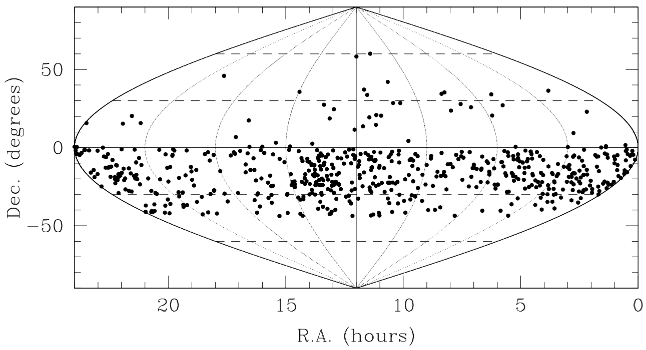

Figure 1. Sky distribution of the 590 sources observed for potential suitability as a VLA calibrator. The lower density of northern Declination sources is due to the upper Declination limit of 0° for the "AT20G" and "Winn" catalogs. Sources south of Declination −48° were not selected.

2010) and a list of southern VLBI sources by Winn et al. (2003), resulted in a total of 590 promising candidate calibrator sources. Being point-like at higher frequencies and/or on longer baselines may indicate a core-dominated compact source, which is a prime attribute for a calibrator source, especially when the high-frequency and low-frequency flux densities are similar (i.e., a likely non- or only slowly-variable flat spectrum source).

During 2017, all these additional sources were observed in C-array, B-array and/or A-array configuration at S-band and positively assessed as sufficiently bright and relatively compact to function as suitable VLASS calibrators.

3.1. *ALMA calibrator list*

The ALMA calibrator list is a catalog of bright compact high-frequency (90-1000 GHz) sources in use by the Atacama Large Millimeter/submillimeter Array (ALMA). These sources are likely compact flat-spectrum cores and should be detectable at lower frequencies with the sensitivity of the VLA. Therefore about 130 calibrators north of Declination −48° that appeared point-like were selected for inclusion in the X-band astrometry survey. While these sources are not included in the current VLA calibrator list, they were detected with the VLA in the S-band observations outlined above. Although these sources in principle should have adequate astrometry from their ALMA calibrator position, they were included here to verify their detectability, compactness and position with VLA BnA/A-array configuration baselines at X-band. The ALMA calibrator sources included in the observations are here referred to as "ALMA targets".

3.2. *AT20G survey*

The AT20G is a 20 GHz (K-band) survey carried out with the Australia Telescope Compact Array (ATCA) of the sky south of Declination 0° with a flux-density limit of 40 mJy/beam (Murphy et al. 2010). Unfortunately it deliberately omits the inner 3° ($b < \pm 1.5°$) of the Galactic Plane due to potential source confusion. About 300 compact AT20G sources north of Declination −48° and that were also detected in the previous S-band observations were included for these X-band observations, excluding the sources already selected using the VLA or ALMA calibrator list. The AT20G sources observed here are referred to as "AT20G targets".

3.3. *Other compilations*

About 110 non-duplicate sources of the catalog of 321 compact sources of Winn et al. (2003) were added. These "Winn targets" are sources in the declination range −30 to 0° observed to be brighter than 50 mJy/beam in X-band using VLBI and appeared point-like in their B-array S-band observations.

Originally intended to provide extra calibrator sources at S-band, single-component low frequency (150 MHz) sources selected from the TGSS-ADR (Intema et al. 2017) were included. These sources were selected using a Declination cut-off, a flat or rising spectral index characteristic, and with an anticipated minimum flux criteria of 50 mJy/beam at 13 GHz. The 45 "TGSS targets" included had earlier passed a point-like structure assessment from earlier observations in C-array and A-array configurations at S-band.

Finally, a couple of point-like "3FGL targets" from the S-band observations originate from the "Unassociated Gamma-Ray Sources from the Third Fermi Large Area Telescope Source Catalog" (Schinzel et al. 2017).

Although it would have been possible to include many more potential calibrator sources form other compilations, the current target list with 590 sources, mostly in the southern sky (Fig. 1), was considered sufficiently large to postpone observing many more candidates to a future opportunity.

4. OBSERVATIONS

The target sources were grouped to areas in the sky with a common astrometric phase-referencing calibrator, where the calibrator would typically have a designation of **"P"** (see Table 3) at X-band in A-array configuration (i.e. one of the VLA *Anchors*) and typically be well within a 10° reach. Occasionally, in particular in the south were the VLA *Anchor* density is lower, this was relaxed to an **"S"**-type calibrator or to slightly further than 10° distance (though never more than 15°).

Table 4. Observing sessions

Date & Start (UT)	Configuration	Duration	Targets
2018-02-10 08:04	BnA	05:29:27	76
2018-02-13 23:34	BnA	05:58:53	121
2018-02-19 07:13	BnA	05:14:38	109
2018-02-22 23:19	BnA to A	01:40:08	34
2018-02-25 01:06	BnA to A	21:12:13	603

Excluding the standard flux density sources, in total 216 VLA calibrators were used for phase-referencing. In some cases one could have selected more nearby calibrators, increasing the total number of calibrators used, but if the calibrator was a **"P"** within 10°, the choice was to reuse calibrators to reduce observing time. All target sources were observed for up to a single one-minute scan, bracketed by a phase-calibrator. This snapshot (u, v)-sampling does not capture the full angular structure of the source, but should allow for a proper astrometric measurement if the source is point-like and the synthesized beam is sufficiently round. The observations took place in 2018 February, in BnA-array configuration and during the BnA to A-array configuration move (Table 4), using an X-band setup that covered about 5 GHz in contiguous bandwidth (7.5-12.5 GHz).

Because the observations were primarily set up for astrometry and not for accurate flux density measurements, the resulting flux densities should be assumed to have up to about a ten percent error.

5. DATA REDUCTION

Given the wide frequency coverage, and the fact that many artificial sources transmit in X-band, severe RFI was present. In order to keep it manageable and speed up the astrometry measurements only one of the 128 MHz subbands was reduced and imaged; this subband was centered on 11.284 GHz, the highest frequency subband that was apparently RFI-free. As calibration typically is performed on a per-subband basis, using a single subband is thus appropriate, and adequate for this purpose. After minimal flagging of bad data, the visibilities were calibrated and imaged with the standard AIPS pipeline procedure PIPEAIPS, applying a fixed pixel size of 43.08 mas for all array configurations used in a 1024-square pixel continuum image.

It should be noted that the results are directly taken from this data reduction and thus are "as-is" from the pipeline. More careful flagging, multiple data inspection and reduction passes, and individual handling of each of the target sources may have yielded better overall results and/or resolve individual discrepancies such as an original anticipated point-like (**"P"**) source not being detected here once more resources are available. Furthermore, improving image quality using hybrid mapping or self-calibration schemes of course would counter the goal of obtaining absolute (calibrator phase-referenced) astrometry.

6. RESULTS & DISCUSSION

A complete overview of results is collected in the Appendix, where Table 5 and Fig. 3 refer to the VLA targets and where Table 6 and Fig. 4 refer to the alternative reference sources. A suggested application – how to use these results in VLA observations – is given in Sect. 6.4.

Again, it should be noted that the analysis was done mostly automatic with a minimal subjective visual check as resources to perform a thorough individual quality check or follow-up were unavailable. It thus may appear that an extended source is resolved out, with a hot-spot remaining in the image yielding an apparent artificial large position shift; in those cases the position therefore is not from the main component and care must be taken in assuming the here measured position. Equally, a genuine point-like source may appear extended due to improper phase-referencing, which could be corrected for with more attention to the data reduction and/or reobservations at a higher elevation in better weather and/or with a different calibrator source. No such attempts were made; the "as-is" results below were obtained with minimum effort.

In the data reduction, all calibrators used for phase referencing, the VLA *Anchors*, were detected. Depending on the Hour Angle and elevation some (mostly southern) calibrators had relatively elongated beam shapes potentially affecting the astrometric solution. Apart from the non-detected target sources, a number of target sources (noted in the Appendix) were detected though yielded insufficient data quality to address their astrometry. This may be improved with a more careful reanalysis of the observations.

In the following sections the results of the phase-calibrators, the VLA *Anchors* used in this experiment are discussed first (Sect. 6.1), followed by an assessment of the questionable VLA calibrators, the VLA targets for which improved astrometry was sought (Sect. 6.2). The alternative reference sources, the 590 additional targets not previously listed as a VLA calibrator are discussed in Sect. 6.3. Finally, Sect. 6.4 suggests the best use of these results.

6.1. *Calibration*

VLA Anchors—The target observations were calibrated with "good", genuine VLA phase-referencing calibra-

Table 7. Targets for astrometric positions observed

Origin	Observed	Point-like	Inconclusive
VLA	353	122^X	231^X
ALMA	133	78	55
AT20G	299	201	98
Winn	111	91	20
TGSS	45	28	17
3FGL	2	1	1

Point-like: single (or single dominant) point-like component yielding good astrometry.
Inconclusive: extended or multi-component source without a dominant point-like component, non-detection at X-band using these longest baselines, or image affected by bad calibration or RFI.
^{X}: Includes sources coded as **"X"** for closure error, i.e., previously deemed unsuitable to be used as a point-like source in A-array configuration at X-band.

Table 8. Questionable Phase-referencing Calibrators.

Name	Codes	ΔRA, ΔDec. (mas)	Shift (mas)	Label
J0019+7327	A, **P**	−0.1, +46.4	46.4	*a*
J0339−0146	A, **P**	−26.3, −7.8	27.4	*b*
J0403−3605	B, **P**	−100.9, +119.2	156.2	*c*
J0428−3756	A, **P**	−1.9, +39.6	39.7	*d*
J0510+1800	A, **P**	−42.0, +42.8	60.0	*e*
J0538−4405	A, **P**	−13.4, −44.5	46.5	*f*
J0555+3948	A, **P**	+39.3, −42.6	58.0	*g*
J0741+3112	A, **P**	−44.9, +29.3	53.6	*h*
J0854+2006	A, **P**	−87.6, +38.0	95.5	*i*
J0921−2618	B, **P**	+4.3, +21.0	21.4	*j*
J1107−4449	B, **P**	−1.1, −31.5	31.6	*k*
J1146+3958	A, **P**	+88.1, −1.4	88.1	*l*
J1608+1029	A, **P**	+36.4, −9.4	37.6	*m*
J2025+3343	A, **P**	−0.1, +44.8	44.8	*n*
J2052+3635	A, **S**	−33.5, −45.8	56.7	*o*
J2322+5057	A, **P**	−55.5, +40.9	68.9	*p*

Codes: positional accuracy code (Table 2) and phase closure error (in bold, Table 3) code references in the VLA calibrator list for A-array configuration and X-band.
Label: see calibrator image in Fig. 2 and see Table 5 and Table 6 for which target is phase-referenced to this calibrator.

tors, the VLA *Anchors*. Their results are discussed in this section. To recall, these are sources that have their position in common (within 50 mas) with VLBI source positions, are bright and are anticipated to be dominated by a point-like source at X-band in BnA/A-array configuration (calibrator code **"P"**). In general this assumption yields good results after examining the images, as almost all of the 216 VLA *Anchors* are detected and appear point-like with the maximum emission in the phase-center. However, there are a few VLA *Anchors* for which the maximum emission does not appear in the reference pixel (512, 513); these calibrators are listed in Table 8 with the coordinate shift of the flux density maximum. Their images are shown in Fig. 2 and it is clear that many have multiple components and seem to have jet-like structures, possibly either by incomplete flagging of bad data or having emerged in the years since their inclusion in the calibrator list. Target sources calibrated with these calibrators, listed in Table 8, may have larger than anticipated remaining systematic astrometric errors and are labeled as such in Table 5 and Table 6 (in the Appendix).

There are some other calibrators that show evidence for asymmetry and/or jet-like structures in the images, but those are not as extreme and do not seem to impact the astrometric results more than the assumed systematic error by selecting on position based on VLBI data.

Target source calibration—For all the different sets of targets below, inconclusive results could benefit from a new look at the data. It may be noticeable that specific sources near each other show similar structure, i.e., they arguably suffer from the same incorrect phase corrections on individual baselines. This is apparent, e.g., when a group of nearby targets show a typical "rocket shape" triangular (or any other commonly shaped) structure pointing in the same direction. Furthermore, phase-referencing between calibrators and targets at low elevation observations, mostly affecting low-declination targets, are more likely to fail for the longer projected baselines. Thus, whereas the individual images may show structure, these may well be artifacts that can be calibrated out. But for the purpose of this report, they are inconclusive in obtaining proper astrometric positions.

Nevertheless, some structure, whether real or not, may be acceptable for using the majority of these sources as potential alternatives to VLA calibrators in lower resolution observations (e.g., in B-array or more compact array configuration or, e.g., in C-band at ∼6 GHz or lower frequencies). See Section 6.3 on alternative VLA reference sources below.

6.2. *VLA targets*

In general, the (at X-band BnA/A-array configuration) dominant point-like VLA targets could benefit from the here measured alternative positions, although

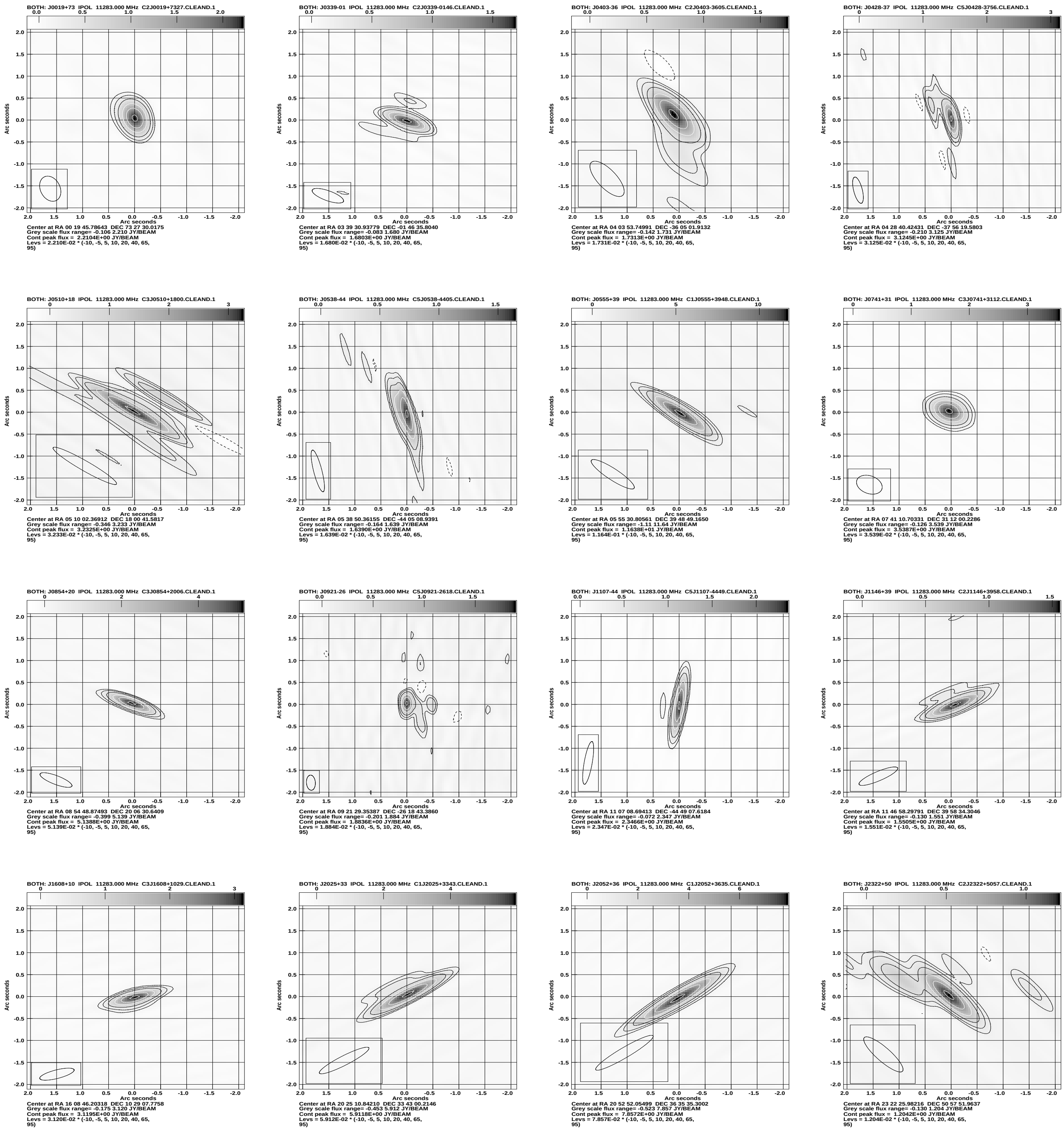

Figure 2. Phase-calibrators, VLA *Anchors* used that do not have their maximum emission at the phase center, potentially leading to questionable astrometry larger than the a-priory accuracy (50 mas). The order of sources plotted is left-to-right and top-to-bottom as the labels *a* through *p* in Table 8. Sources calibrated with any of these calibrators may have some remaining systematic astrometry issues and are labeled as such in Table 5 and Table 6 (in the Appendix). Other VLA *Anchors* with apparent structure have a dominant point-like feature at the phase-center causing less concern about systematic residuals in astrometric accuracy.

the differences are typically small; a small fraction of an arcsecond. However, some individual cases should be updated with positions up to 3 arcseconds differing from the calibrator list position.

A large number of non-point-like sources among the VLA targets is likely a remnant of the selection of suitable calibrators, e.g. from the Westerbork catalog, in the early days (i.e., for the longer wavelengths in the shorter array configurations). As they are point-like for e.g. 21-cm work in D-array configuration they were kept but also withheld or assigned a non-suitable calibrator code for, in this case, X-band A-array configuration (similarly the "Q-band only" calibrators do not have an X-band A-array calcode). It should be pointed out that some sources are not detected at all in X-band A-array configuration, suggesting that there is no real core component and the emission is located only in the diffuse lobes like in Compact Symmetric Objects. Many of the multi-component VLA targets seem to be originally positioned somewhere near the weighted center of the X-band emission and thus are off-set from the VLBI core position.

Also, whereas some calibrator sources are quite suitable in the more compact array configurations and/or at the lower frequency bands, they may show near-equal double structure at X-band in the BnA/A-array configuration that may also resolve into a single dominant core at the higher frequency bands (or VLBI baselines) and thus are just not suitable under the conditions of this experiment. Overall, it seems not useful to modify these multi-component positions to their core as clearly the VLA is sensitive to emission that does not share the same center as the VLBI-scale emission.

6.3. *Alternative VLA reference sources*

ALMA targets—Nearly all of the 133 ALMA targets were detected. The clear non-detections were the ALMA calibrator sources J0449−0057, J1217−0029 and J2156−0037. Looking at the source names it is apparent that the source coordinates, with a Declination between −1 and 0 (i.e., −00°) were not properly parsed into the target list and hence were observed at the mirrored positive Declination (i.e., +00°).

Of the remaining 130 targets, 55 were not dominated by a point source or were of bad data quality (see Fig. 4) and are thus not listed as alternative VLA reference sources in Table 6. As these are known calibrators (for ALMA), the initial positions are generally already reliable. As mentioned, these are mainly included to confirm these high-frequency sources as suitable calibrators using the VLA at X-band and possibly at other VLA receiver bands.

AT20G targets—The majority, 299 of 590 (50.7%) non-VLA targets are drawn from the AT20G catalog. Unsurprisingly this survey provided the largest contribution of new point-like detections, but it is also the survey with the largest collective corrections needed (excepting the low resolution, low frequency TGSS) of typically a couple to a few arcseconds when phase-referencing with the VLA *Anchors*. A smaller fraction (33%) than for the ALMA sources (42%) lacked the dominance of a point-like source (see Fig. 4), preventing 98 sources to be listed as alternative VLA reference sources in Table 6.

Winn targets—The 111 Winn targets, with a-priori VLBI X-band positions, could potentially expose more extended structure and associated position shift when using the VLA. Whereas most sources agree in position well within 100 mas, the exception is an extended double source (J1418−2958) deviating about 370 mas. Most targets were detected and typically are dominated by a point-like component. That is, 81% are listed as alternative VLA reference sources in Table 6 (see also Fig. 4).

TGSS targets—All TGSS targets were detected and most are point-like. As these originally were drawn from a low-frequency survey, and mostly sensitive to extended lobe emission, the position corrections for this sample are the largest compared to the others (followed by AT20G).

3FGL targets—Of the two 3FGL targets one, J1204−0710, is a clear point-like source. The other field, J1745−2900 and anticipated to be displaced by a few arcseconds from the VLA calibrator Sgr A* (both designated J1745−2900 by IAU naming convention) did not yield a detection other than Sgr A* itself. The former 3FGL target is listed as an alternative VLA reference source in Table 6, the latter is not.

6.4. *Use of these results*

The sources in Tables 5 and 6 (see Appendix) have been included in a new public source catalog in the SCT; next to the original "*VLA*" calibrator list one can find the "*VLA Alternatives*" catalog. However, given the above explanation on observations, calibration and limitations, sources in this list should not be blindly trusted for being good calibrators. It is also anticipated that this *VLA Alternatives* catalog will be an evolving resource, with updated positions and new sources, whereas the original *VLA* calibrator list will be kept frozen at this time.

For a successful calibration of VLA observations, it is recommended to select a suitable source from the *VLA* calibrator list adhering to the general advice given in the extensive VLA observing documentation. If a suitable calibrator is found, one may check Table 5 or the *VLA Alternatives* catalog if an updated position is listed, and if so, whether the image in Fig. 3 gives sufficient credence to use the updated position or whether to stick with the original *VLA* catalog entry.

If no suitable calibrator is found in the *VLA* list, or such calibrator is deemed non-optimal, one can search for a potential suitable calibrator in the *VLA Alternatives* catalog. Before using this alternative source as a calibrator, one **absolutely must check** the image in Fig. 4. If dominated by a point-like component, the next check would be the (11.3 GHz) flux density in Table 6 to deduce the approximate flux density at the observing frequency (e.g., using the original catalog data or more general surveys like VLASS) to judge whether it may be sufficiently bright for the observation. If not detected or in case of a complex structure, one should discard this source and search for another, using the same procedure.

7. FUTURE PROSPECTS

The astrometry of this sample, for the sources that are indeed dominated by a point-like component, can be improved by managing the editing of bad data and a more focused attention during the data reduction process as noted above. For the very southern sources, and perhaps others, phase referencing to an alternative, closer VLA reference source from Table 6 instead of a genuine VLA *Anchor* separated more in angle might be an option when considering new observations. The astrometry for the other sources may only succeed in a different (lower) frequency range and/or in more compact array configurations. Whether these sources are detectable will follow from other programs like TCAL0008, after which astrometry measurements at a more optimum frequency and array configurations can be re-attempted.

Alternative astrometry may be obtained by cross-correlating this sample with, e.g., data products from the VLASS survey and the optical Gaia astrometric survey, where again one should caution for different emission mechanisms and angular structure sensitivity.

Finally, it would be prudent to (re-)develop a (numeric) measure for the "point-likeness" structure of a source that captures suitability to use as a calibrator source. The current calibrator code designations of **"P"**, **"S"**, etc., are a good parametric start but may need more finesse in the future, when production of observing schedules and selection of calibrator sources become more automated.

8. CONCLUSIONS

By performing new phase-referenced X-band A-array configuration observations of (non-VLBI)calibrators from the VLA calibrator list, 122 positions deviating more than 50 mas from the original have been remeasured. The maximum difference between old and new VLA calibrator positions was 6.6 arcseconds (for J0220−0156), although this is likely from a different, unrelated source in the field of view. Another 399 VLA-accurate positions from sources taken from ALMA, AT20G, Winn et al., TGSS and 3FGL catalogs have been collected. For 422 sources in the X-band A-array configuration observations, a single position could not be assigned; these sources individually may still be good calibrators on shorter wavelengths and/or shorter baselines. These results were obtained "as-is" using standard pipelines and minimal intervention, and could be significantly improved with additional resources and reprocessing of the available data. The results are collected in the Appendix and in the *VLA Alternatives* source catalog in the SCT of the VLA Observation Preparation Tool and must be used with extreme care as described in Sect. 6.4.

The National Radio Astronomy Observatory is a facility of the National Science Foundation operated under cooperative agreement by Associated Universities, Inc. The author wishes to thank Ylva Pihlström for carefully reading and improving this memo.

REFERENCES

Belokurov, V., Erkal, D., Deason, A.J., et al. 2017, MNRAS, 446, 4711

Charlot, P., Jacobs, C. S., Gordon, D., et al. 2020, A&A, 644, A159. doi:10.1051/0004-6361/202038368

Intema, H. T., Jagannathan, P., Mooley, K. P., & Frail, D. A. 2017, A&A, 598, A78

Lacy, M., Baum, S. A., Chandler, C. J., et al. 2020, PASP, 132, 035001. doi:10.1088/1538-3873/ab63eb

Murphy, T., Sadler, E. M., Ekers, R. D., et al. 2010, MNRAS, 402, 2403

Schinzel, F. K., Petrov, L., Taylor, G. B., & Edwards, P. G. 2017, ApJ, 838, 139

Winn, J. N., Patnaik, A. R., & Wrobel, J. M. 2003, ApJS, 145, 83

APPENDIX

This Appendix lists the details and shows the images obtained for all the "targets"; first the sources from the VLA calibrator list (Table 5, Fig. 3) and then the alternative VLA reference sources from other catalogs (Table 6, Fig. 4). The tables are sorted on RA, one row per source. The figures are sorted on RA, horizontally from upper left to upper right and then similarly row-like all the way down to lower right.

Whereas a large number of targets have their measured positions blanked[10], as it appears that the position is not properly defined in these observations, manual inspection of individual images may help to decide whether a particular target seems a viable point-like source in array configurations with less angular resolution and/or at lower frequency bands, or perhaps potentially may be more point-like at higher frequency bands. Therefore most sources, with their here measured positions (i.e., also for many "Extended" sources still dominated by a point-like core), are retained in a new *VLA Alternatives* catalog in the SCT.

As the majority of the new sources seem indeed to be dominated by a single point-like component, judgment for calibration suitability of individual sources and for specific observing goals is left to the reader upon consultation of the here presented images. Be warned however, that some of the larger shifts may indicate the detection of a lobe hot-spot instead of marking the position of the core emission. That is, when using for phase-referencing one has to decide whether to use the reported position of maximum emission (i.e., as in Table 5 or Table 6) or to use the center RA/DEC as given in the figure caption (which are from the original input catalogs). Also note the peak flux density in the figure caption and the gray scale range, which is auto-scaled.

Do not blindly use the positions as reported in the new *VLA Alternatives* catalog in the SCT; consult the images first as described in Sect. 6.4. Future observations at lower (or higher) frequency bands and/or in more compact array configurations may yield more reliable or sufficiently accurate positions for general use.

[10] Be aware that the *VLA Alternatives* catalog does list a position associated with the maximum flux density in the image also for these sources, but it is not suggested to use that data as a phase-reference position – check the images for calibration suitability!

Table 5. Alternative Positions and X-band Flux Densities of Existing VLA Calibrators

IAU Name J2000	Code	Measured RA (h m s)	Measured Dec. (° ′ ″)	Error RA (s)	Error Dec. (″)	Flux Dens. Jy beam^{-1}	ΔRA (mas)	ΔDec. (mas)	Shift (mas)
J0003−1727		Extended Source, Multiple Components							
J0004+2019		00 04 35.75746	+20 19 42.3106	0.0000131	0.000143	1.54	2.0	61.6	61.6
J0006−0004		Extended Source, Multiple Components							
J0010+2047		00 10 28.74373	+20 47 49.7930	0.0000234	0.000258	0.26	−17.3	80.0	81.8
J0012−3954	**P**	Inadequate Data							
J0018−1242		Extended Source							
J0020+1540		Extended Source, Multiple Components							
J0024+2439		00 24 27.32964	+24 39 26.2168	0.0000188	0.000191	0.27	32.1	−83.2	89.2
J0025−2602	**X**	Inadequate Data							
J0035−2003		Extended Source, Multiple Components							
J0040+0125		00 40 13.52529	+01 25 46.3421	0.0000065	0.000110	0.75	−1.4	39.1	39.1
J0040+3310		Extended Source, Multiple Components							
J0042−4414		Not Detected							
J0044−3530		Not Detected							
J0046+2456		00 46 07.82589	+24 56 32.5277	0.0000105	0.000114	0.97	45.0	−79.4	91.2
J0047+2435		00 47 43.87117	+24 35 16.0037	0.0000130	0.000145	0.44	57.7	−69.4	90.2
J0054−0333		Extended Source, Multiple Components							
J0059−1700		Extended Source							
J0103+1526		01 03 26.00273	+15 26 24.6600	0.0000200	0.000257	0.24	−7.7	−15.0	16.9
J0112+3208		Extended Source							
J0116−2052	**X**	01 16 51.40496	−20 52 06.8977	0.0000064	0.000146	0.65	−9.2	−84.7	85.2
J0120−1520		Extended Source							
J0122+2954		01 22 45.43012	+29 54 12.6452	0.0000110	0.000114	2.20	−28.9	41.1	50.3
J0129+2338		Extended Source							
J0134−0931	**X**	Extended Source							
J0134−3843	**S**	Extended Source, Multiple Components							
J0135+0811		Extended Source							
J0137+3122		01 37 08.73273	+31 22 35.8321	0.0000609	0.000551	0.60	−0.4	43.1	43.1
J0141+1353		Extended Source, Multiple Components							
J0141−2706		Extended Source							
J0157−1043	**X**	Multiple Compact Components							
J0200+2523		02 00 20.63823	+25 23 54.6503	0.0000152	0.000194	0.23	15.8	−43.6	46.4
J0201−1132		Multiple Compact Components							
J0203−4349		Extended Source, Multiple Components							
J0220−0156		02 20 54.01305	−01 56 57.0040	0.0002954	0.002846	0.04	4002.0	−5204.0	6564.9
J0221+3556	**X**	02 21 05.46347	+35 56 13.6638	0.0000795	0.000668	0.44	119.4	−127.2	174.5
J0224+2750		Multiple Compact Components							
J0231−3935	**S**	Extended Source, Multiple Components							
J0242−0000		Extended Source							
J0252+1718		02 52 07.71872	+17 18 42.6886	0.0000097	0.000144	0.59	1.2	1.6	1.9
J0301+3142		03 01 23.25562	+31 42 08.4819	0.0000469	0.000374	0.05	3.5	43.9	44.0
J0309+2738		03 09 22.09644	+27 38 54.3708	0.0000174	0.000229	0.07	0.9	−0.2	0.9
J0312−1449		Extended Source, Multiple Components							
J0323+0534	**X**	03 23 20.26212	+05 34 11.9024	0.0000104	0.000168	0.34	−7.8	11.5	13.9
J0324+3410		03 24 41.16072	+34 10 45.8479	0.0000277	0.000203	0.32	−1.5	42.9	42.9
J0336+0545[b]		Not Detected							

Code: Closure phase error (Sect. 4) references in the VLA calibrator list for A-array configuration and X-band.
[a] : Calibrated with source *a* in Table 8, [b] with source *b*, etc.

Table 5. Alternative Positions and X-band Flux Densities of Existing VLA Calibrators (Continued..)

IAU Name J2000	Code	Measured RA (h m s)	Measured Dec. (° ′ ″)	Error RA (s)	Error Dec. (″)	Flux Dens. Jy beam^{-1}	ΔRA (mas)	ΔDec. (mas)	Shift (mas)
J0337+0137[b]	**W**	03 37 17.10824	+01 37 22.7537	0.0000136	0.000234	0.06	77.3	−18.4	79.5
J0338+2243		03 38 17.81155	+22 43 35.9937	0.0000263	0.000337	0.41	28.4	−43.3	51.7
J0348+3353		03 48 46.91069	+33 53 15.5145	0.0000291	0.000227	0.29	−77.1	549.5	554.9
J0355+3909		03 55 16.59368	+39 09 09.8234	0.0000369	0.000260	0.24	−28.9	−0.6	28.9
J0356+2903		03 56 08.46204	+29 03 42.3184	0.0000083	0.000099	0.59	−25.4	41.4	48.6
J0407−3303	**P**	Extended Source							
J0409−1757	**X**	04 09 06.67553	−17 57 10.0772	0.0000337	0.000376	0.78	349.2	−38.2	351.3
J0409+3848		Multiple Compact Components							
J0411+0843		04 11 33.85746	+08 43 11.4210	0.0000127	0.000208	0.62	0.6	13.0	13.0
J0413−3430		Multiple Compact Components							
J0422+3058		04 22 21.22279	+30 58 09.7100	0.0000374	0.000265	0.29	36.1	42.0	55.4
J0423+3451		Extended Source							
J0425+1755	**X**	Multiple Compact Components							
J0429−3426	**X**	04 29 46.91543	−34 26 41.0836	0.0003290	0.005244	0.05	3779.9	676.4	3840.0
J0432+3131		04 32 06.44361	+31 31 13.3416	0.0000449	0.000313	0.30	7.5	41.6	42.3
J0433+2905		04 33 37.82932	+29 05 55.4788	0.0000123	0.000156	0.22	46.9	18.8	50.5
J0438+3004		04 38 04.94848	+30 04 45.5277	0.0000527	0.000363	0.65	40.5	38.7	56.0
J0441−3340[d]	**S**	Extended Source							
J0449−3911[d]	**P**	Extended Source							
J0455−2034		04 55 23.72106	−20 34 16.0583	0.0002684	0.006026	0.02	−808.4	−1547.3	1745.8
J0502+2516[e]		Inadequate Data							
J0519+2744[e]		Inadequate Data							
J0521−2047		Multiple Compact Components							
J0534+1927[e]		Inadequate Data							
J0535+3910[g]		05 35 55.12632	+39 10 58.5237	0.0001275	0.001239	0.18	−96.8	126.7	159.4
J0536−3401	**P**	Extended Source							
J0550+2326	**?**	Inadequate Data							
J0604+2021		Extended Source, Multiple Components							
J0604+2429[f]	**X**	Inadequate Data							
J0604−4225	**P**	Inadequate Data							
J0613+1708	**W**	Inadequate Data							
J0617−3634	**X**	Extended Source, Multiple Components							
J0625+1440	**X**	Inadequate Data							
J0627−0553		Extended Source							
J0632+1022	**S**	Inadequate Data							
J0632+1554		Inadequate Data							
J0641−0320	**P**	Multiple Compact Components							
J0643+0857	**S**	Inadequate Data							
J0644−3459	**P**	Extended Source, Multiple Components							
J0646+3041		Extended Source, Multiple Components							
J0653−0625	**P**	06 53 00.59662	−06 25 32.6962	0.0000097	0.000183	0.12	31.1	−176.2	179.0
J0656−0323	**S**	06 56 11.12007	−03 23 06.7870	0.0000048	0.000086	0.45	33.5	−149.0	152.7
J0702−1015		07 02 35.75612	−10 15 06.4219	0.0000085	0.000170	0.09	−28.3	−61.9	68.1
J0703−0051	**S**	07 03 19.08644	−00 51 03.1590	0.0000044	0.000077	0.18	303.9	1790.0	1815.6
J0706−2311		Extended Source, Multiple Components							
J0707+2917[h]	**W**	07 07 26.00071	+29 17 18.7487	0.0002155	0.001875	0.09	−185.8	82.7	203.4

Code: Closure phase error (Sect. 4) references in the VLA calibrator list for A-array configuration and X-band.
[a] : Calibrated with source *a* in Table 8, [b] with source *b*, etc.

Table 5. Alternative Positions and X-band Flux Densities of Existing VLA Calibrators (Continued..)

IAU Name J2000	Code	Measured RA (h m s)	Measured Dec. (° ′ ″)	Error RA (s)	Error Dec. (″)	Flux Dens. Jy beam^{-1}	ΔRA (mas)	ΔDec. (mas)	Shift (mas)
J0709−1127		07 09 10.40652	−11 27 48.4577	0.0000065	0.000134	0.10	−1.7	−13.7	13.8
J0710−0343	**S**	07 10 20.13278	−03 43 27.8712	0.0000058	0.000106	0.14	19.8	−76.2	78.7
J0714+1436		Extended Source							
J0724−0715	**W**	07 24 17.29277	−07 15 20.3588	0.0000066	0.000128	0.46	95.6	−99.8	138.2
J0728+1437		Extended Source, Multiple Components							
J0729−3639	**S**	Inadequate Data							
J0731−2224		Extended Source							
J0735+2036		07 35 52.74000	+20 36 38.8290	0.0000790	0.000699	0.50	43.6	2.0	43.6
J0735+3307[h]	**X**	07 35 55.54958	+33 07 09.4494	0.0000306	0.000248	0.83	206.2	39.3	209.9
J0736+2604[h]		07 36 58.07559	+26 04 49.9717	0.0000946	0.000857	0.27	−33.6	88.7	94.8
J0738−3025		Extended Source, Multiple Components							
J0744−0629	**X**	Extended Source							
J0744+3753		Multiple Compact Components							
J0746−1555	**W**	07 46 18.23592	−15 55 34.7328	0.0000110	0.000236	0.08	−6.1	−260.8	260.8
J0747−3310	**P**	Inadequate Data							
J0748−1639	**S**	07 48 03.08400	−16 39 50.2530	0.0000066	0.000144	2.09	57.5	−93.1	109.4
J0749−4412		07 49 42.37337	−44 12 26.5731	0.0002656	0.009118	0.05	−1266.2	2945.9	3206.5
J0801+1414		Extended Source, Multiple Components							
J0804+1015	**X**	Multiple Compact Components							
J0805+2106		Extended Source							
J0808+0514		08 08 38.84693	+05 14 39.9416	0.0000070	0.000114	0.25	12.9	0.6	12.9
J0814+3237		Extended Source							
J0814−3538		Extended Source							
J0815−0308		Extended Source, Multiple Components							
J0821+2857		08 21 54.06595	+28 57 39.5661	0.0000959	0.000822	0.37	32.1	2.1	32.2
J0825+2704		Extended Source, Multiple Components							
J0827−2026		Extended Source, Multiple Components							
J0837−1951	**X**	08 37 11.16554	−19 51 56.7309	0.0000039	0.000081	0.88	232.2	79.1	245.3
J0853−2047		Not Detected							
J0858+1409[i]		Multiple Compact Components							
J0911+3349		09 11 47.76372	+33 49 16.8137	0.0000233	0.000169	0.07	6.0	−9.3	11.1
J0921+0805		09 21 01.06456	+08 05 05.6460	0.0000081	0.000136	0.19	3.5	−25.0	25.3
J0921+1350[i]		09 21 31.37404	+13 50 48.2294	0.0000995	0.000806	0.05	−6.4	−0.6	6.5
J0925+3127		09 25 43.64995	+31 27 10.7939	0.0000313	0.000186	1.99	35.2	−39.1	52.6
J0939+8315		Extended Source							
J0948+0022		09 48 57.32148	+00 22 25.5629	0.0000106	0.000174	0.59	−8.7	−0.1	8.7
J0949+1752		09 49 39.76542	+17 52 49.4226	0.0000499	0.000364	0.33	−38.9	0.6	38.9
J0949+6614		Multiple Compact Components							
J1008+0730		Multiple Compact Components							
J1011+0624		Extended Source							
J1018−3144	**X**	10 18 09.26769	−31 44 14.0994	0.0000102	0.000314	0.88	−2.4	−116.4	116.4
J1020−4251[k]		Not Detected							
J1021+2159	**X**	Extended Source							
J1022+3041	**S**	10 22 30.29849	+30 41 05.1365	0.0000563	0.000307	2.17	9.2	203.5	203.7
J1033−3418		Extended Source							
J1041+0242		Extended Source, Multiple Components							

Code: Closure phase error (Sect. 4) references in the VLA calibrator list for A-array configuration and X-band.
[a] : Calibrated with source *a* in Table 8, [b] with source *b*, etc.

Table 5. Alternative Positions and X-band Flux Densities of Existing VLA Calibrators (Continued..)

IAU Name J2000	Code	Measured RA (h m s)	Measured Dec. (° ′ ″)	Error RA (s)	Error Dec. (″)	Flux Dens. Jy beam^{-1}	ΔRA (mas)	ΔDec. (mas)	Shift (mas)
J1106−2108		Extended Source							
J1109+3744	**X**	Extended Source							
J1114+4037		Extended Source							
J1117+4120		11 17 53.33384	+41 20 16.2765	0.0000214	0.000133	0.54	0.7	0.5	0.9
J1119−0302		11 19 25.29276	−03 02 51.2723	0.0000384	0.000696	0.05	108.4	47.7	118.4
J1120+2327		Extended Source							
J1120−2508[l]	**X**	Extended Source, Multiple Components							
J1123+0530		Extended Source, Multiple Components							
J1125+2005		Extended Source, Multiple Components							
J1131+3114		11 31 09.48205	+31 14 05.4931	0.0000242	0.000118	0.79	−30.1	3.1	30.3
J1132+0034		11 32 45.61831	+00 34 27.8313	0.0000067	0.000117	0.35	8.9	10.3	13.6
J1139+6547		Not Detected							
J1139+7654		11 39 51.53222	+76 54 32.3349	0.0001158	0.000239	1.94	58.0	45.9	74.0
J1142−1141		11 42 34.93429	−11 41 48.6954	0.0000235	0.000416	0.04	1051.8	−857.5	1357.1
J1143+2206		Extended Source, Multiple Components							
J1145+4946		Extended Source, Multiple Components							
J1148+5254	**S**	Extended Source							
J1154−3505	**X**	Extended Source							
J1156+3128		Extended Source, Multiple Components							
J1200+7300		Extended Source							
J1206+6413		Extended Source, Multiple Components							
J1209+1810		Extended Source, Multiple Components							
J1209−3214	**P**	Extended Source, Multiple Components							
J1209+4339		Extended Source, Multiple Components							
J1220+2916	**W**	Not Detected							
J1220+3431		12 20 08.29340	+34 31 21.7641	0.0001198	0.000924	0.09	−34.7	43.1	55.3
J1221+0510		12 21 52.33221	+05 10 16.0746	0.0000423	0.000292	0.68	34.2	2.6	34.3
J1235−4153	**X**	Extended Source							
J1236+3920		12 36 51.45204	+39 20 27.6940	0.0001062	0.000809	0.15	−34.0	0.0	34.0
J1242−0446		Extended Source, Multiple Components							
J1248+2022		Extended Source							
J1252+5634		Extended Source, Multiple Components							
J1256+4720		Extended Source, Multiple Components							
J1308−0950		Extended Source							
J1308+3546	**P**	Extended Source							
J1308+6544	**X**	Multiple Compact Components							
J1310+0044		13 10 28.50321	+00 44 08.8898	0.0000113	0.000184	0.35	−7.7	19.8	21.2
J1311−2216		Extended Source, Multiple Components							
J1321+1106		Extended Source, Multiple Components							
J1330+2509	**X**	Inadequate Data							
J1338−0627		Not Detected							
J1338+3851		13 38 50.00901	+38 51 10.1935	0.0026398	0.028819	0.02	−2678.6	−1656.5	3149.4
J1341+2816		Extended Source							
J1342+6021		Extended Source, Multiple Components							
J1343+2844		13 43 00.17568	+28 44 07.5248	0.0000667	0.000341	0.78	50.2	27.8	57.4
J1344+1409	**X**	13 44 23.74515	+14 09 14.9039	0.0000498	0.000317	0.64	−44.4	47.9	65.3

Code: Closure phase error (Sect. 4) references in the VLA calibrator list for A-array configuration and X-band.
[a] : Calibrated with source a in Table 8, [b] with source b, etc.

Table 5. Alternative Positions and X-band Flux Densities of Existing VLA Calibrators (Continued..)

IAU Name J2000	Code	Measured RA (h m s)	Measured Dec. (° ′ ″)	Error RA (s)	Error Dec. (″)	Flux Dens. Jy beam^{-1}	ΔRA (mas)	ΔDec. (mas)	Shift (mas)
J1345+4946		Extended Source							
J1347−0803		13 47 01.69897	−08 03 22.5927	0.0000565	0.001119	0.01	−2613.5	1247.3	2895.9
J1349−3922		Extended Source, Multiple Components							
J1352+3126		Extended Source, Multiple Components							
J1353+1435		13 53 22.83966	+14 35 39.2521	0.0000519	0.000312	0.74	0.6	−7.9	7.9
J1353+7532		Extended Source, Multiple Components							
J1357+4353	**X**	13 57 40.59273	+43 53 59.7657	0.0000251	0.000109	2.77	902.1	94.7	907.1
J1400+6210	**S**	14 00 28.64949	+62 10 38.5733	0.0000416	0.000129	4.01	21.8	47.3	52.1
J1404+6551		14 04 05.27694	+65 51 37.5719	0.0000326	0.000089	2.11	−5.7	55.9	56.2
J1411+5212		Extended Source, Multiple Components							
J1420+1703		14 20 20.88858	+17 03 29.1910	0.0000371	0.000217	1.41	44.7	−8.0	45.4
J1421+4144		Extended Source, Multiple Components							
J1425−2959		Extended Source, Multiple Components							
J1427+2348		14 27 00.38882	+23 48 00.0404	0.0000402	0.000219	1.83	86.2	−0.6	86.2
J1428−2741		Extended Source							
J1429+6316		14 29 05.30828	+63 16 04.6518	0.0000359	0.000109	0.53	−5.3	−4.2	6.7
J1438+6211	**X**	14 38 44.78393	+62 11 54.4013	0.0000276	0.000093	1.54	23.6	4.3	23.9
J1439−1659		Extended Source, Multiple Components							
J1449+6316		Extended Source, Multiple Components							
J1501−3918		Extended Source							
J1504+2854		Extended Source							
J1506+8319		Extended Source							
J1507+5857		15 07 47.38758	+58 57 27.6546	0.0000320	0.000108	0.89	−11.4	6.6	13.2
J1520+2016		Extended Source							
J1539+2744		Extended Source							
J1541+5348		15 41 25.46407	+53 48 13.0354	0.0000344	0.000133	0.61	0.3	−1.6	1.6
J1547+4937		15 47 21.13813	+49 37 05.8037	0.0000260	0.000112	2.23	2.6	−6.2	6.8
J1549+2125		Extended Source							
J1556+2004		Inadequate Data							
J1604+0117^{m}		Multiple Compact Components							
J1604−4441	**?**	Multiple Compact Components							
J1605−1734		Extended Source							
J1610+2414		Extended Source							
J1623−1140		Extended Source, Multiple Components							
J1625−3108		Multiple Compact Components							
J1627+1216^{m}		16 27 37.02445	+12 16 07.1563	0.0000618	0.000405	0.44	110.7	42.3	118.5
J1629+1500^{m}		16 29 44.79413	+15 00 18.6104	0.0000675	0.000472	0.43	79.3	−6.6	79.6
J1629+6757	**X**	16 29 51.84090	+67 57 14.9589	0.0000610	0.000188	0.66	17.4	10.9	20.6
J1634+6245	**X**	Extended Source							
J1636+2112^{m}		Extended Source							
J1638+6234	**X**	Extended Source							
J1639+8631	**S**	16 39 25.02476	+86 31 53.1506	0.0004375	0.000292	0.94	85.0	−43.4	95.4
J1641+2257		Inadequate Data							
J1642−0621		Inadequate Data							
J1642+2523		Multiple Compact Components							
J1646−2227		Extended Source							

Code: Closure phase error (Sect. 4) references in the VLA calibrator list for A-array configuration and X-band.
[a] : Calibrated with source a in Table 8, [b] with source b, etc.

Table 5. Alternative Positions and X-band Flux Densities of Existing VLA Calibrators (Continued..)

IAU Name J2000	Code	Measured RA (h m s)	Measured Dec. (° ′ ″)	Error RA (s)	Error Dec. (″)	Flux Dens. Jy beam^{-1}	ΔRA (mas)	ΔDec. (mas)	Shift (mas)
J1647+2705		Multiple Compact Components							
J1658−0739	**S**	Inadequate Data							
J1659+2629		Extended Source							
J1701−2954		Multiple Compact Components							
J1710+4601		Extended Source							
J1712−2809		Extended Source, Multiple Components							
J1714−2514	**X**	Extended Source, Multiple Components							
J1717−3342		Extended Source, Multiple Components							
J1717−3948		Extended Source, Multiple Components							
J1720−3552	**X**	Extended Source, Multiple Components							
J1722+2815		Extended Source							
J1726+2717		17 26 53.40613	+27 17 16.3114	0.0000643	0.000406	0.52	86.2	−82.6	119.4
J1738+3224		17 38 40.50136	+32 24 09.0231	0.0000353	0.000187	1.37	43.6	−41.9	60.4
J1743−3058	**S**	Extended Source, Multiple Components							
J1744−3116	**S**	Extended Source, Multiple Components							
J1745−0753	**P**	17 45 27.10431	−07 53 03.9512	0.0000082	0.000157	0.56	−4.6	−351.1	351.2
J1755+3350		17 55 11.24322	+33 50 59.8103	0.0000659	0.000355	0.63	−6.4	38.3	38.8
J1801+1351	**X**	Multiple Compact Components							
J1803+0341		Extended Source, Multiple Components							
J1803+0934		18 03 33.66010	+09 34 25.8239	0.0000945	0.000758	0.50	−118.4	−86.1	146.4
J1805+1101		Extended Source, Multiple Components							
J1811−2055	**X**	18 11 06.79527	−20 55 03.2714	0.0000153	0.000365	0.36	66.3	172.6	184.9
J1812−0648	**X**	18 12 50.92444	−06 48 23.5328	0.0000139	0.000258	0.16	260.3	321.0	413.3
J1818−1108		18 18 19.31368	−11 08 48.3286	0.0000166	0.000321	0.16	43.0	0.4	43.0
J1820−0947		Multiple Compact Components							
J1822−0938	**X**	Multiple Compact Components							
J1822−1309	**X**	18 22 10.91317	−13 09 43.5708	0.0000275	0.000555	0.01	−148.5	659.2	675.7
J1822+8257		18 22 03.06013	+82 57 20.6785	0.0001465	0.000241	0.32	3.4	−1.5	3.7
J1825−0737	**W**	18 25 37.61147	−07 37 30.0010	0.0000125	0.000231	0.12	−140.8	222.0	262.9
J1825−1718	**W**	Extended Source, Multiple Components							
J1828+2626		Extended Source, Multiple Components							
J1830−3602		Extended Source, Multiple Components							
J1832−1035	**P**	Extended Source, Multiple Components							
J1833−2103	**X**	Inadequate Data							
J1834−0301		18 34 14.07416	−03 01 19.6286	0.0000170	0.000287	0.35	−2199.8	1496.5	2660.6
J1834−1237		18 34 19.21175	−12 37 40.7990	0.0000273	0.000527	0.03	69.5	146.0	161.7
J1849+3024		18 49 20.10321	+30 24 14.2309	0.0000484	0.000306	1.26	42.6	41.9	59.7
J1850+4959		18 50 22.24052	+49 59 21.4421	0.0000471	0.000292	2.53	−4.0	0.1	4.1
J1851+0035	**S**	Extended Source							
J1859+1259		Extended Source							
J1900+2722		19 00 34.67846	+27 22 30.8654	0.0001338	0.000999	0.36	−42.1	1.5	42.2
J1902−2329		Extended Source							
J1912+0518	**W**	Extended Source							
J1914+1636	**X**	Inadequate Data							
J1919+0619		Inadequate Data							
J1926+4209		19 26 31.04989	+42 09 59.0328	0.0001170	0.000788	0.18	5.6	41.7	42.1

Code: Closure phase error (Sect. 4) references in the VLA calibrator list for A-array configuration and X-band.
[a] : Calibrated with source a in Table 8, [b] with source b, etc.

Table 5. Alternative Positions and X-band Flux Densities of Existing VLA Calibrators (Continued..)

IAU Name J2000	Code	Measured RA (h m s)	Measured Dec. (° ′ ″)	Error RA (s)	Error Dec. (″)	Flux Dens. Jy beam^{-1}	ΔRA (mas)	ΔDec. (mas)	Shift (mas)
J1930+1532	**X**	Inadequate Data							
J1933+1504		Inadequate Data							
J1937+8356		Extended Source							
J1941+1026	**X**	Extended Source, Multiple Components							
J1941−1524		Extended Source, Multiple Components							
J1952+2526	**X**	Inadequate Data							
J1956−0736		Multiple Compact Components							
J1956+2820	**S**	Extended Source, Multiple Components							
J1956−3225	**S**	Extended Source, Multiple Components							
J2005+1825		Extended Source, Multiple Components							
J2005−3723	**S**	Extended Source, Multiple Components							
J2007+3722	**W**	20 07 45.39926	+37 22 02.3234	0.0000555	0.000439	0.66	−265.3	216.3	342.4
J2007−4434	**S**	Extended Source, Multiple Components							
J2008+5213		20 08 56.28769	+52 13 33.0341	0.0001330	0.001025	0.30	1197.3	1075.1	1609.2
J2009+1318		20 09 27.22184	+13 18 14.4279	0.0000133	0.000189	0.49	−13.7	−30.2	33.1
J2009+2505		Extended Source, Multiple Components							
J2010+3322[n]	**P**	20 10 49.72301	+33 22 13.8413	0.0000705	0.000545	0.79	−209.3	214.2	299.5
J2016+3600	**W**	20 16 45.62052	+36 00 33.3940	0.0000554	0.000455	0.38	38.6	−43.0	57.8
J2021+2318		Inadequate Data							
J2024+2736		Inadequate Data							
J2033+2146		Inadequate Data							
J2035+1857	**X**	Inadequate Data							
J2035−3454		Not Detected							
J2039+2152		Inadequate Data							
J2047−0236		Extended Source, Multiple Components							
J2053+2248		Inadequate Data							
J2057+5058		Extended Source, Multiple Components							
J2104+7633		Extended Source							
J2106+2135		Inadequate Data							
J2106+2500		Inadequate Data							
J2107+4214[o]		Extended Source							
J2114−2541		Extended Source, Multiple Components							
J2114−3502	**X**	Extended Source							
J2114+8204		21 14 01.15487	+82 04 48.3403	0.0001771	0.000489	0.73	50.7	−7.7	51.3
J2130+1643		Multiple Compact Components							
J2131−2036		Extended Source, Multiple Components							
J2133+1443		21 33 37.38957	+14 43 46.4691	0.0000074	0.000117	0.25	−3.9	−1.9	4.4
J2134+4050		Extended Source, Multiple Components							
J2137−2042		Extended Source, Multiple Components							
J2137+5101	**P**	Extended Source, Multiple Components							
J2139+1718		21 39 37.14733	+17 18 26.0696	0.0000109	0.000170	0.12	0.9	−1.4	1.7
J2148+6107	**S**	Extended Source, Multiple Components							
J2149−1304	**X**	Multiple Compact Components							
J2150+1449	**S**	21 50 23.60790	+14 49 47.9041	0.0000099	0.000138	0.26	−91.3	−3.9	91.4
J2152−2828		Extended Source, Multiple Components							
J2156+4830		Multiple Compact Components							

Code: Closure phase error (Sect. 4) references in the VLA calibrator list for A-array configuration and X-band.
[a] : Calibrated with source *a* in Table 8, [b] with source *b*, etc.

Table 5. Alternative Positions and X-band Flux Densities of Existing VLA Calibrators (Continued..)

IAU Name J2000	Code	Measured RA (h m s)	Measured Dec. (° ′ ″)	Error RA (s)	Error Dec. (″)	Flux Dens. Jy beam^{-1}	ΔRA (mas)	ΔDec. (mas)	Shift (mas)
J2200+1030		22 00 07.93315	+10 30 07.9036	0.0000134	0.000198	0.20	5.2	0.6	5.3
J2203+6240		Multiple Compact Components							
J2212+0152	**S**	22 12 37.97510	+01 52 51.1842	0.0000132	0.000206	0.47	28.5	33.2	43.8
J2219−2756	**X**	Not Detected							
J2224+6016	**X**	Inadequate Data							
J2231+5409[p]	**X**	Inadequate Data							
J2232+6249		Extended Source							
J2242+1741		22 42 47.95573	+17 41 44.1647	0.0000117	0.000162	0.01	11.0	−11.2	15.7
J2250+1419	**X**	22 50 25.34321	+14 19 52.0486	0.0000192	0.000279	0.05	2860.0	1448.6	3205.9
J2250+7129[a]		Multiple Compact Components							
J2251+1848	**X**	22 51 34.72708	+18 48 40.0151	0.0000199	0.000294	0.03	163.6	−129.9	208.9
J2255+1313	**X**	Extended Source, Multiple Components							
J2257−3627	**P**	Extended Source, Multiple Components							
J2307+1450		23 07 34.00203	+14 50 17.9755	0.0000115	0.000172	0.01	−515.6	−430.0	671.3
J2307−4132		Not Detected							
J2312+0919		Extended Source, Multiple Components							
J2316+0405		Extended Source, Multiple Components							
J2316+1618		23 16 39.69814	+16 18 06.7464	0.0000123	0.000173	0.02	8.1	3.4	8.7
J2321−1623		Extended Source							
J2321+3204		Inadequate Data							
J2325−1207		23 25 19.73138	−12 07 27.1634	0.0000198	0.000396	0.13	610.4	−72.4	614.7
J2325+4346	**X**	Inadequate Data							
J2326+1507		23 26 52.89175	+15 07 39.7105	0.0000142	0.000206	0.03	12.4	−19.6	23.1
J2326−4027		Extended Source, Multiple Components							
J2339+6010[p]	**S**	Extended Source							
J2340+1333	**X**	23 40 33.23870	+13 33 00.8872	0.0000194	0.000272	0.15	−199.8	−22.8	201.1
J2341+0018		Extended Source							
J2341−3506	**X**	Multiple Compact Components							
J2343+5348[p]		Multiple Compact Components							
J2345+6557[a]		Multiple Compact Components							
J2350+6440[a]		Multiple Compact Components							

Code: Closure phase error (Sect. 4) references in the VLA calibrator list for A-array configuration and X-band.
[a] : Calibrated with source *a* in Table 8, [b] with source *b*, etc.

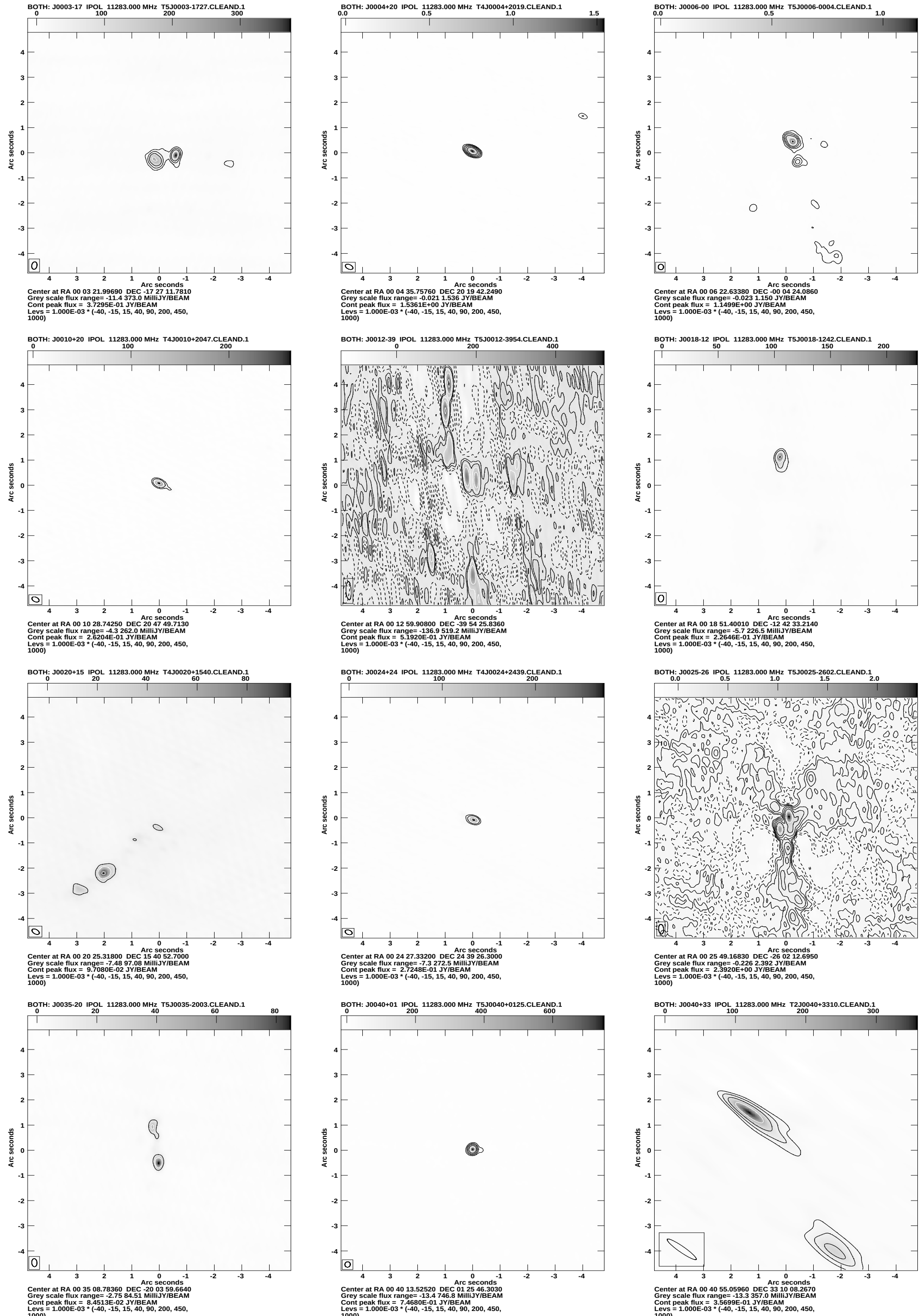

Figure 3. Images for "VLA targets", sorted in RA.

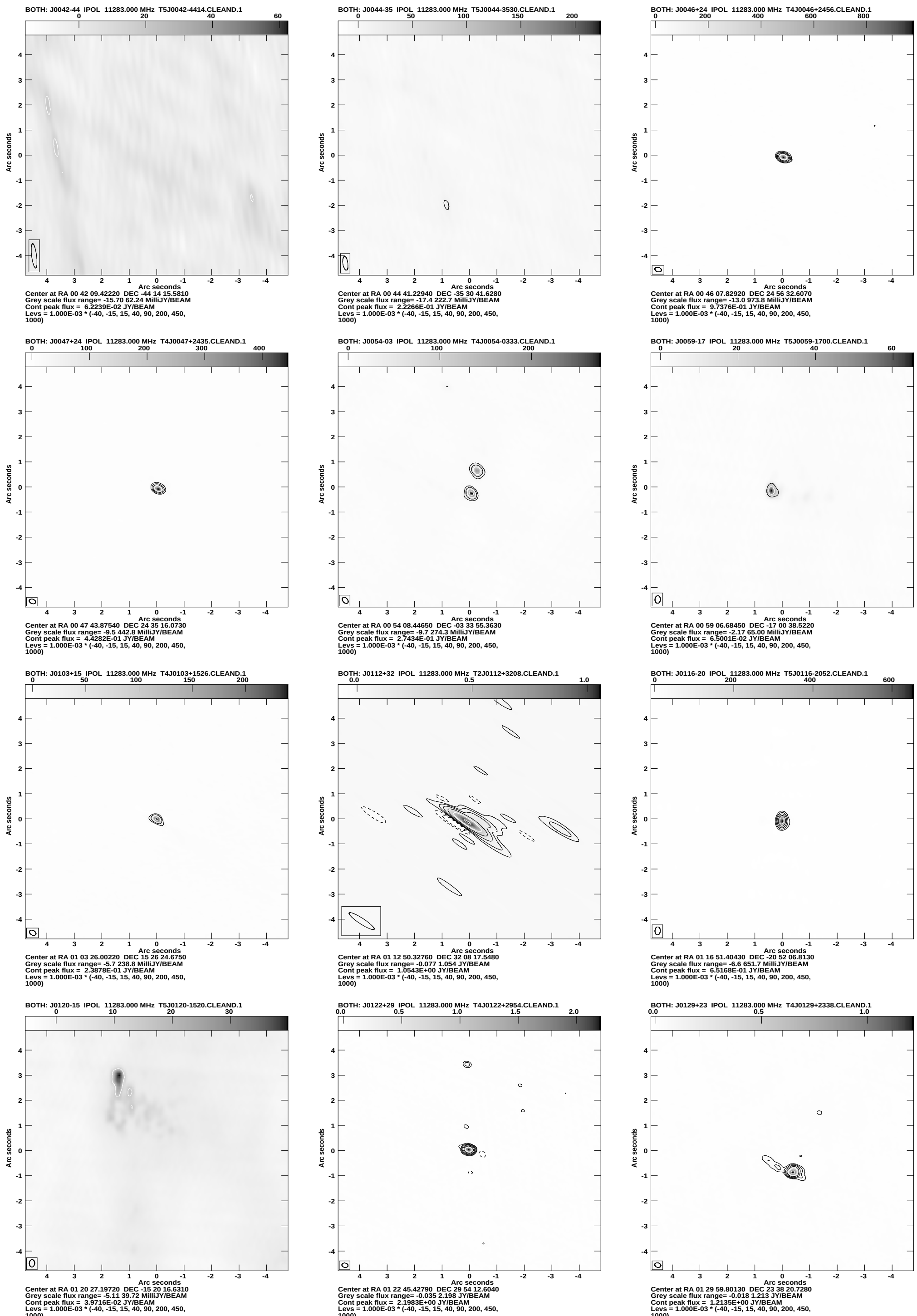

Figure 3. Images for "VLA targets", sorted in RA. (continued)

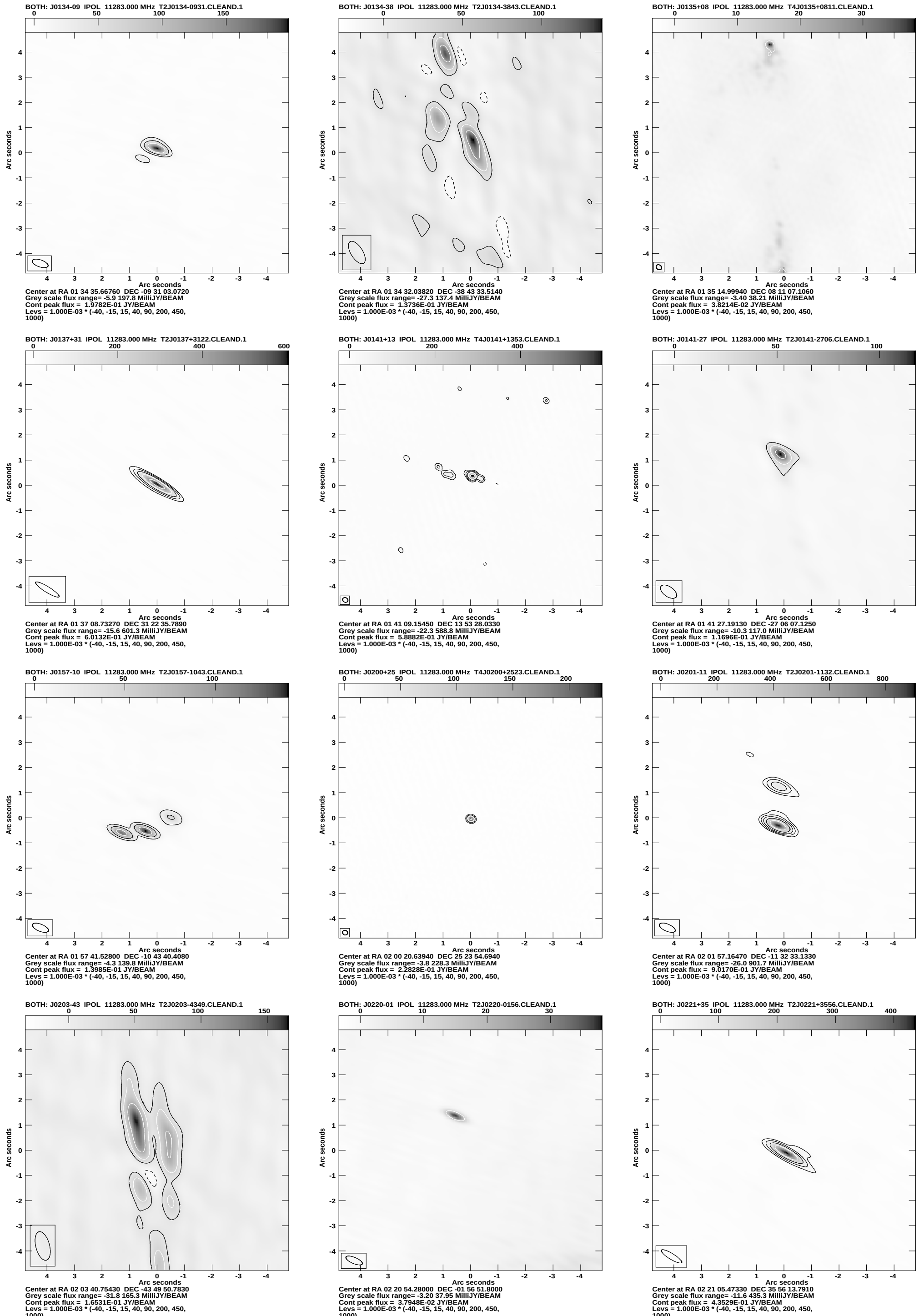

Figure 3. Images for "VLA targets", sorted in RA. (continued)

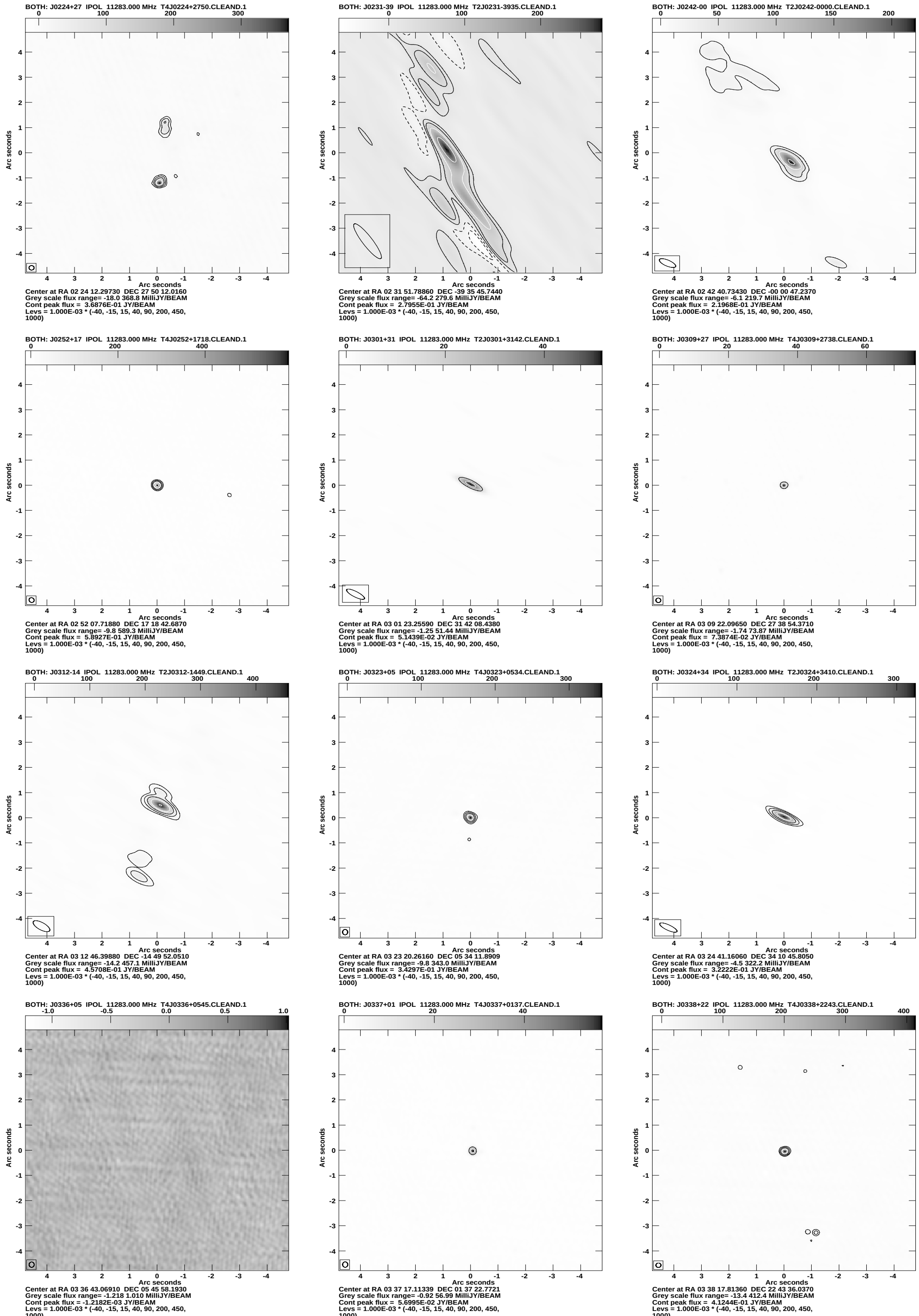

Figure 3. Images for "VLA targets", sorted in RA. (continued)

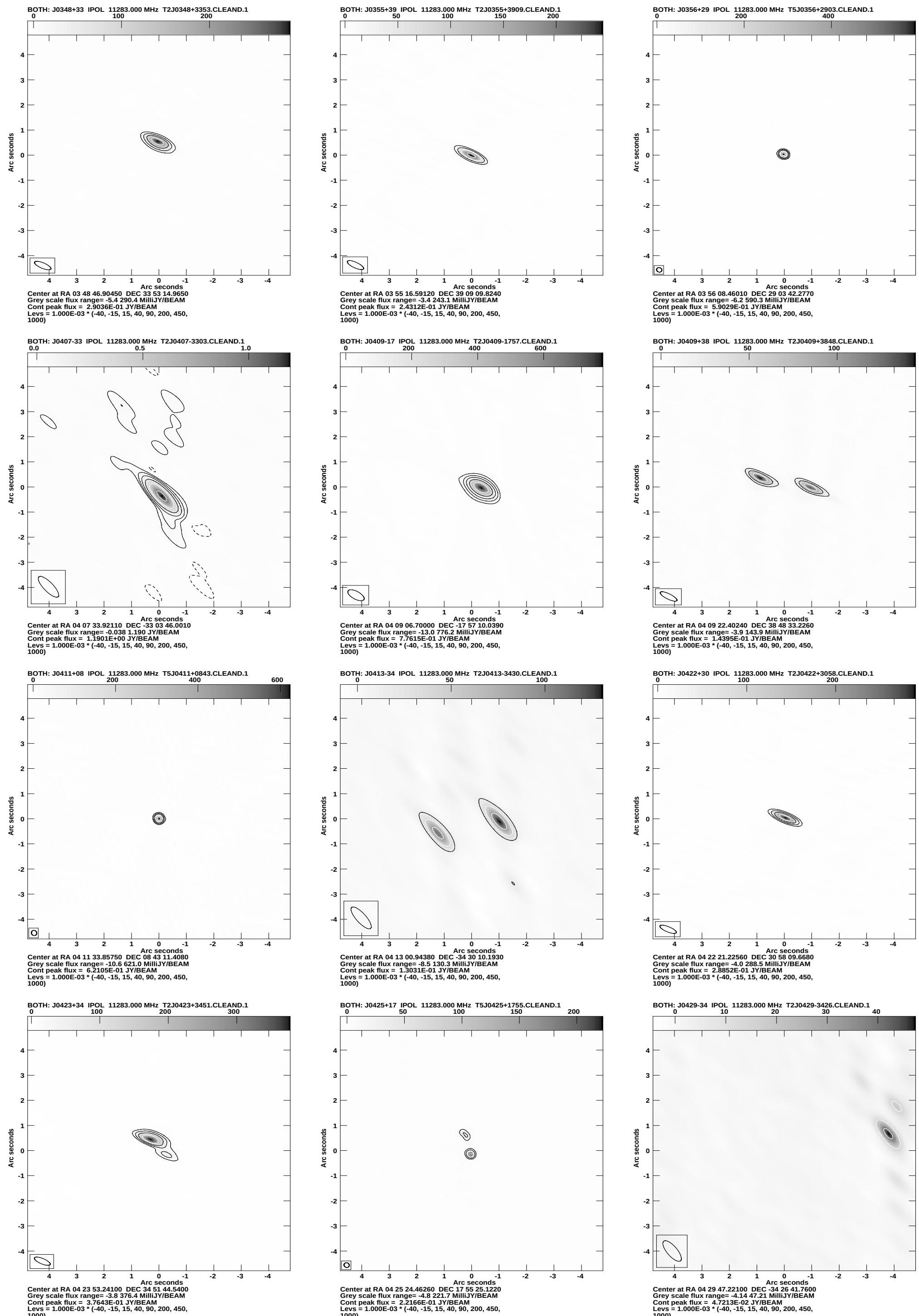

Figure 3. Images for "VLA targets", sorted in RA. (continued)

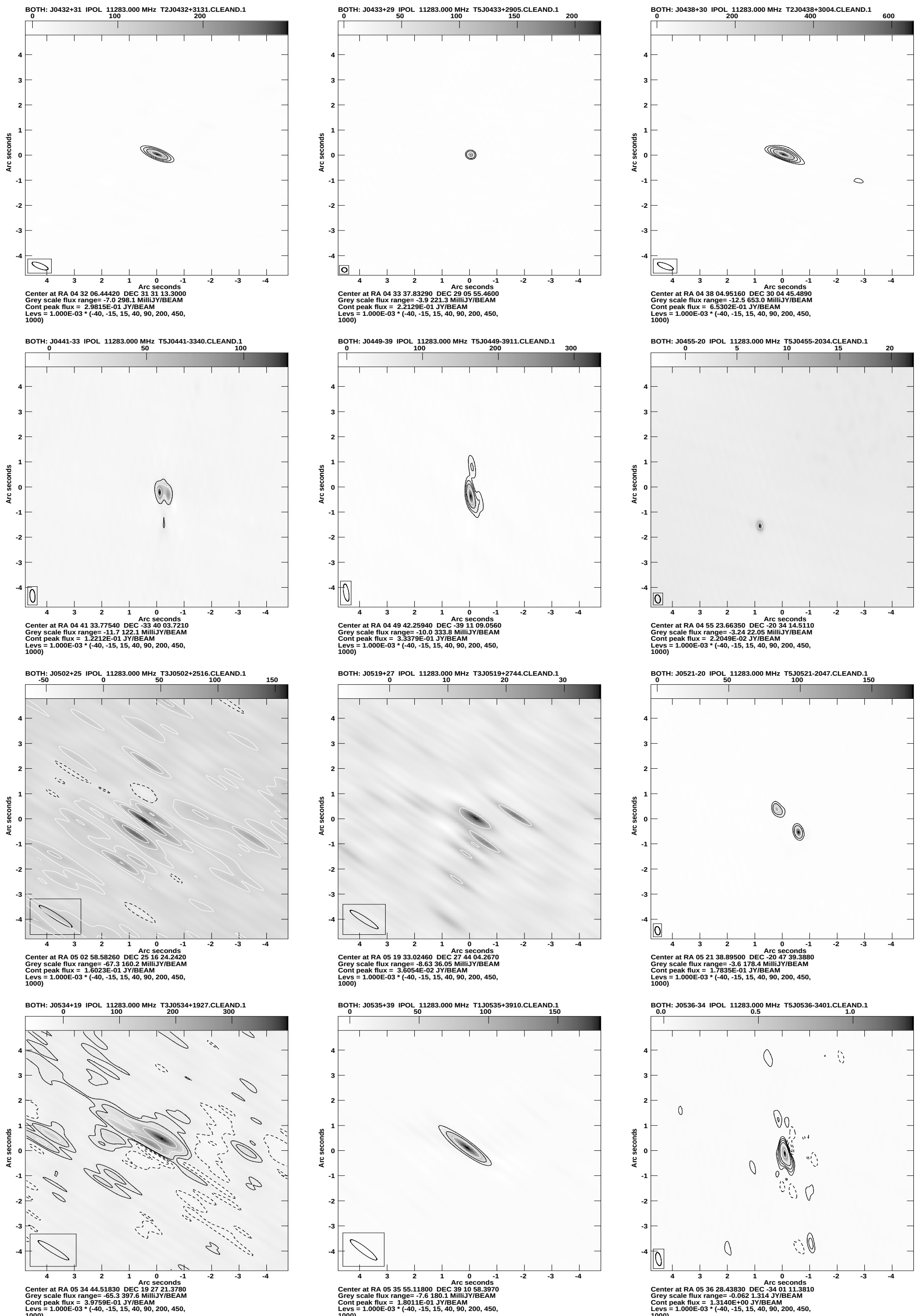

Figure 3. Images for "VLA targets", sorted in RA. (continued)

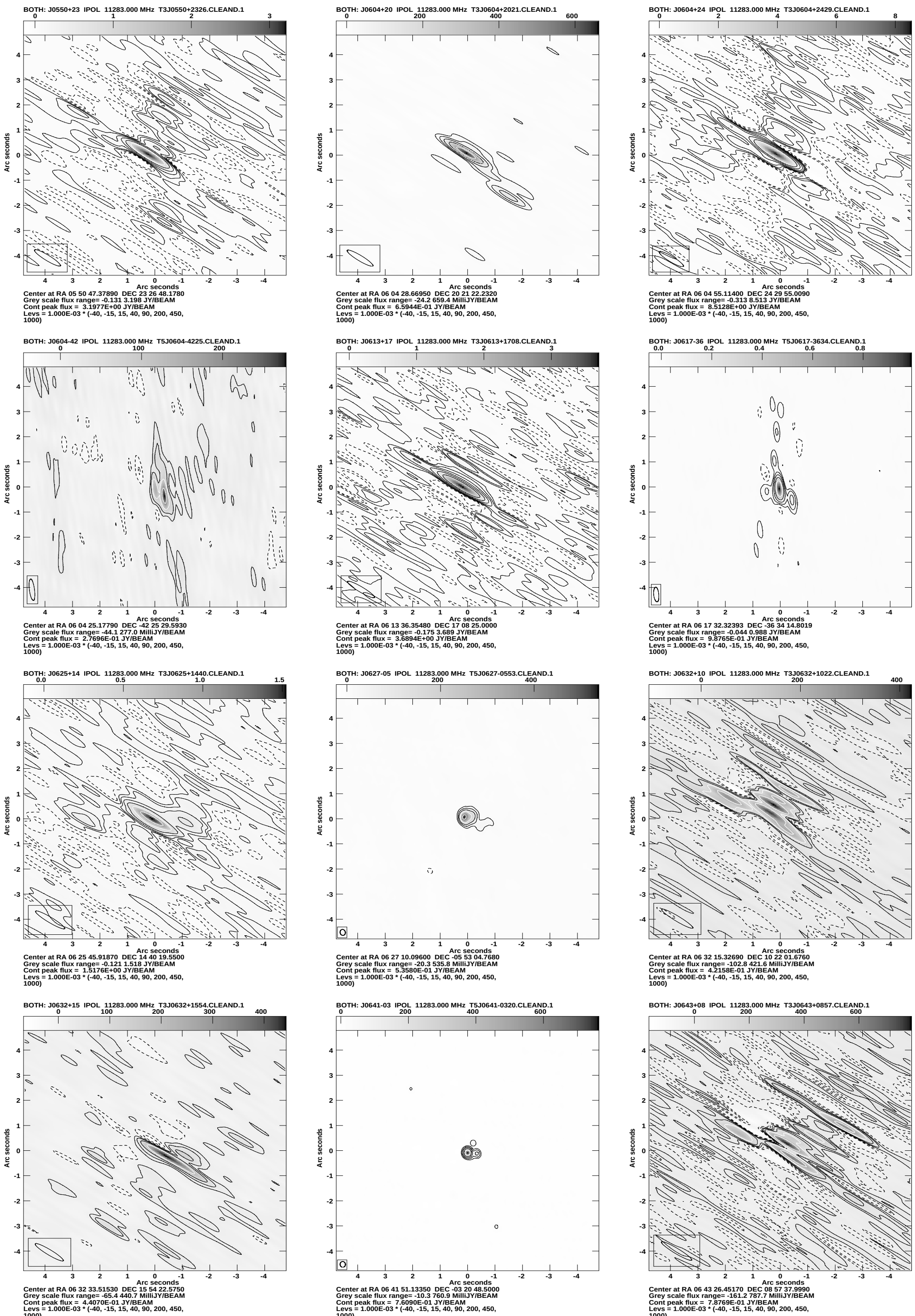

Figure 3. Images for “VLA targets”, sorted in RA. (continued)

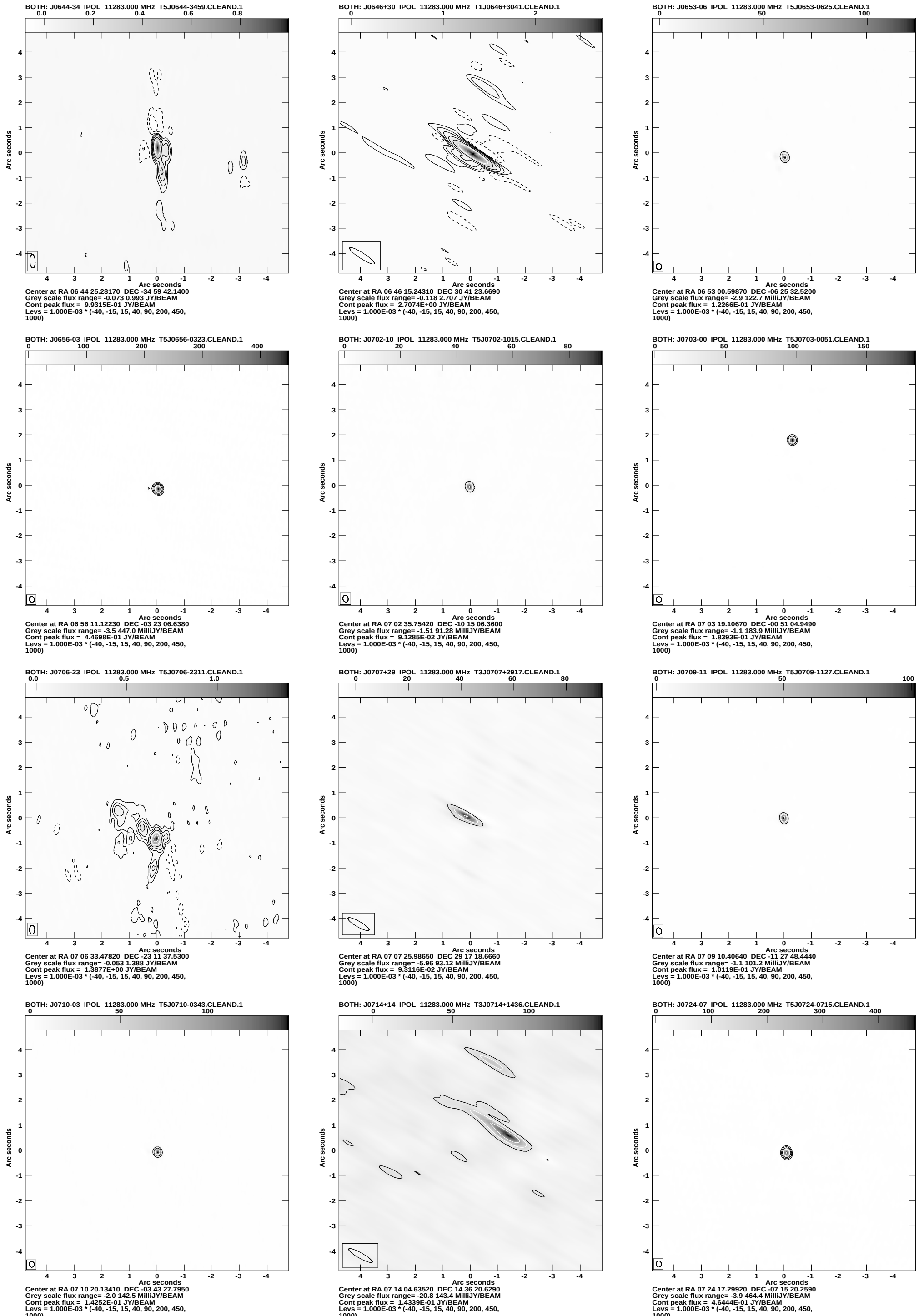

Figure 3. Images for “VLA targets”, sorted in RA. (continued)

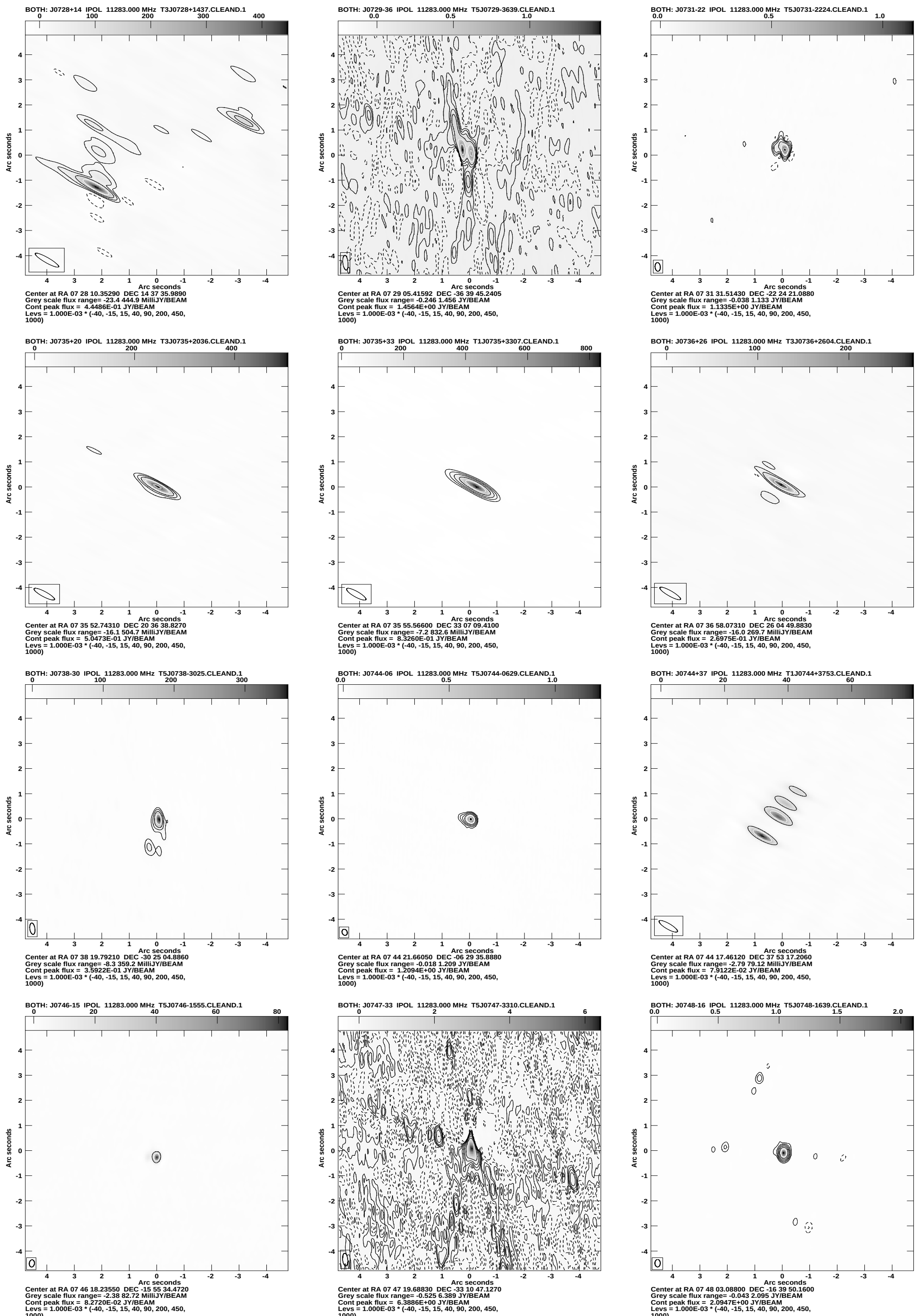

Figure 3. Images for "VLA targets", sorted in RA. (continued)

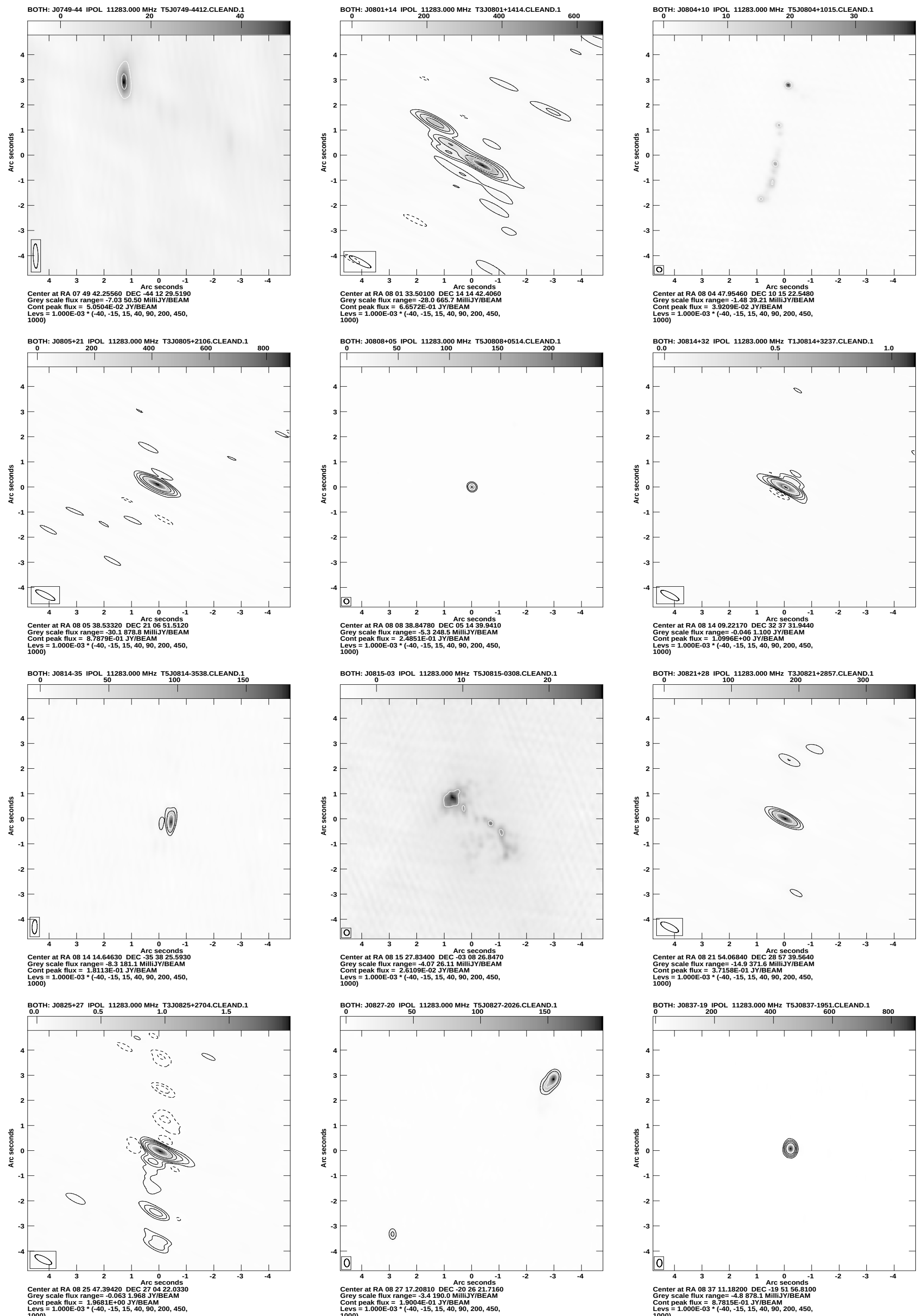

Figure 3. Images for “VLA targets”, sorted in RA. (continued)

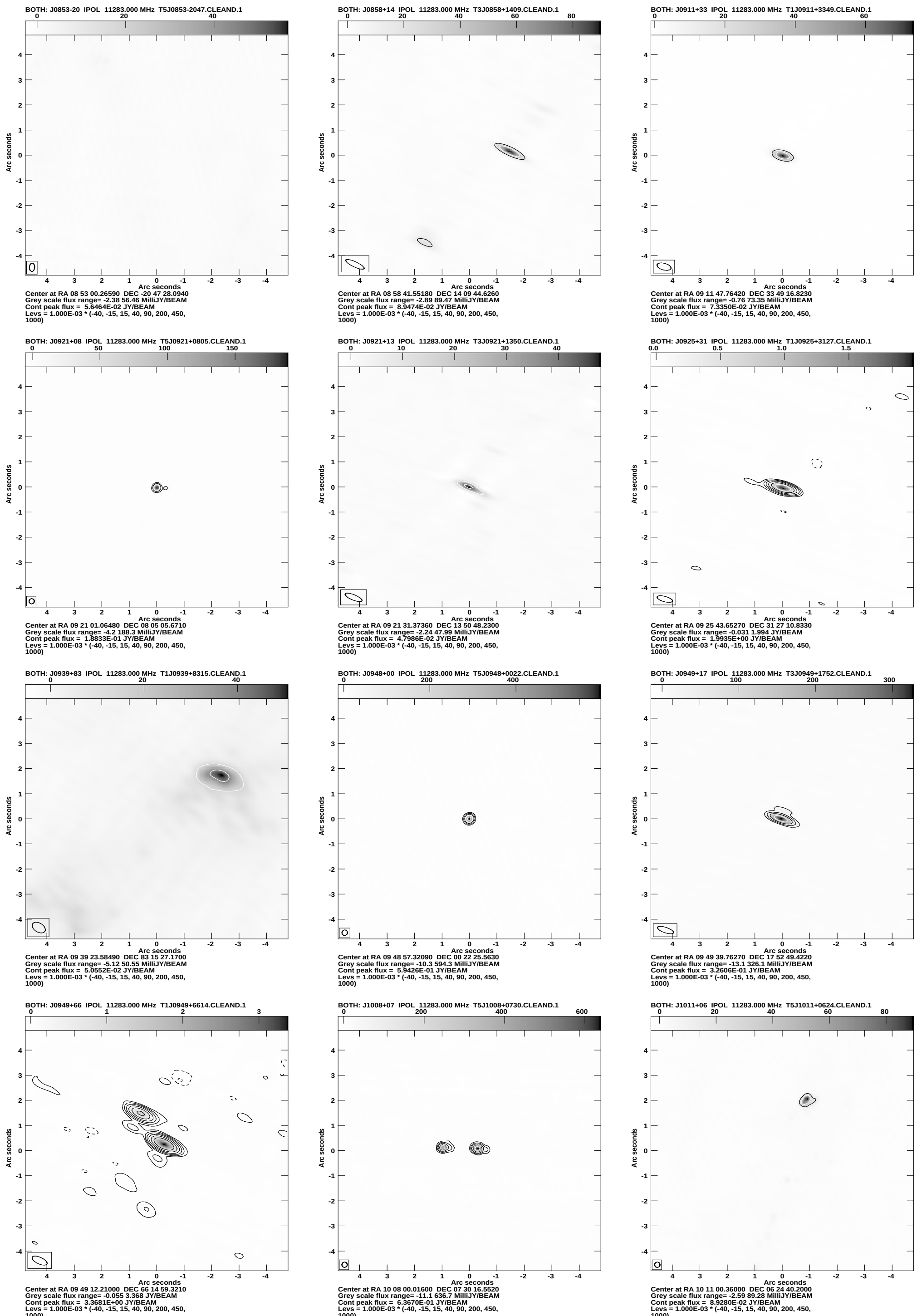

Figure 3. Images for “VLA targets”, sorted in RA. (continued)

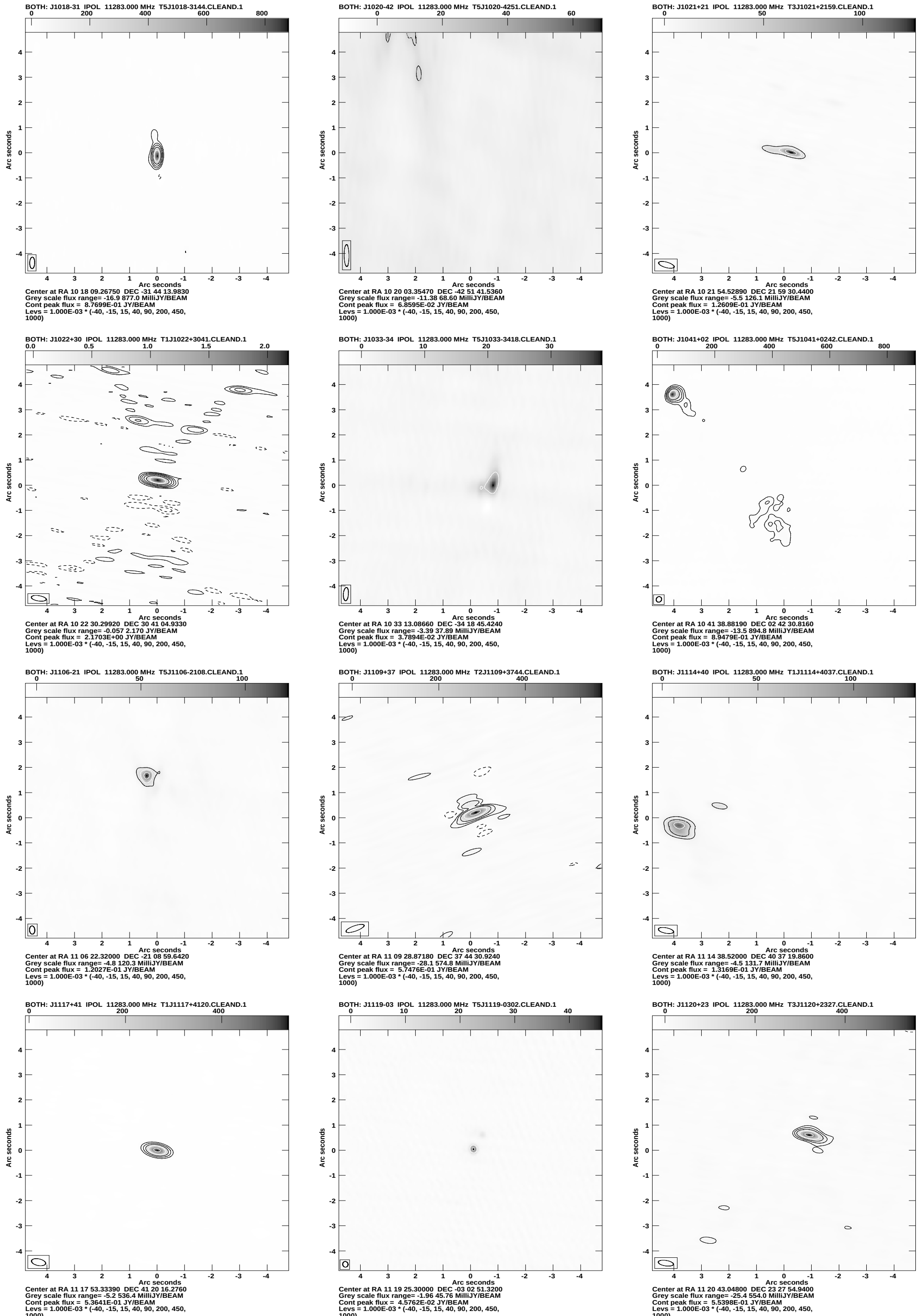

Figure 3. Images for "VLA targets", sorted in RA. (continued)

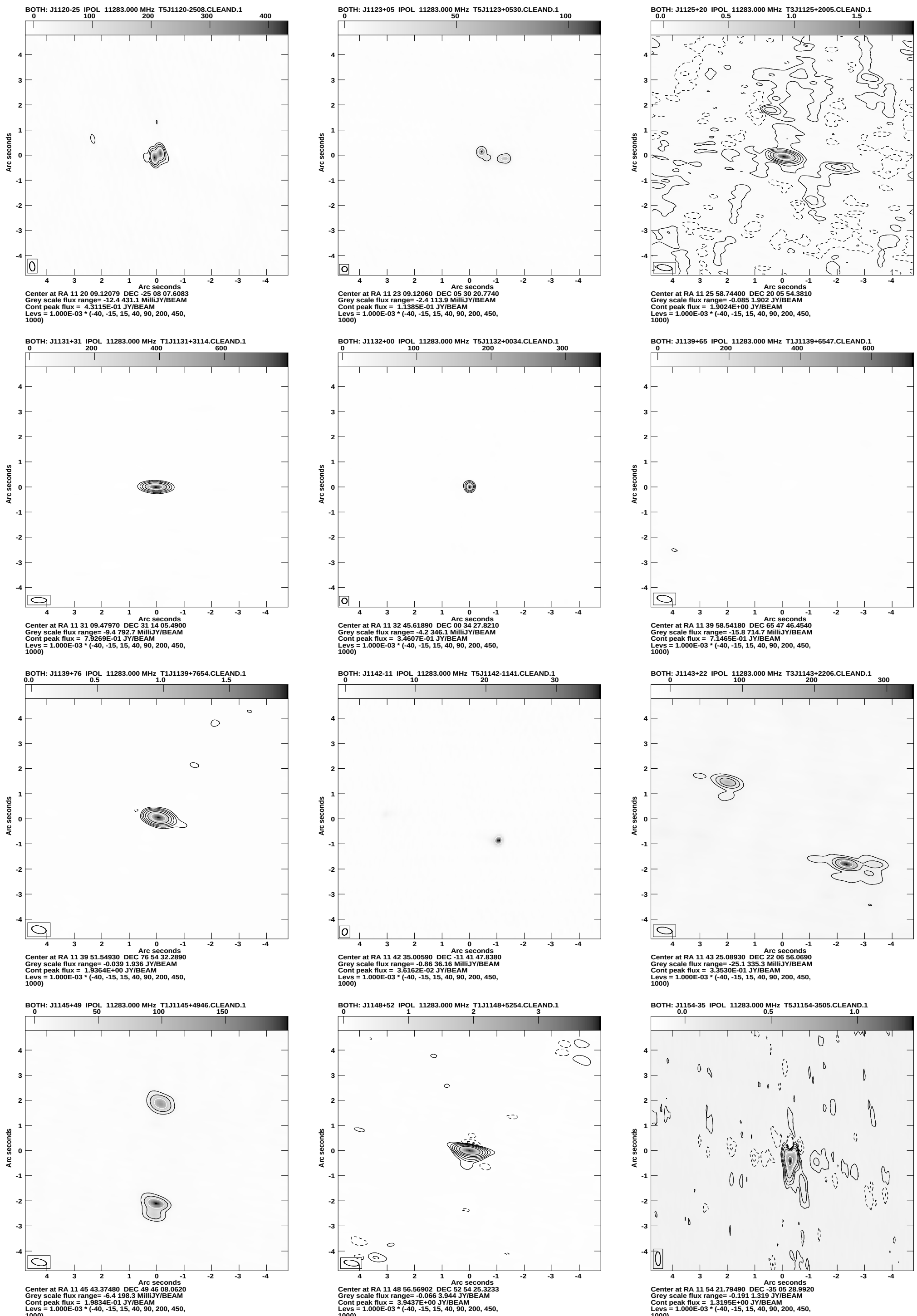

Figure 3. Images for “VLA targets”, sorted in RA. (continued)

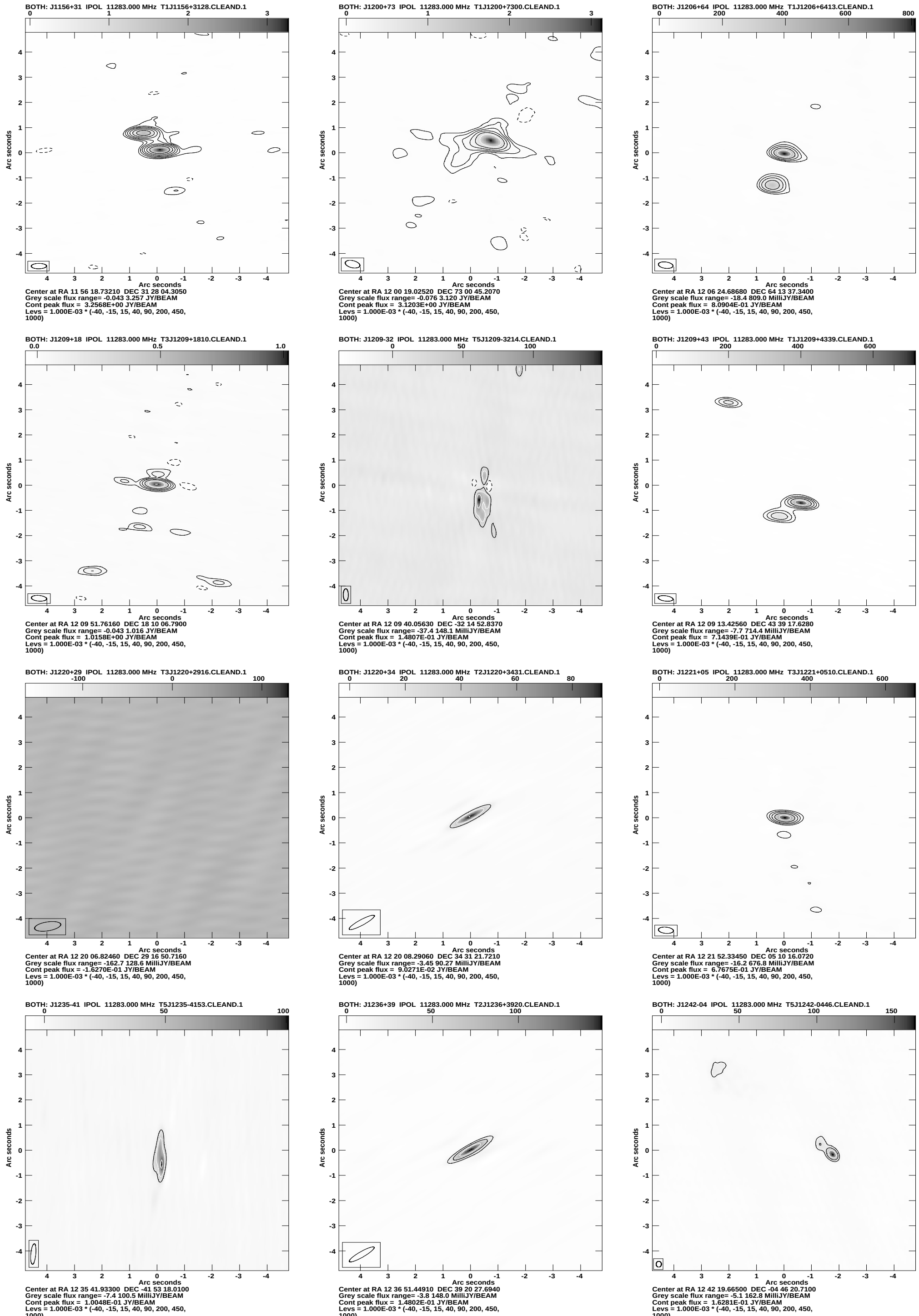

Figure 3. Images for “VLA targets”, sorted in RA. (continued)

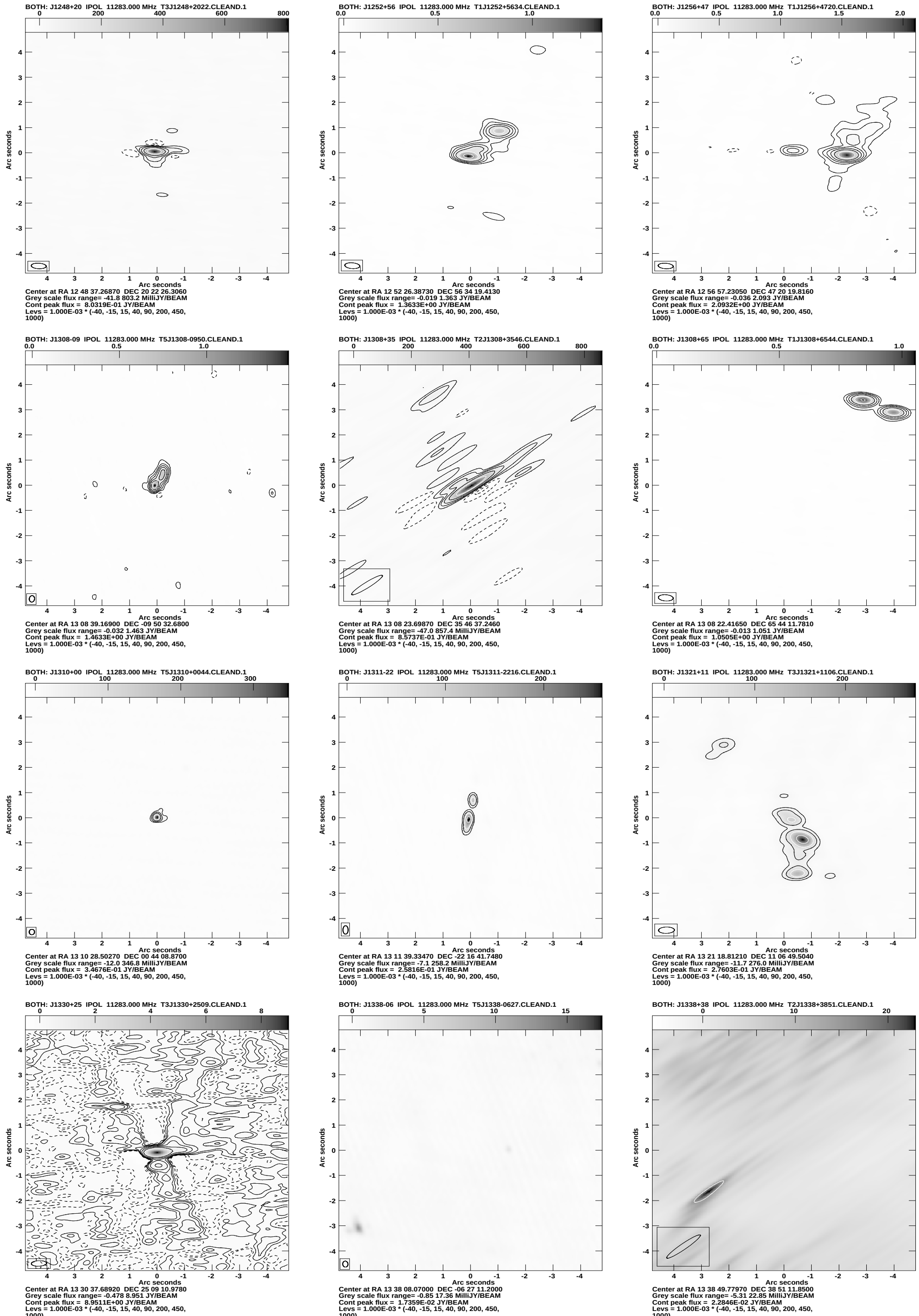

Figure 3. Images for "VLA targets", sorted in RA. (continued)

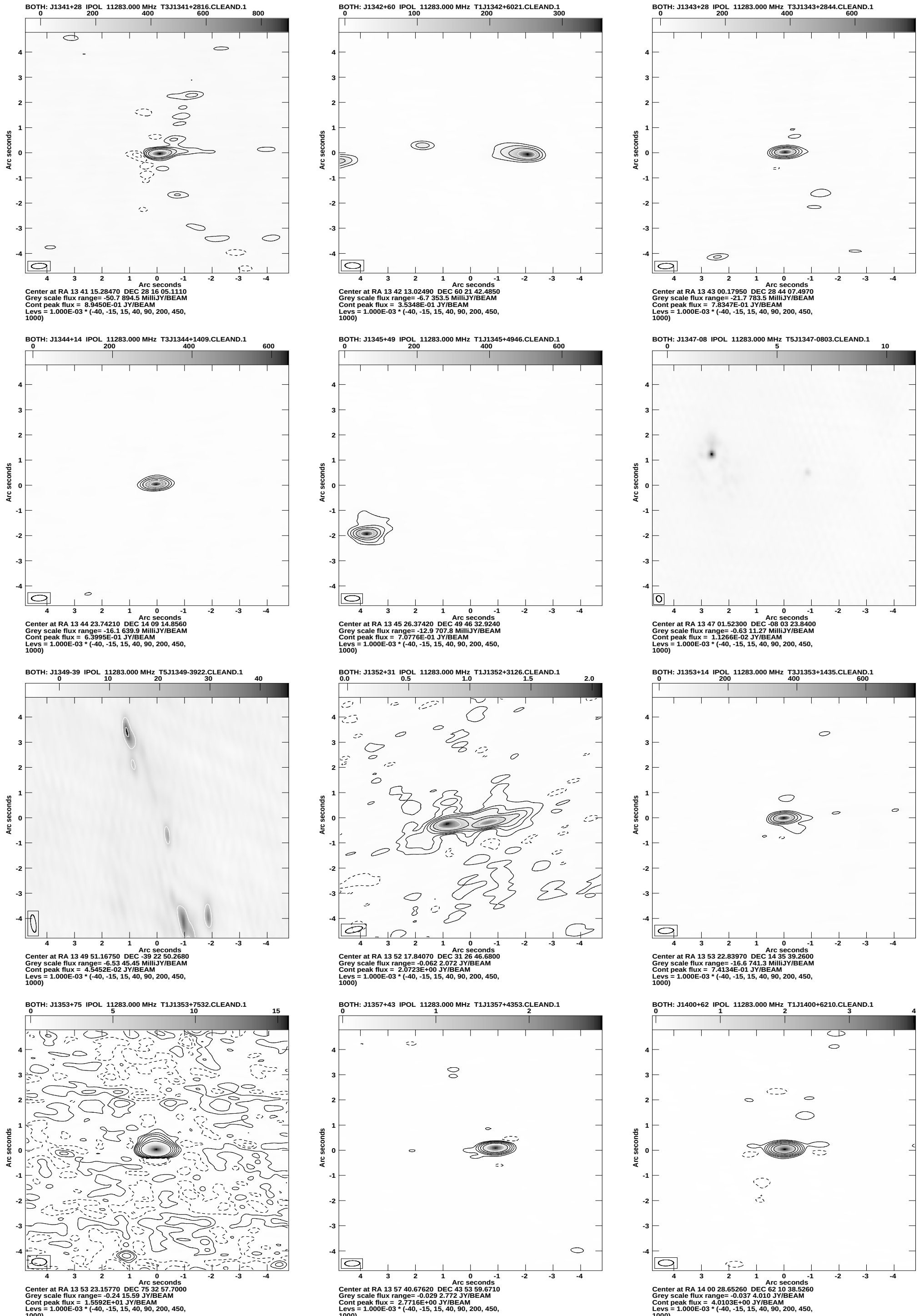

Figure 3. Images for "VLA targets", sorted in RA. (continued)

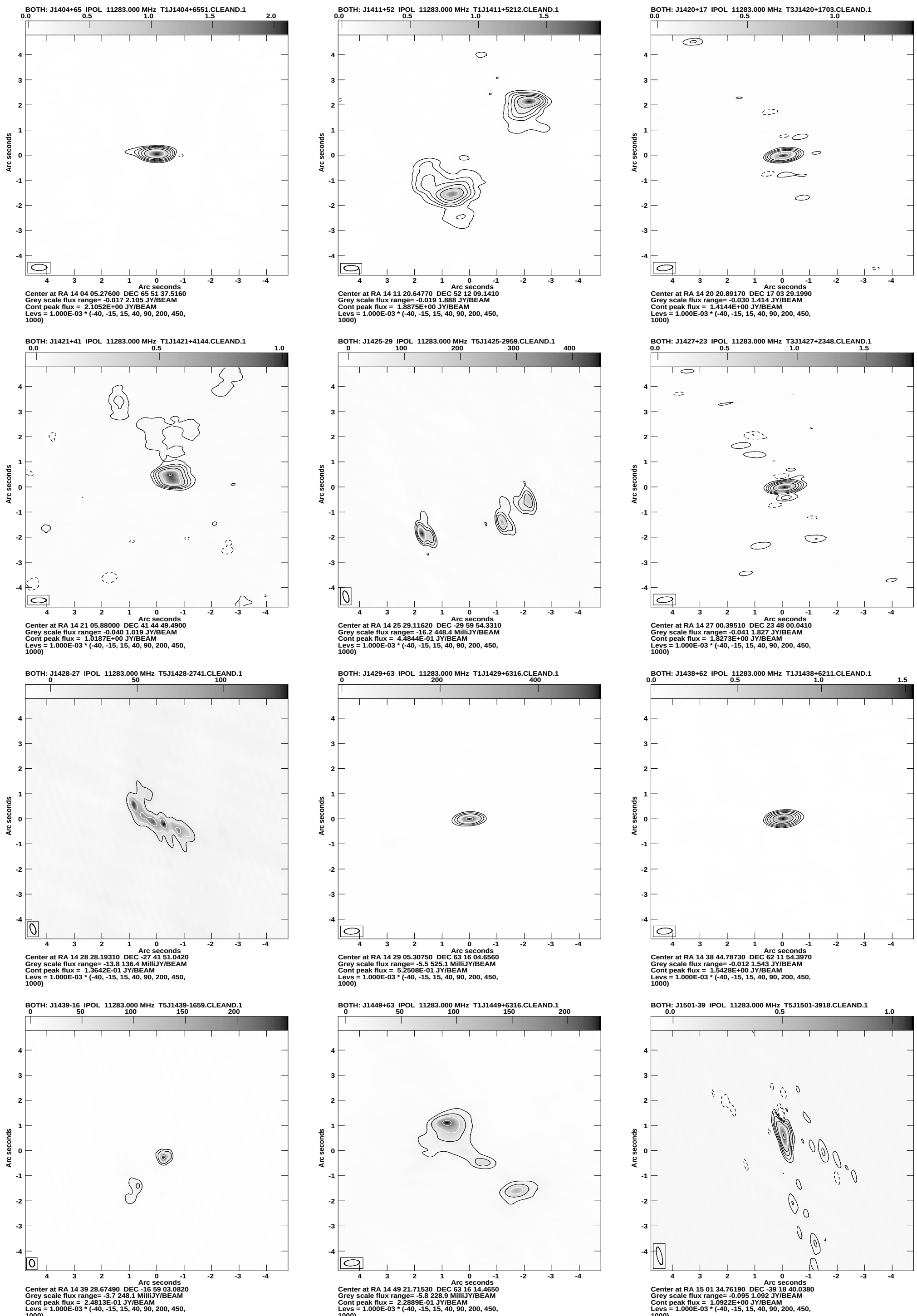

Figure 3. Images for “VLA targets”, sorted in RA. (continued)

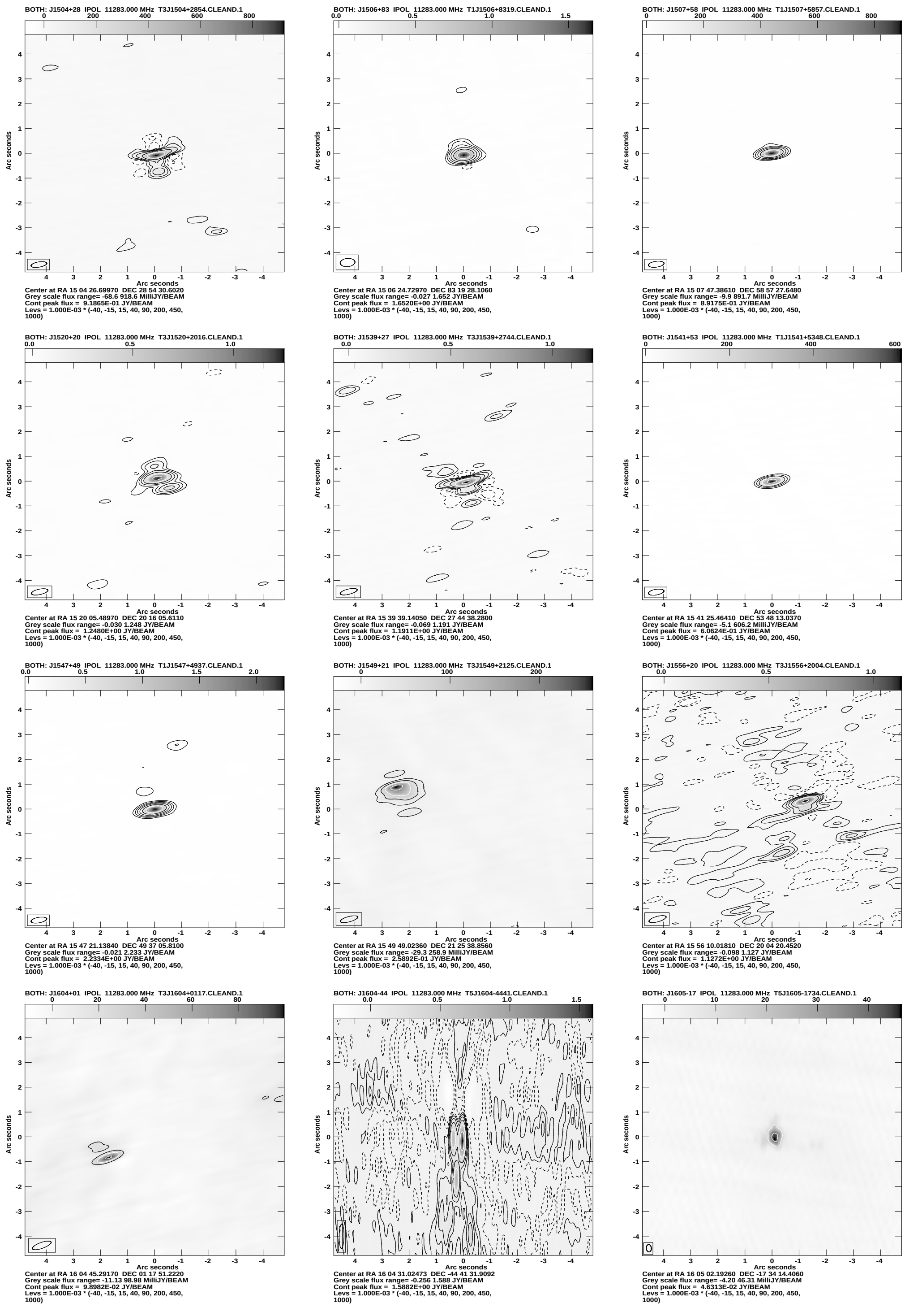

Figure 3. Images for "VLA targets", sorted in RA. (continued)

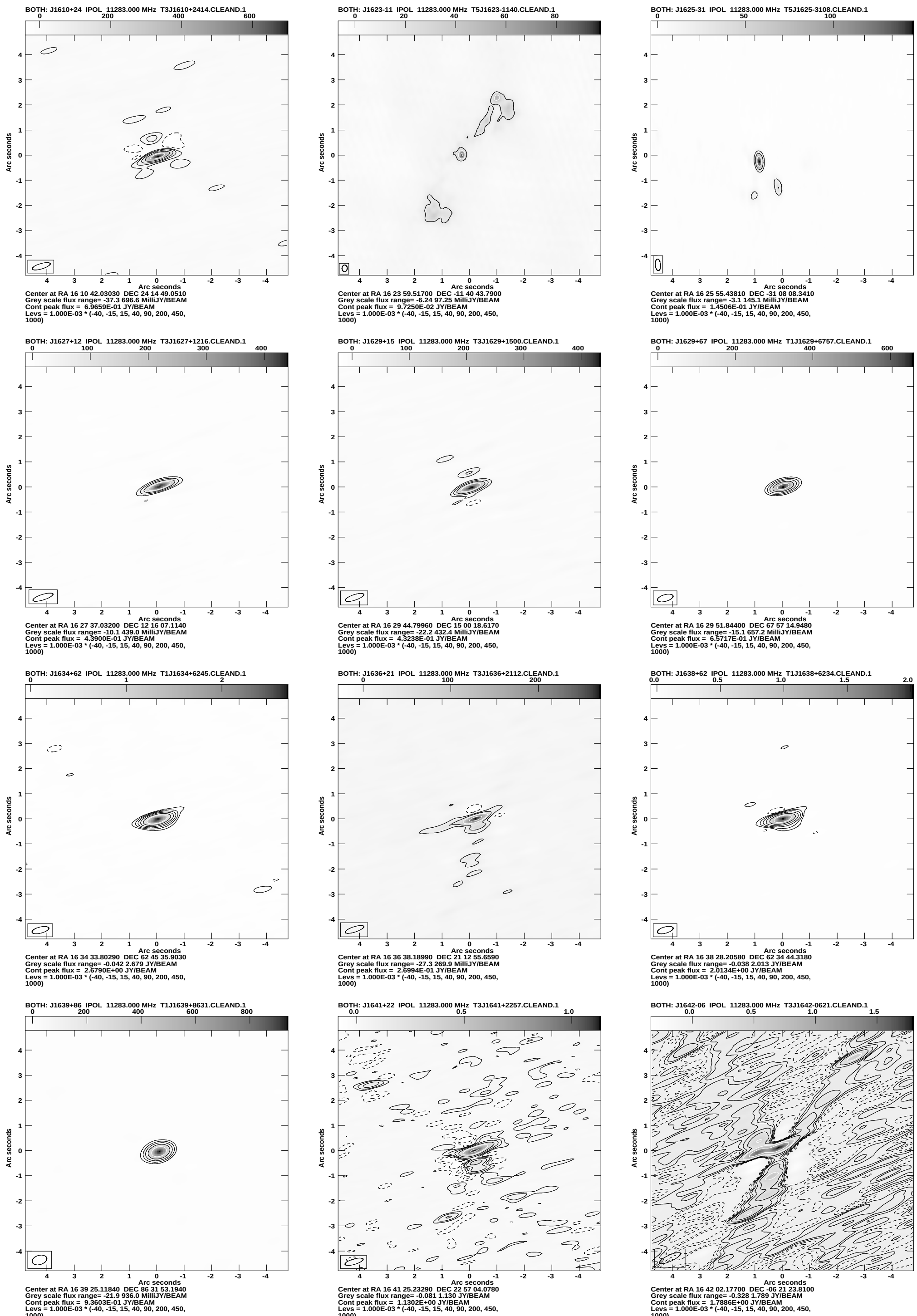

Figure 3. Images for “VLA targets”, sorted in RA. (continued)

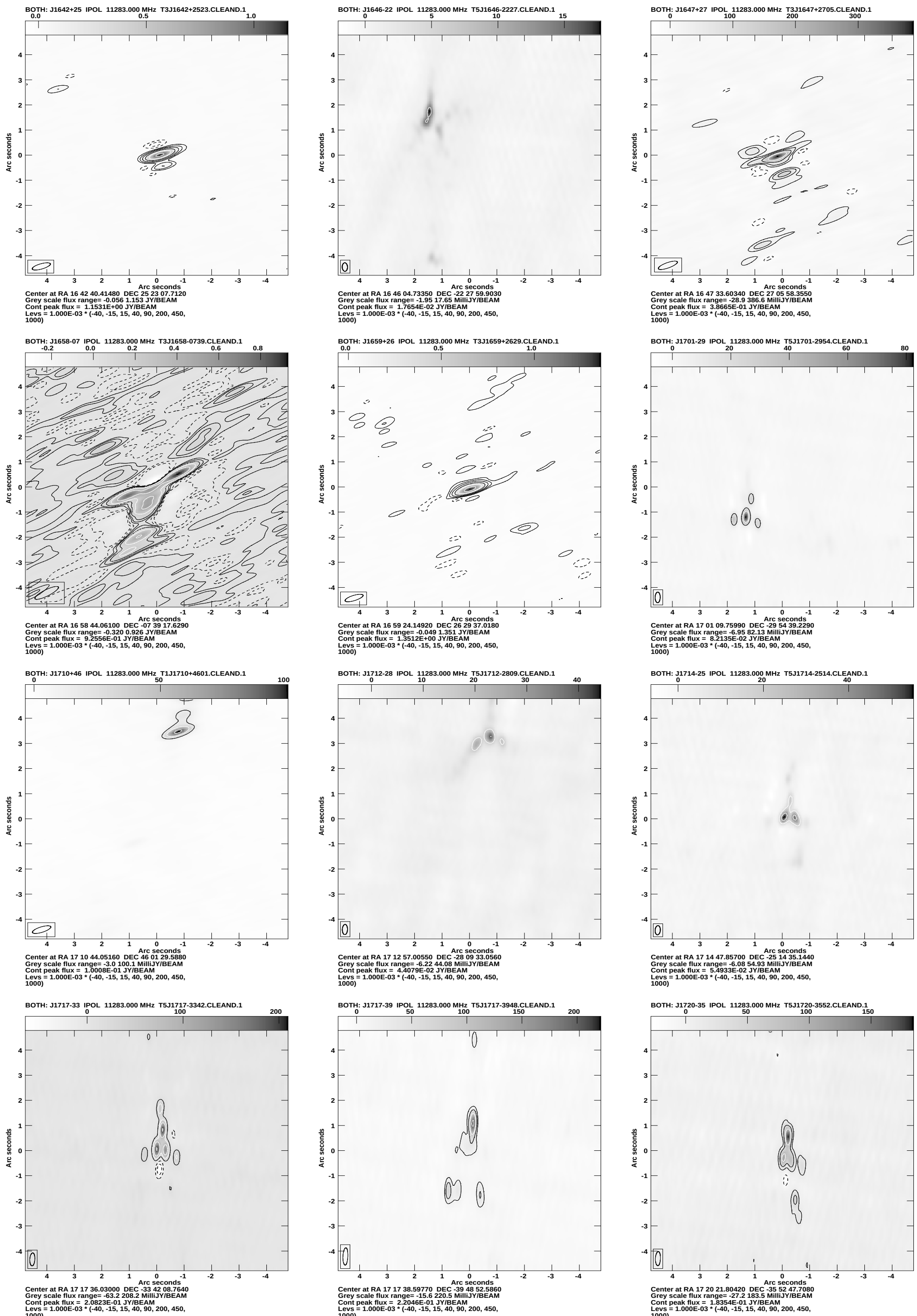

Figure 3. Images for "VLA targets", sorted in RA. (continued)

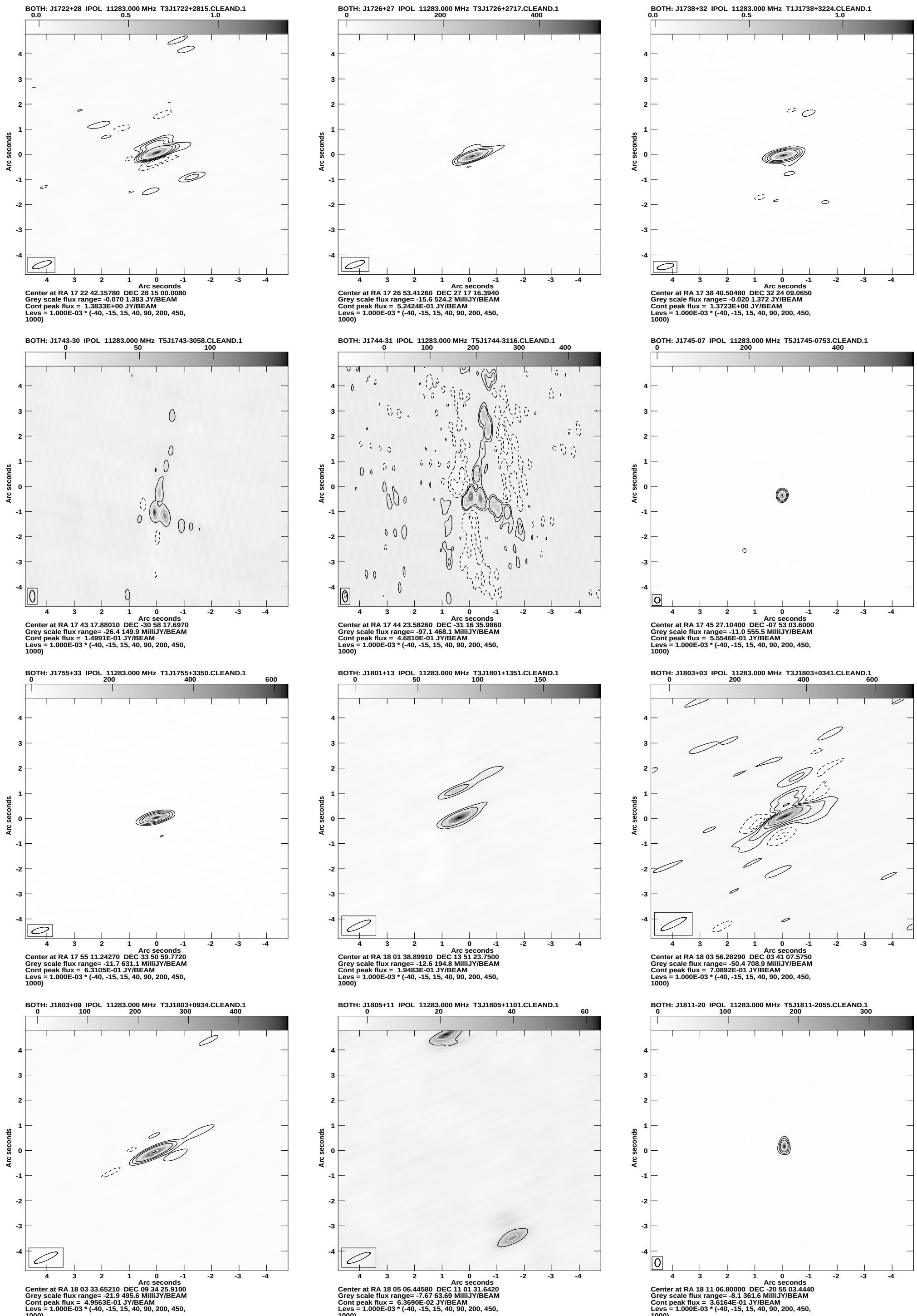

Figure 3. Images for "VLA targets", sorted in RA. (continued)

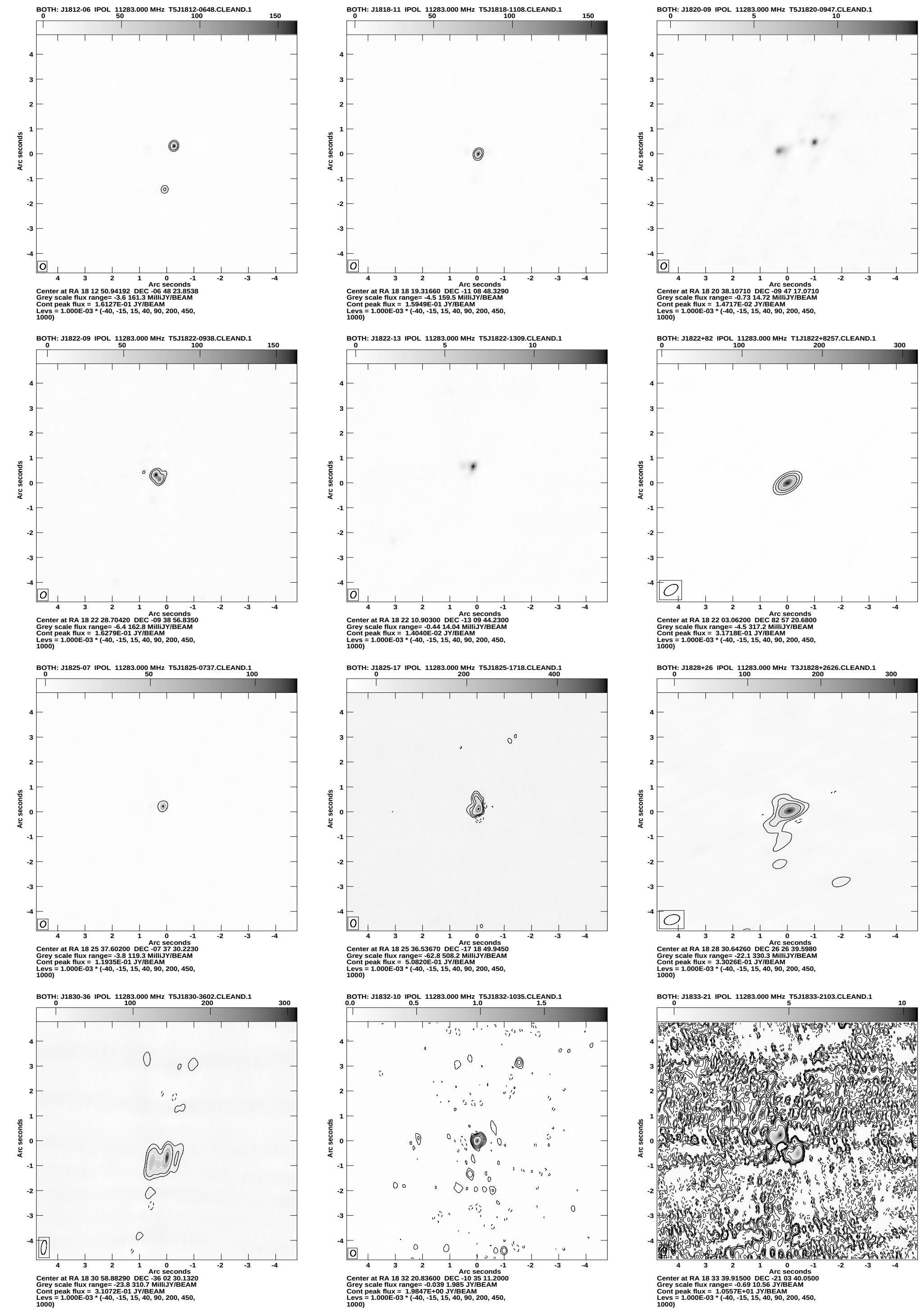

Figure 3. Images for "VLA targets", sorted in RA. (continued)

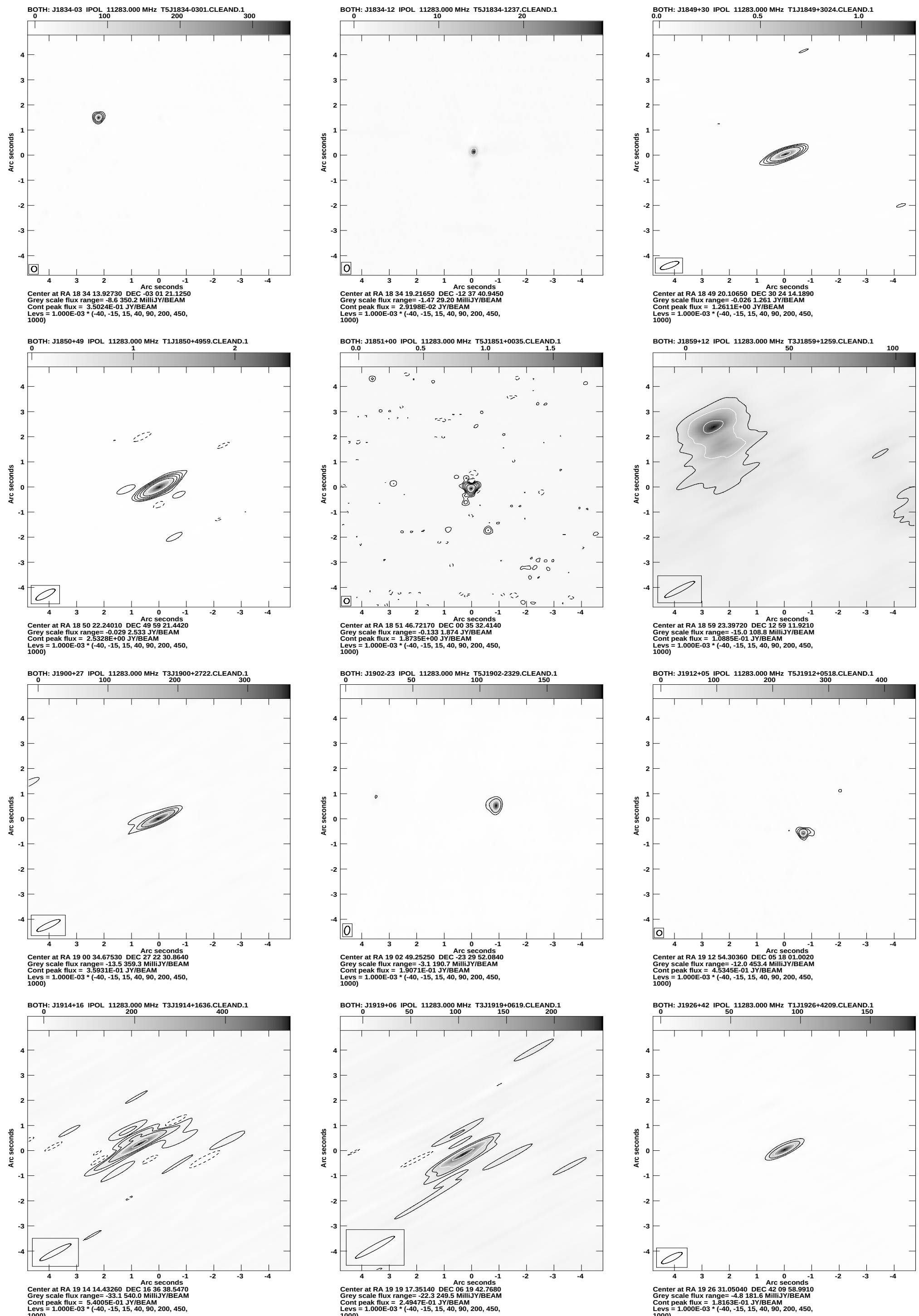

Figure 3. Images for "VLA targets", sorted in RA. (continued)

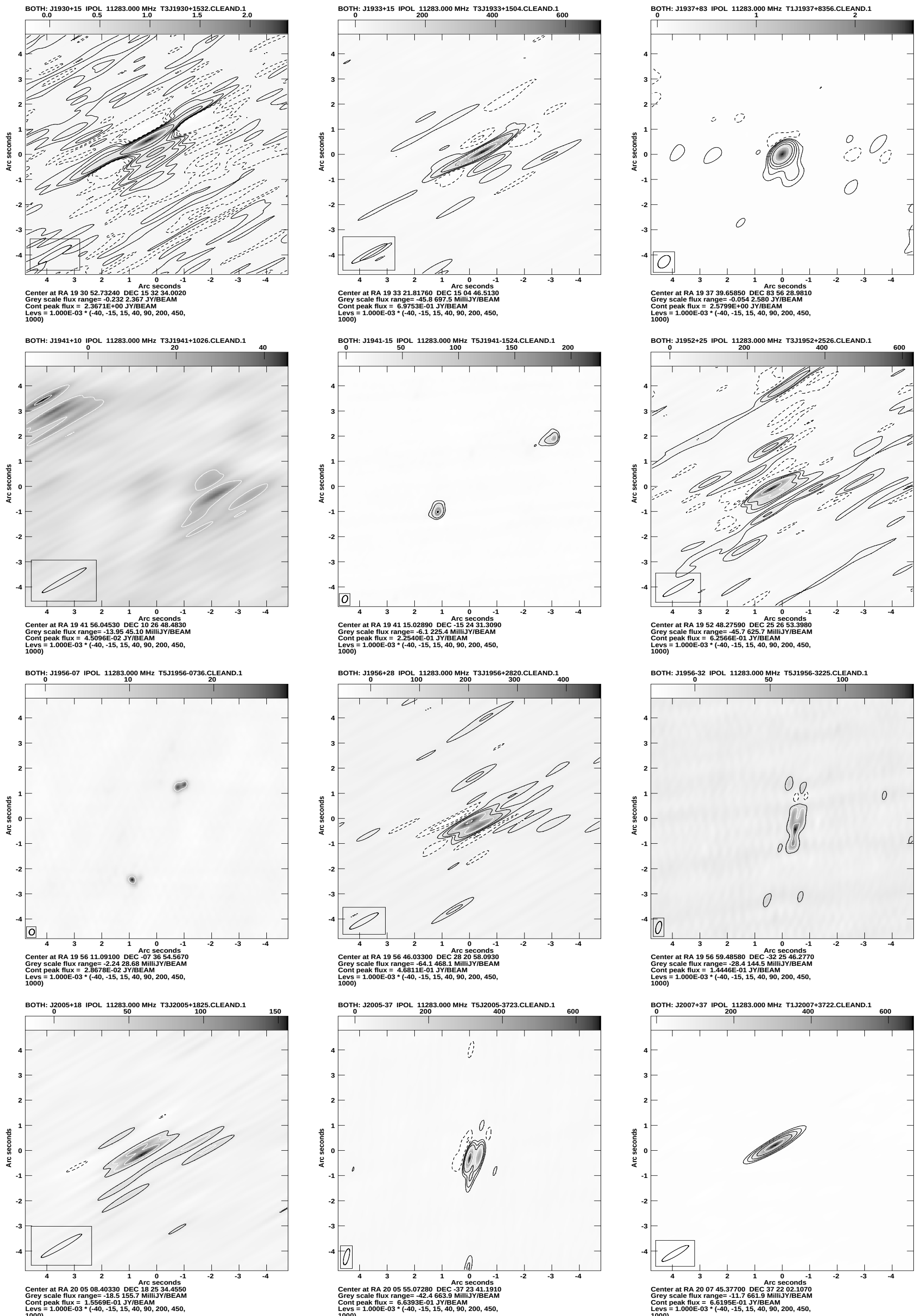

Figure 3. Images for “VLA targets”, sorted in RA. (continued)

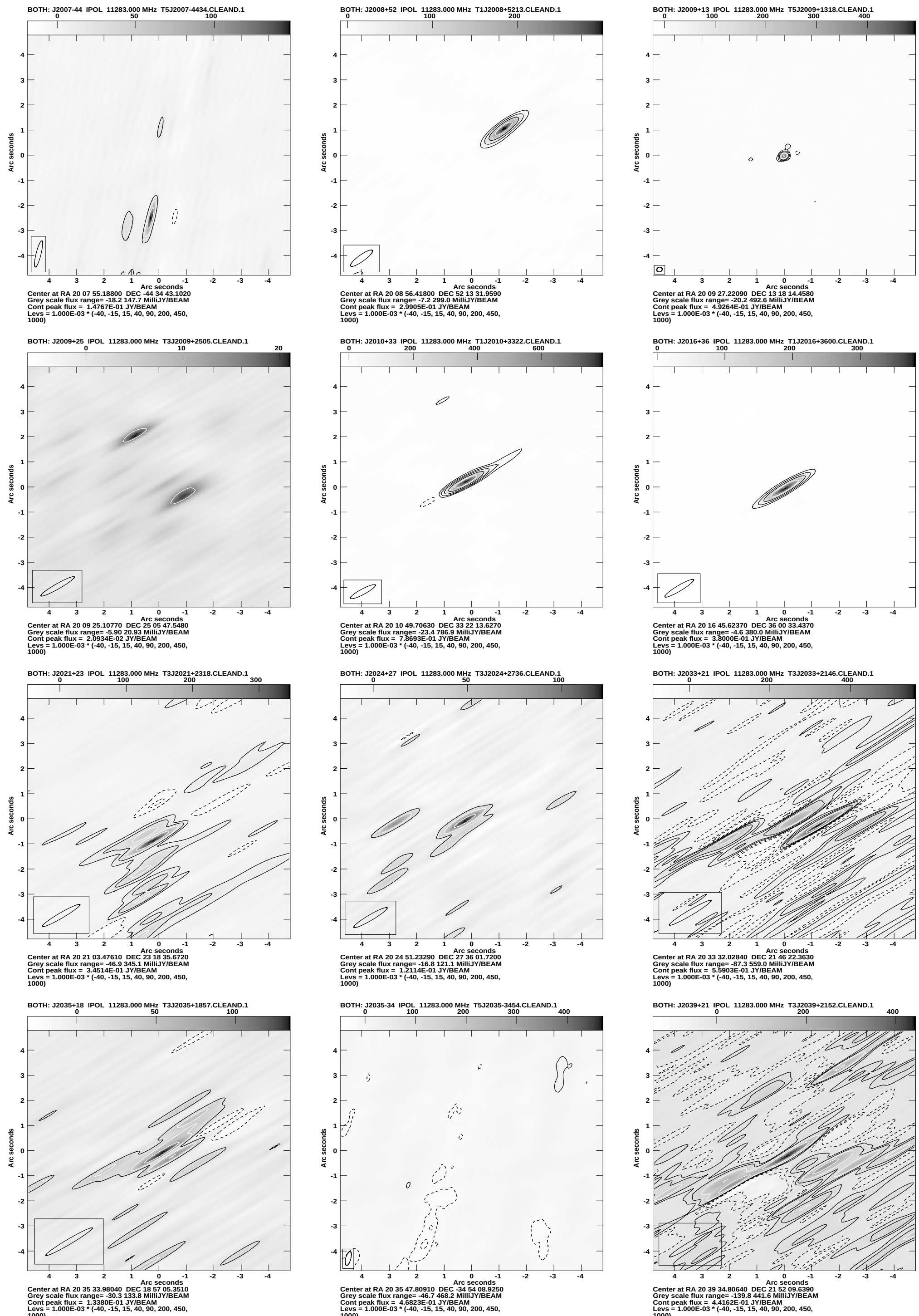

Figure 3. Images for "VLA targets", sorted in RA. (continued)

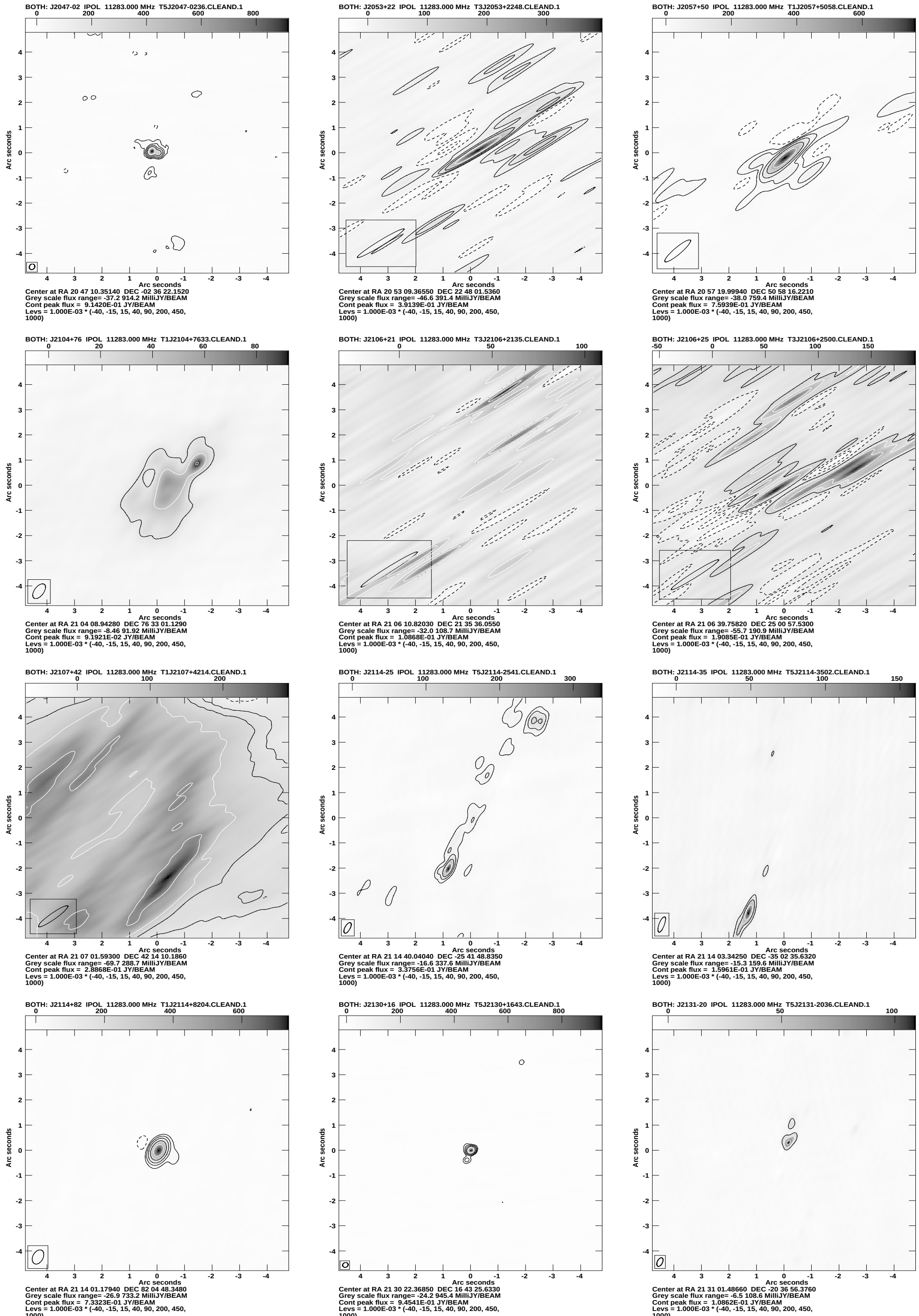

Figure 3. Images for “VLA targets”, sorted in RA. (continued)

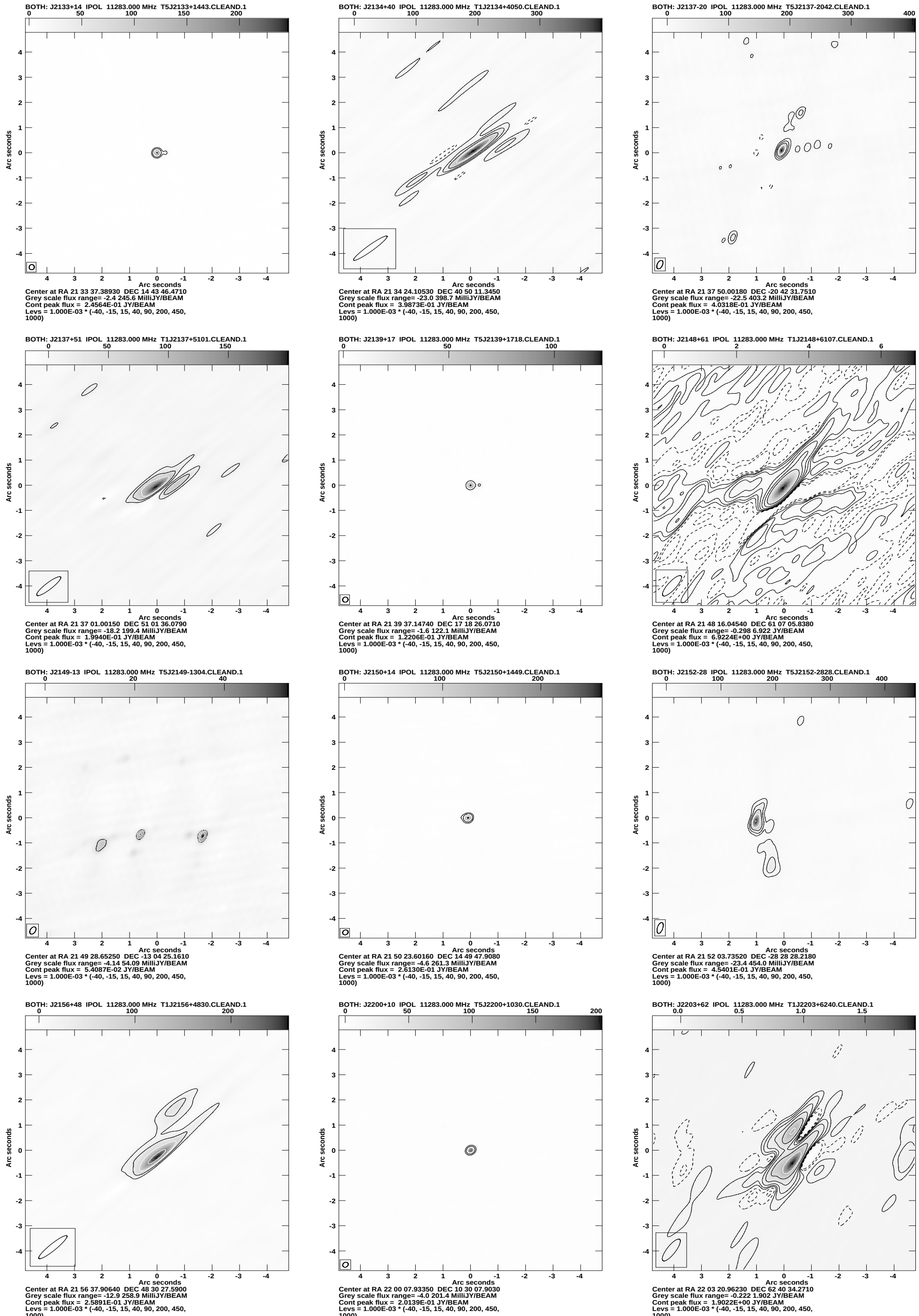

Figure 3. Images for "VLA targets", sorted in RA. (continued)

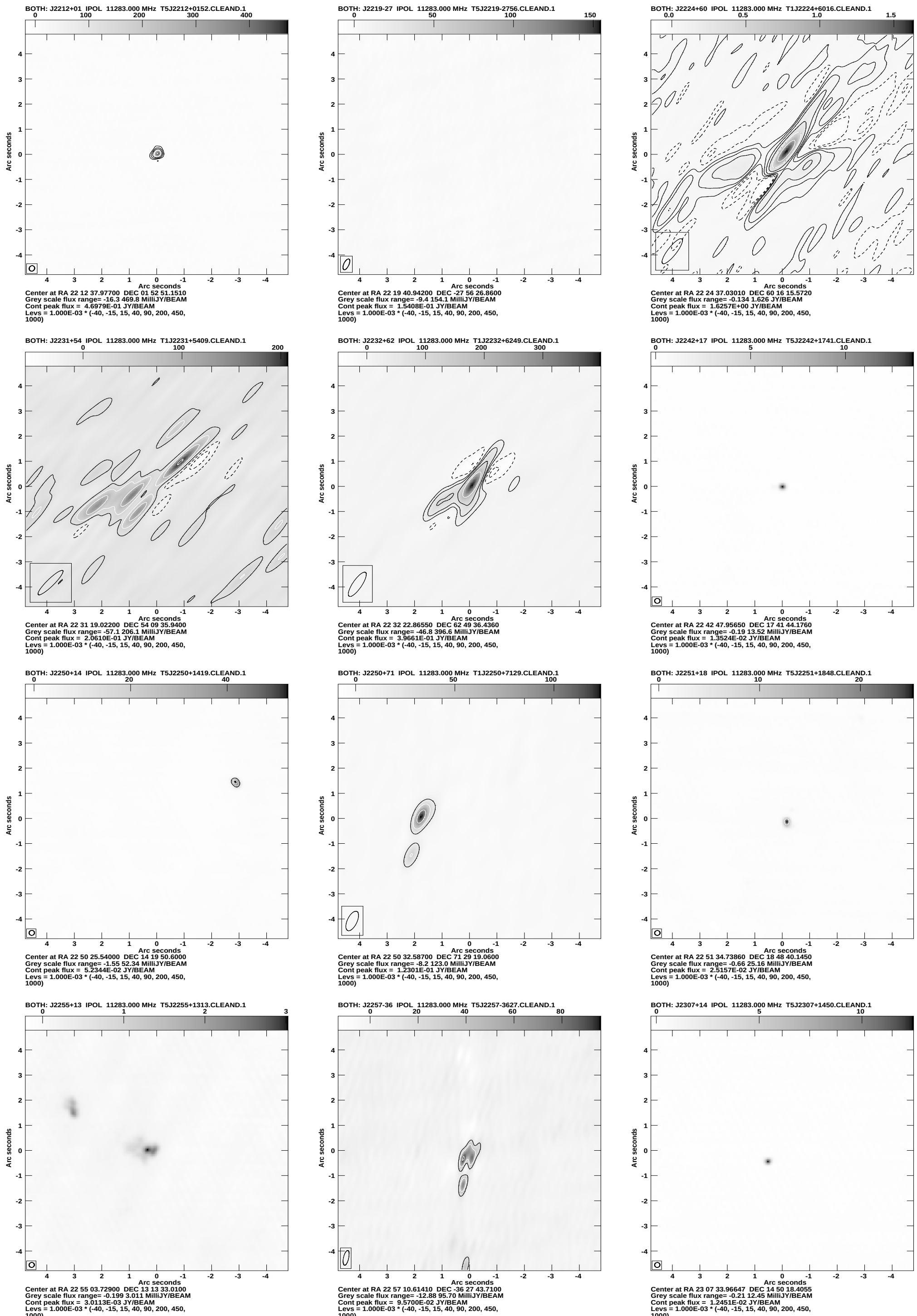

Figure 3. Images for "VLA targets", sorted in RA. (continued)

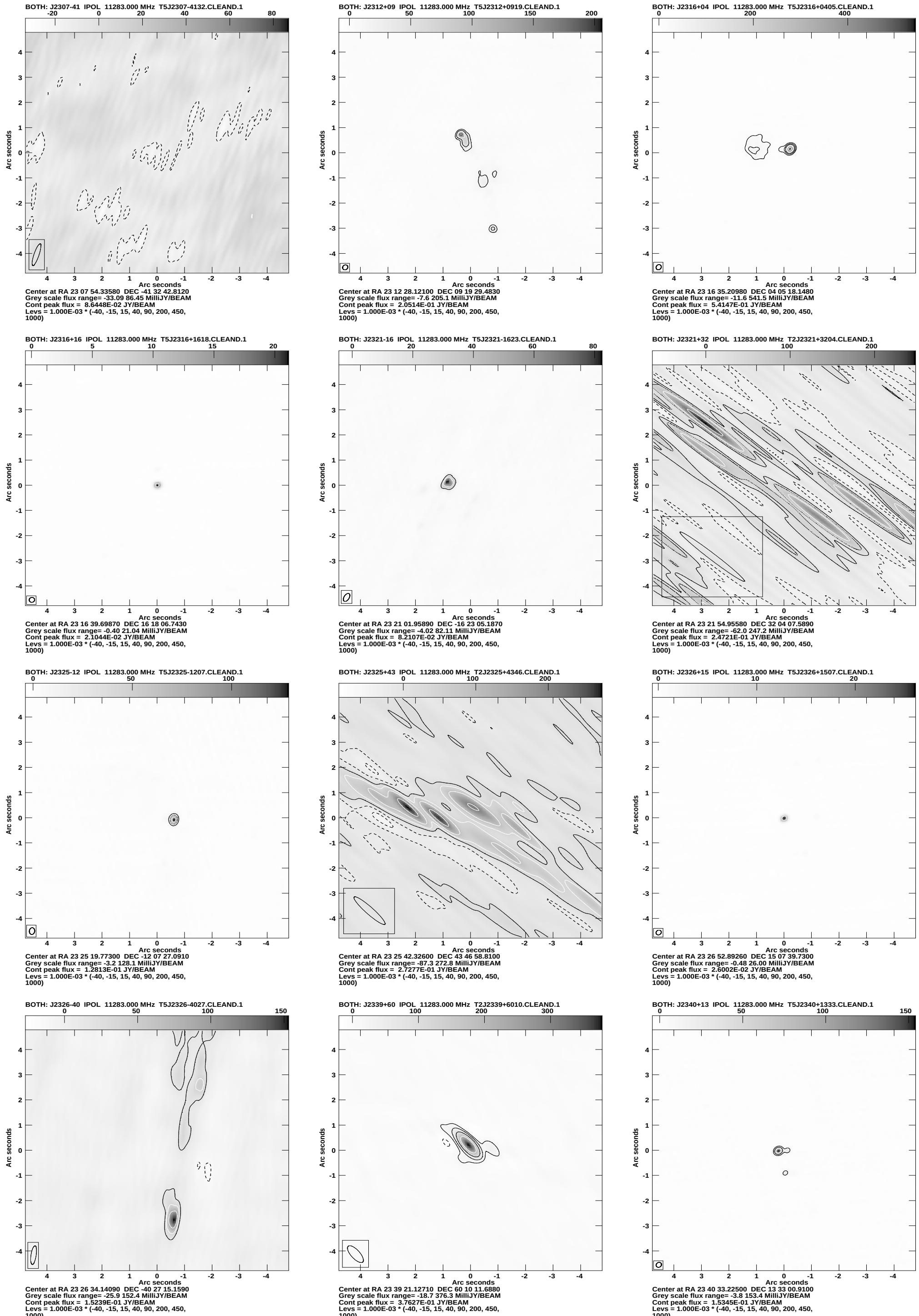

Figure 3. Images for "VLA targets", sorted in RA. (continued)

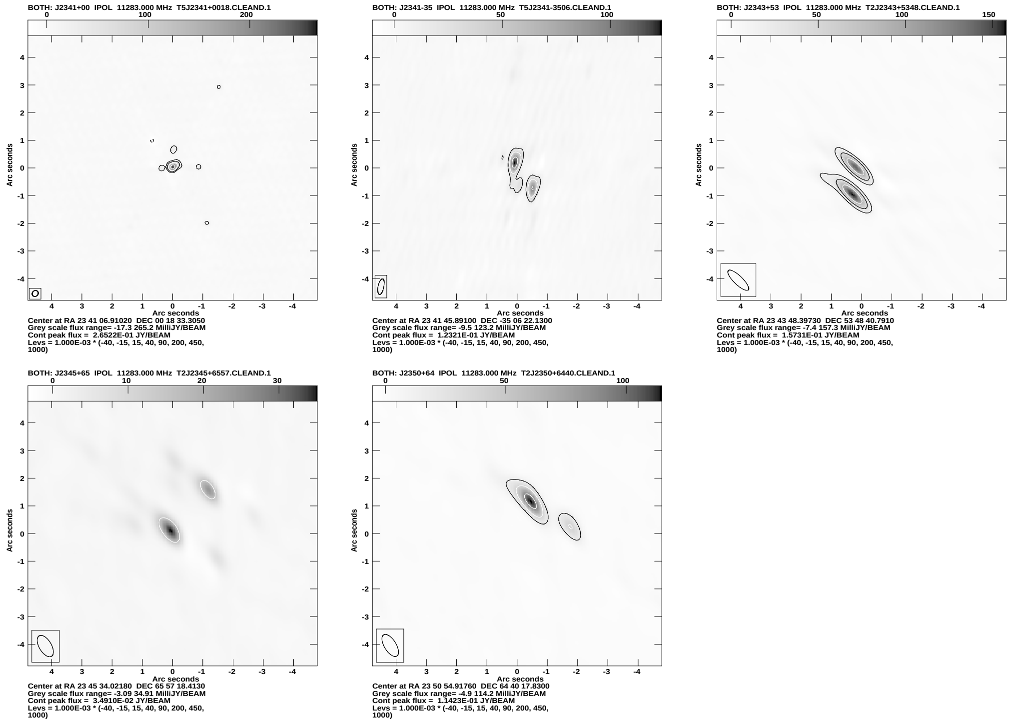

Figure 3. Images for "VLA targets", sorted in RA. (continued)

Table 6. Positions and X-band Flux Densities of Alternative VLA Reference Sources

IAU Name J2000	Measured RA (h m s)	Measured Dec. (° ′ ″)	Error RA (s)	Error Dec. (″)	Flux Dens. Jy beam^{-1}	Origin	ΔRA (mas)	ΔDec. (mas)	Shift (mas)
J0001−0746	00 01 18.02533	−07 46 26.9206	0.0000081	0.000157	0.40	AT20G	218.1	−120.6	249.2
J0001−1551	00 01 05.32829	−15 51 07.0754	0.0000134	0.000287	0.46	AT20G	1323.3	124.6	1329.2
J0003−1927	00 03 18.67472	−19 27 22.3595	0.0000202	0.000465	0.19	Winn	23.8	−17.4	29.5
J0004−1148	00 04 04.91577	−11 48 58.3791	0.0000116	0.000234	1.57	ALMA	−11.4	10.9	15.8
J0005−1648	00 05 17.93411	−16 48 04.6729	0.0000149	0.000330	0.30	Winn	−41.7	−23.0	47.6
J0006−2955	00 06 01.12637	−29 55 50.0901	0.0000193	0.000564	0.42	AT20G	177.2	−490.1	521.2
J0008−2339	Extended Source, Multiple Components					AT20G			
J0008−2559	Extended Source, Multiple Components					AT20G			
J0008−3945	Multiple Compact Components					AT20G			
J0010−0433	00 10 00.38840	−04 33 48.5084	0.0000072	0.000130	1.06	ALMA	8.9	1.6	9.1
J0010−2157	Extended Source					AT20G			
J0011−1434	00 11 40.45592	−14 34 04.6307	0.0000122	0.000253	0.35	AT20G	−231.1	−430.8	488.8
J0013−0423	00 13 54.13101	−04 23 52.2967	0.0000084	0.000152	1.16	ALMA	−0.1	−6.7	6.7
J0014−0205	00 14 25.54015	−02 05 55.7899	0.0000227	0.000366	0.11	TGSS	−676.8	1220.1	1395.2
J0015−1812	Extended Source					AT20G			
J0016−2343	Multiple Compact Components					Winn			
J0017−0512	00 17 35.81731	−05 12 41.7836	0.0000124	0.000228	0.32	ALMA	−4.6	−13.6	14.4
J0017−2748	Extended Source, Multiple Components					AT20G			
J0024−0412	00 24 45.98312	−04 12 01.5488	0.0000087	0.000158	0.56	Winn	−22.7	−26.8	35.2
J0024−0811	00 24 00.67257	−08 11 10.0498	0.0000127	0.000240	0.40	AT20G	258.8	−249.8	359.7
J0025−2227	00 25 24.24721	−22 27 47.5629	0.0000351	0.000803	0.32	AT20G	−99.9	37.0	106.6
J0026−3512	Extended Source, Multiple Components					ALMA			
J0029−0113	00 29 00.98693	−01 13 41.7543	0.0000075	0.000131	0.69	AT20G	345.9	−54.3	350.2
J0030−0211	00 30 31.82394	−02 11 56.1340	0.0000068	0.000120	1.83	AT20G	240.7	66.0	249.6
J0031−1426	Multiple Compact Components					Winn			
J0032+0136	00 32 08.00543	+01 36 55.5971	0.0000329	0.000493	0.09	TGSS	−666.2	−92.9	672.6
J0032−2849	Extended Source, Multiple Components					AT20G			
J0034−2303	00 34 54.79624	−23 03 35.2621	0.0000181	0.000443	0.12	AT20G	466.0	−862.1	980.0
J0037−2145	00 37 14.82597	−21 45 24.7146	0.0000160	0.000397	0.19	AT20G	474.1	−814.6	942.5
J0038−2459	Multiple Compact Components					ALMA			
J0039−1111	Extended Source					AT20G			
J0040−3225	Not Detected					AT20G			
J0046−2631	00 46 13.77552	−26 31 54.4613	0.0000231	0.000616	0.13	AT20G	−476.7	−161.2	503.2
J0049−1006	00 49 54.10537	−10 06 14.6826	0.0000185	0.000330	0.39	TGSS	112.7	−172.5	206.1
J0050−0452	00 50 21.53506	−04 52 20.5987	0.0000112	0.000195	1.36	ALMA	−0.9	−8.7	8.7
J0053−0727	00 53 36.51507	−07 27 29.6276	0.0000318	0.000564	0.24	Winn	25.7	−23.6	34.9
J0058−0539	00 58 05.06690	−05 39 52.2792	0.0000104	0.000179	1.30	ALMA	−13.4	0.8	13.4
J0058−3347	00 58 15.64079	−33 47 57.4496	0.0000641	0.002117	0.12	AT20G	738.0	−349.5	816.6
J0101−2831	01 01 52.38896	−28 31 20.4174	0.0000227	0.000638	0.19	Winn	1.9	28.6	28.7
J0102−2646	01 02 56.35304	−26 46 36.5247	0.0000285	0.000727	0.10	AT20G	1164.5	−524.7	1277.3
J0104−2416	01 04 58.20492	−24 16 28.4709	0.0000117	0.000294	0.23	AT20G	616.4	429.1	751.0
J0106−2718	Extended Source, Multiple Components					ALMA			
J0109−3854	01 09 17.79747	−38 54 55.9907	0.0000380	0.001616	0.13	AT20G	29.6	1209.3	1209.7
J0113−0630	01 13 16.24592	−06 30 52.5317	0.0000131	0.000247	0.38	AT20G	−88.2	−831.7	836.3
J0115−2804	Extended Source					ALMA			
J0117−0425	01 17 27.85842	−04 25 10.4603	0.0000136	0.000243	0.69	AT20G	173.1	−860.3	877.5

[a] : Calibrated with source a in Table 8, [b] with source b, etc.

Table 6. Positions and X-band Flux Densities of Alternative VLA Reference Sources (Continued..)

IAU Name J2000	Measured RA (h m s)	Measured Dec. (° ′ ″)	Error RA (s)	Error Dec. (″)	Flux Dens. Jy beam^{-1}	Origin	ΔRA (mas)	ΔDec. (mas)	Shift (mas)
J0117−1507	01 17 38.93192	−15 07 55.0075	0.0000233	0.000507	0.08	Winn	−46.7	15.5	49.2
J0117−2111	01 17 48.78007	−21 11 06.6288	0.0000064	0.000154	0.33	ALMA	−0.9	1.2	1.5
J0120+2256	01 20 33.36976	+22 56 36.7399	0.0000293	0.000344	0.11	TGSS	−397.2	−10.1	397.4
J0122−0018		Extended Source				AT20G			
J0122−0056	01 22 17.47016	−00 56 15.6942	0.0000193	0.000317	0.48	AT20G	147.5	−594.2	612.2
J0123−0348	01 23 35.77491	−03 48 39.2898	0.0000171	0.000294	0.42	AT20G	225.8	−689.8	725.8
J0131−1211	01 31 12.54764	−12 11 00.6921	0.0000215	0.000422	0.18	Winn	−3.4	−4.1	5.4
J0134+0003	01 34 12.70387	+00 03 45.1373	0.0000112	0.000188	0.48	Winn	33.4	12.4	35.6
J0138−0540	01 38 51.84961	−05 40 08.2540	0.0000318	0.000279	0.40	AT20G	304.4	−554.0	632.1
J0138−2254	01 38 57.46212	−22 54 47.3862	0.0000406	0.000462	0.67	AT20G	523.3	−686.2	863.0
J0138−2711		Extended Source				AT20G			
J0142−0544	01 42 38.87509	−05 44 01.5581	0.0000273	0.000236	0.25	Winn	50.9	−40.1	64.8
J0142−1714	01 42 23.40494	−17 14 35.4085	0.0000389	0.000410	0.15	Winn	13.8	37.5	40.0
J0143−3200	01 43 10.13204	−32 00 56.6566	0.0000621	0.000829	0.51	ALMA	−0.6	−6.6	6.7
J0144−3938	01 44 54.10702	−39 38 10.3355	0.0001746	0.003123	0.25	AT20G	−81.1	464.5	471.5
J0147−0445	01 47 21.12304	−04 45 42.1341	0.0000307	0.000255	0.14	AT20G	−792.8	−134.1	804.1
J0147−2144	01 47 07.35087	−21 44 42.5270	0.0000412	0.000477	0.36	Winn	0.4	−2.0	2.0
J0149+3628	01 49 46.07265	+36 28 32.6263	0.0001109	0.001045	0.08	TGSS	−550.6	216.3	591.5
J0151−1719	01 51 48.05186	−17 19 55.0538	0.0000385	0.000393	0.09	AT20G	−169.9	−953.8	968.8
J0151−1732	01 51 06.08605	−17 32 44.7200	0.0000281	0.000297	0.35	AT20G	199.6	−220.1	297.1
J0151−3435	01 51 23.49390	−34 35 13.7972	0.0000755	0.001130	0.24	AT20G	445.8	−897.2	1001.9
J0152−1412	01 52 32.01532	−14 12 39.3805	0.0000352	0.000349	0.33	AT20G	−513.6	−180.5	544.4
J0153−1906	01 53 01.51201	−19 06 56.7000	0.0000328	0.000351	0.10	AT20G	255.0	−0.0	255.0
J0154−2329	01 54 46.10326	−23 29 53.9573	0.0000616	0.000700	0.08	AT20G	−732.7	42.7	733.9
J0202−1948	02 02 13.84888	−19 48 19.4878	0.0000246	0.000261	0.16	AT20G	1286.0	512.2	1384.2
J0205−3444	02 05 55.50850	−34 44 09.1544	0.0000788	0.001143	0.08	AT20G	−474.5	−154.4	499.0
J0206−1150	02 06 26.08334	−11 50 39.7458	0.0000280	0.000268	0.57	AT20G	97.8	54.2	111.8
J0206−2212	02 06 20.07397	−22 12 19.6628	0.0000412	0.000457	0.15	Winn	−55.1	−47.9	73.0
J0208−2650		Extended Source				AT20G			
J0210−1444	02 10 23.17980	−14 44 59.0301	0.0000369	0.000352	0.11	Winn	−36.2	−34.1	49.7
J0213−2943		Extended Source				AT20G			
J0216−3009		Extended Source				TGSS			
J0217−0121	02 17 54.99860	−01 21 50.7220	0.0000348	0.000309	0.13	Winn	−14.9	2.0	15.1
J0217−0820	02 17 02.66406	−08 20 52.3490	0.0000213	0.000196	0.59	ALMA	−30.5	1.0	30.6
J0217−1631	02 17 57.24884	−16 31 10.4814	0.0000333	0.000339	0.24	Winn	8.1	−33.4	34.4
J0219−1842	02 19 21.16226	−18 42 38.7432	0.0000224	0.000240	0.24	AT20G	678.2	−43.2	679.6
J0220−2151	02 20 35.14873	−21 51 12.1122	0.0000563	0.000653	0.10	AT20G	992.2	87.8	996.1
J0222−1615	02 22 00.72368	−16 15 16.5529	0.0000283	0.000280	0.22	AT20G	811.1	47.1	812.5
J0223−1656	02 23 43.76244	−16 56 37.6990	0.0000260	0.000268	0.17	AT20G	251.9	301.0	392.5
J0226−1843	02 26 47.62944	−18 43 39.2358	0.0000404	0.000444	0.24	AT20G	718.2	−435.8	840.1
J0227−0621	02 27 44.46213	−06 21 06.7405	0.0000460	0.000430	0.34	Winn	5.6	0.5	5.6
J0229−3643		Extended Source, Multiple Components				AT20G			
J0236−2953		Extended Source, Multiple Components				AT20G			
J0237+0919	02 37 40.52935	+09 19 01.6422	0.0000076	0.000124	0.71	TGSS	−301.2	372.2	478.8
J0237−2623	02 37 16.75927	−26 23 53.1945	0.0000905	0.001134	0.11	AT20G	−259.0	−394.5	471.9
J0239−1348	02 39 26.02095	−13 48 43.3876	0.0000412	0.000408	0.15	Winn	29.9	−42.6	52.0

[a] : Calibrated with source a in Table 8, [b] with source b, etc.

Table 6. Positions and X-band Flux Densities of Alternative VLA Reference Sources (Continued..)

IAU Name J2000	Measured RA (h m s)	Measured Dec. (° ′ ″)	Error RA (s)	Error Dec. (″)	Flux Dens. Jy beam^{-1}	Origin	ΔRA (mas)	ΔDec. (mas)	Shift (mas)
J0240−0504	02 40 56.17224	−05 04 42.2001	0.0000273	0.000236	0.18	AT20G	116.0	299.9	321.6
J0243−0550	02 43 12.46886	−05 50 55.2966	0.0000207	0.000183	0.46	ALMA	2.0	3.4	4.0
J0243−3204		Extended Source				AT20G			
J0245−1107	02 45 24.95256	−11 07 16.8099	0.0000210	0.000204	0.19	AT20G	109.6	290.1	310.1
J0246−1236	02 46 58.46986	−12 36 30.8063	0.0000253	0.000251	0.32	ALMA	2.1	−6.2	6.6
J0250−2627	02 50 35.56588	−26 27 42.5451	0.0000554	0.000683	0.27	AT20G	−347.5	−345.1	489.7
J0252−2219	02 52 47.95394	−22 19 25.4612	0.0000353	0.000400	0.37	AT20G	84.1	−561.2	567.5
J0252−2933	02 52 34.97934	−29 33 46.7331	0.0000916	0.001219	0.12	AT20G	−774.2	−433.0	887.1
J0256−2137	02 56 12.83893	−21 37 29.1430	0.0000417	0.000477	0.37	AT20G	15.0	−643.1	643.2
J0257−1212	02 57 41.00412	−12 12 01.3863	0.0000173	0.000160	0.42	ALMA	12.9	−6.3	14.3
J0259−0019	02 59 28.51539	−00 19 59.9742	0.0000245	0.000212	0.90	AT20G	1719.2	−474.2	1783.4
J0300−0531	03 00 01.29969	−05 31 20.3781	0.0009528	0.010286	0.04	AT20G	303.2	−178.1	351.7
J0301−1652	03 01 16.62273	−16 52 45.0767	0.0000602	0.000645	0.75	AT20G	247.9	1123.3	1150.3
J0301−1812	03 01 06.71651	−18 12 17.7758	0.0000449	0.000506	0.74	AT20G	1332.1	424.2	1398.0
J0303−2407		Extended Source				AT20G			
J0304−4333		Extended Source				AT20G			
J0315−1031		Extended Source				ALMA			
J0315−1656	03 15 27.67787	−16 56 29.7209	0.0000374	0.000373	0.25	AT20G	1178.4	−120.9	1184.6
J0319−1613		Extended Source				AT20G			
J0325−2415	03 25 13.34266	−24 15 48.0817	0.0000342	0.000410	0.26	AT20G	−173.1	218.2	278.6
J0327−2202	03 27 59.92443	−22 02 06.3760	0.0000479	0.000555	0.57	AT20G	633.6	−176.0	657.6
J0331−2524	03 31 08.92053	−25 24 43.2817	0.0000368	0.000455	0.39	AT20G	399.3	−681.7	790.1
J0337−1204[b]	03 37 55.45769	−12 04 04.4517	0.0000540	0.000537	0.14	AT20G	−2019.7	648.3	2121.2
J0339−1736	03 39 13.69936	−17 36 00.7827	0.0000529	0.000591	0.11	Winn	77.7	2.3	77.8
J0340−2152	03 40 03.40969	−21 52 01.3901	0.0000559	0.000664	0.10	Winn	0.1	−3.1	3.1
J0347−3616[c]	03 47 59.07871	−36 16 36.5038	0.0000839	0.001309	0.15	AT20G	257.5	−303.8	398.2
J0348−1610		Extended Source				ALMA			
J0349−2102	03 49 57.82372	−21 02 47.7399	0.0000500	0.000543	0.87	ALMA	45.9	0.1	45.9
J0349−2401	03 49 15.38695	−24 01 14.3625	0.0000488	0.000579	0.10	Winn	29.5	−49.5	57.6
J0350−3232		Extended Source				ALMA			
J0352−2514		Extended Source				ALMA			
J0356−4021		Extended Source				AT20G			
J0357−0751	03 57 43.29297	−07 51 14.5397	0.0000361	0.000343	0.11	AT20G	996.1	−1939.7	2180.5
J0359−2615	03 59 33.68194	−26 15 31.3675	0.0000666	0.000820	0.57	AT20G	−833.3	−567.5	1008.2
J0406−1749	04 06 12.24786	−17 49 57.9110	0.0000352	0.000371	0.56	AT20G	−1968.6	689.0	2085.7
J0408−0529	04 08 59.64946	−05 29 40.5509	0.0000427	0.000396	0.32	AT20G	306.7	49.1	310.6
J0409−1655	04 09 37.33533	−16 55 35.5298	0.0000371	0.000380	0.66	AT20G	1071.6	170.2	1085.0
J0417−0250	04 17 58.26015	−02 50 19.3332	0.0000200	0.000208	0.39	ALMA	−2.2	−3.2	3.9
J0422−2034	04 22 48.46027	−20 34 56.0295	0.0000432	0.000471	0.18	Winn	4.6	−2.5	5.2
J0427−0700	04 27 26.16019	−07 00 31.2526	0.0000285	0.000266	0.27	AT20G	−2.9	−52.6	52.7
J0428−1230	04 28 44.86588	−12 30 17.0926	0.0000472	0.000479	0.27	AT20G	353.2	−292.6	458.7
J0431−0406	04 31 28.08733	−04 06 27.3584	0.0000359	0.000316	0.47	ALMA	25.0	−38.5	45.9
J0432−1614	04 32 29.08140	−16 14 05.6755	0.0000334	0.000341	0.84	AT20G	1275.9	−175.5	1287.9
J0433−0229	04 33 54.88959	−02 29 56.0373	0.0000053	0.000094	0.53	AT20G	605.6	−437.3	747.0
J0437−2813	04 37 48.22414	−28 13 39.3399	0.0000095	0.000278	0.19	AT20G	606.0	460.1	760.9
J0438−0716	04 38 21.67213	−07 16 19.1936	0.0000169	0.000322	0.11	TGSS	−671.5	−713.6	979.9

[a] : Calibrated with source a in Table 8, [b] with source b, etc.

Table 6. Positions and X-band Flux Densities of Alternative VLA Reference Sources (Continued..)

IAU Name J2000	Measured RA (h m s)	Measured Dec. (° ′ ″)	Error RA (s)	Error Dec. (″)	Flux Dens. Jy beam^{-1}	Origin	ΔRA (mas)	ΔDec. (mas)	Shift (mas)
J0438−0848	04 38 37.87588	−08 48 21.4881	0.0000234	0.000423	0.25	Winn	19.5	3.9	19.9
J0438−1251	04 38 35.02107	−12 51 03.3631	0.0000082	0.000170	0.74	ALMA	−1.1	−3.1	3.2
J0438−2012	04 38 50.48941	−20 12 26.3644	0.0000127	0.000285	0.76	AT20G	853.0	−264.3	893.0
J0442−2825	04 42 37.65720	−28 25 30.8596	0.0000127	0.000356	0.55	ALMA	−2.6	−19.6	19.7
J0447−0152	04 47 42.60765	−01 52 47.3155	0.0000128	0.000223	0.04	Winn	−14.3	3.5	14.7
J0448−0935	04 48 49.46949	−09 35 31.4857	0.0000106	0.000206	0.06	Winn	1.6	9.3	9.4
J0448−2109	04 48 17.38213	−21 09 44.8316	0.0000066	0.000156	0.30	ALMA	−1.8	−1.6	2.4
J0449−0057	Observed at the wrong Declination					ALMA			
J0450−1837	04 50 35.90958	−18 37 00.3947	0.0000061	0.000136	0.68	AT20G	858.8	105.2	865.3
J0453−1233	04 53 40.98853	−12 33 54.6005	0.0000108	0.000214	0.36	ALMA	−7.8	−0.5	7.8
J0457−0849	04 57 20.21251	−08 49 05.4738	0.0000094	0.000178	0.09	Winn	22.1	6.2	22.9
J0457−1819	04 57 54.32533	−18 19 16.0393	0.0000181	0.000400	0.52	AT20G	493.7	60.7	497.4
J0457−4025[d]	04 57 16.03278	−40 25 20.6083	0.0000811	0.002618	0.06	AT20G	−31.7	−408.3	409.5
J0459+2706[e]	Not Detected					TGSS			
J0501−1706	05 01 42.64323	−17 06 08.5959	0.0000138	0.000292	0.60	AT20G	1100.6	304.1	1141.8
J0503−0638	05 03 56.04751	−06 38 03.4560	0.0000126	0.000237	0.07	AT20G	186.0	−556.0	586.3
J0503+3403	05 03 56.78645	+34 03 28.1155	0.0000553	0.000398	0.63	TGSS	93.8	395.5	406.5
J0504−0744	05 04 34.49271	−07 44 36.8739	0.0000074	0.000139	0.23	AT20G	257.0	−473.9	539.1
J0505−0419	05 05 51.23862	−04 19 26.6150	0.0000104	0.000193	0.09	AT20G	−128.9	−315.0	340.4
J0505−1615	05 05 57.16120	−16 15 58.0198	0.0000148	0.000314	0.24	AT20G	846.7	480.2	973.4
J0513−0032	05 13 02.60397	−00 32 25.2590	0.0000143	0.000242	0.04	Winn	11.0	0.0	11.0
J0514−0733	05 14 29.03746	−07 33 12.9409	0.0000102	0.000200	0.07	AT20G	335.2	159.1	371.0
J0517−0520	05 17 28.10983	−05 20 40.8414	0.0000092	0.000175	0.17	ALMA	2.5	−1.4	2.9
J0517−1756	05 17 24.04725	−17 56 24.1590	0.0000108	0.000240	0.45	AT20G	39.2	341.0	343.3
J0522−1627	05 22 44.65518	−16 27 52.4177	0.0000118	0.000253	0.41	AT20G	644.8	82.3	650.0
J0523−2614	05 23 18.46936	−26 14 09.5359	0.0000119	0.000311	1.49	AT20G	412.3	564.1	698.7
J0525−2338	05 25 06.50599	−23 38 10.8088	0.0000076	0.000196	4.95	ALMA	0.1	1.2	1.2
J0526−2342	05 26 48.38522	−23 42 55.8530	0.0000119	0.000306	0.44	AT20G	−1033.0	−153.0	1044.2
J0529−0519	05 29 53.53392	−05 19 41.6167	0.0000096	0.000174	1.32	AT20G	−357.2	683.3	771.0
J0532−0307	05 32 07.51934	−03 07 07.0326	0.0000065	0.000116	1.55	ALMA	−5.0	7.4	9.0
J0533−2344	05 33 54.60337	−23 44 29.9863	0.0000106	0.000259	0.82	AT20G	91.1	213.8	232.4
J0535−1202	05 35 33.29987	−12 02 22.4292	0.0000111	0.000219	0.65	AT20G	−291.5	170.7	337.8
J0541−0211	05 41 21.69652	−02 11 08.3842	0.0000060	0.000103	1.20	AT20G	202.0	515.8	553.9
J0542−0913	Inadequate Data					ALMA			
J0544−0917	05 44 09.09693	−09 17 41.0642	0.0000174	0.000302	0.90	Winn	−3.4	2.8	4.3
J0549+2031	Inadequate Data					TGSS			
J0557−2214	05 57 29.89097	−22 14 39.0950	0.0000125	0.000294	0.18	AT20G	−707.7	405.0	815.4
J0558−1317	05 58 02.54682	−13 17 41.1964	0.0000066	0.000136	0.57	ALMA	2.7	3.6	4.5
J0603−1716	06 03 57.73208	−17 16 28.2226	0.0000064	0.000143	0.26	Winn	−8.3	24.4	25.7
J0606−0724	Multiple Compact Components					AT20G			
J0608−1520	06 08 01.53195	−15 20 36.9868	0.0000047	0.000104	0.28	AT20G	261.1	−186.8	321.1
J0612−4337[f]	Multiple Compact Components					AT20G			
J0617−2200	06 17 02.04204	−22 00 28.1609	0.0000148	0.000349	0.13	AT20G	−306.4	739.0	800.0
J0618−0954	06 18 20.66748	−09 54 25.7262	0.0000101	0.000200	0.14	AT20G	−258.3	73.8	268.7
J0620−2515	Extended Source					ALMA			
J0622−0846	06 22 37.99951	−08 46 18.2651	0.0000222	0.000426	0.04	AT20G	155.5	34.9	159.4

[a] : Calibrated with source *a* in Table 8, [b] with source *b*, etc.

Table 6. Positions and X-band Flux Densities of Alternative VLA Reference Sources (Continued..)

IAU Name J2000	Measured RA (h m s)	Measured Dec. (° ′ ″)	Error RA (s)	Error Dec. (″)	Flux Dens. Jy beam^{-1}	Origin	ΔRA (mas)	ΔDec. (mas)	Shift (mas)
J0630−1323	06 30 53.90294	−13 23 34.4861	0.0000073	0.000150	0.52	ALMA	0.8	3.9	4.0
J0631−1410	06 31 20.22597	−14 10 31.7372	0.0000087	0.000190	0.45	ALMA	0.4	2.8	2.9
J0634+2550	Inadequate Data					TGSS			
J0636−0547	06 36 48.33005	−05 47 07.5474	0.0000248	0.000483	0.07	AT20G	−0.7	252.7	252.7
J0643−1335	06 43 32.36196	−13 35 49.8746	0.0000059	0.000125	0.48	ALMA	0.6	5.4	5.4
J0643−2451	Extended Source, Multiple Components					AT20G			
J0649−1839	06 49 46.67670	−18 39 11.2312	0.0000128	0.000276	0.16	AT20G	−237.4	−31.2	239.4
J0650−1306	Extended Source, Multiple Components					AT20G			
J0654−1053	06 54 10.63931	−10 53 36.9686	0.0000090	0.000181	0.14	ALMA	−4.6	1.4	4.8
J0654−1309	06 54 50.40939	−13 09 30.3935	0.0000071	0.000149	0.11	AT20G	447.1	−293.5	534.8
J0658+2754	Extended Source, Multiple Components					TGSS			
J0709−0255	07 09 45.05435	−02 55 17.4977	0.0000050	0.000089	0.17	ALMA	9.7	2.2	10.0
J0710−2033	07 10 46.62165	−20 33 23.9637	0.0000150	0.000352	0.25	AT20G	819.5	236.3	852.9
J0723+3519	07 23 55.44293	+35 19 36.4173	0.0000615	0.000512	1.11	TGSS	1432.7	687.3	1589.0
J0724−0624	07 24 29.07898	−06 24 33.2785	0.0000079	0.000148	0.11	AT20G	−282.9	1421.5	1449.3
J0727−3813	Extended Source					AT20G			
J0730−0241	07 30 25.87729	−02 41 24.8988	0.0000074	0.000128	0.14	ALMA	10.6	1.2	10.7
J0730−0535	07 30 28.43703	−05 35 46.9092	0.0000159	0.000296	0.03	AT20G	−254.2	90.8	269.9
J0735+2341	Extended Source					TGSS			
J0735+3428[h]	07 35 55.99808	+34 28 50.6418	0.0000316	0.000264	0.27	TGSS	468.8	731.8	869.1
J0737−0720	07 37 07.13324	−07 20 38.0421	0.0000086	0.000162	0.06	AT20G	−1089.7	457.9	1181.9
J0737−3954	Extended Source					AT20G			
J0741−2647	07 41 55.68170	−26 47 30.5121	0.0000128	0.000335	0.58	AT20G	−156.7	−112.1	192.6
J0743−0440	07 43 52.40620	−04 40 20.5327	0.0000072	0.000131	0.27	AT20G	−690.8	767.2	1032.4
J0747−1237	07 47 10.05602	−12 37 18.1432	0.0000097	0.000208	0.08	AT20G	−2283.8	756.8	2405.9
J0755−1028	07 55 17.83948	−10 28 27.5288	0.0000085	0.000167	0.06	AT20G	302.6	−28.7	304.0
J0759−1821	07 59 43.70046	−18 21 59.1834	0.0000143	0.000326	0.19	AT20G	−6.6	−583.4	583.4
J0800−3959	Extended Source					AT20G			
J0802−1042	08 02 05.92864	−10 42 16.7199	0.0000093	0.000189	0.09	AT20G	−127.4	−319.9	344.3
J0806−1724	08 06 24.96636	−17 24 44.3331	0.0000118	0.000265	0.54	AT20G	767.7	−33.1	768.4
J0807−1531	08 07 05.30957	−15 31 25.3924	0.0000167	0.000352	0.18	AT20G	1451.6	−92.4	1454.5
J0812−1810	Multiple Compact Components					AT20G			
J0821−0323	Multiple Compact Components					AT20G			
J0824−1527	08 24 51.62222	−15 27 45.9260	0.0000107	0.000227	0.28	ALMA	−17.6	−6.0	18.6
J0824−1827	08 24 04.06668	−18 27 40.8347	0.0000096	0.000218	0.27	AT20G	474.1	−134.7	492.9
J0824−2428	08 24 49.25913	−24 28 52.5360	0.0000158	0.000388	0.24	AT20G	285.0	−136.0	315.8
J0837−3409	Extended Source, Multiple Components					ALMA			
J0847−0520	Multiple Compact Components					ALMA			
J0847−0703	Multiple Compact Components					ALMA			
J0847−2337	08 47 01.56583	−23 37 01.6839	0.0000143	0.000349	0.16	AT20G	−492.4	116.1	505.9
J0856−1105	Multiple Compact Components					ALMA			
J0902−1721	09 03 00.01909	−17 21 05.2181	0.0000085	0.000187	0.35	AT20G	−1705.1	3781.9	4148.5
J0903−3117	09 03 37.93566	−31 17 39.1650	0.0000189	0.000578	0.19	AT20G	−72.5	−65.0	97.4
J0904−2552	09 04 52.18576	−25 52 51.7589	0.0000075	0.000203	0.83	AT20G	732.0	1941.2	2074.6
J0904−3111	09 04 20.51632	−31 11 25.7129	0.0000121	0.000363	0.55	ALMA	−4.2	−43.0	43.2
J0912−4137	Multiple Compact Components					AT20G			

[a] : Calibrated with source a in Table 8, [b] with source b, etc.

Table 6. Positions and X-band Flux Densities of Alternative VLA Reference Sources (Continued..)

IAU Name J2000	Measured RA (h m s)	Measured Dec. (° ′ ″)	Error RA (s)	Error Dec. (″)	Flux Dens. Jy beam^{-1}	Origin	ΔRA (mas)	ΔDec. (mas)	Shift (mas)
J0914−3314	Extended Source					AT20G			
J0915−3029	09 15 40.89529	−30 29 49.4617	0.0000156	0.000462	0.26	AT20G	319.4	−261.7	412.9
J0917−1345	09 17 39.00032	−13 45 42.2359	0.0000061	0.000130	0.51	AT20G	432.5	−1135.9	1215.4
J0922−0529	Extended Source					ALMA			
J0923−2135	Extended Source					ALMA			
J0928−0409	09 28 33.46918	−04 09 08.8489	0.0000096	0.000169	0.16	ALMA	−2.8	1.1	3.0
J0932−3405	Extended Source					AT20G			
J0933−0819	Multiple Compact Components					ALMA			
J0933−1139	Multiple Compact Components					ALMA			
J0938−0708	Multiple Compact Components					ALMA			
J0939−1731	09 39 19.19465	−17 31 35.7749	0.0000212	0.000428	0.19	AT20G	−352.6	2325.1	2351.7
J0942−0759	09 42 21.46123	−07 59 53.2037	0.0000108	0.000203	0.97	ALMA	−3.4	−3.7	5.0
J0946+0419	Extended Source					TGSS			
J0946−2020[j]	09 46 50.21096	−20 20 44.4522	0.0000206	0.000455	0.13	AT20G	−154.1	−152.2	216.6
J0948−3544[j]	09 48 41.59579	−35 44 29.1760	0.0000397	0.001277	0.08	AT20G	1025.3	−1275.9	1636.8
J0952+2828	09 52 06.08398	+28 28 32.4035	0.0000627	0.000356	0.34	TGSS	79.4	−376.5	384.7
J0952−3006[j]	Extended Source					ALMA			
J0958−4110	Inadequate Data					AT20G			
J1006−2159	10 06 46.41375	−21 59 20.4062	0.0000083	0.000197	0.48	AT20G	782.3	393.7	875.8
J1008−0933	10 08 43.86548	−09 33 23.3504	0.0000095	0.000187	0.79	Winn	9.2	20.6	22.5
J1010−0200	10 10 51.66616	−02 00 19.5692	0.0000042	0.000074	3.02	ALMA	12.6	0.8	12.6
J1011−0423	10 11 30.23940	−04 23 27.7044	0.0000063	0.000113	1.64	Winn	−14.9	32.7	35.9
J1011−2301	10 11 20.48175	−23 01 19.4729	0.0000210	0.000500	0.13	Winn	0.7	2.1	2.2
J1011+4204	10 11 54.17654	+42 04 33.3797	0.0000273	0.000154	0.54	TGSS	−763.2	−3280.3	3367.9
J1013+2829	10 13 02.99891	+28 29 10.9329	0.0000535	0.000338	0.46	TGSS	−1014.0	2.9	1014.0
J1016−3533	Extended Source					AT20G			
J1019−2219	10 19 49.02396	−22 19 59.7702	0.0000225	0.000538	0.13	AT20G	−193.7	−470.2	508.6
J1019−2708	10 19 08.48331	−27 08 55.6622	0.0000173	0.000467	0.18	Winn	13.2	31.8	34.5
J1024−3234	10 24 00.42408	−32 34 16.0889	0.0000125	0.000419	0.42	ALMA	−1.0	−28.9	28.9
J1027−2230	10 27 08.45723	−22 30 09.8596	0.0000110	0.000270	0.21	AT20G	−516.0	340.4	618.1
J1028−0236	Multiple Compact Components					ALMA			
J1028−0844	Multiple Compact Components					Winn	−3.4	−3.7	5.0
J1029−1852	10 29 33.09800	−18 52 50.2883	0.0000052	0.000118	0.76	ALMA			
J1031−0423	Multiple Compact Components					AT20G			
J1031−2228	10 31 52.31212	−22 28 24.9815	0.0000062	0.000156	0.44	AT20G	386.5	−281.5	478.1
J1036−0605	Multiple Compact Components					Winn			
J1037−2823	10 37 42.45748	−28 23 04.1013	0.0000068	0.000194	0.36	Winn	4.1	−5.3	6.8
J1038−4325[k]	Extended Source, Multiple Components					ALMA			
J1042−4143[k]	Extended Source, Multiple Components					ALMA			
J1047−1308	Extended Source					AT20G			
J1048+6008	10 48 33.70097	+60 08 45.6444	0.0000505	0.000196	0.72	TGSS	254.1	224.4	339.0
J1049−2231	10 49 21.86895	−22 31 07.4879	0.0000098	0.000241	0.28	AT20G	−678.2	512.1	849.8
J1052+2029	Inadequate Data					TGSS			
J1057−2342	10 57 24.42072	−23 42 01.7031	0.0000097	0.000241	0.97	AT20G	−834.0	96.8	839.6
J1058−0309	10 58 11.01116	−03 09 27.2599	0.0000093	0.000160	0.94	Winn	2.1	3.1	3.7
J1059−1134	10 59 12.42619	−11 34 22.7870	0.0000106	0.000216	0.14	ALMA	−2.8	−7.0	7.5

[a] : Calibrated with source *a* in Table 8, [b] with source *b*, etc.

Table 6. Positions and X-band Flux Densities of Alternative VLA Reference Sources (Continued..)

IAU Name J2000	Measured RA (h m s)	Measured Dec. (° ′ ″)	Error RA (s)	Error Dec. (″)	Flux Dens. Jy beam^{-1}	Origin	ΔRA (mas)	ΔDec. (mas)	Shift (mas)
J1100−1251	11 00 11.06784	−12 51 11.9309	0.0000115	0.000237	0.08	AT20G	177.8	−430.9	466.2
J1100−4249[k]		Extended Source				AT20G			
J1104−2431	11 04 46.17633	−24 31 25.7954	0.0000100	0.000254	0.60	ALMA	−4.5	4.7	6.5
J1105+2052		Extended Source				TGSS			
J1108+1435		Inadequate Data				TGSS			
J1108−4329[k]		Extended Source				AT20G			
J1110−0756	11 10 16.95388	−07 56 50.1837	0.0000172	0.000325	0.06	AT20G	388.1	216.3	444.3
J1110−1858	11 10 00.40705	−18 58 48.7428	0.0000095	0.000215	0.16	AT20G	41.9	−142.8	148.8
J1112−0842	11 12 12.64641	−08 42 19.3854	0.0000144	0.000275	0.07	AT20G	646.4	−1285.4	1438.8
J1113−2300	11 13 54.78750	−23 00 43.6751	0.0000083	0.000208	0.39	ALMA	6.9	−15.1	16.6
J1114−0247	11 14 39.66414	−02 47 31.7515	0.0000117	0.000213	0.28	ALMA	−2.2	−11.5	11.7
J1114−0816	11 14 32.54989	−08 16 39.0133	0.0000117	0.000228	0.29	ALMA	16.4	−13.3	21.1
J1116−2828	11 16 11.79940	−28 28 30.5651	0.0000131	0.000331	0.20	AT20G	−123.9	734.9	745.2
J1118−1232	11 18 17.14085	−12 32 54.2662	0.0000073	0.000150	0.64	ALMA	2.2	−6.2	6.5
J1120−1243	11 20 12.07998	−12 43 37.8352	0.0000076	0.000155	0.22	AT20G	−1462.9	864.8	1699.4
J1120−1420	11 20 55.56338	−14 20 29.9262	0.0000072	0.000149	0.22	AT20G	241.5	273.8	365.1
J1120−2719[l]	11 20 16.19145	−27 19 06.3826	0.0000150	0.000408	1.54	AT20G	−1352.1	1617.4	2108.1
J1121−0553	11 21 25.10771	−05 53 56.4552	0.0000136	0.000251	0.23	ALMA	4.4	−15.2	15.8
J1121−0711	11 21 42.12213	−07 11 06.3619	0.0000128	0.000234	0.19	AT20G	−775.8	138.1	788.0
J1122−2532[l]	11 22 05.74305	−25 32 33.8556	0.0000133	0.000338	0.65	AT20G	−1124.0	−355.6	1179.0
J1124+1919	11 24 43.87192	+19 19 29.4961	0.0000767	0.000477	1.01	TGSS	1.2	−463.8	463.8
J1126+3345	11 26 23.66168	+33 45 26.8319	0.0000299	0.000163	0.74	TGSS	−644.5	481.8	804.7
J1127−0735	11 27 12.43600	−07 35 12.1766	0.0000135	0.000256	0.11	AT20G	−386.5	1223.4	1283.0
J1129−0446	11 29 35.51208	−04 46 59.4937	0.0000164	0.000310	0.15	Winn	12.3	4.3	13.0
J1135+3708	11 35 05.93209	+37 08 40.7938	0.0000452	0.000367	0.08	TGSS	−216.3	83.8	231.9
J1136−0330	11 36 24.57709	−03 30 29.4989	0.0000046	0.000083	0.94	AT20G	941.8	−1099.0	1447.3
J1139−1552	11 39 29.57598	−15 52 51.6536	0.0000058	0.000123	0.40	Winn	−9.7	−2.6	10.1
J1142+1338		Extended Source				TGSS			
J1142−2442[l]	11 42 24.74896	−24 42 57.2978	0.0000141	0.000361	0.21	Winn	0.5	2.2	2.2
J1148−0404	11 48 55.88512	−04 04 09.5619	0.0000065	0.000118	0.40	AT20G	3364.7	138.0	3367.5
J1150−1930	11 50 31.52571	−19 30 49.5450	0.0000091	0.000206	0.42	AT20G	−2908.5	−345.0	2928.9
J1151−1723	11 51 03.20278	−17 23 59.8404	0.0000081	0.000176	0.48	Winn	18.9	1.6	18.9
J1152−0841	11 52 17.20917	−08 41 03.3157	0.0000033	0.000065	2.22	ALMA	12.4	−5.7	13.6
J1153−1105	11 53 22.31509	−11 05 12.5814	0.0000183	0.000329	0.18	Winn	−39.5	26.6	47.7
J1154−3242		Extended Source				AT20G			
J1155−1216	11 55 36.81943	−12 16 35.5092	0.0000088	0.000174	0.12	Winn	−13.7	14.8	20.1
J1159+5820	11 59 48.77170	+58 20 20.3139	0.0000325	0.000123	1.45	TGSS	−52.8	−376.1	379.8
J1202−0528	12 02 34.22487	−05 28 02.4817	0.0000512	0.001005	0.19	ALMA	1.9	8.3	8.5
J1203−2628[l]	12 03 33.28431	−26 28 10.6925	0.0000131	0.000340	0.36	AT20G	210.7	−92.5	230.1
J1204−0710	12 04 16.66481	−07 10 08.9999	0.0000127	0.000236	0.29	3FGL	−964.6	1510.1	1791.9
J1204+1129	12 04 26.66586	+11 29 10.1479	0.0000701	0.000490	0.35	TGSS	134.5	258.0	290.9
J1207−0106		Not Detected				AT20G			
J1208−0435	12 08 02.38185	−04 35 33.0150	0.0000161	0.000299	0.17	AT20G	−2270.5	−3215.0	3936.0
J1212−2221[l]	12 12 03.69776	−22 21 51.4939	0.0000134	0.000327	0.48	AT20G	3499.0	−694.0	3567.1
J1213−1003	12 13 22.94514	−10 03 25.2761	0.0000098	0.000198	0.38	AT20G	−814.3	1123.9	1387.9
J1213−2724[l]	12 13 40.06945	−27 24 22.5588	0.0000140	0.000393	0.42	AT20G	1605.3	1141.3	1969.6

[a] : Calibrated with source a in Table 8, [b] with source b, etc.

Table 6. Positions and X-band Flux Densities of Alternative VLA Reference Sources (Continued..)

IAU Name J2000	Measured RA (h m s)	Measured Dec. (° ′ ″)	Error RA (s)	Error Dec. (″)	Flux Dens. Jy beam^{-1}	Origin	ΔRA (mas)	ΔDec. (mas)	Shift (mas)
J1213−4343	Extended Source					AT20G			
J1216−3546	12 16 24.93624	−35 46 34.1802	0.0000613	0.002042	0.05	AT20G	167.4	−1380.2	1390.3
J1217−0029	Observed at the wrong Declination					ALMA			
J1218−0119	12 18 34.92821	−01 19 54.3480	0.0000461	0.000353	0.92	AT20G	−2072.6	−1248.0	2419.3
J1221−3423	Extended Source					AT20G			
J1222−3046	12 22 24.76382	−30 46 21.8298	0.0000176	0.000530	0.16	AT20G	3430.6	2970.2	4537.7
J1223−0546	12 23 46.05579	−05 46 58.0165	0.0000697	0.000601	0.28	AT20G	−1280.3	783.5	1501.0
J1228−0304	12 28 36.91444	−03 04 39.3049	0.0000592	0.000457	0.40	Winn	39.8	−7.9	40.6
J1230−3121	12 30 44.93299	−31 21 23.3466	0.0000164	0.000507	0.13	AT20G	986.4	−246.6	1016.8
J1232−1015	12 32 15.86014	−10 15 25.1718	0.0000054	0.000109	0.39	ALMA	−2.1	−1.9	2.8
J1238−0656	12 38 38.48625	−06 56 12.1726	0.0000106	0.000201	0.22	AT20G	−2773.3	−872.6	2907.3
J1244−2633	12 44 14.64108	−26 33 24.9540	0.0000174	0.000456	0.09	AT20G	1998.2	346.0	2027.9
J1245−1616	Multiple Compact Components					ALMA			
J1247−2348	12 47 59.35012	−23 48 59.2095	0.0000220	0.000536	0.15	AT20G	−138.9	−209.5	251.3
J1248−0632	12 48 22.97543	−06 32 09.8142	0.0000065	0.000123	0.93	ALMA	8.4	5.9	10.3
J1249−2324	12 49 05.03456	−23 24 21.9343	0.0000337	0.000832	0.12	AT20G	−62.7	−234.4	242.6
J1251−1717	12 51 14.47601	−17 17 13.1544	0.0000109	0.000239	0.42	ALMA	−14.5	5.6	15.6
J1256−2155	12 56 25.51015	−21 55 21.1434	0.0000065	0.000158	0.60	AT20G	−280.3	−543.4	611.4
J1259−0150	12 59 06.61492	−01 50 58.3552	0.0000108	0.000191	0.16	Winn	1.2	10.8	10.9
J1259−2310	12 59 08.46236	−23 10 38.6395	0.0000141	0.000358	0.75	ALMA	−5.0	10.5	11.6
J1300−1302	13 00 18.74002	−13 02 53.6778	0.0000117	0.000246	0.21	Winn	−17.8	30.2	35.1
J1300−3253	13 00 42.42636	−32 53 12.1217	0.0000127	0.000384	0.17	AT20G	171.8	−521.7	549.2
J1303−1051	13 03 13.86753	−10 51 17.1256	0.0000074	0.000151	0.43	Winn	18.7	14.4	23.6
J1303−2405	13 03 19.64708	−24 05 03.0346	0.0000150	0.000380	0.14	AT20G	450.8	65.4	455.5
J1303+2433	13 03 03.21962	+24 33 55.7165	0.0000500	0.000275	2.34	ALMA	−35.8	−13.4	38.2
J1305−2850	Extended Source					ALMA			
J1306−1718	Multiple Compact Components					AT20G			
J1306−2147	13 06 42.04917	−21 47 50.9733	0.0000175	0.000421	0.13	Winn	29.6	22.7	37.3
J1308−2422	13 08 42.01185	−24 22 57.9392	0.0000144	0.000366	0.13	Winn	−47.1	−69.2	83.7
J1309−3948	Inadequate Data					AT20G			
J1311+1839	13 11 57.24369	+18 39 30.7725	0.0000594	0.000363	0.67	TGSS	1127.1	212.6	1146.9
J1312−0424	13 12 50.90144	−04 24 49.8891	0.0000121	0.000217	0.79	ALMA	−6.6	0.9	6.7
J1313−2722	13 13 01.42043	−27 22 58.8324	0.0000143	0.000394	0.17	Winn	70.1	62.6	94.0
J1317−1345	13 17 36.53855	−13 45 32.6497	0.0000050	0.000105	0.10	AT20G	−1290.2	−1149.6	1728.1
J1317−2031	13 17 26.14842	−20 31 38.1125	0.0000139	0.000327	0.18	Winn	1.1	41.5	41.5
J1318−0607	13 18 33.70925	−06 07 23.8251	0.0000118	0.000209	0.12	AT20G	−287.1	−25.1	288.2
J1318−1807	13 18 56.70671	−18 07 40.4257	0.0000174	0.000384	0.03	AT20G	1187.4	−325.7	1231.3
J1321−2636	13 21 14.03590	−26 36 10.4401	0.0000088	0.000230	0.65	AT20G	−347.4	−440.1	560.7
J1322−0937	13 22 36.91276	−09 37 37.7986	0.0000116	0.000226	0.09	Winn	−20.1	−25.6	32.5
J1323−4101	Extended Source, Multiple Components					AT20G			
J1324−1049	13 24 25.79314	−10 49 23.1337	0.0000063	0.000128	0.28	ALMA	−2.1	−3.7	4.3
J1325−1117	13 25 13.21996	−11 17 39.0831	0.0000074	0.000148	0.07	ALMA	0.6	−3.1	3.1
J1326−0500	13 26 54.61294	−05 00 58.9857	0.0000144	0.000267	0.07	Winn	−3.6	−25.7	26.0
J1327−4214	Extended Source					AT20G			
J1330−2056	13 30 07.70087	−20 56 16.5541	0.0000186	0.000432	0.05	AT20G	1528.9	−154.1	1536.6
J1331−0341	13 31 29.16091	−03 41 14.1121	0.0000139	0.000254	0.08	ALMA	1.4	−2.1	2.5

[a] : Calibrated with source a in Table 8, [b] with source b, etc.

Table 6. Positions and X-band Flux Densities of Alternative VLA Reference Sources (Continued..)

IAU Name J2000	Measured RA (h m s)	Measured Dec. (° ′ ″)	Error RA (s)	Error Dec. (″)	Flux Dens. Jy beam^{-1}	Origin	ΔRA (mas)	ΔDec. (mas)	Shift (mas)
J1331−4230	Extended Source					AT20G			
J1332−0509	13 32 04.46486	−05 09 43.3069	0.0000131	0.000238	0.14	ALMA	2.2	3.1	3.8
J1332−1402	13 32 30.92818	−14 02 13.1835	0.0000075	0.000159	0.08	AT20G	−1137.7	216.5	1158.1
J1333−1950	13 33 45.17603	−19 50 42.3357	0.0000135	0.000307	0.09	ALMA	−0.5	4.3	4.3
J1333−2356	Extended Source, Multiple Components					AT20G			
J1333+2725	13 33 07.49012	+27 25 18.3749	0.0000407	0.000212	2.36	ALMA	−1.6	5.0	5.2
J1334−1150	13 34 04.19072	−11 50 14.2721	0.0000076	0.000151	0.09	AT20G	−891.4	−172.1	907.8
J1335−0511	13 35 56.47694	−05 11 41.6612	0.0000163	0.000301	0.05	ALMA	0.9	−1.2	1.6
J1335−3911	Extended Source					AT20G			
J1336−0829	13 36 08.25999	−08 29 51.7999	0.0000060	0.000120	0.42	ALMA	0.1	0.1	0.2
J1337−0601	13 37 19.51065	−06 01 47.1212	0.0000237	0.000460	0.02	AT20G	1332.9	−1021.2	1679.1
J1339−0637	13 39 07.14567	−06 37 04.8767	0.0000150	0.000289	0.05	AT20G	213.5	−476.7	522.3
J1339−2401	Extended Source, Multiple Components					ALMA			
J1340−0137	13 40 04.61441	−01 37 46.5582	0.0000065	0.000110	0.88	AT20G	2183.1	−758.2	2311.0
J1342−2051	Extended Source, Multiple Components					ALMA			
J1342−2900	Extended Source, Multiple Components					ALMA			
J1342−3010	Multiple Compact Components					Winn			
J1343−1747	13 43 37.41405	−17 47 55.4502	0.0000094	0.000209	0.21	ALMA	−0.7	−0.2	0.8
J1343−2357	13 43 26.81147	−23 57 31.9947	0.0000151	0.000365	0.46	Winn	36.1	28.3	45.9
J1347−3750	Extended Source					AT20G			
J1349−1110	13 49 03.19292	−11 10 00.8204	0.0000081	0.000164	0.08	ALMA	1.2	−0.3	1.2
J1349−1132	13 49 31.44352	−11 32 53.8268	0.0000076	0.000161	0.13	Winn	8.5	−17.8	19.8
J1349−1413	13 49 16.02252	−14 13 16.8393	0.0000147	0.000310	0.03	Winn	4.1	−18.3	18.7
J1349−2334	13 49 24.68831	−23 34 31.1189	0.0000153	0.000371	0.62	AT20G	−664.1	581.1	882.5
J1350−1634	13 50 36.14411	−16 34 49.5271	0.0000113	0.000250	0.10	ALMA	−1.6	−17.1	17.1
J1350−2204	Extended Source, Multiple Components					AT20G			
J1351−3442	Extended Source					AT20G			
J1352+0232	13 52 30.69893	+02 32 47.1303	0.0000092	0.000119	0.53	TGSS	285.7	−269.7	392.9
J1352−1817	13 52 50.27929	−18 17 28.4066	0.0000205	0.000447	0.03	Winn	−28.3	39.3	48.5
J1354−1041	13 54 46.51851	−10 41 02.6621	0.0000078	0.000156	0.23	Winn	14.5	−28.1	31.6
J1354−2357	Extended Source, Multiple Components					Winn			
J1356−1101	13 56 46.83206	−11 01 29.2338	0.0000103	0.000209	0.07	Winn	10.9	−30.8	32.6
J1356−1724	13 56 06.95376	−17 24 31.8227	0.0000133	0.000298	0.07	AT20G	948.0	1277.3	1590.7
J1401−0916	14 01 05.33196	−09 16 31.5974	0.0000119	0.000238	0.12	ALMA	0.6	−27.4	27.4
J1401−3004	Extended Source					Winn			
J1405−1440	14 05 32.86718	−14 40 18.3105	0.0000107	0.000231	0.09	AT20G	−2716.2	−1510.5	3107.9
J1405−3907	Extended Source, Multiple Components					AT20G			
J1406−0707	Extended Source					ALMA			
J1406−0848	Extended Source					AT20G			
J1407−2701	Extended Source					AT20G			
J1408−2900	Extended Source					ALMA			
J1409−2315	Extended Source					AT20G			
J1416−1705	Extended Source					AT20G			
J1416−2131	Extended Source					AT20G			
J1418−2958	Extended Source					Winn			
J1419−0838	Multiple Compact Components					ALMA			

[a] : Calibrated with source a in Table 8, [b] with source b, etc.

Table 6. Positions and X-band Flux Densities of Alternative VLA Reference Sources (Continued..)

IAU Name J2000	Measured RA (h m s)	Measured Dec. (° ′ ″)	Error RA (s)	Error Dec. (″)	Flux Dens. Jy beam^{-1}	Origin	ΔRA (mas)	ΔDec. (mas)	Shift (mas)
J1419−1928		Extended Source				Winn			
J1421−0643	14 21 07.75615	−06 43 56.3536	0.0000124	0.000233	0.46	Winn	−2.2	1.4	2.6
J1422−2308		Extended Source				ALMA			
J1426−0215	14 26 55.48454	−02 15 44.2751	0.0000065	0.000112	0.90	AT20G	381.6	−775.1	864.0
J1429−2157		Extended Source				TGSS			
J1438−3122		Extended Source				ALMA			
J1441−3303		Extended Source				AT20G			
J1449−0045	14 49 16.59010	−00 45 19.2345	0.0000532	0.000395	1.24	AT20G	−1501.4	−734.5	1671.5
J1449−2139	14 49 39.97422	−21 39 24.7174	0.0000190	0.000461	0.26	AT20G	−198.3	282.6	345.2
J1450−3319		Extended Source				AT20G			
J1451−0127	14 51 47.41444	−01 27 35.2775	0.0000656	0.000489	1.00	AT20G	−666.3	1022.5	1220.5
J1451−2329		Extended Source				AT20G			
J1453−2522		Extended Source				AT20G			
J1455−1700	14 55 02.81041	−17 00 13.9551	0.0000096	0.000213	0.31	AT20G	−436.2	144.9	459.7
J1455−2159		Extended Source				Winn			
J1455−3158		Extended Source				AT20G			
J1458+3542		Inadequate Data				TGSS			
J1500−2358		Extended Source				AT20G			
J1506−0919		Multiple Compact Components				Winn			
J1509−4340		Extended Source, Multiple Components				ALMA			
J1513−4221		Extended Source, Multiple Components				ALMA			
J1517−0710	15 17 14.05623	−07 10 14.0737	0.0000081	0.000154	1.06	ALMA	−3.4	26.3	26.5
J1522−2936		Extended Source				Winn			
J1524−3012		Extended Source				ALMA			
J1525+0308		Extended Source, Multiple Components				TGSS			
J1533−0421	15 33 14.20519	−04 21 16.6291	0.0000139	0.000249	0.76	AT20G	1567.6	−729.1	1728.9
J1551−1755		Extended Source, Multiple Components				AT20G			
J1553−2422	15 53 31.62814	−24 22 06.0186	0.0000188	0.000515	0.19	ALMA	−2.0	21.4	21.5
J1555−0326	15 55 30.74902	−03 26 49.4973	0.0000101	0.000179	0.83	AT20G	−883.7	602.7	1069.7
J1555−4150		Extended Source, Multiple Components				ALMA			
J1559−2442		Extended Source, Multiple Components				AT20G			
J1600−0037	16 00 01.01531	−00 37 22.5867	0.0000295	0.000484	0.10	Winn	−25.6	3.2	25.8
J1603−0139	16 03 48.50644	−01 39 00.6171	0.0000126	0.000215	0.50	TGSS	803.0	−7.2	803.1
J1604−2223	16 04 01.47122	−22 23 40.9996	0.0000178	0.000435	0.14	Winn	−0.3	−21.5	21.5
J1611−3018	16 11 03.73405	−30 18 26.1265	0.0000284	0.000826	0.08	AT20G	−570.5	−1526.5	1629.6
J1617−1941	16 17 27.09336	−19 41 32.0296	0.0000248	0.000516	0.10	AT20G	1788.5	270.4	1808.8
J1624−0649		Extended Source, Multiple Components				Winn			
J1624−3213	16 24 59.61969	−32 13 24.4429	0.0000283	0.000873	0.17	ALMA	4.0	−2.9	5.0
J1624−3516		Extended Source, Multiple Components				AT20G			
J1628−1415		Extended Source, Multiple Components				Winn			
J1631−4345		Extended Source, Multiple Components				AT20G			
J1632−0033		Extended Source				Winn			
J1634−2058		Extended Source				ALMA			
J1638−0340		Extended Source, Multiple Components				Winn			
J1638−1415		Extended Source, Multiple Components				Winn			
J1647−1044		Extended Source				TGSS	−363.8	252.0	442.5

[a] : Calibrated with source *a* in Table 8, [b] with source *b*, etc.

Table 6. Positions and X-band Flux Densities of Alternative VLA Reference Sources (Continued..)

IAU Name J2000	Measured RA (h m s)	Measured Dec. (° ′ ″)	Error RA (s)	Error Dec. (″)	Flux Dens. Jy beam^{-1}	Origin	ΔRA (mas)	ΔDec. (mas)	Shift (mas)
J1647+1720	Extended Source, Multiple Components					TGSS			
J1647−2912	16 47 57.87592	−29 12 44.3926	0.0000302	0.000876	0.10	AT20G	708.0	207.4	737.8
J1652−3005	16 52 12.87455	−30 05 42.8755	0.0000530	0.001538	0.02	Winn	−25.3	96.5	99.7
J1653−1551	16 53 34.20694	−15 51 29.8652	0.0000150	0.000307	0.05	AT20G	332.7	−1565.2	1600.2
J1656−0206	Inadequate Data					Winn			
J1709+0645	Extended Source					TGSS			
J1710−0355	Extended Source, Multiple Components					Winn			
J1711−3338	Multiple Compact Components					AT20G			
J1711−3744	Multiple Compact Components					ALMA			
J1713−0259	Extended Source					Winn			
J1722−0503	17 22 03.53860	−05 03 25.0070	0.0000138	0.000260	0.10	AT20G	319.7	−1407.0	1442.9
J1739−4137	Multiple Compact Components					AT20G			
J1745−2900	Inadequate Data					3FGL			
J1759−1505	17 59 57.24604	−15 05 49.1805	0.0000172	0.000360	0.02	Winn	19.8	−27.5	33.9
J1805−0438	18 05 31.11602	−04 38 09.7211	0.0000203	0.000364	0.02	Winn	−0.3	−0.0	0.3
J1818−0814	18 18 33.49202	−08 14 42.3742	0.0000170	0.000329	0.05	Winn	2.6	15.8	16.0
J1819−0258	18 19 17.40958	−02 58 07.8607	0.0000107	0.000183	0.25	AT20G	605.5	−560.8	825.3
J1826−2924	Extended Source					ALMA			
J1827−0405	18 27 45.04046	−04 05 44.5745	0.0000142	0.000250	0.34	AT20G	−755.0	−374.4	842.7
J1838−3427	Extended Source					AT20G			
J1848−2718	Extended Source, Multiple Components					AT20G			
J1850−2740	Extended Source, Multiple Components					AT20G			
J1901−1416	19 01 46.14638	−14 16 26.6408	0.0000242	0.000493	0.06	Winn	7.6	23.2	24.4
J1908−2942	Multiple Compact Components					AT20G			
J1912−1223	19 12 29.51466	−12 23 00.8220	0.0000161	0.000317	0.16	AT20G	−947.3	1378.0	1672.2
J1913−0151	19 13 39.12476	−01 51 47.0234	0.0000201	0.000342	0.24	TGSS	−416.2	176.6	452.1
J1916−1519	Multiple Compact Components					ALMA			
J1928−2035	19 28 09.18325	−20 35 43.7727	0.0000414	0.000956	0.11	AT20G	1358.6	427.3	1424.2
J1934−2416	Extended Source					AT20G			
J1938−1749	19 38 04.95931	−17 49 20.3761	0.0000094	0.000204	0.17	ALMA	−18.7	13.9	23.2
J1942−3130	Extended Source					AT20G			
J1945−0153	Extended Source					ALMA			
J1947−0103	Multiple Compact Components					AT20G			
J1950−0436	Multiple Compact Components					AT20G			
J1951−0509	Multiple Compact Components					ALMA			
J2000−1921	20 00 08.56007	−19 21 37.5307	0.0000128	0.000285	0.24	AT20G	−142.6	−130.7	193.4
J2000−4214	Extended Source, Multiple Components					AT20G			
J2005+4556	20 05 48.04743	+45 56 33.1283	0.0000735	0.000528	0.25	TGSS	−390.4	348.3	523.2
J2006−1222	20 06 48.34295	−12 22 55.2915	0.0000135	0.000270	0.18	AT20G	249.8	−791.5	829.9
J2008−0418	20 08 24.42929	−04 18 29.2976	0.0000315	0.000509	0.07	Winn	−11.8	−27.6	30.0
J2015−1252	Multiple Compact Components					AT20G			
J2015−3445	Extended Source, Multiple Components					AT20G			
J2023−0123	Multiple Compact Components					ALMA			
J2024−4127	Extended Source					AT20G			
J2025−2845	Extended Source, Multiple Components					ALMA			
J2036−2146	20 36 51.17205	−21 46 36.7444	0.0000369	0.000811	0.60	AT20G	389.4	455.7	599.3

[a] : Calibrated with source a in Table 8, [b] with source b, etc.

Table 6. Positions and X-band Flux Densities of Alternative VLA Reference Sources (Continued..)

IAU Name J2000	Measured RA (h m s)	Measured Dec. (° ′ ″)	Error RA (s)	Error Dec. (″)	Flux Dens. Jy beam^{-1}	Origin	ΔRA (mas)	ΔDec. (mas)	Shift (mas)
J2036−2830	Extended Source, Multiple Components					AT20G			
J2048−3112	20 48 51.97022	−31 12 49.3767	0.0000289	0.000767	0.28	AT20G	−900.8	523.3	1041.8
J2054−2016	Extended Source, Multiple Components					AT20G			
J2054−4242	Extended Source					AT20G			
J2059−3645	Multiple Compact Components					AT20G			
J2110−3635	Multiple Compact Components					AT20G			
J2118−0636	21 18 43.24249	−06 36 17.9928	0.0000175	0.000309	0.28	AT20G	261.0	−92.8	277.0
J2118−3752	Multiple Compact Components					AT20G			
J2119−1106	21 19 39.88113	−11 06 14.7083	0.0000157	0.000288	0.64	Winn	1.1	−28.3	28.3
J2124−1941	21 24 44.64099	−19 41 43.3439	0.0000320	0.000641	0.14	AT20G	−296.4	156.1	335.0
J2126−0119	Extended Source					AT20G			
J2130−0927	Multiple Compact Components					ALMA			
J2132+1541	21 32 09.09117	+15 41 08.8770	0.0000084	0.000134	0.17	TGSS	−450.1	−213.0	498.0
J2135−3312	21 35 11.67634	−33 12 42.2197	0.0000555	0.001589	0.16	AT20G	−205.1	−119.7	237.5
J2146−2902	21 46 59.90196	−29 02 11.5404	0.0000205	0.000526	0.22	AT20G	−419.2	159.6	448.6
J2146−2935	Multiple Compact Components					AT20G			
J2147−3601	Extended Source, Multiple Components					AT20G			
J2148−1723	21 48 36.80070	−17 23 43.9773	0.0000332	0.000636	0.71	ALMA	4.3	42.6	42.9
J2151−2742	Extended Source					ALMA			
J2156−0037	Observed at the wrong Declination					ALMA			
J2156−2012	21 56 33.75645	−20 12 30.8683	0.0000222	0.000471	0.06	Winn	−35.9	66.7	75.7
J2157−1319	21 57 02.97691	−13 19 02.9683	0.0000126	0.000259	0.08	AT20G	45.1	631.7	633.3
J2157−1807	21 57 29.12380	−18 07 02.8529	0.0000220	0.000455	0.16	AT20G	88.4	47.1	100.2
J2159−0105	21 59 34.27609	−01 05 54.8892	0.0000143	0.000240	0.08	Winn	−19.4	−32.2	37.6
J2200−1632	22 00 54.87921	−16 32 32.6804	0.0000185	0.000387	0.09	Winn	−23.1	17.6	29.0
J2200−1945	22 00 07.76156	−19 45 47.3536	0.0000253	0.000537	0.06	Winn	−20.6	32.4	38.4
J2202−2335	22 02 56.00018	−23 35 10.2321	0.0000330	0.000772	0.13	ALMA	−2.5	17.9	18.1
J2210+2013	22 10 51.65201	+20 13 24.0514	0.0000137	0.000175	0.34	ALMA	−0.1	1.4	1.4
J2211−1328	22 11 24.10020	−13 28 09.7347	0.0000150	0.000284	0.20	ALMA	−17.4	−14.7	22.8
J2211−3707	Multiple Compact Components					AT20G			
J2218+1520	22 18 10.91405	+15 20 35.7254	0.0000139	0.000185	0.99	ALMA	−0.7	5.4	5.4
J2223−1607	22 23 41.17186	−16 07 05.1549	0.0000264	0.000526	0.07	Winn	22.2	38.0	44.0
J2224−1126	22 24 07.96184	−11 26 21.1000	0.0000224	0.000405	0.15	ALMA	17.1	10.0	19.8
J2225−1113	22 25 43.71841	−11 13 40.6902	0.0000246	0.000458	0.03	Winn	16.0	30.8	34.7
J2227−1946	22 27 41.43951	−19 46 36.0221	0.0000790	0.001535	0.02	Winn	−3.0	−3.1	4.3
J2228−0753	22 28 52.60696	−07 53 46.6381	0.0000183	0.000334	0.15	ALMA	15.5	1.9	15.6
J2232−1659	22 32 22.56507	−16 59 01.9029	0.0000331	0.000653	0.15	Winn	−0.9	0.1	1.0
J2234−1759	22 34 02.62697	−17 58 58.8628	0.0000597	0.000811	0.02	TGSS	−1112.4	1127.2	1583.7
J2234−2055	22 34 57.43968	−20 55 03.2150	0.0000432	0.000929	0.12	Winn	−2.5	45.0	45.0
J2236−0406	22 36 16.77425	−04 06 19.6706	0.0000176	0.000294	0.22	AT20G	86.0	129.4	155.4
J2236−1706	22 36 09.52226	−17 06 21.9946	0.0000180	0.000358	0.19	Winn	4.9	−18.6	19.2
J2240−1209	22 40 25.90190	−12 09 33.0003	0.0000160	0.000304	0.10	Winn	−7.4	−13.3	15.2
J2240−1839	22 40 37.56894	−18 39 28.8171	0.0000278	0.000569	0.05	Winn	−3.5	−22.1	22.4
J2240−3621	Extended Source, Multiple Components					AT20G			
J2242−4204	Extended Source, Multiple Components					AT20G			
J2243−0609	22 43 08.76072	−06 09 02.5646	0.0000183	0.000323	0.05	AT20G	287.6	−664.6	724.2

[a] : Calibrated with source *a* in Table 8, [b] with source *b*, etc.

Table 6. Positions and X-band Flux Densities of Alternative VLA Reference Sources (Continued..)

IAU Name J2000	Measured RA (h m s)	Measured Dec. (° ′ ″)	Error RA (s)	Error Dec. (″)	Flux Dens. Jy beam^{-1}	Origin	ΔRA (mas)	ΔDec. (mas)	Shift (mas)
J2247+0000	22 47 30.19601	+00 00 06.4660	0.0000124	0.000195	0.42	Winn	23.9	1.0	23.9
J2247−1237	22 47 52.64138	−12 37 19.7218	0.0000115	0.000230	0.35	AT20G	126.1	−621.8	634.4
J2248−0541	22 48 00.07882	−05 41 18.1958	0.0000169	0.000275	0.06	AT20G	−430.2	−995.8	1084.8
J2249−1251	22 49 59.61047	−12 51 16.8025	0.0000254	0.000487	0.27	TGSS	446.5	1957.5	2007.8
J2250−2806	22 50 44.49211	−28 06 39.3230	0.0000132	0.000348	0.28	ALMA	−1.4	7.0	7.2
J2251−1848	22 51 31.38649	−18 48 07.9011	0.0000297	0.000669	0.04	Winn	−15.4	−23.1	27.8
J2252−2047	22 52 28.68048	−20 47 31.5512	0.0000173	0.000400	0.06	Winn	40.9	−2.2	41.0
J2254−4139	Extended Source, Multiple Components					AT20G	434.1	−820.9	928.6
J2256−1249	22 56 45.91492	−12 49 55.7419	0.0000133	0.000250	0.15	AT20G	659.3	−742.0	992.6
J2256−2011	Multiple Compact Components					ALMA			
J2256−2735	22 56 00.15718	−27 35 56.1195	0.0000168	0.000414	0.12	ALMA	−15.7	0.5	15.7
J2300−2644	23 00 25.50070	−26 44 22.7856	0.0000165	0.000456	0.10	Winn	−1.3	−17.6	17.7
J2301−0158	Multiple Compact Components					ALMA			
J2303−1841	23 03 02.97613	−18 41 25.8636	0.0000285	0.000629	0.13	ALMA	−1.9	−43.6	43.6
J2307−2247	23 07 38.65679	−22 47 53.0228	0.0000291	0.000673	0.13	AT20G	874.1	277.2	917.0
J2313−3704	Extended Source					AT20G			
J2318−4032	Extended Source					AT20G			
J2323−0150	23 23 04.62953	−01 50 48.1016	0.0000141	0.000235	0.40	Winn	16.0	0.4	16.0
J2328−4035	Multiple Compact Components					ALMA			
J2330−1656	23 30 55.45338	−16 56 39.6046	0.0000194	0.000408	0.32	Winn	3.2	11.4	11.9
J2332−1423	23 32 31.77823	−14 23 20.5057	0.0000179	0.000368	0.14	Winn	17.0	12.2	20.9
J2332−4118	Multiple Compact Components					AT20G			
J2333−0131	23 33 16.68861	−01 31 07.3733	0.0000207	0.000332	0.21	AT20G	1520.4	326.7	1555.1
J2335−0131	23 35 20.41237	−01 31 09.5765	0.0000118	0.000197	0.62	ALMA	−5.6	13.5	14.6
J2335−2907	Multiple Compact Components					Winn			
J2336−4115	Inadequate Data					ALMA			
J2342−0322	23 42 56.60067	−03 22 26.2642	0.0000101	0.000177	0.25	Winn	−20.6	−5.3	21.3
J2345−1555	23 45 12.46228	−15 55 07.8403	0.0000065	0.000141	2.88	ALMA	−4.1	−10.3	11.1
J2347−1856	23 47 08.62577	−18 56 18.8592	0.0000185	0.000414	0.58	AT20G	−365.7	−559.2	668.1
J2348−0425	23 48 11.75737	−04 25 56.3933	0.0000134	0.000237	0.43	AT20G	1534.9	806.8	1734.0
J2349−0438	23 49 10.16571	−04 38 03.3883	0.0000124	0.000223	0.41	AT20G	961.2	611.7	1139.3
J2354−0019	23 54 09.17606	−00 19 47.9596	0.0000119	0.000206	0.57	Winn	2.2	−25.6	25.7
J2354−0405	23 54 51.68181	−04 05 03.4837	0.0000301	0.000450	0.12	Winn	−51.1	−35.7	62.3
J2354−4106	Extended Source, Multiple Components					AT20G			
J2355+1541	Multiple Compact Components					TGSS			
J2357−0152	23 57 25.13849	−01 52 15.5105	0.0000134	0.000234	0.32	Winn	−31.4	−31.5	44.5
J2357−2451	23 57 23.84901	−24 51 03.1265	0.0000430	0.001058	0.17	Winn	−11.0	−9.5	14.5
J2359−0031	23 59 36.82108	−00 31 12.8661	0.0000172	0.000294	0.19	AT20G	2683.7	1433.9	3042.8

[a] : Calibrated with source *a* in Table 8, [b] with source *b*, etc.

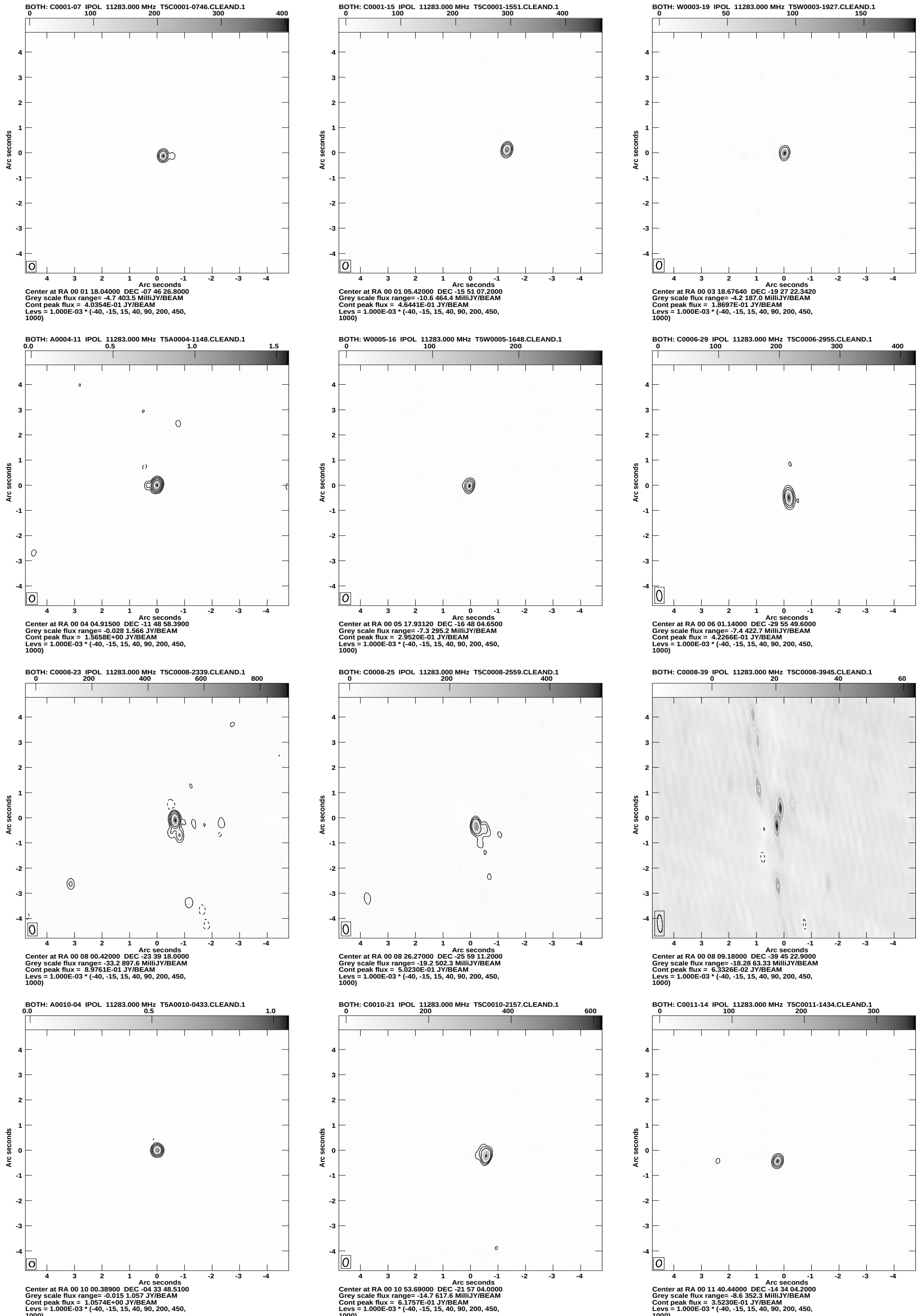

Figure 4. Images for alternative VLA reference sources, sorted in RA.

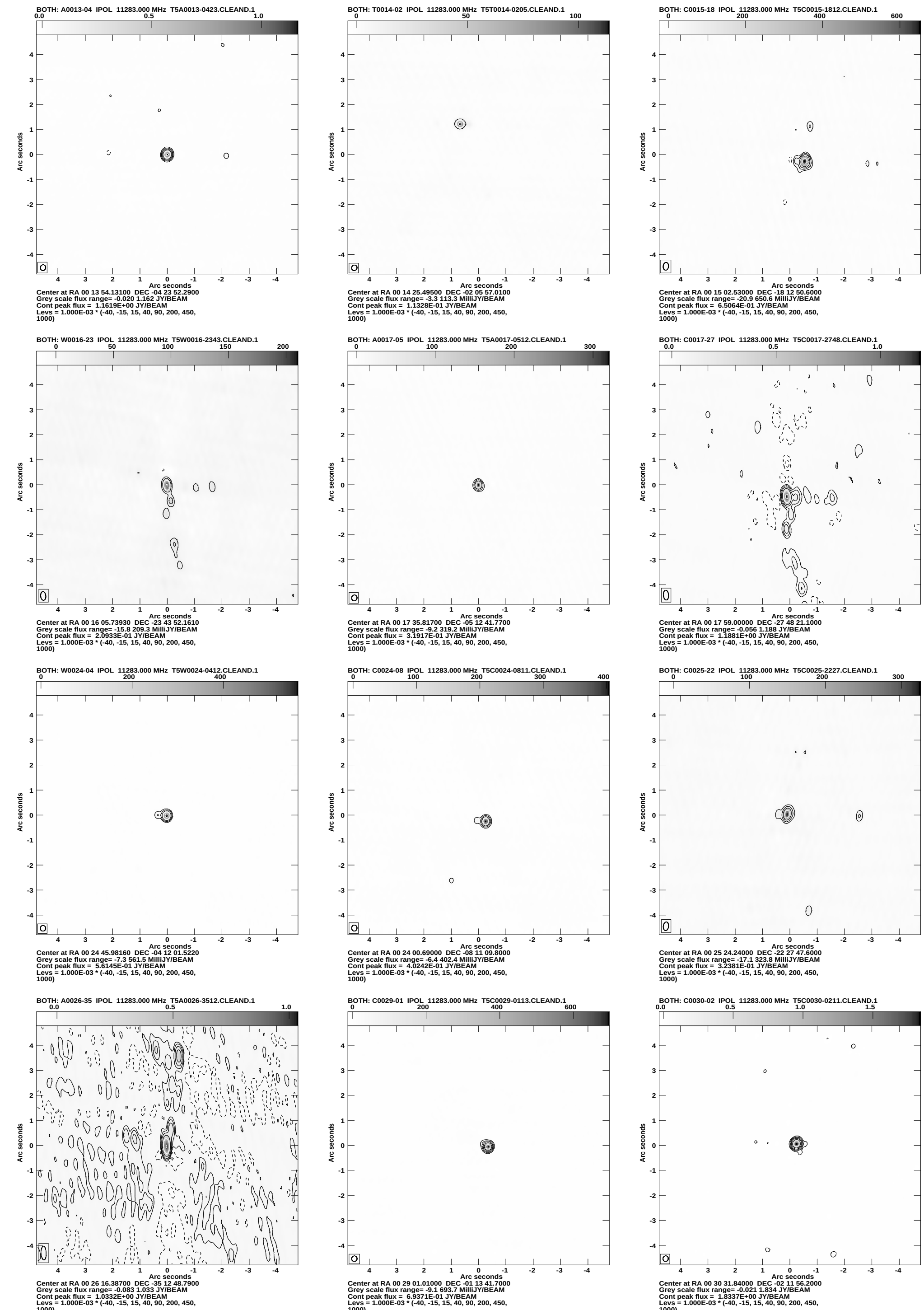

Figure 4. Images for alternative VLA reference sources, sorted in RA. (continued)

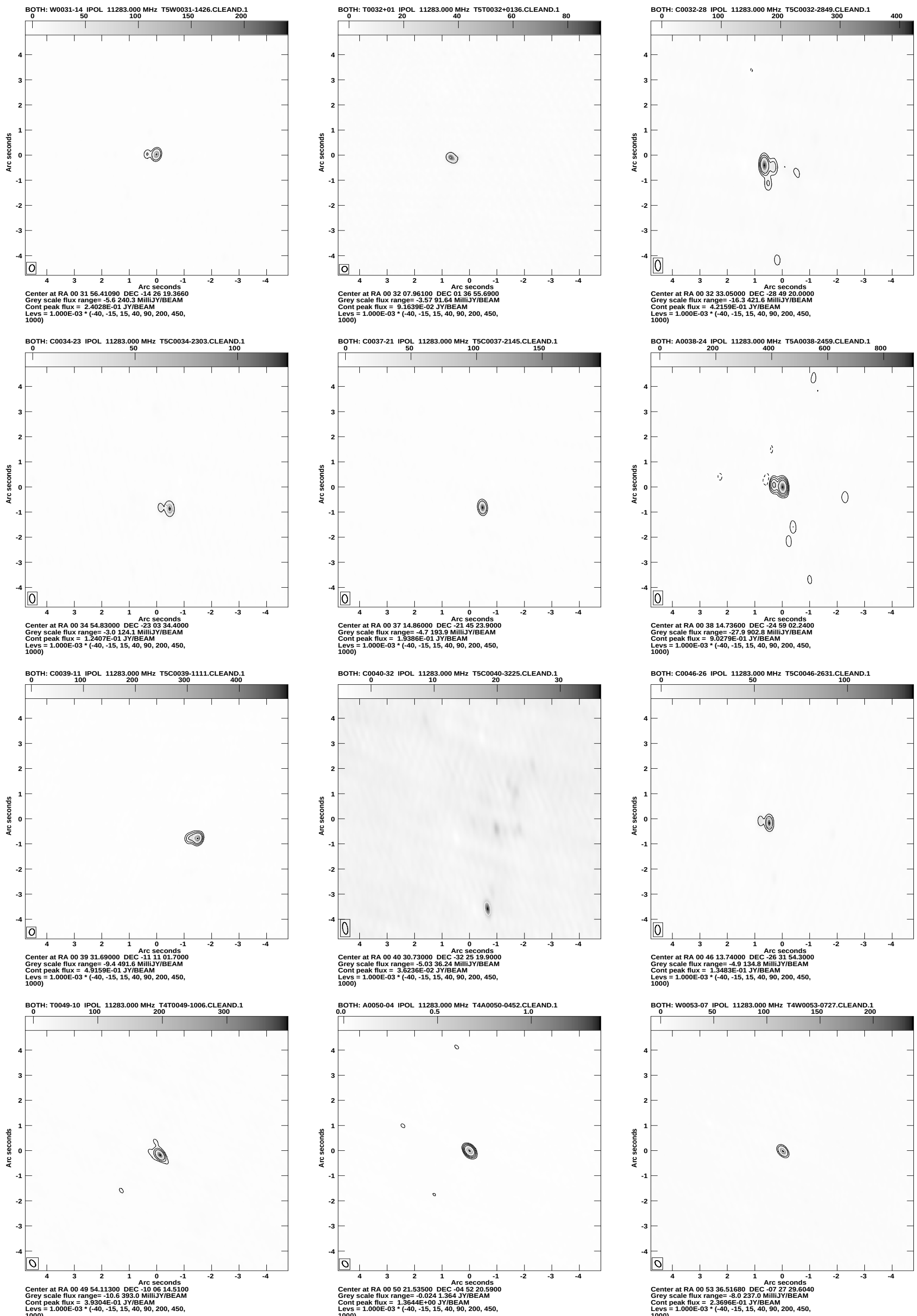

Figure 4. Images for alternative VLA reference sources, sorted in RA. (continued)

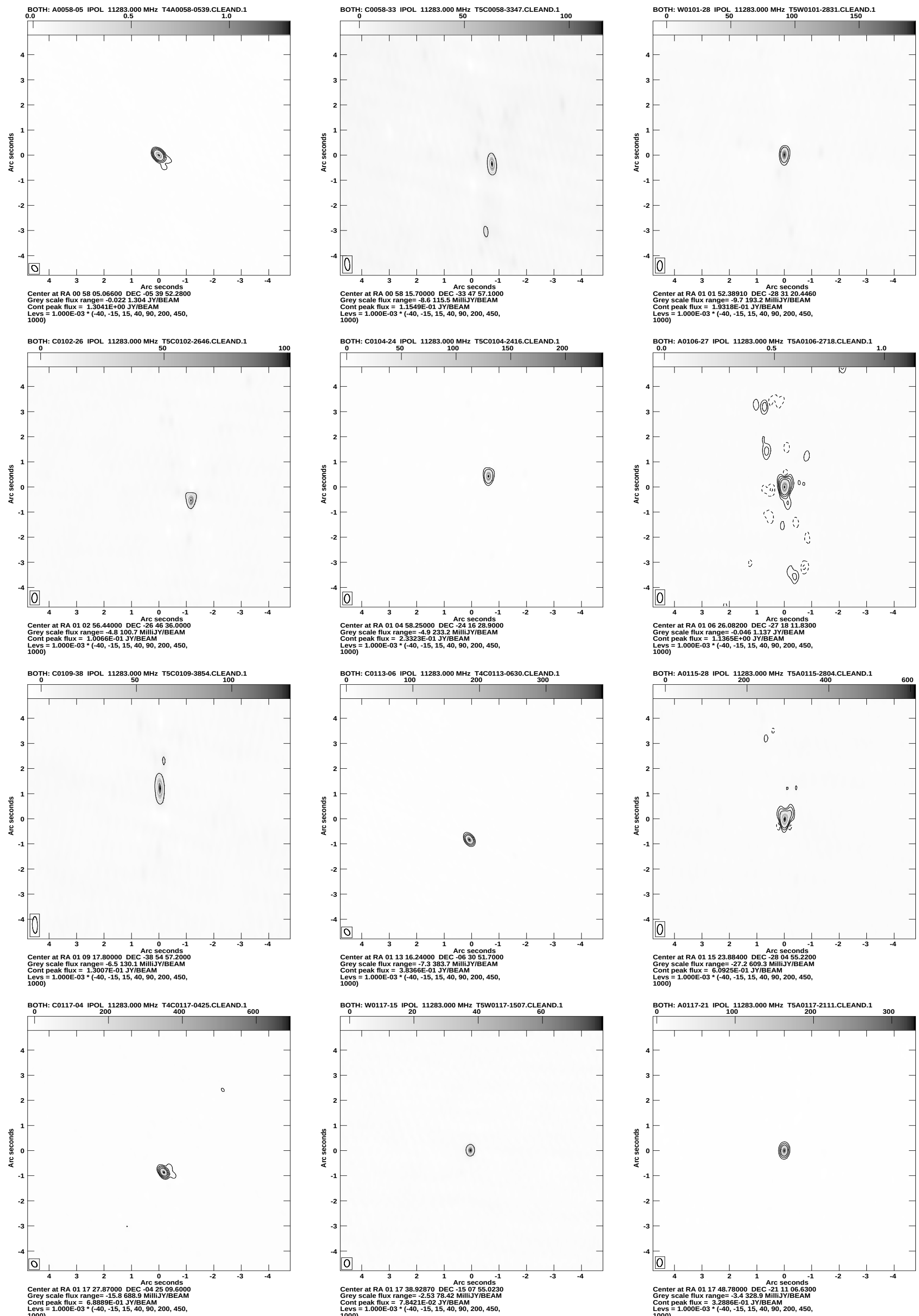

Figure 4. Images for alternative VLA reference sources, sorted in RA. (continued)

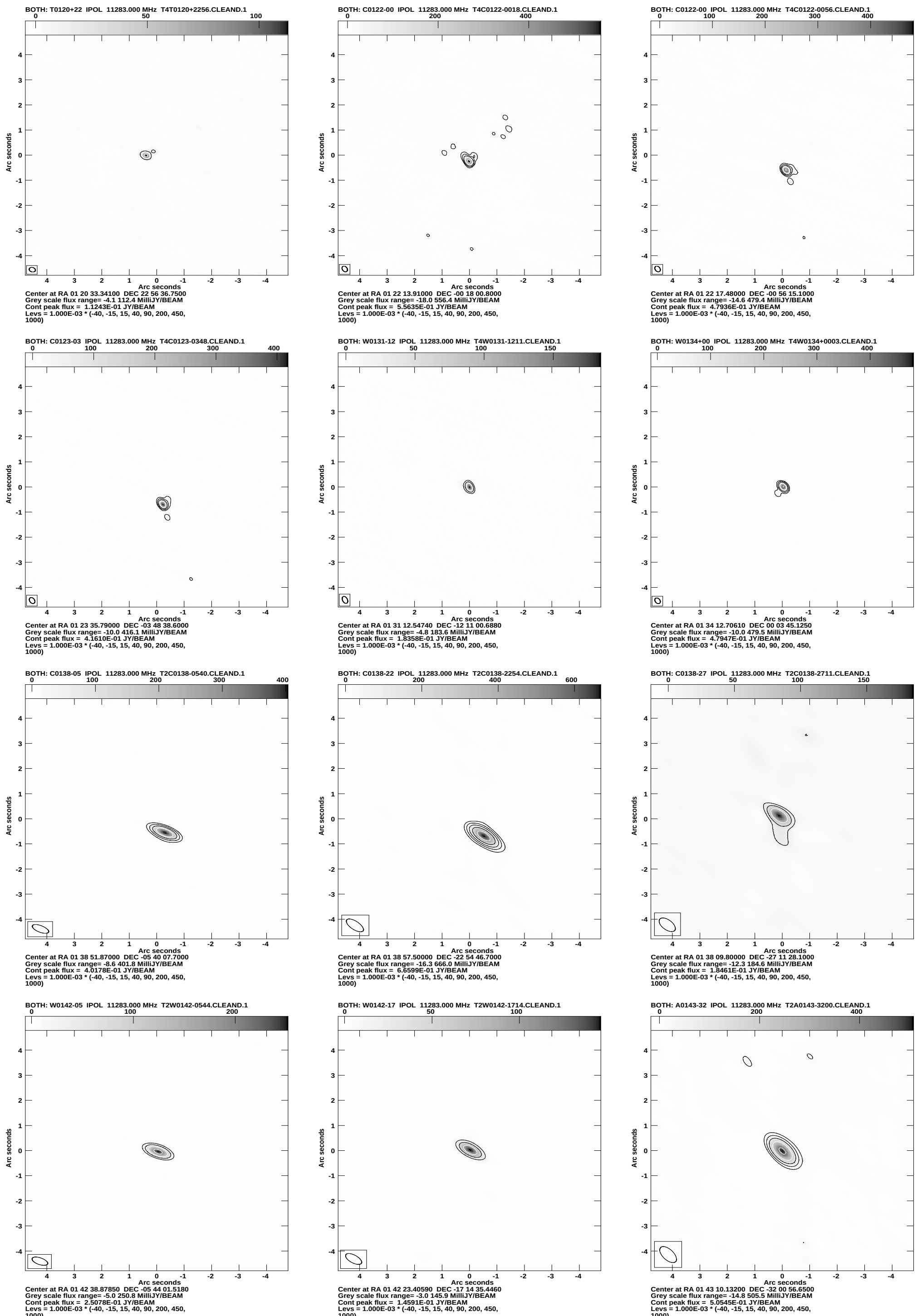

Figure 4. Images for alternative VLA reference sources, sorted in RA. (continued)

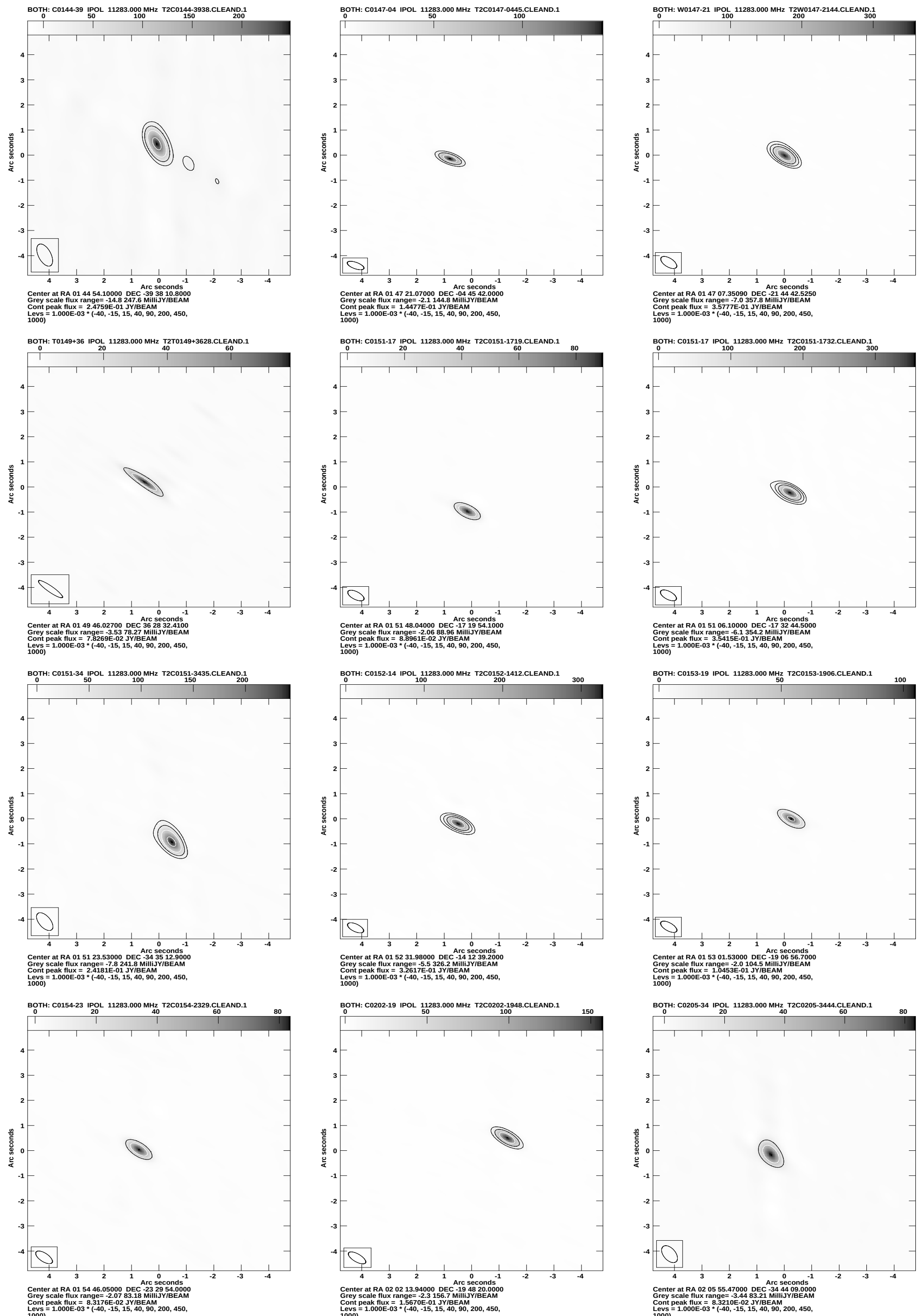

Figure 4. Images for alternative VLA reference sources, sorted in RA. (continued)

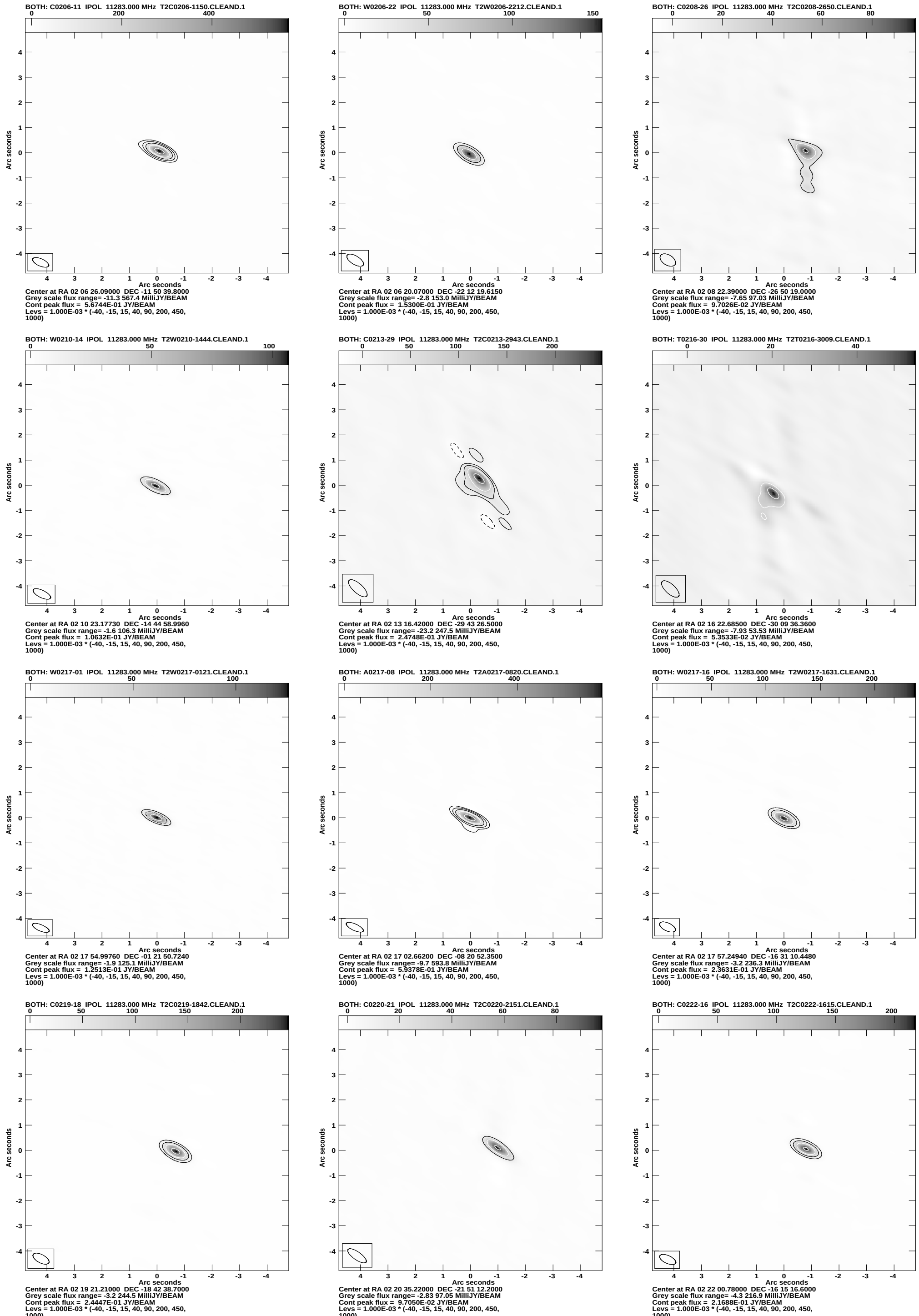

Figure 4. Images for alternative VLA reference sources, sorted in RA. (continued)

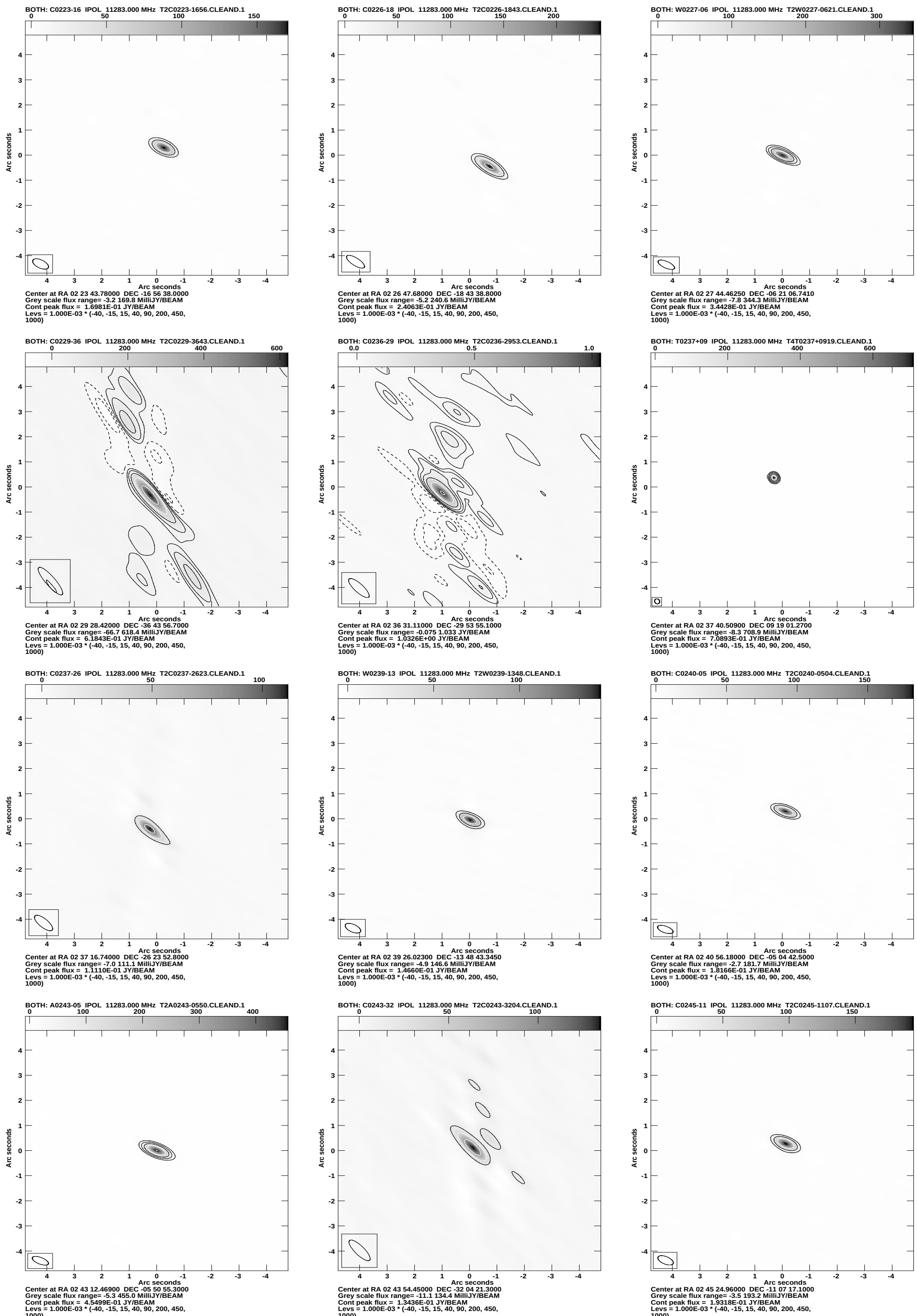

Figure 4. Images for alternative VLA reference sources, sorted in RA. (continued)

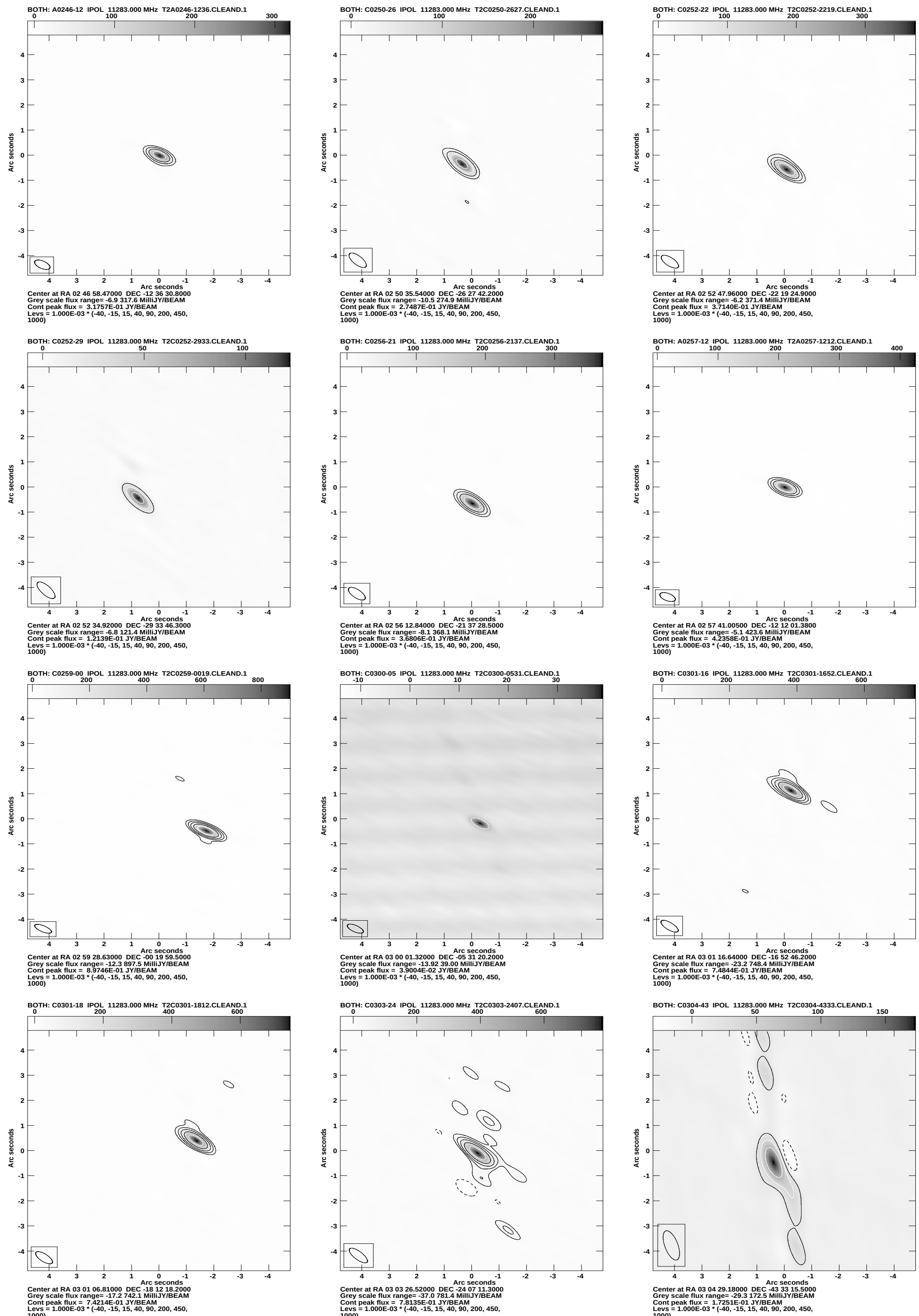

Figure 4. Images for alternative VLA reference sources, sorted in RA. (continued)

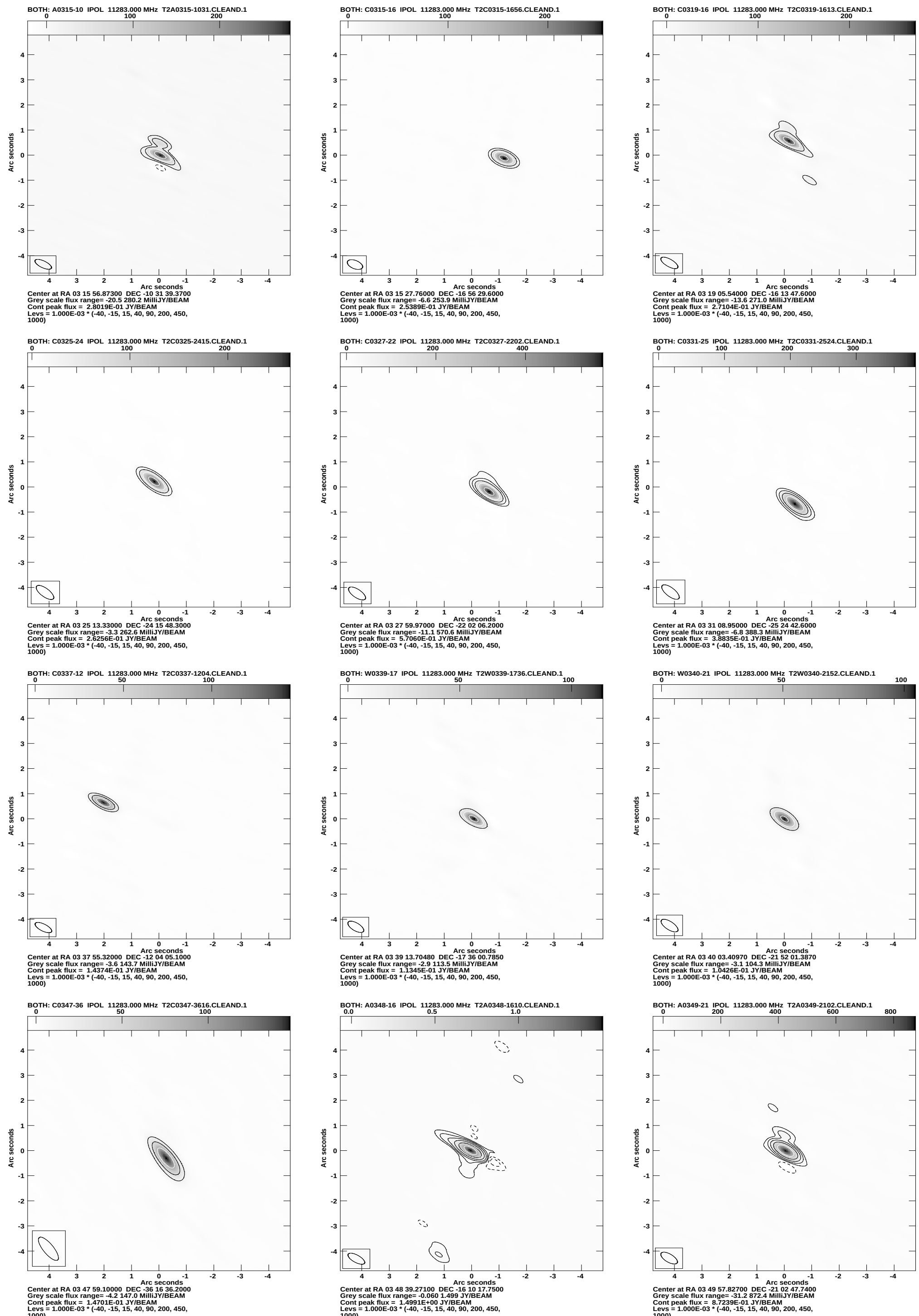

Figure 4. Images for alternative VLA reference sources, sorted in RA. (continued)

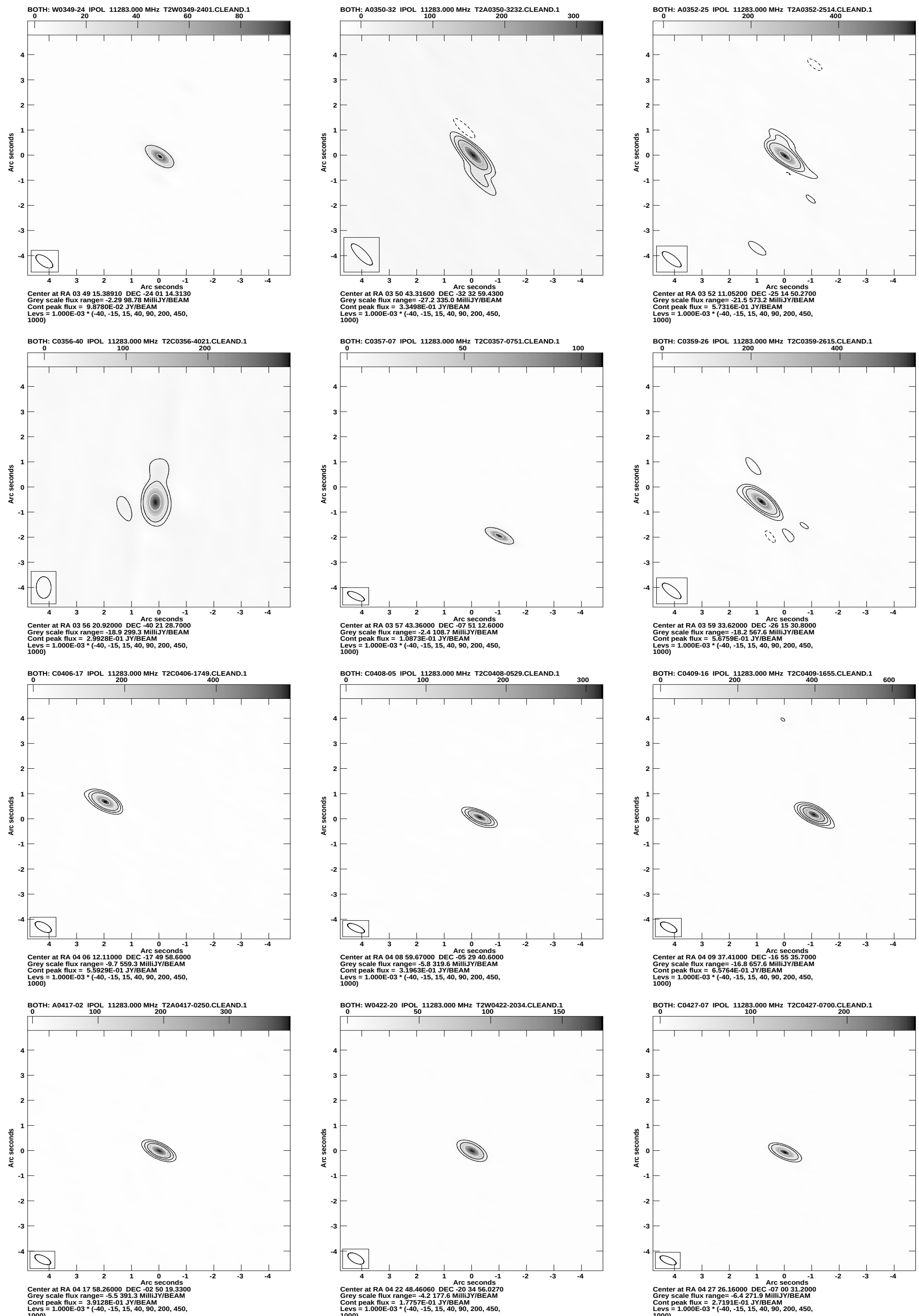

Figure 4. Images for alternative VLA reference sources, sorted in RA. (continued)

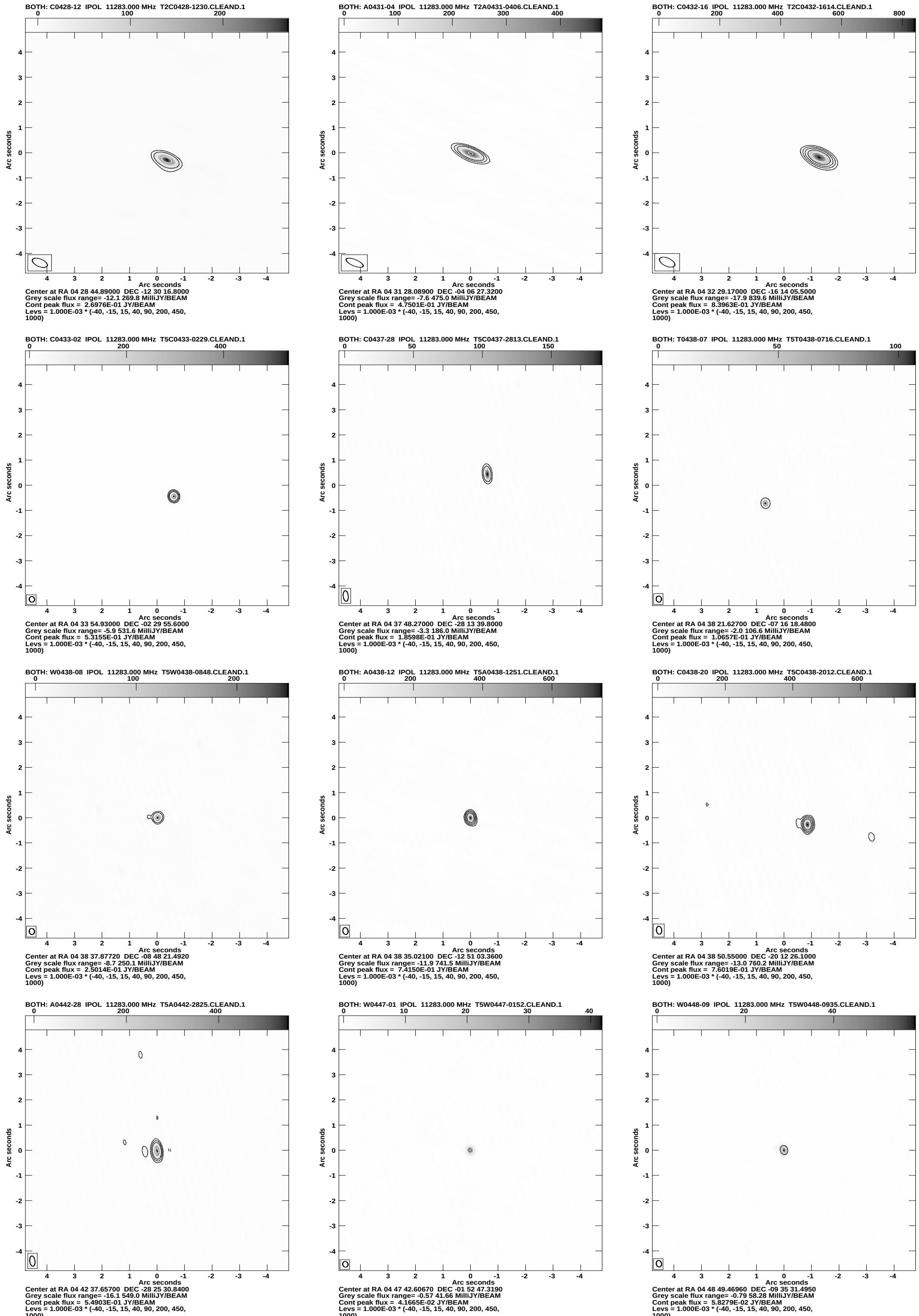

Figure 4. Images for alternative VLA reference sources, sorted in RA. (continued)

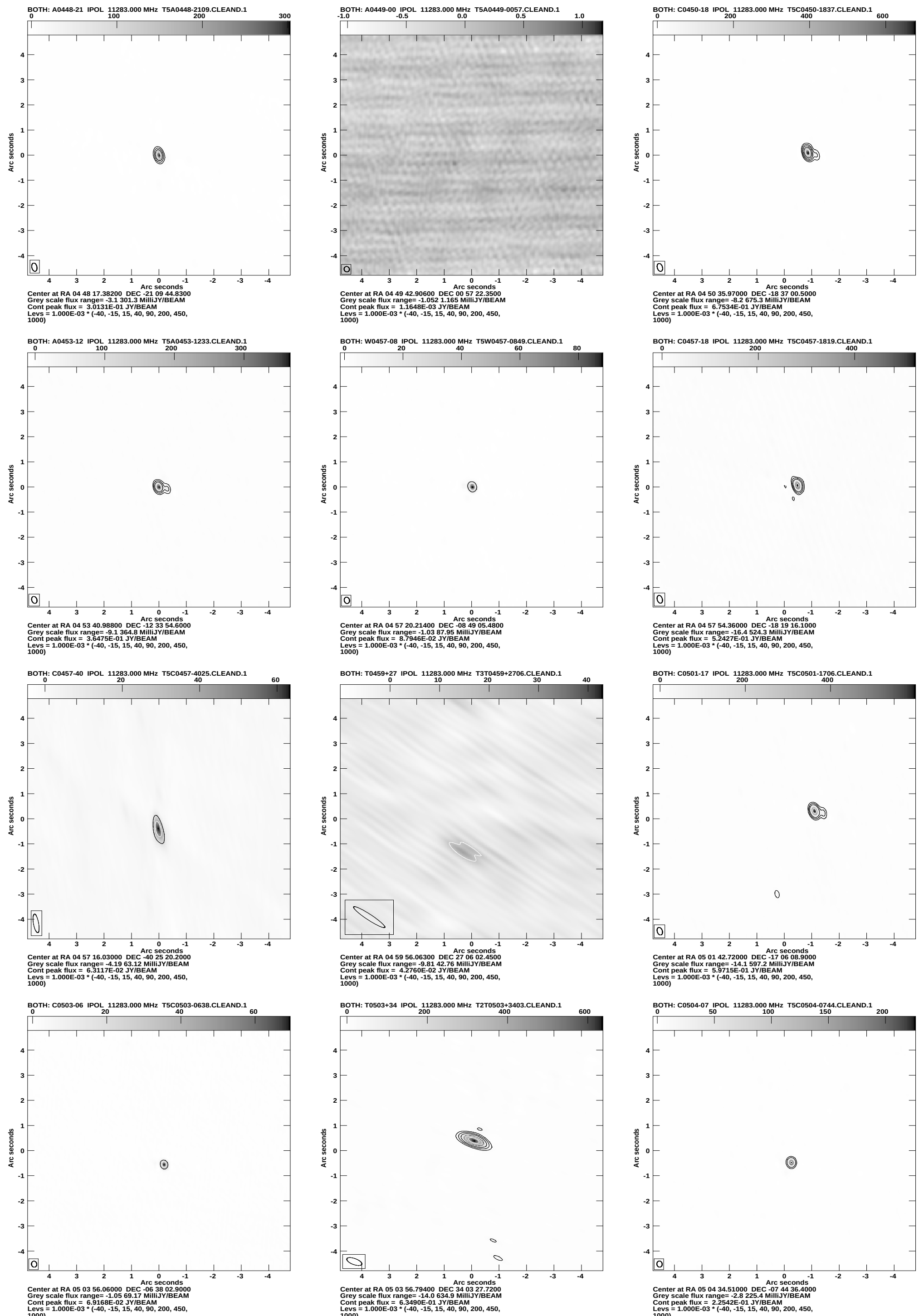

Figure 4. Images for alternative VLA reference sources, sorted in RA. (continued)

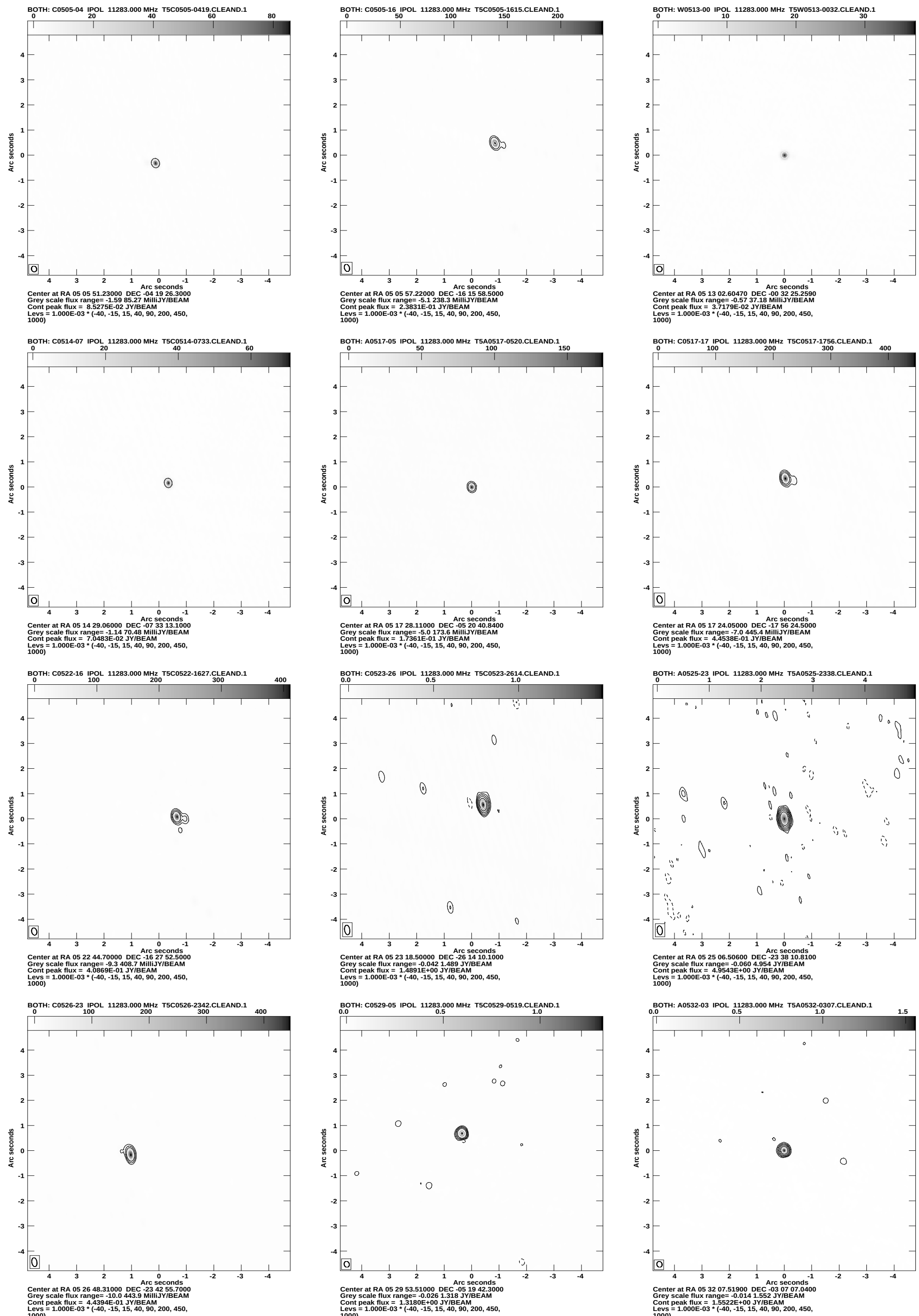

Figure 4. Images for alternative VLA reference sources, sorted in RA. (continued)

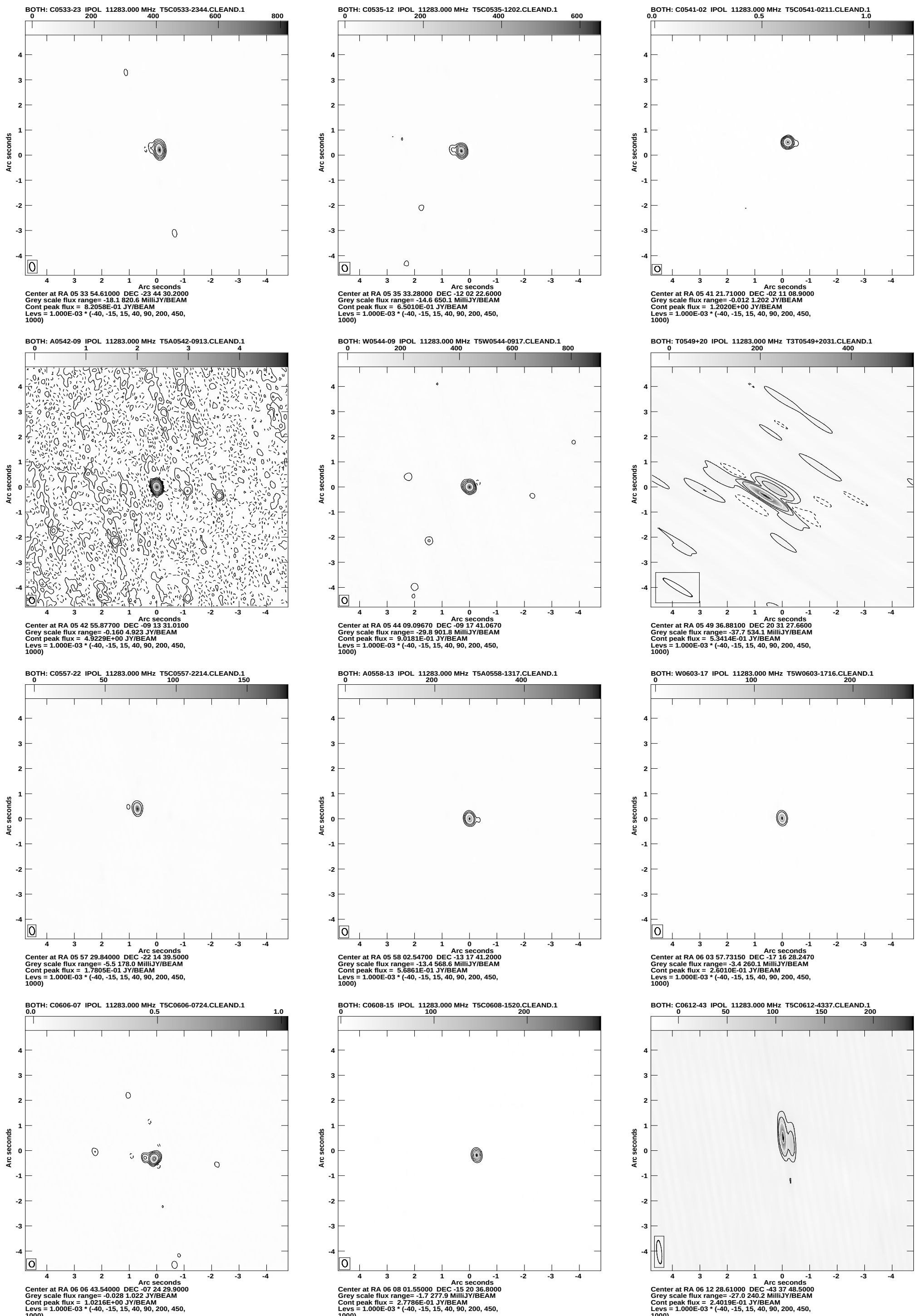

Figure 4. Images for alternative VLA reference sources, sorted in RA. (continued)

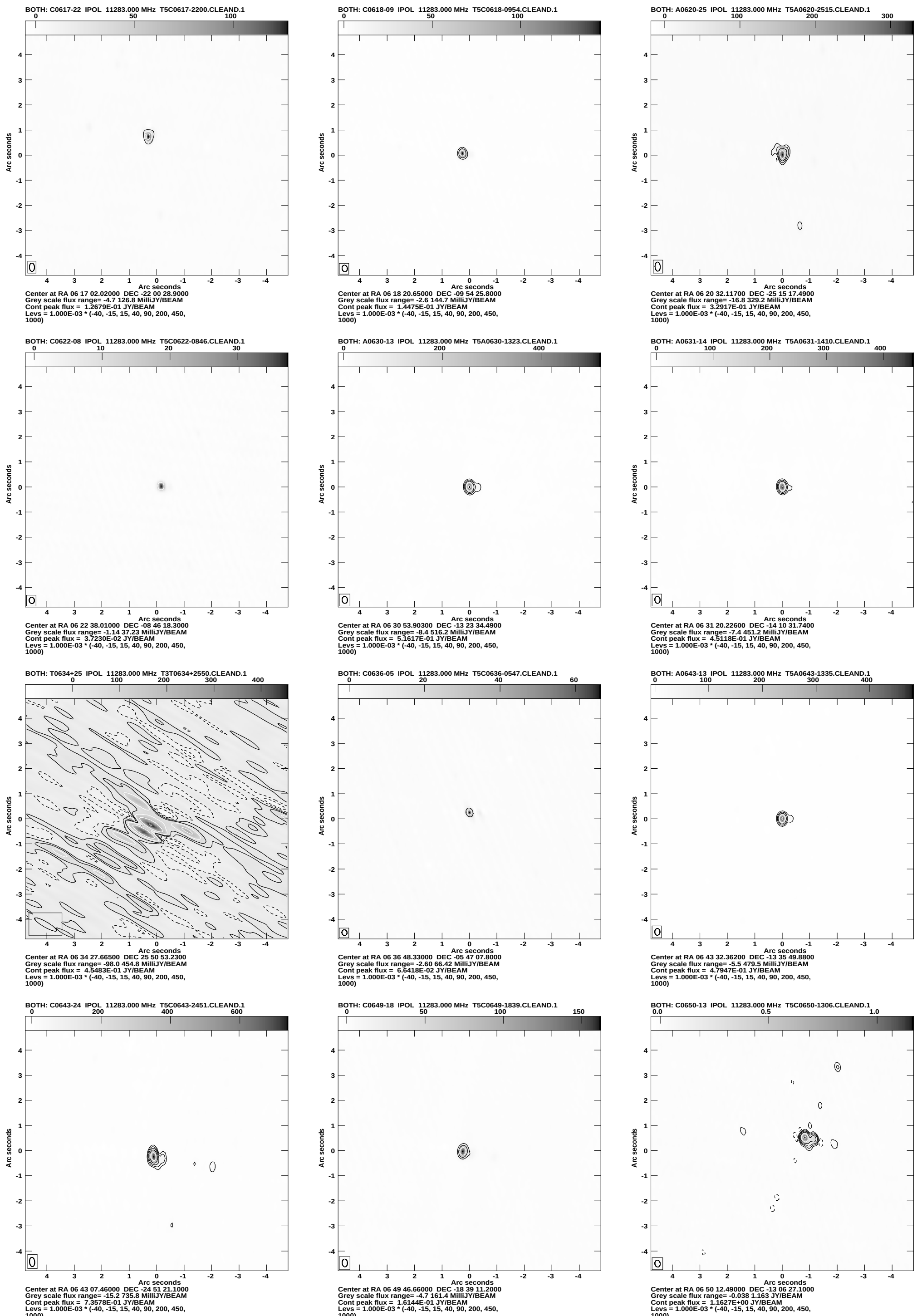

Figure 4. Images for alternative VLA reference sources, sorted in RA. (continued)

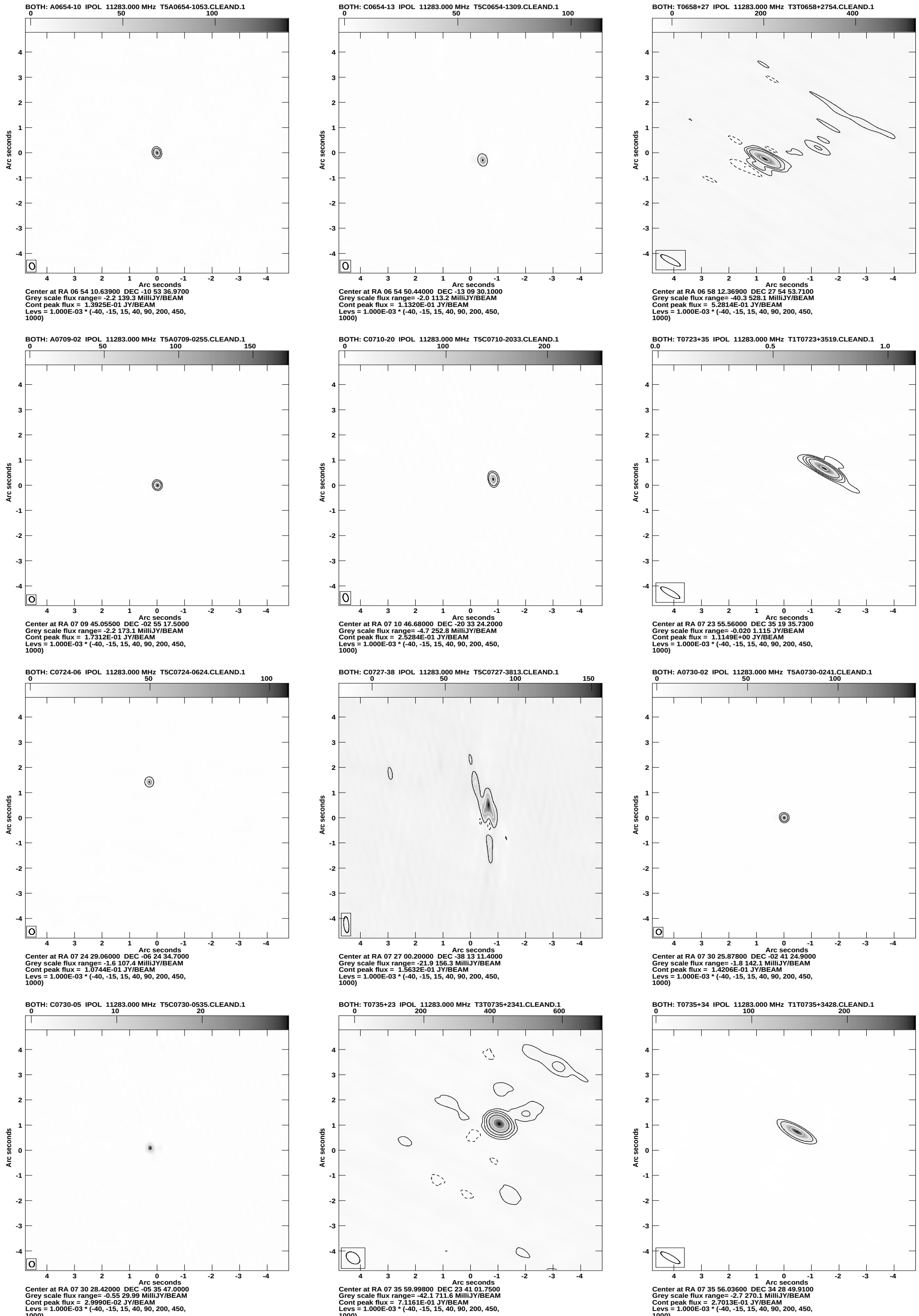

Figure 4. Images for alternative VLA reference sources, sorted in RA. (continued)

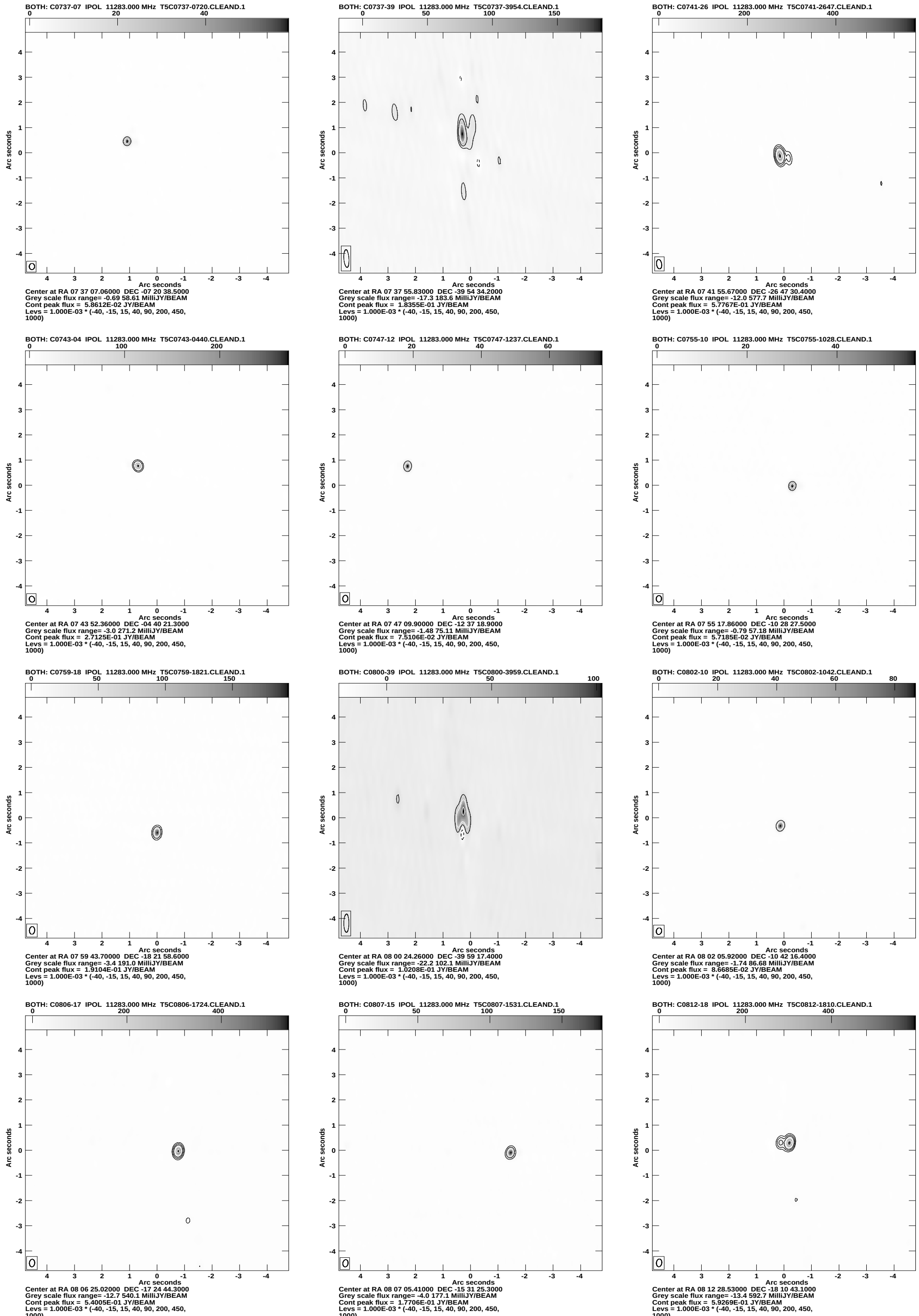

Figure 4. Images for alternative VLA reference sources, sorted in RA. (continued)

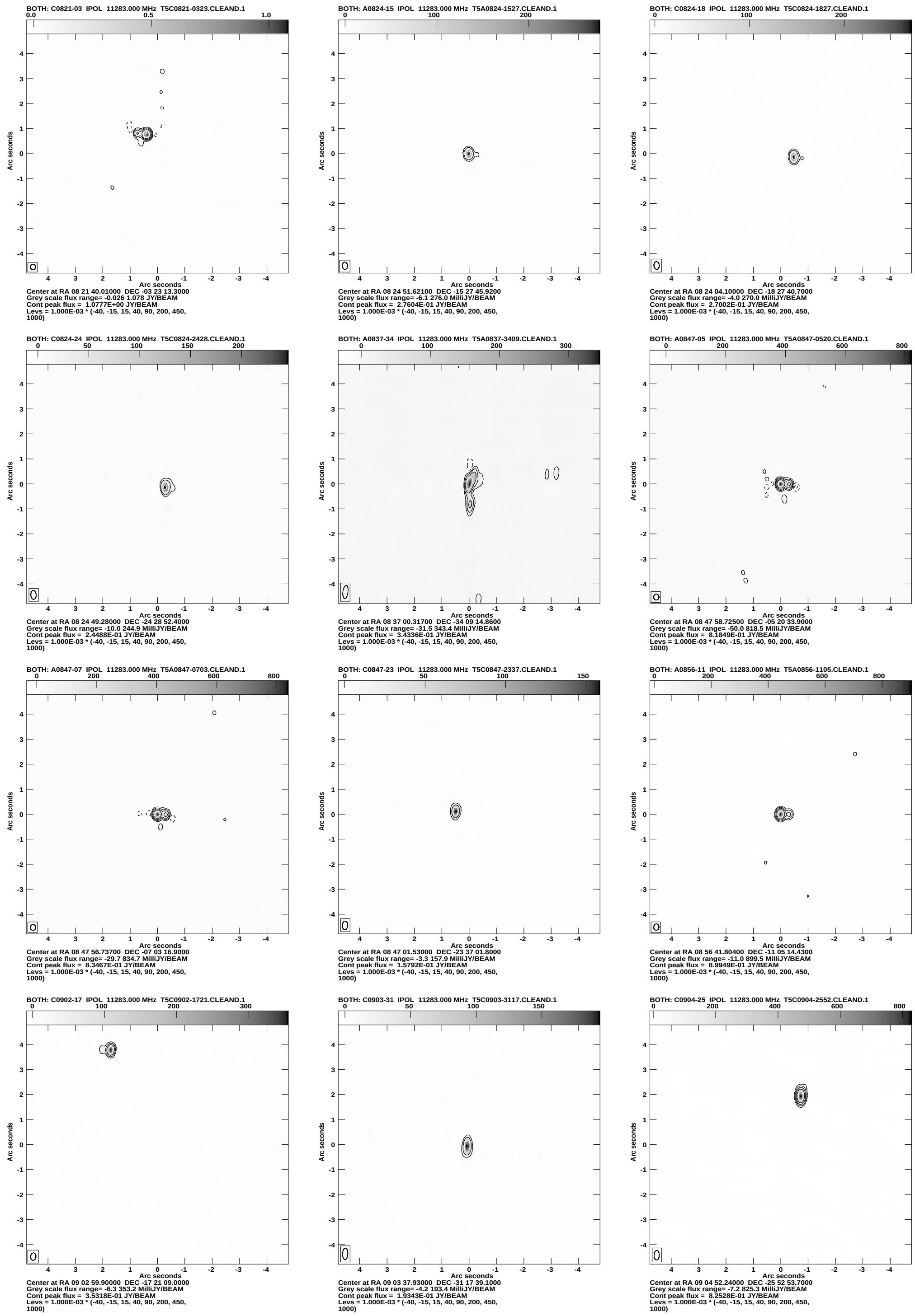

Figure 4. Images for alternative VLA reference sources, sorted in RA. (continued)

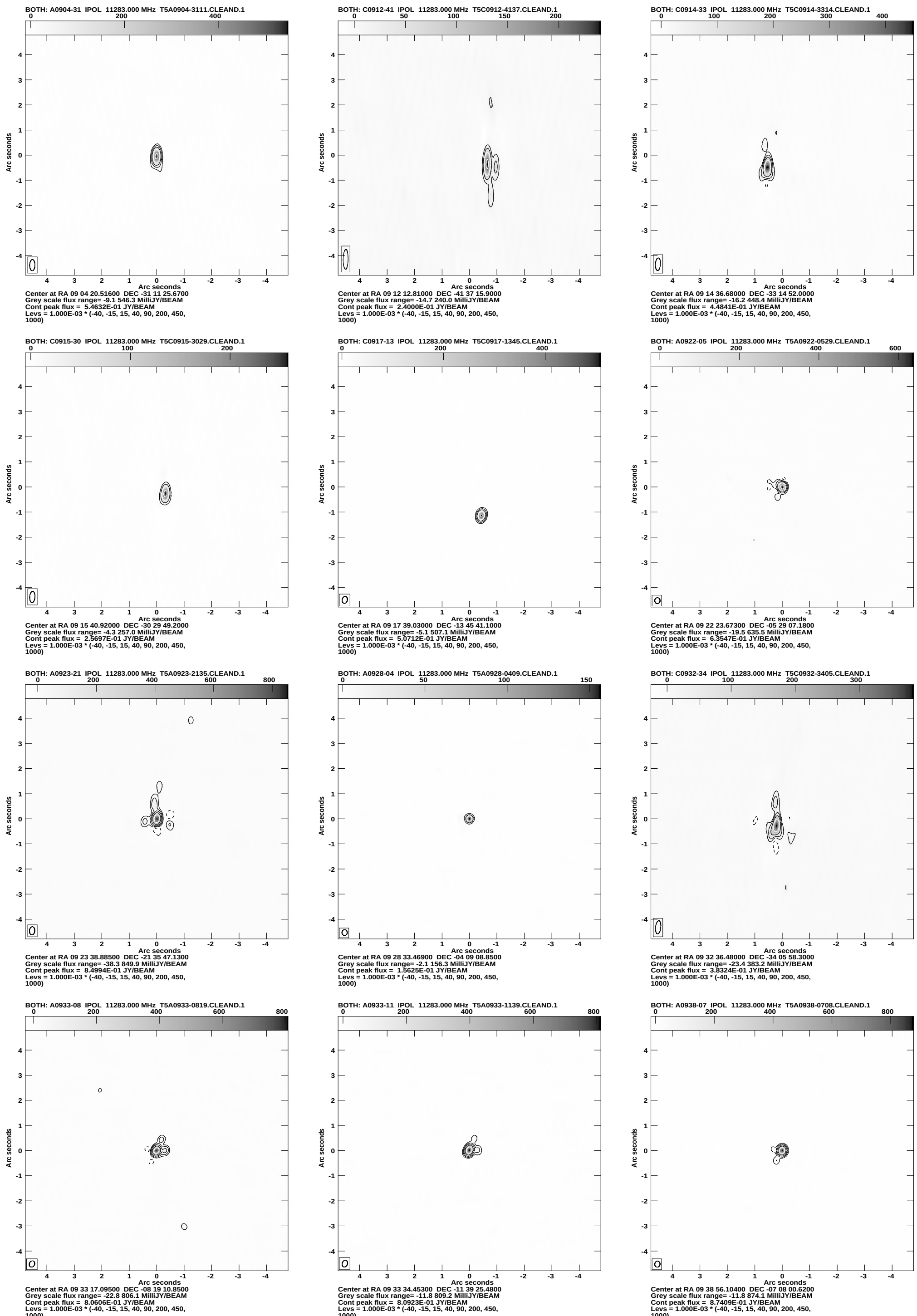

Figure 4. Images for alternative VLA reference sources, sorted in RA. (continued)

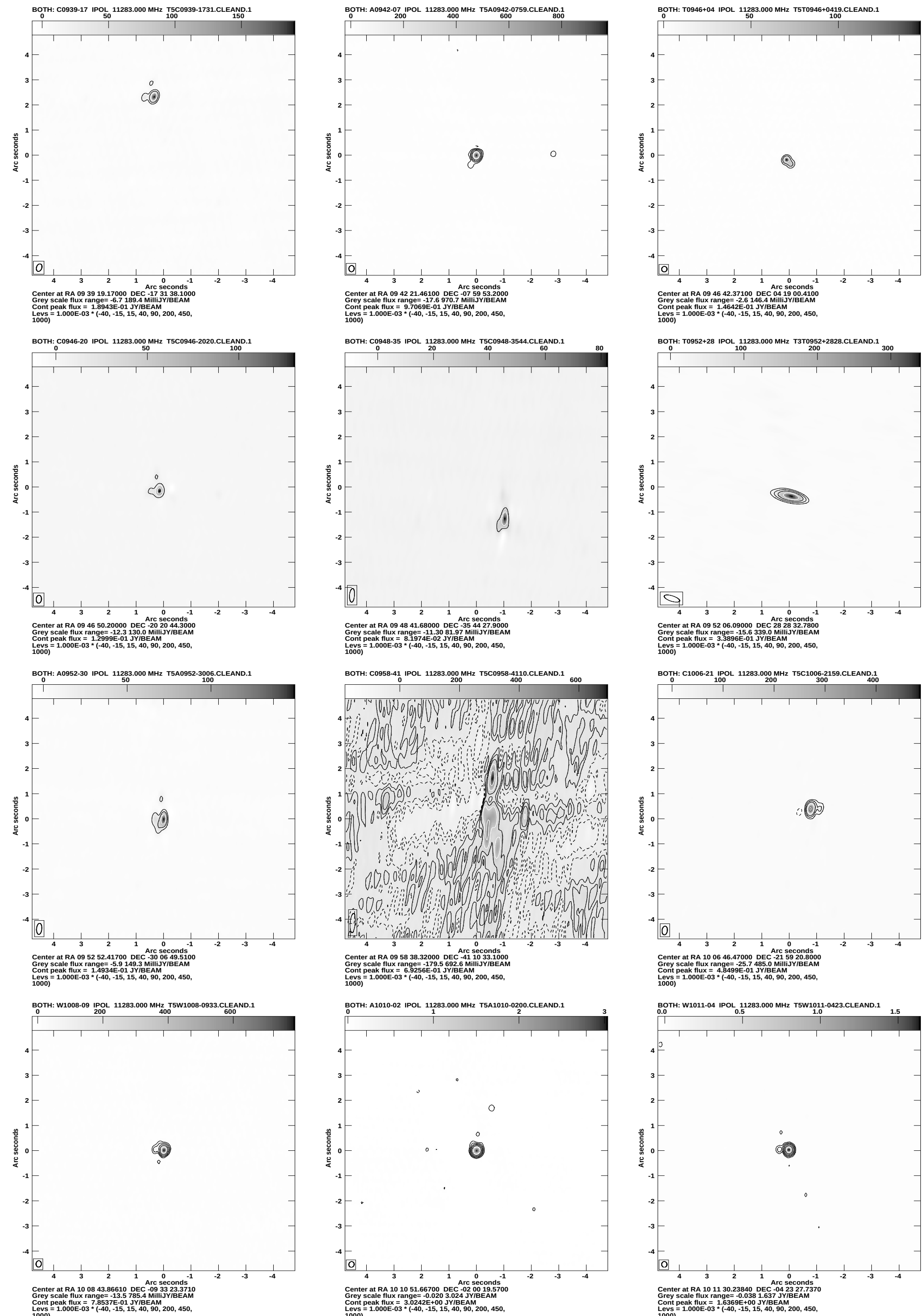

Figure 4. Images for alternative VLA reference sources, sorted in RA. (continued)

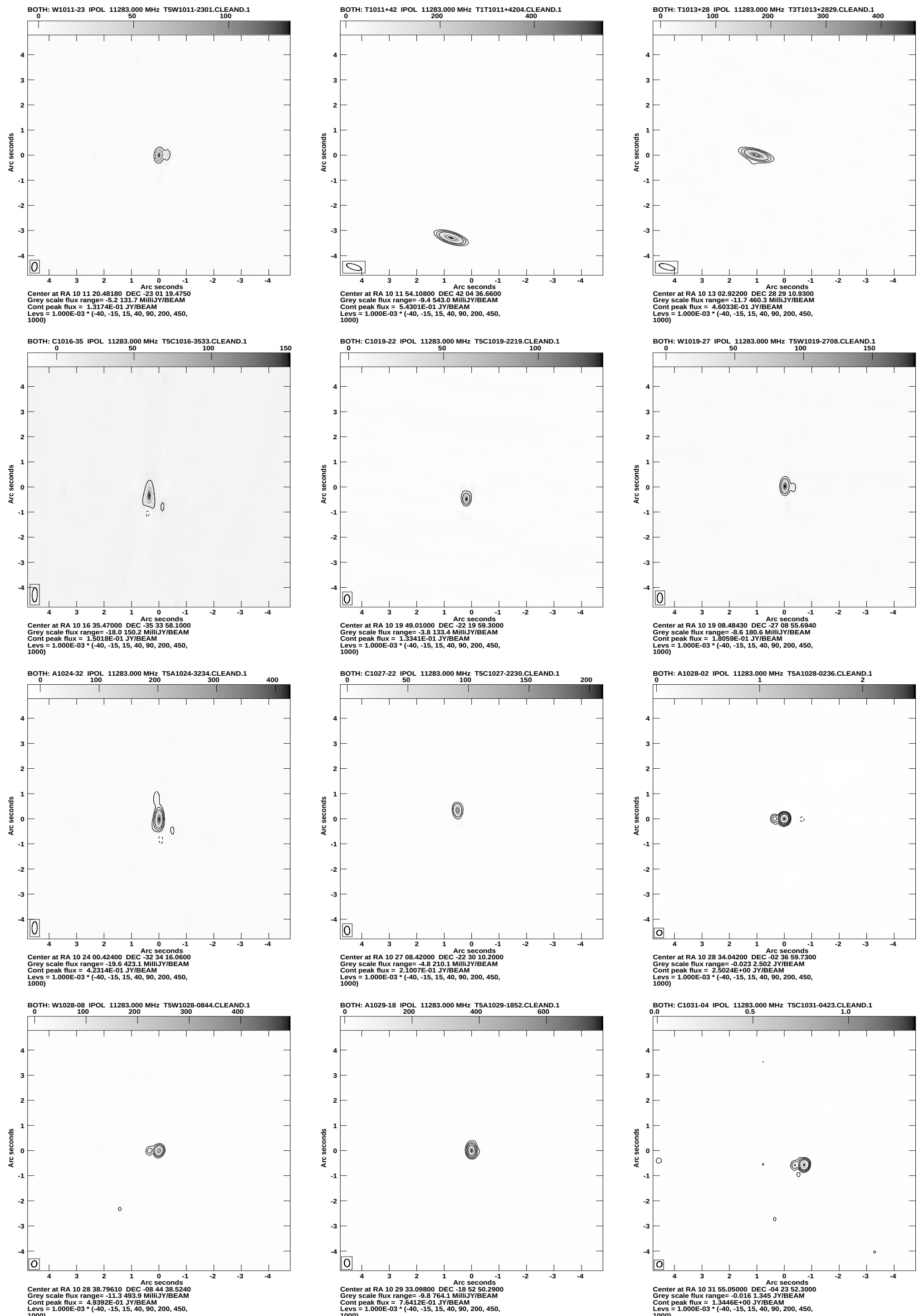

Figure 4. Images for alternative VLA reference sources, sorted in RA. (continued)

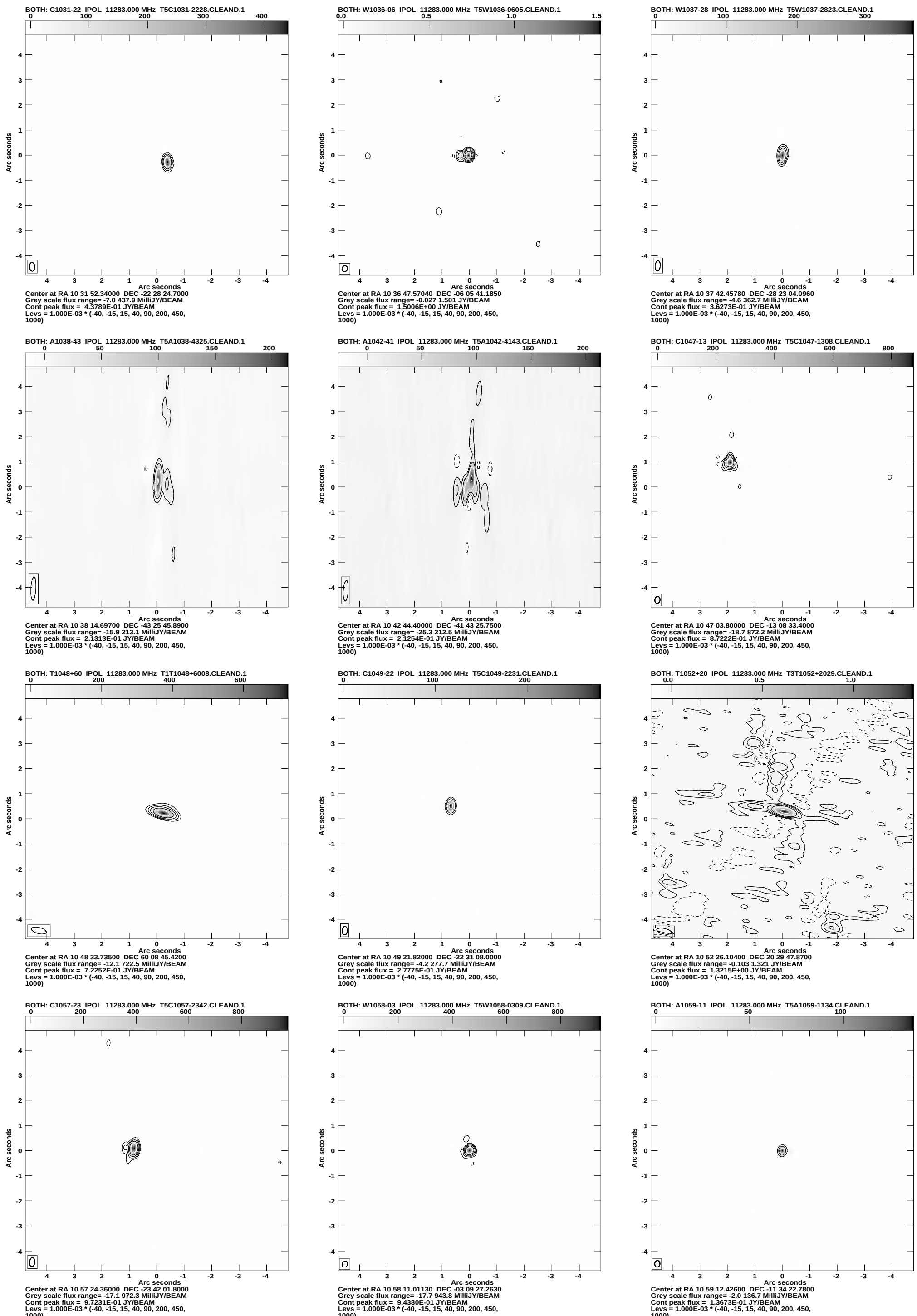

Figure 4. Images for alternative VLA reference sources, sorted in RA. (continued)

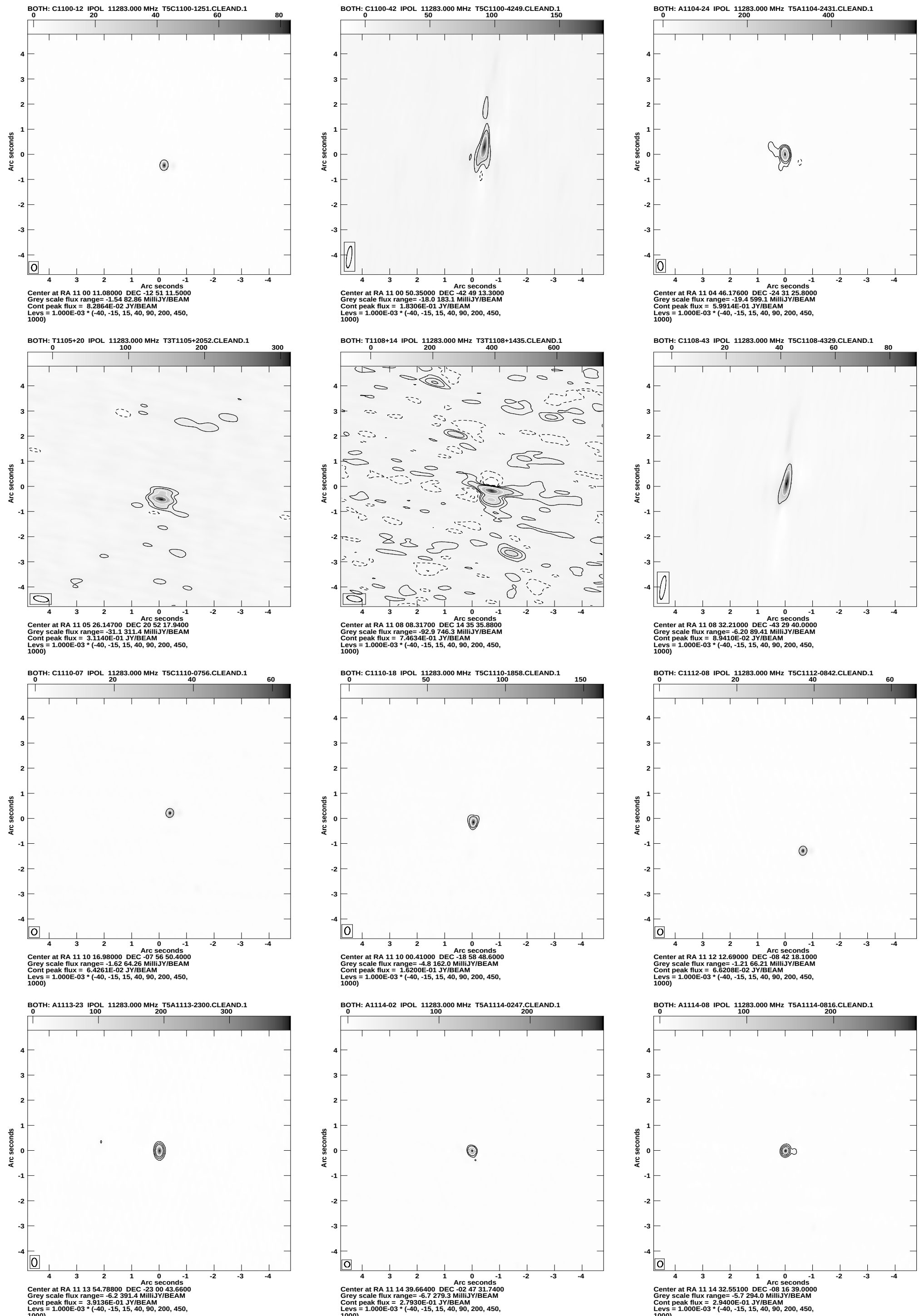

Figure 4. Images for alternative VLA reference sources, sorted in RA. (continued)

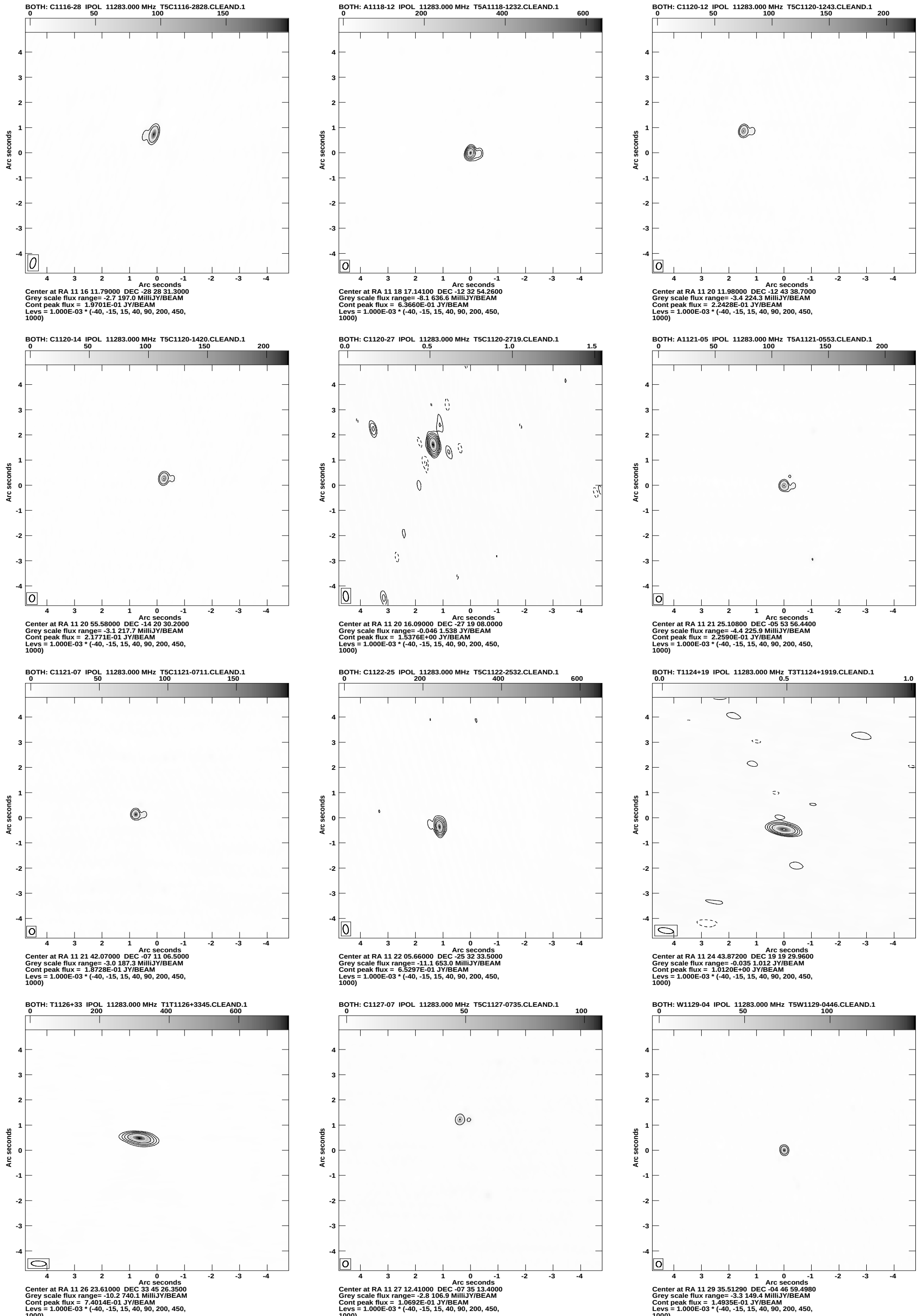

Figure 4. Images for alternative VLA reference sources, sorted in RA. (continued)

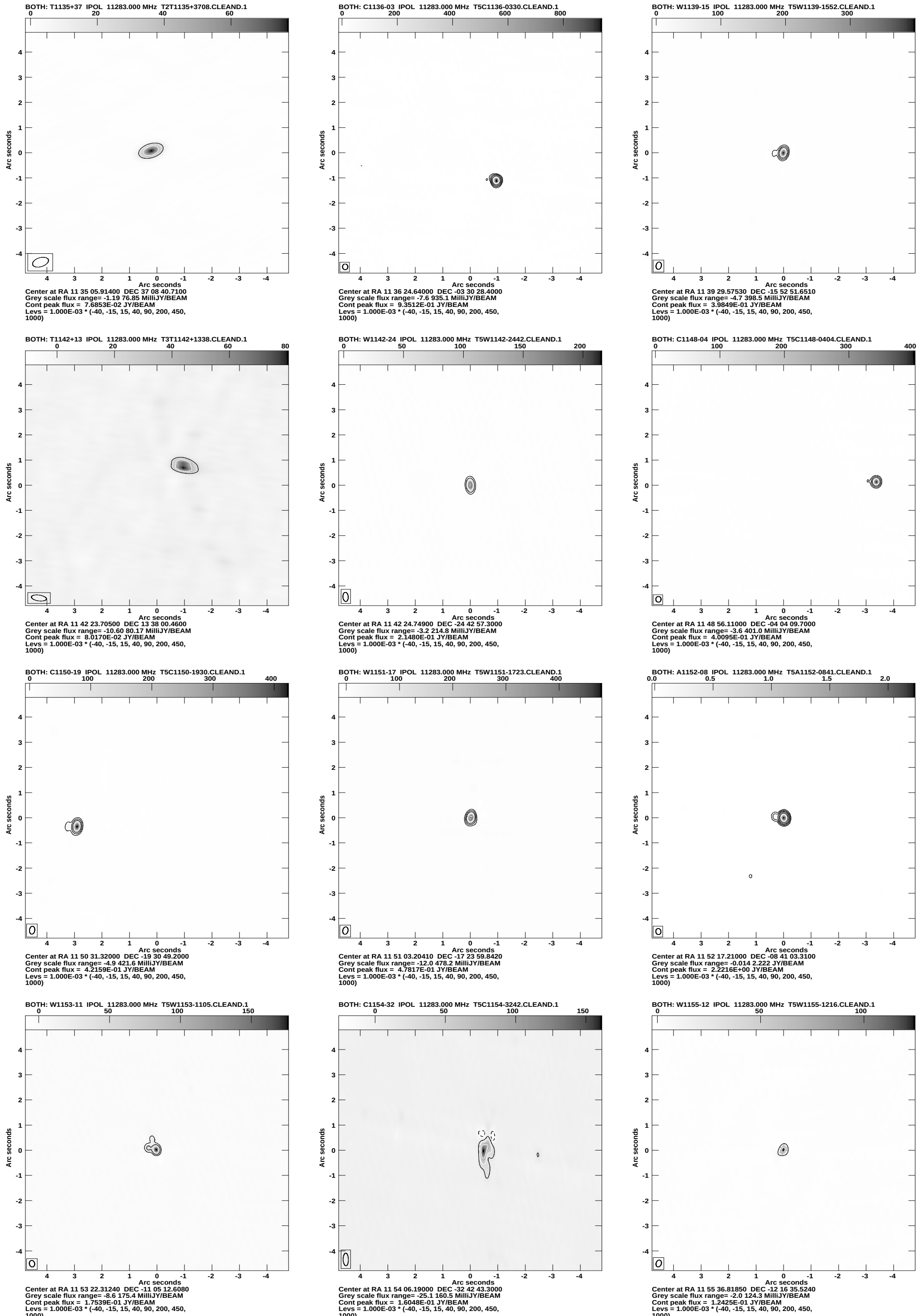

Figure 4. Images for alternative VLA reference sources, sorted in RA. (continued)

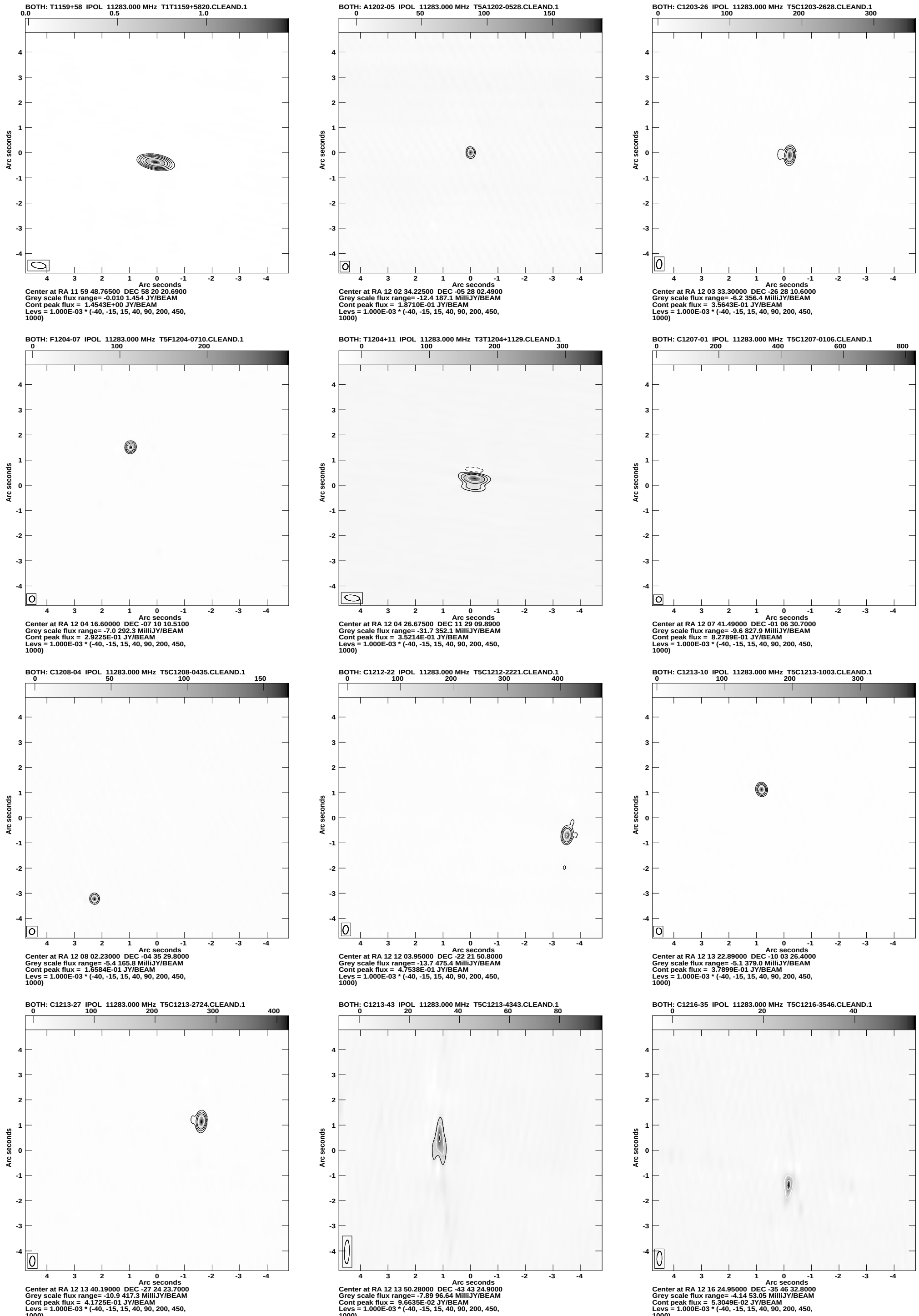

Figure 4. Images for alternative VLA reference sources, sorted in RA. (continued)

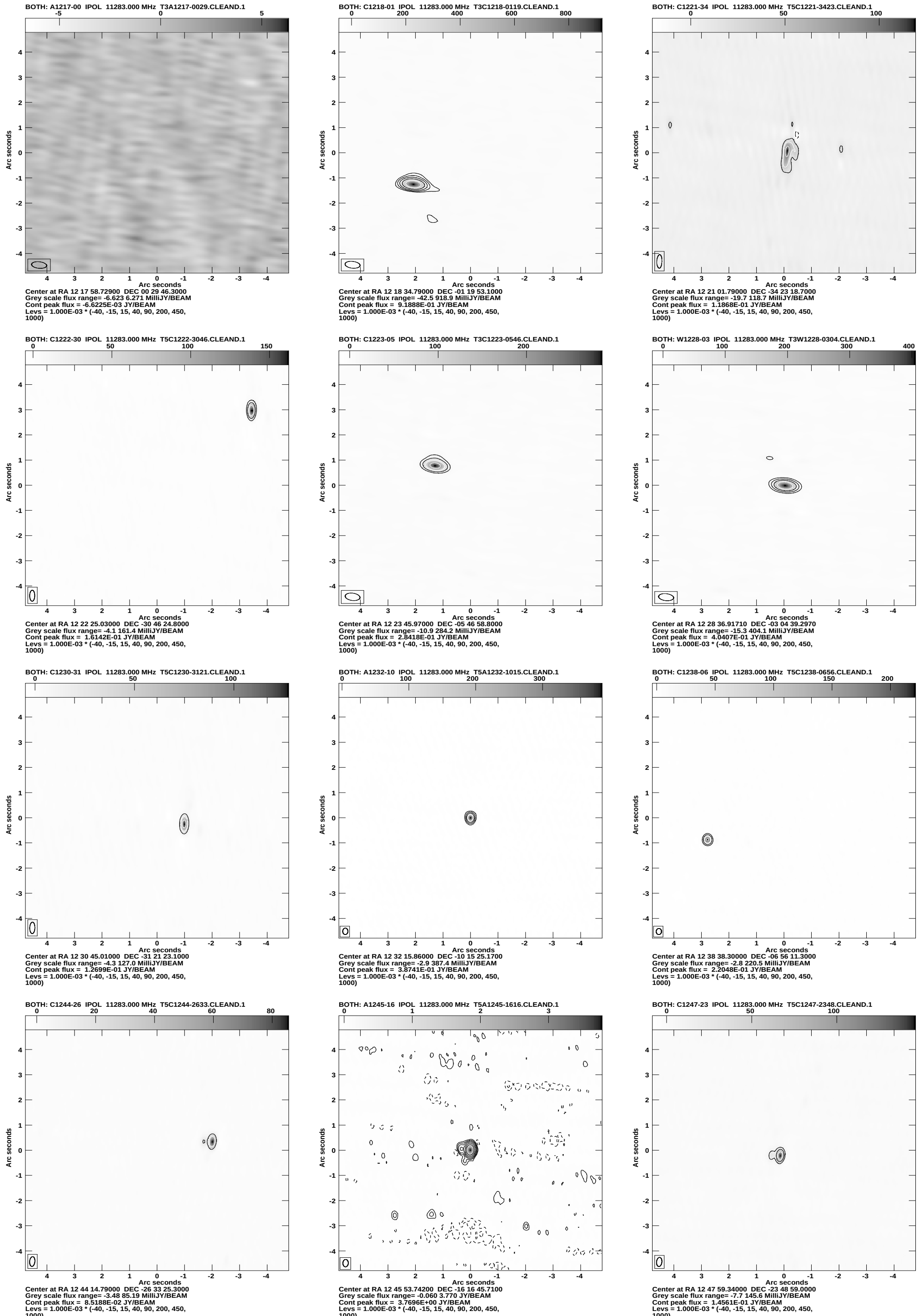

Figure 4. Images for alternative VLA reference sources, sorted in RA. (continued)

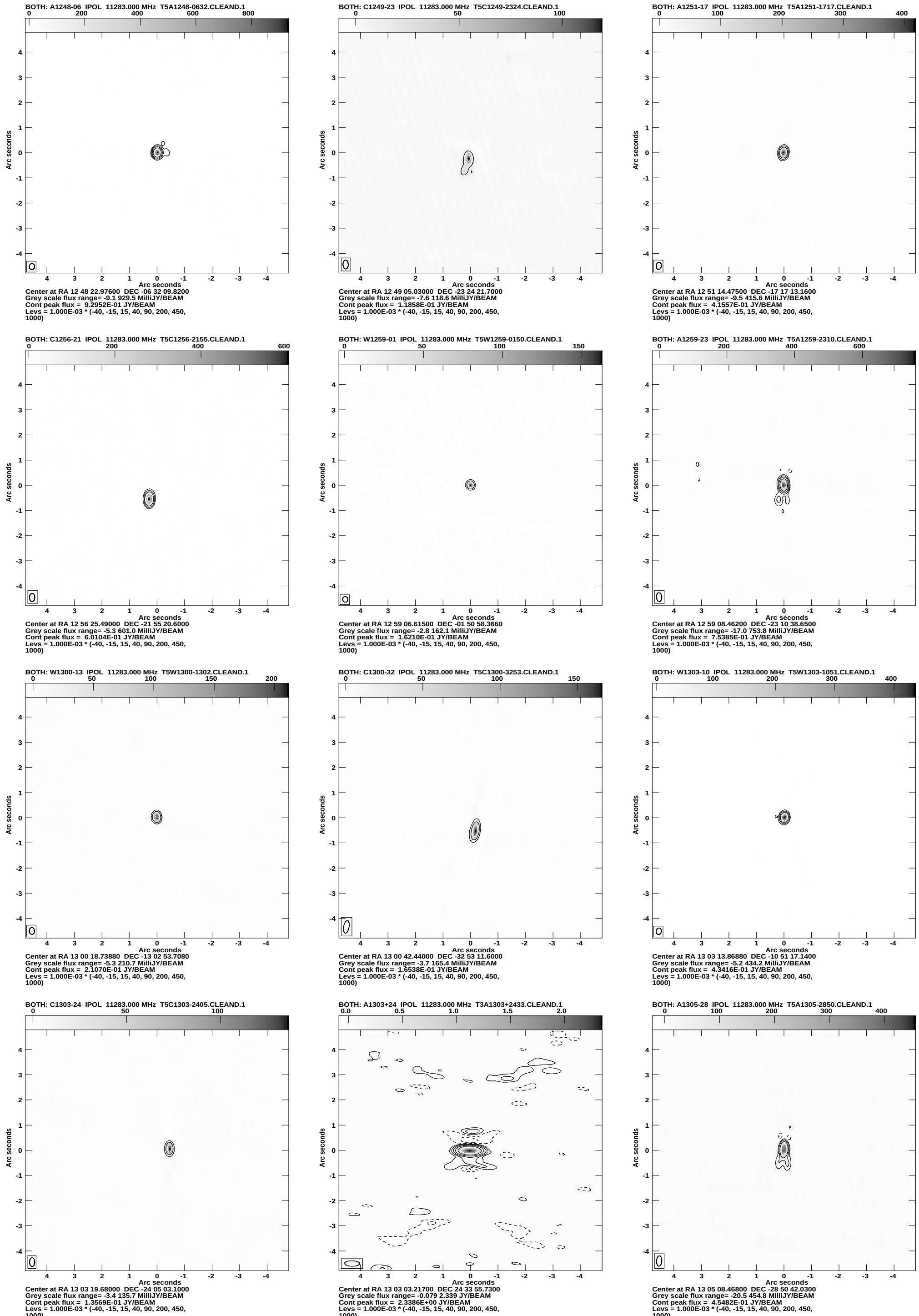

Figure 4. Images for alternative VLA reference sources, sorted in RA. (continued)

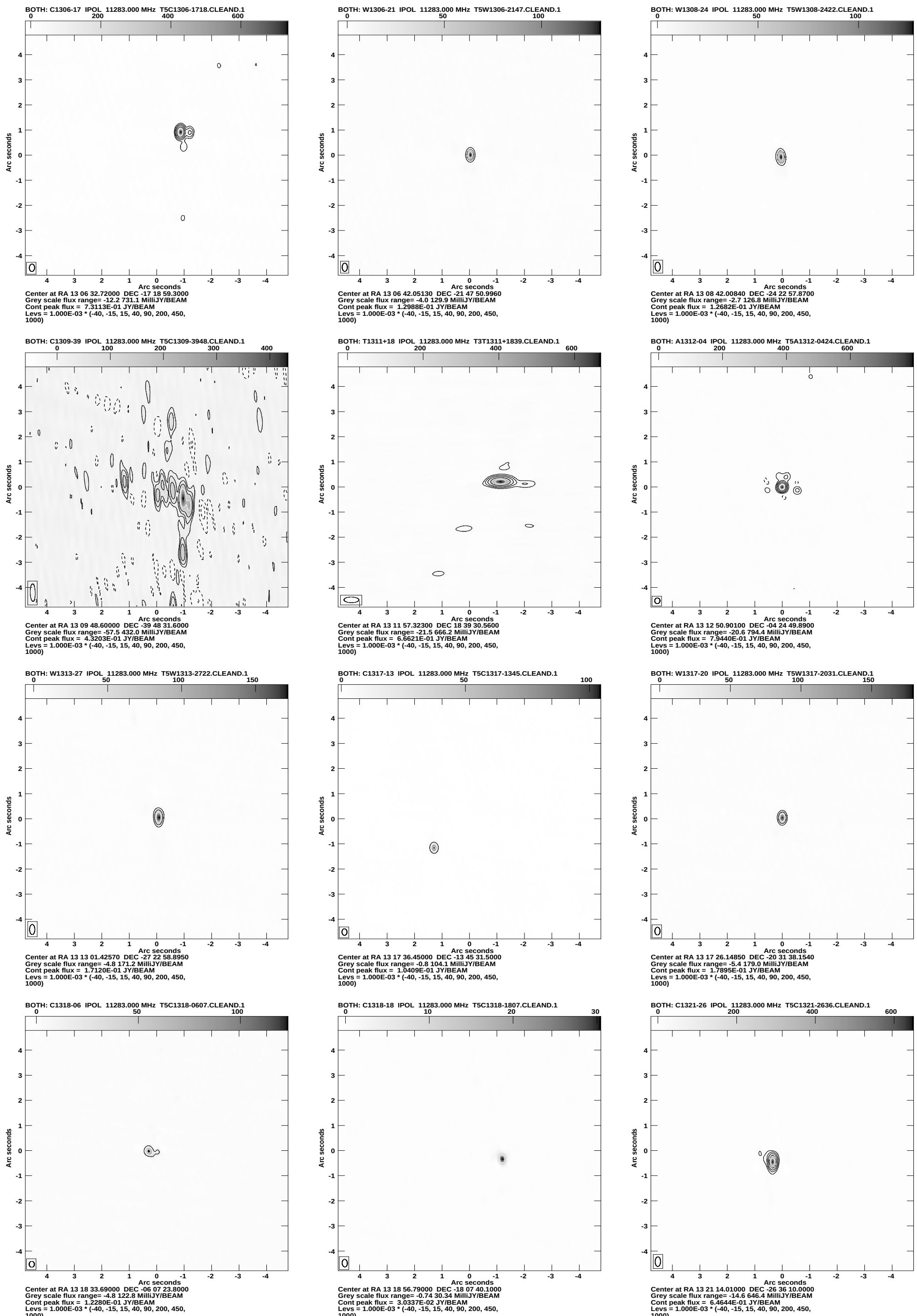

Figure 4. Images for alternative VLA reference sources, sorted in RA. (continued)

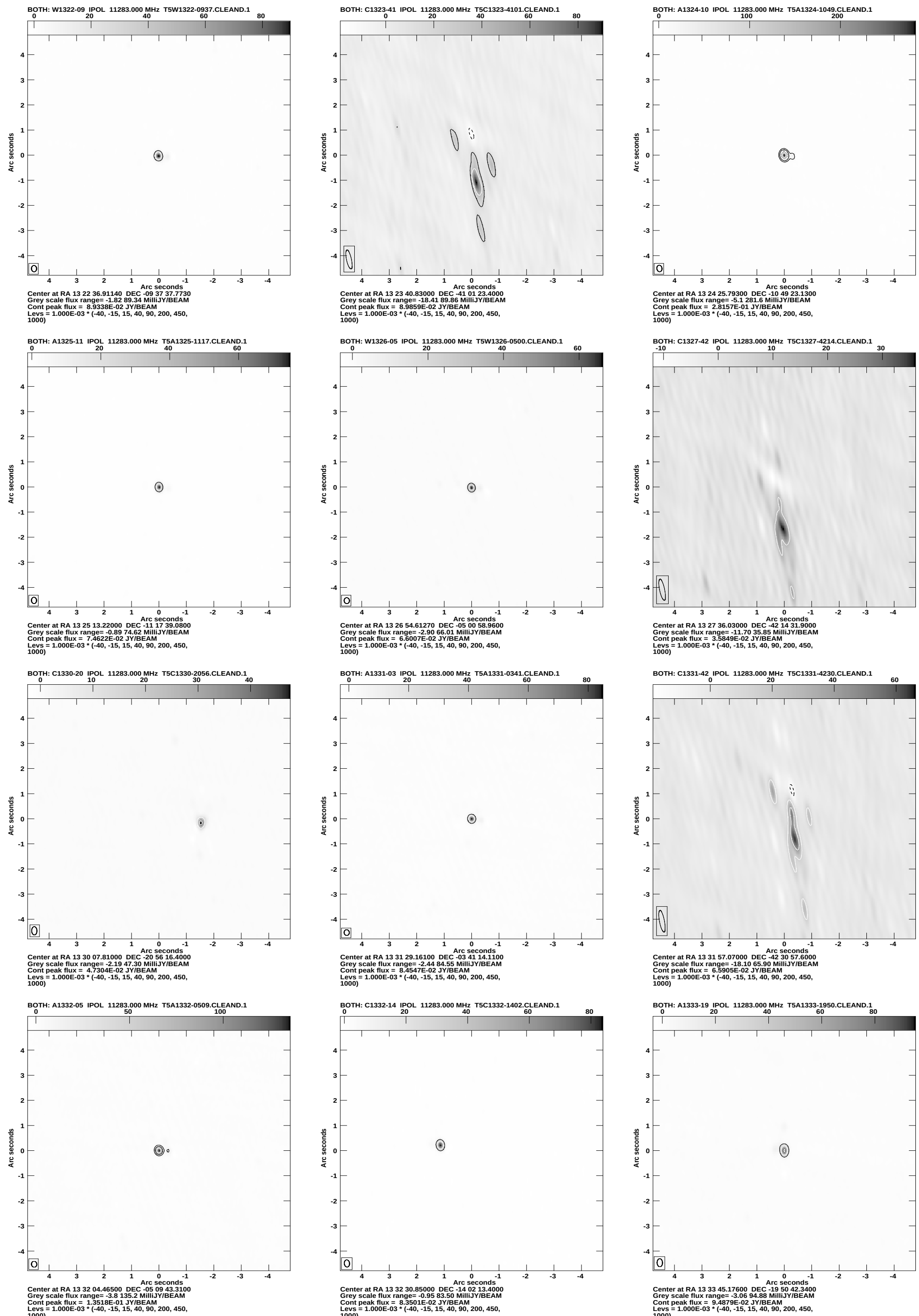

Figure 4. Images for alternative VLA reference sources, sorted in RA. (continued)

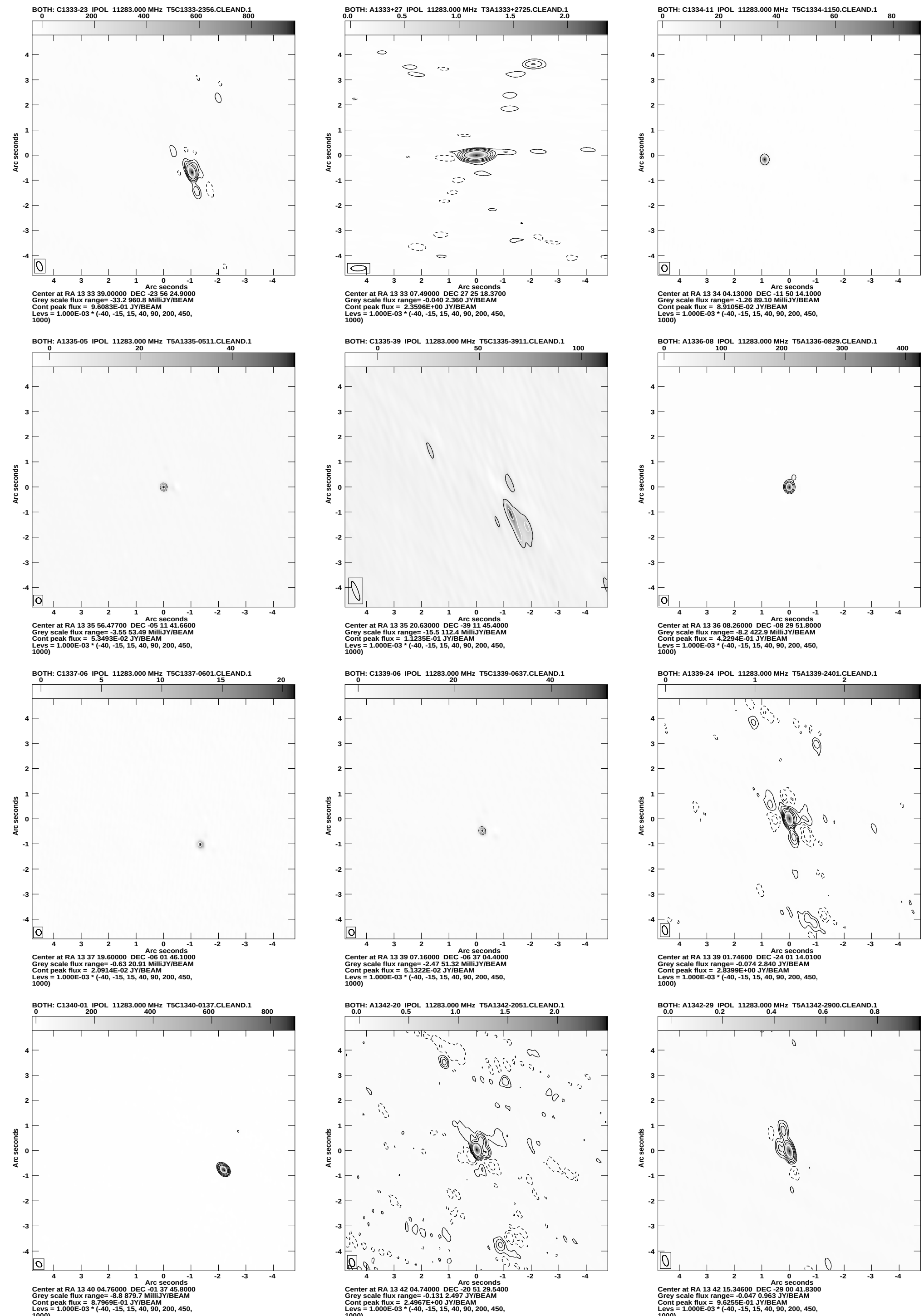

Figure 4. Images for alternative VLA reference sources, sorted in RA. (continued)

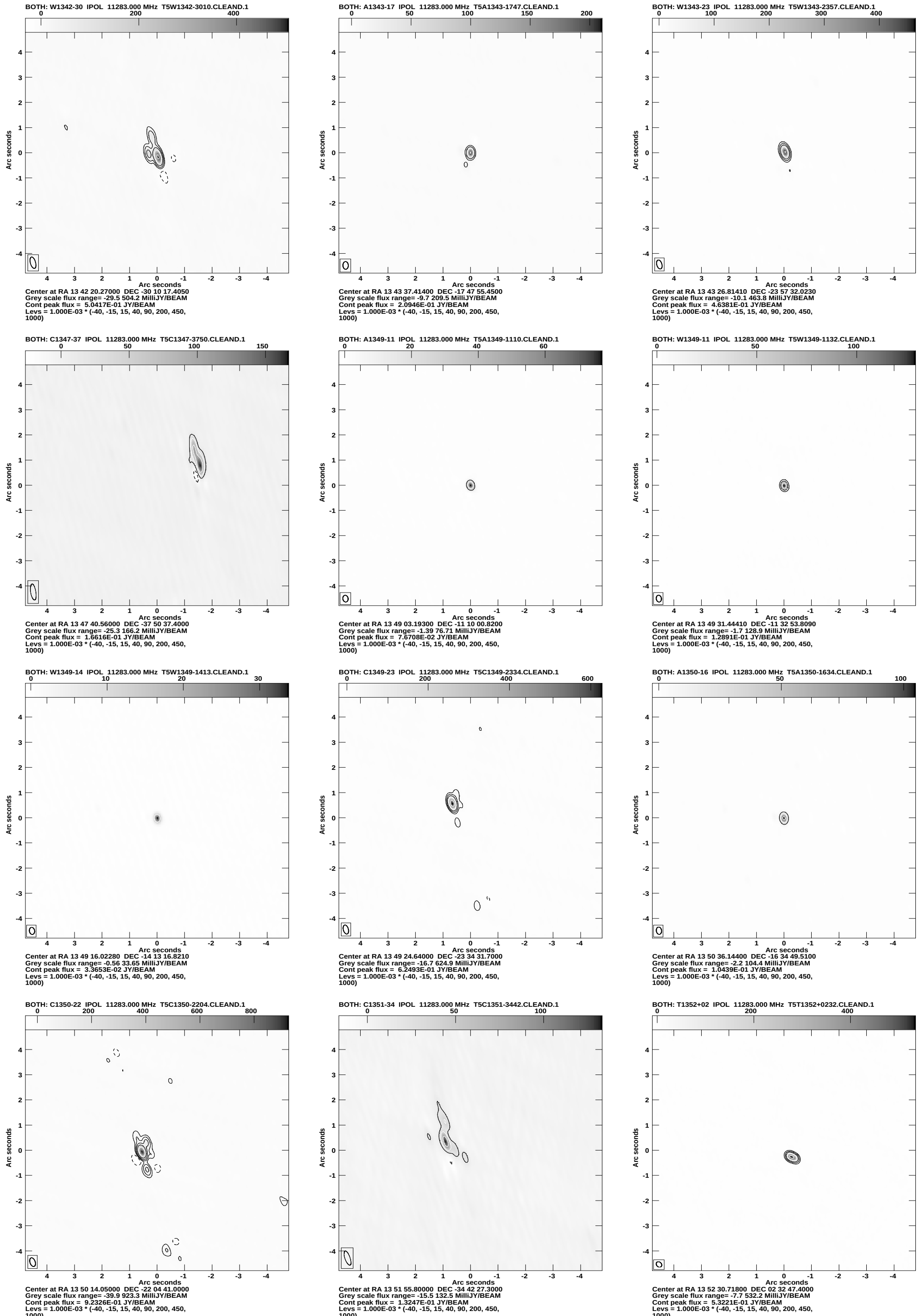

Figure 4. Images for alternative VLA reference sources, sorted in RA. (continued)

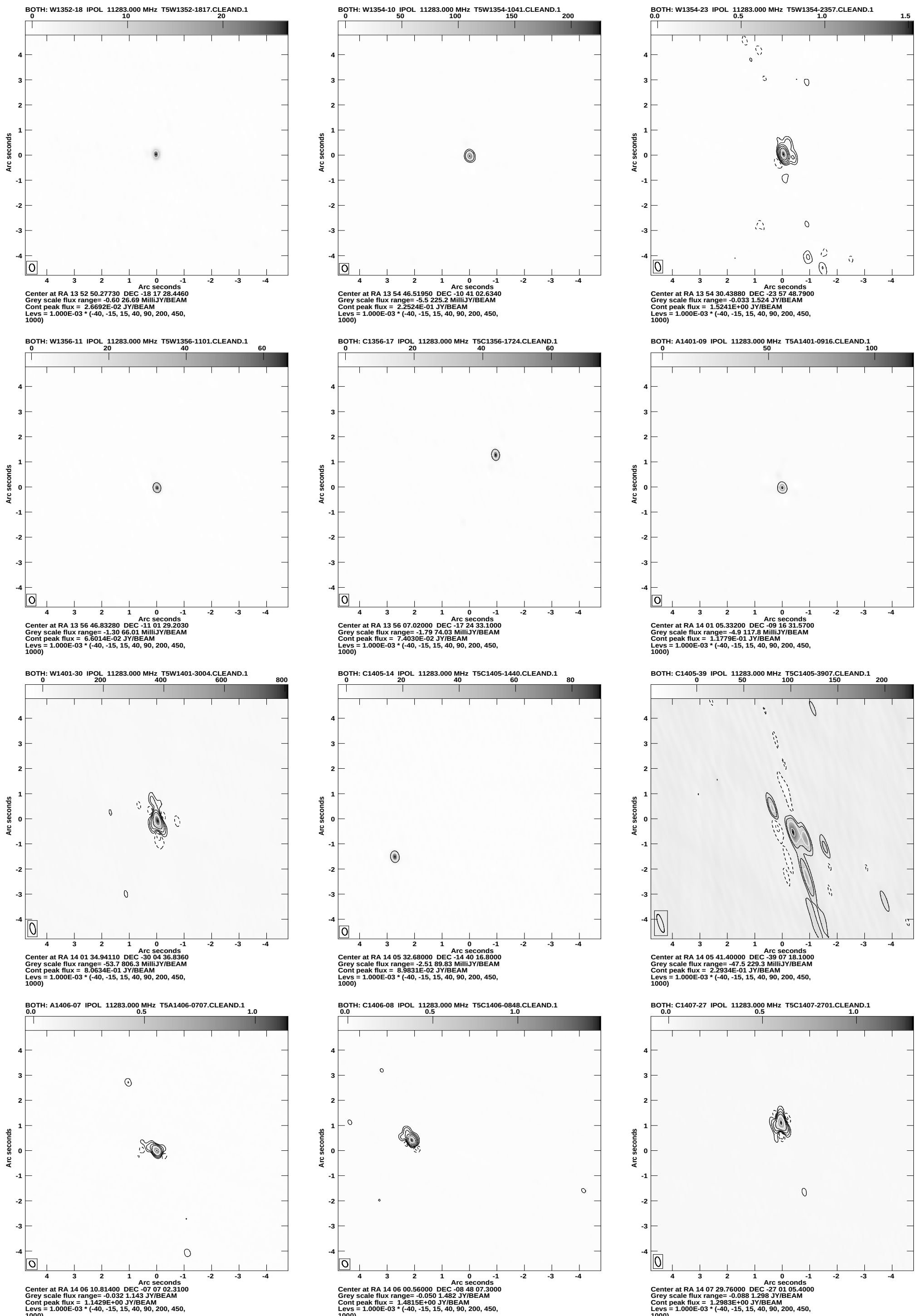

Figure 4. Images for alternative VLA reference sources, sorted in RA. (continued)

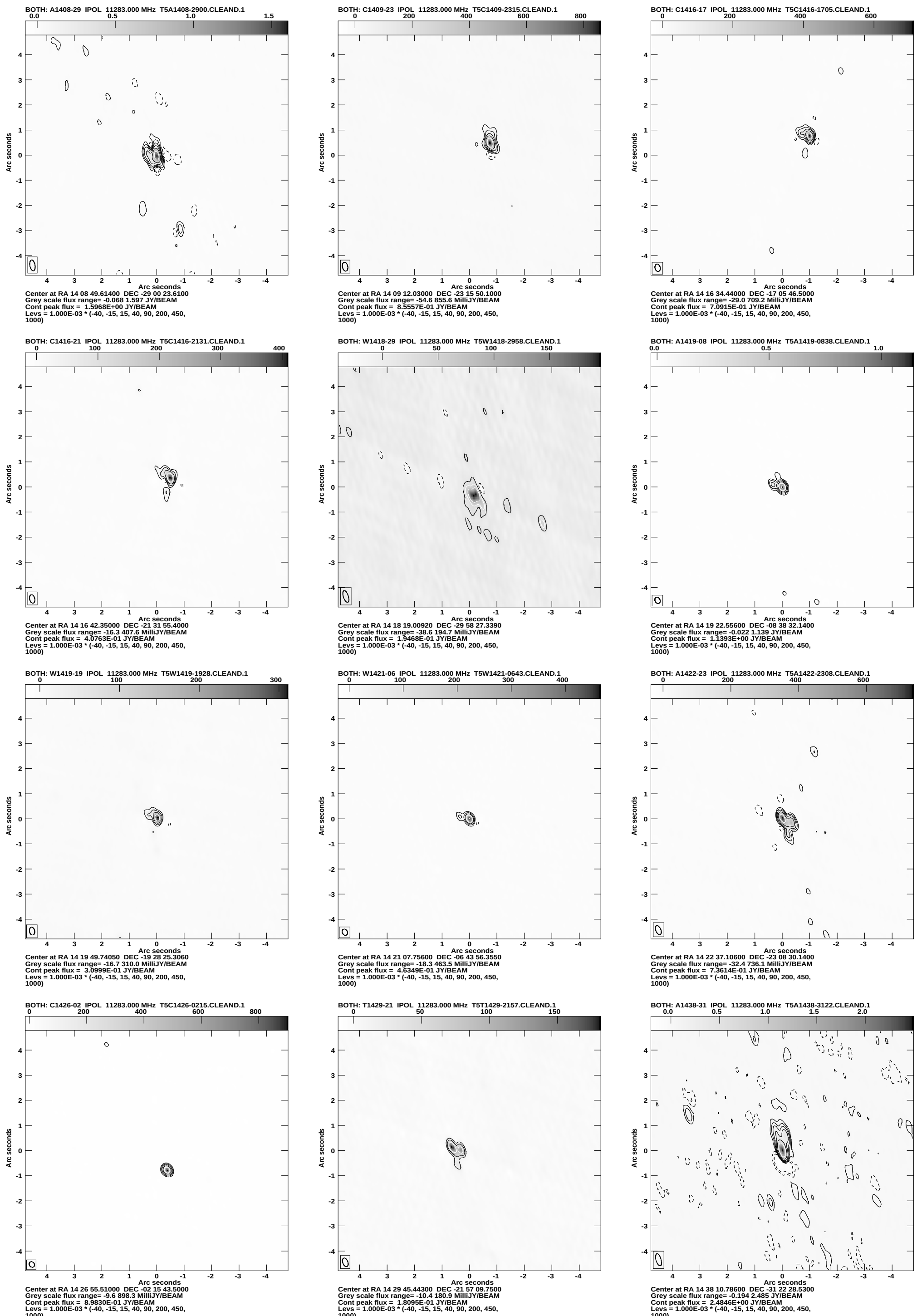

Figure 4. Images for alternative VLA reference sources, sorted in RA. (continued)

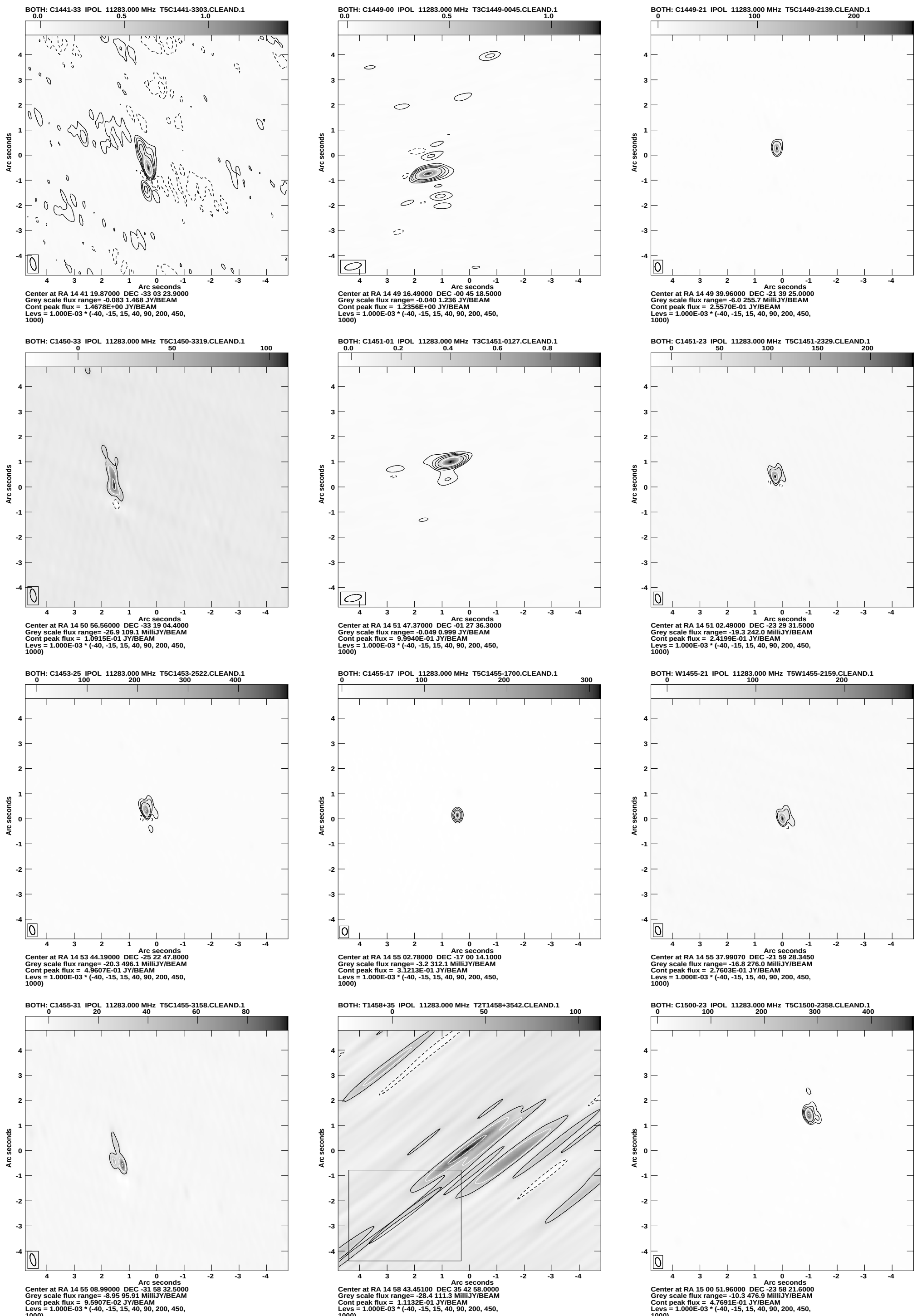

Figure 4. Images for alternative VLA reference sources, sorted in RA. (continued)

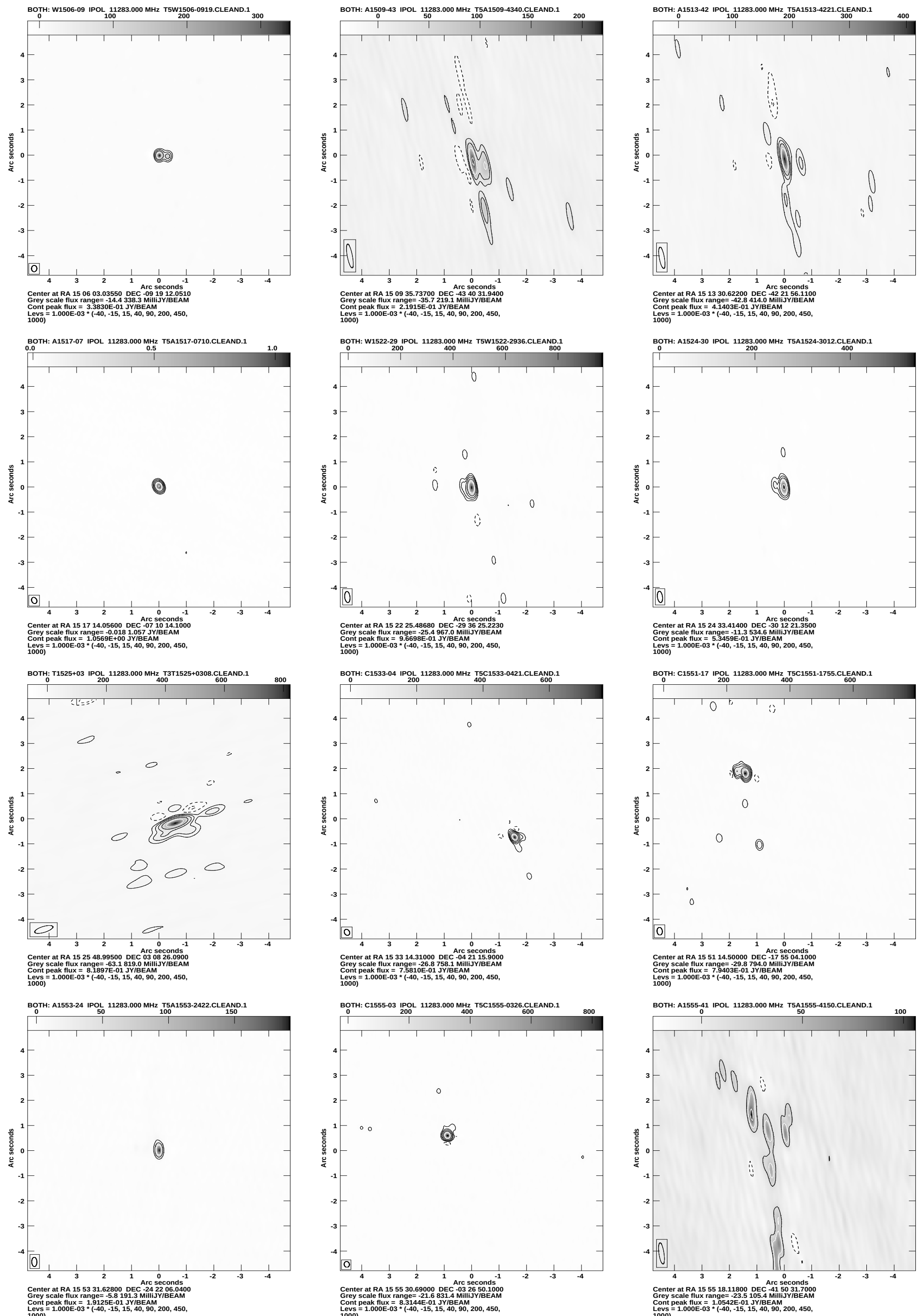

Figure 4. Images for alternative VLA reference sources, sorted in RA. (continued)

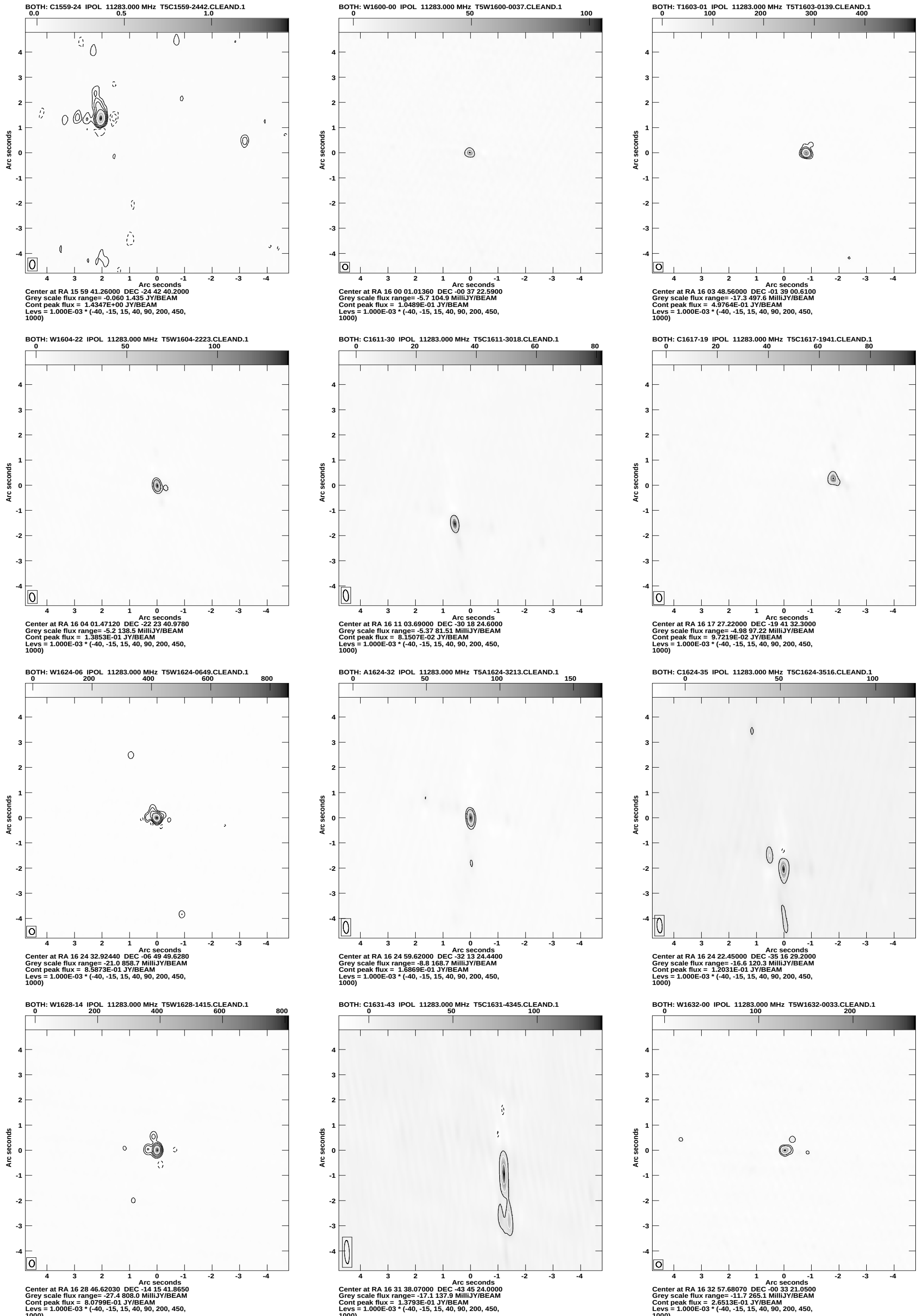

Figure 4. Images for alternative VLA reference sources, sorted in RA. (continued)

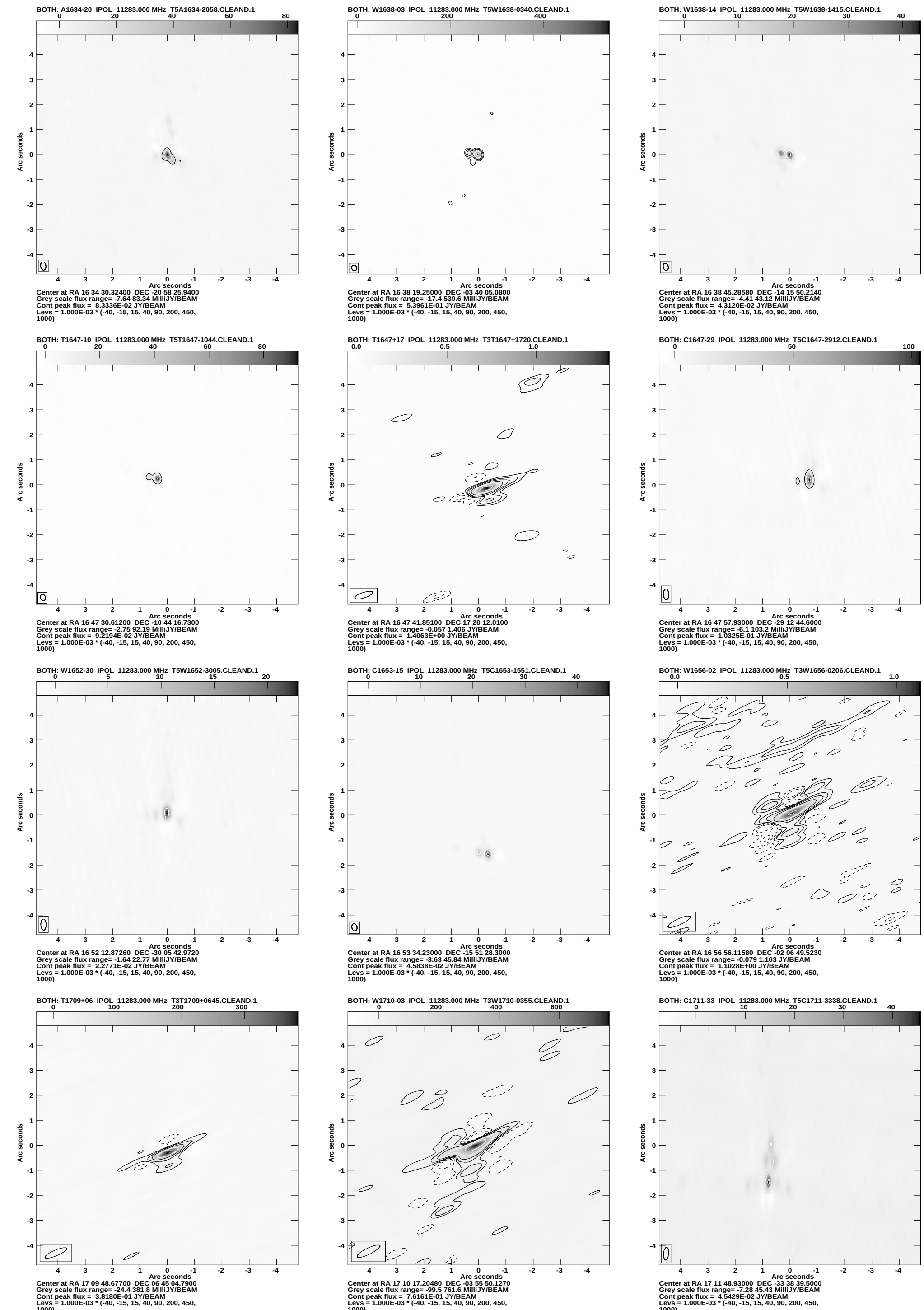

Figure 4. Images for alternative VLA reference sources, sorted in RA. (continued)

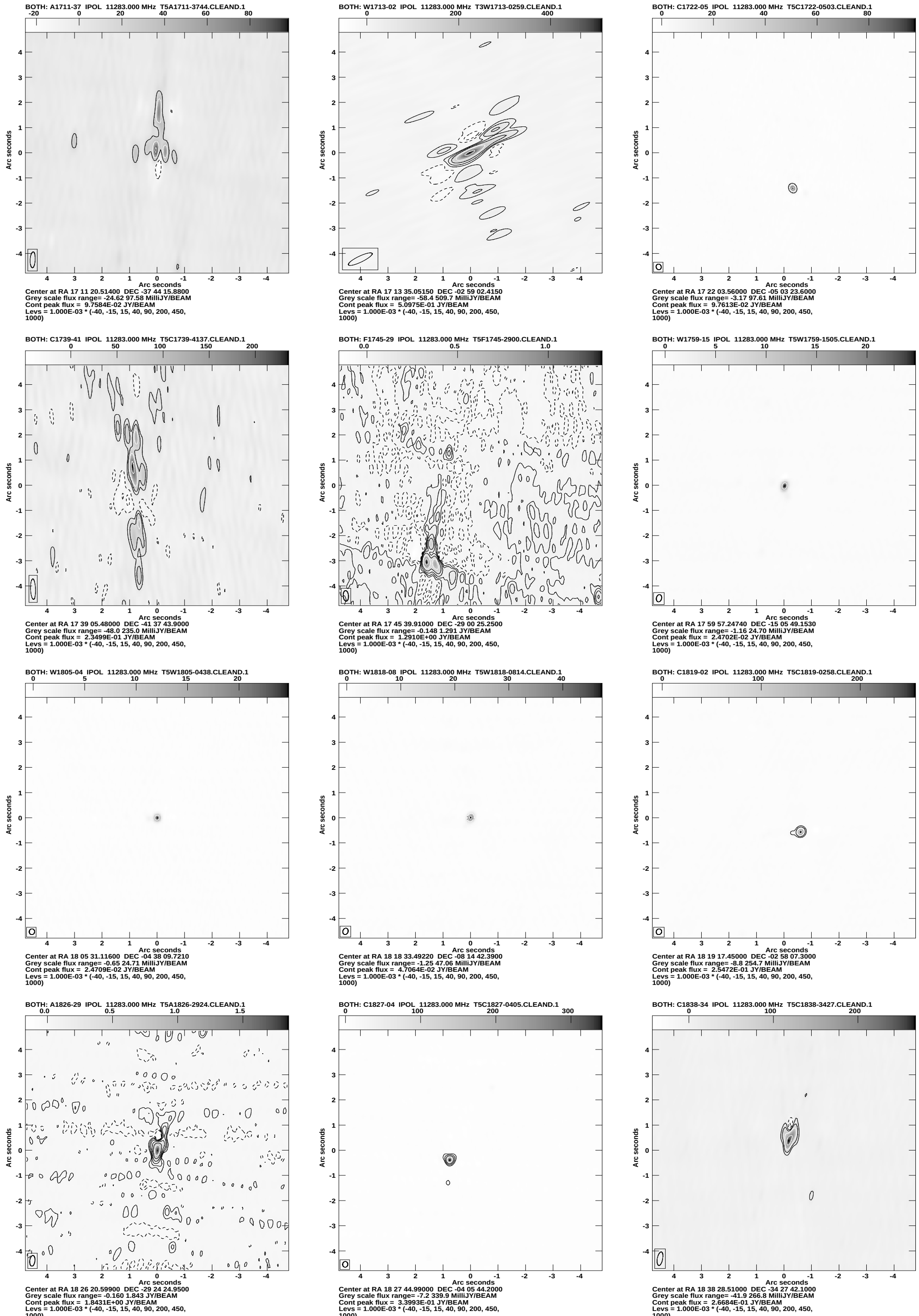

Figure 4. Images for alternative VLA reference sources, sorted in RA. (continued)

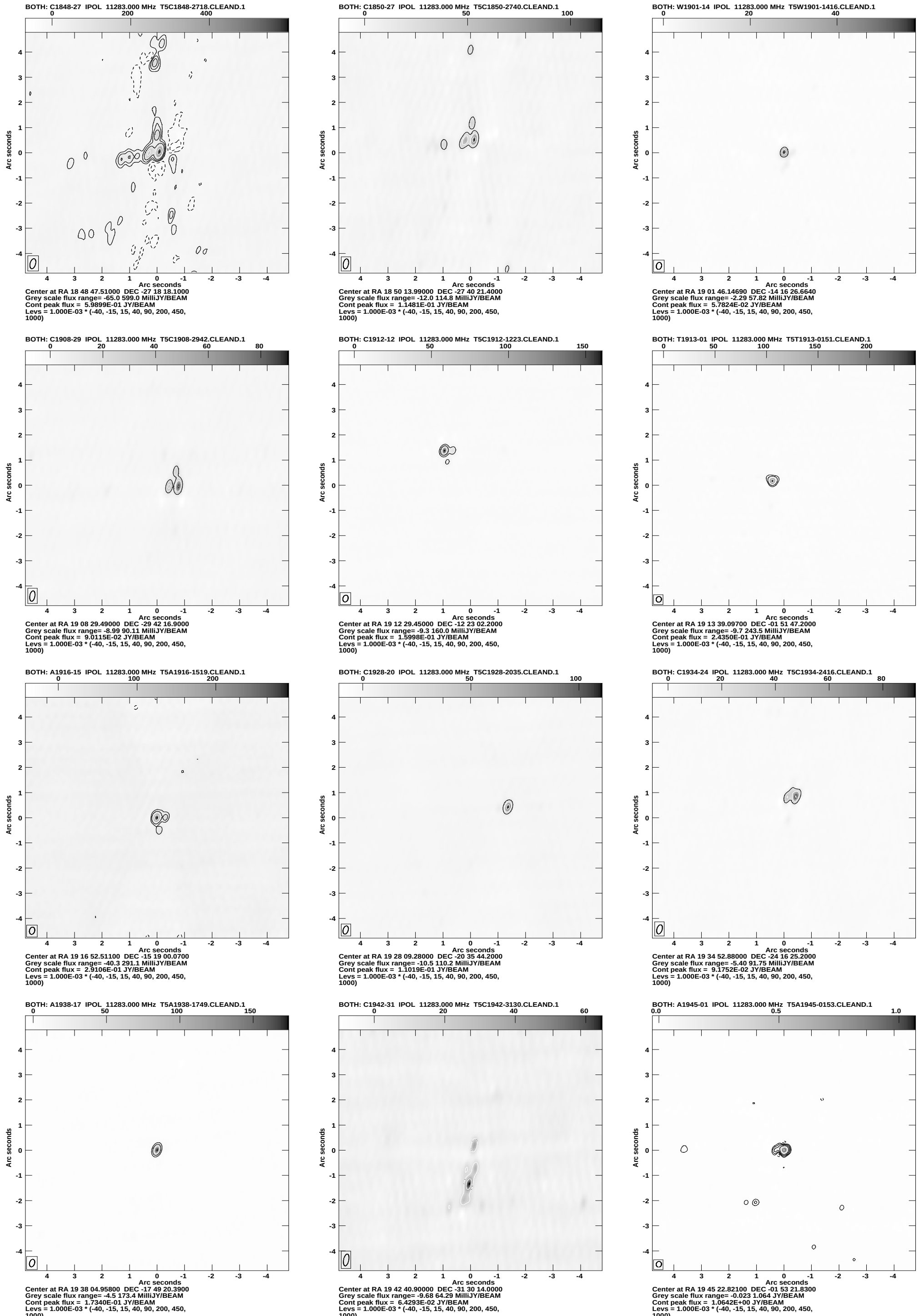

Figure 4. Images for alternative VLA reference sources, sorted in RA. (continued)

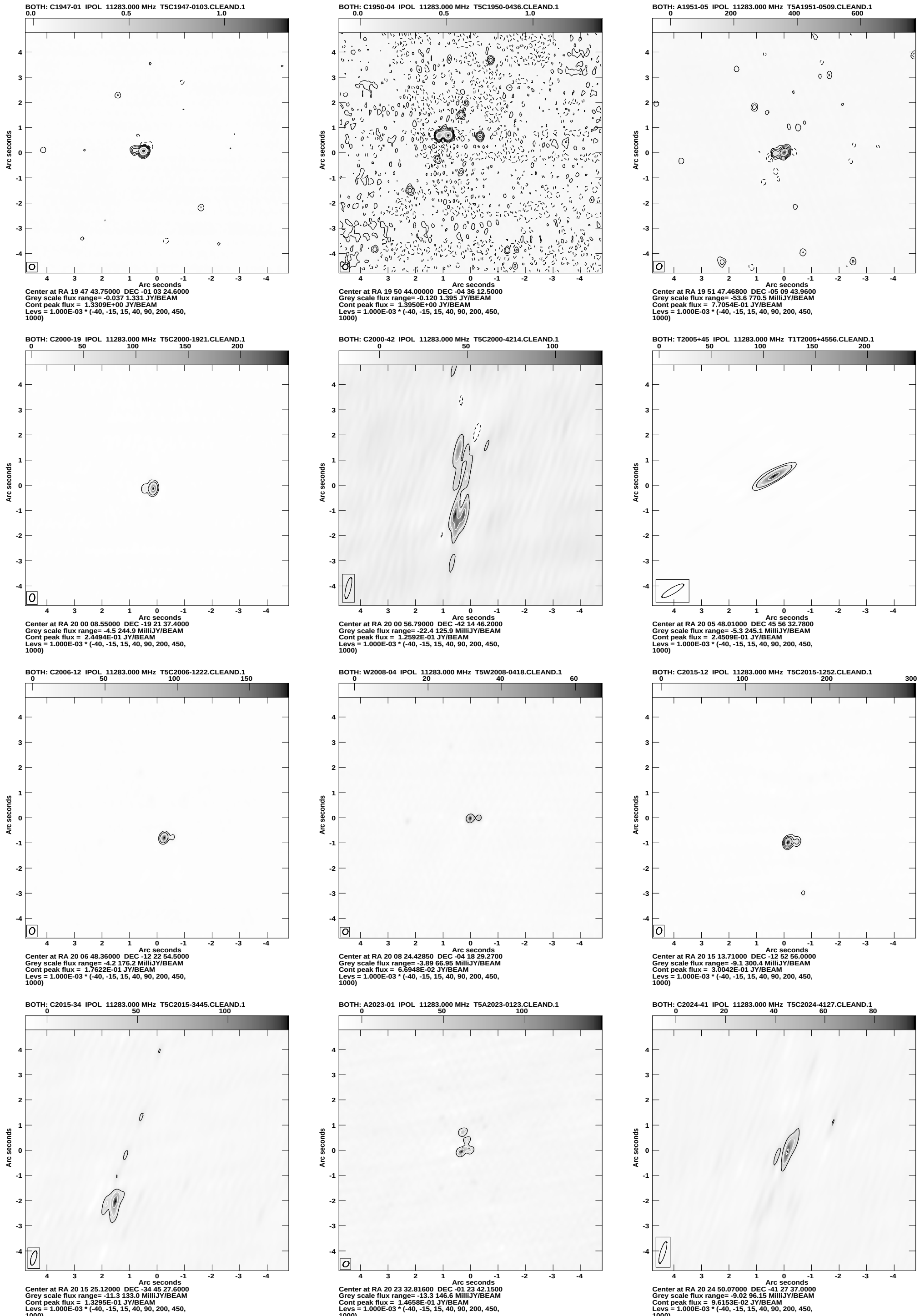

Figure 4. Images for alternative VLA reference sources, sorted in RA. (continued)

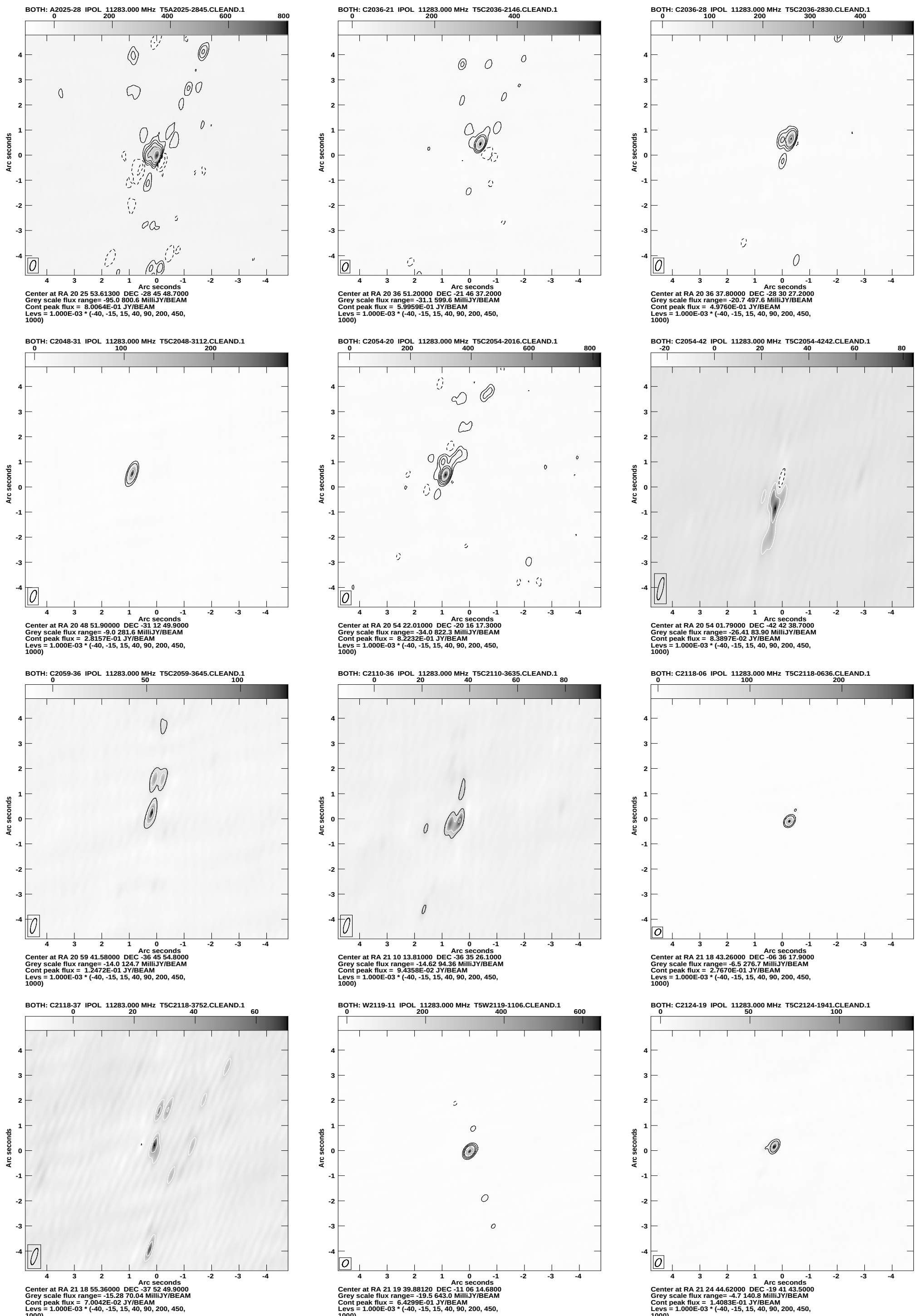

Figure 4. Images for alternative VLA reference sources, sorted in RA. (continued)

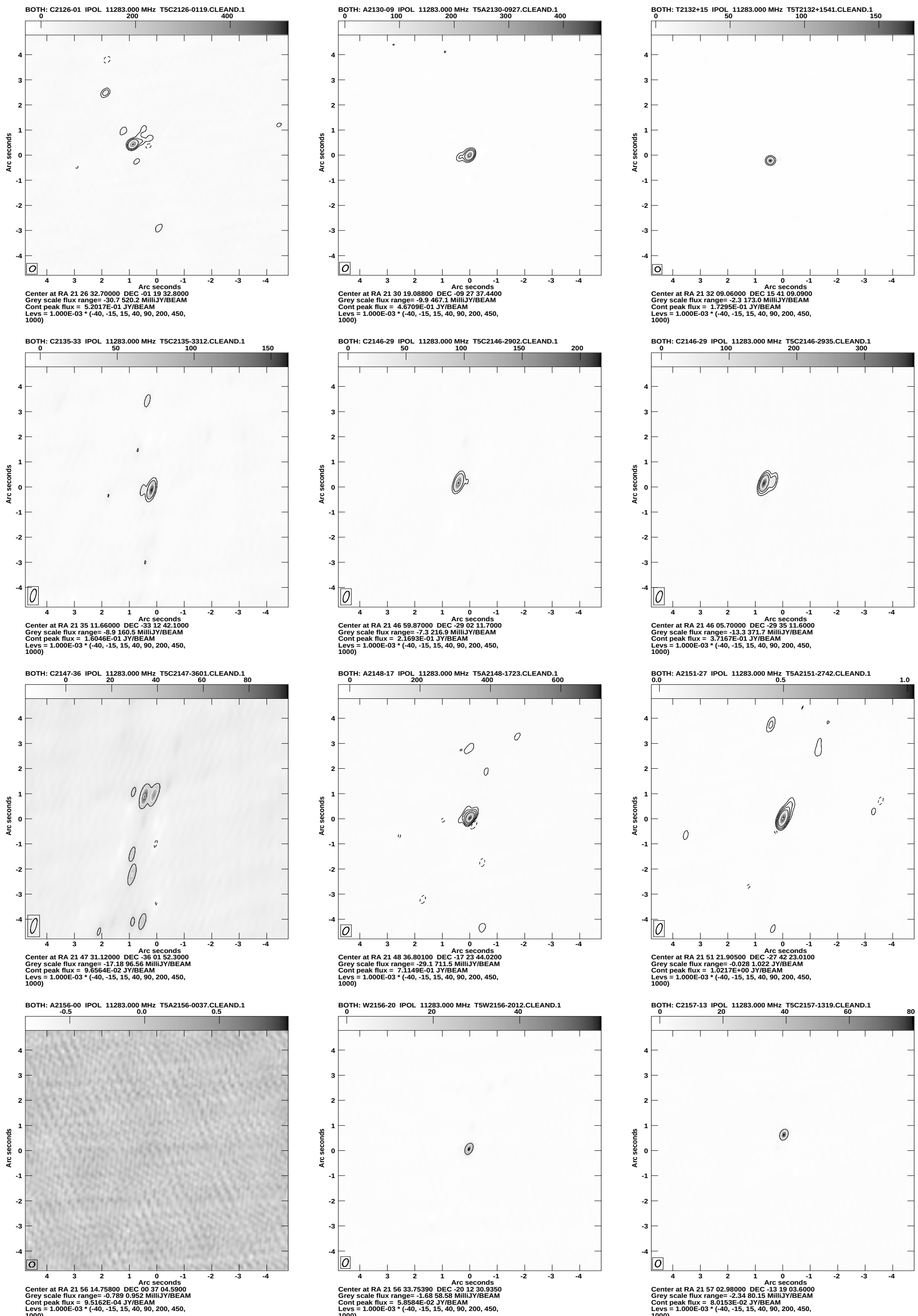

Figure 4. Images for alternative VLA reference sources, sorted in RA. (continued)

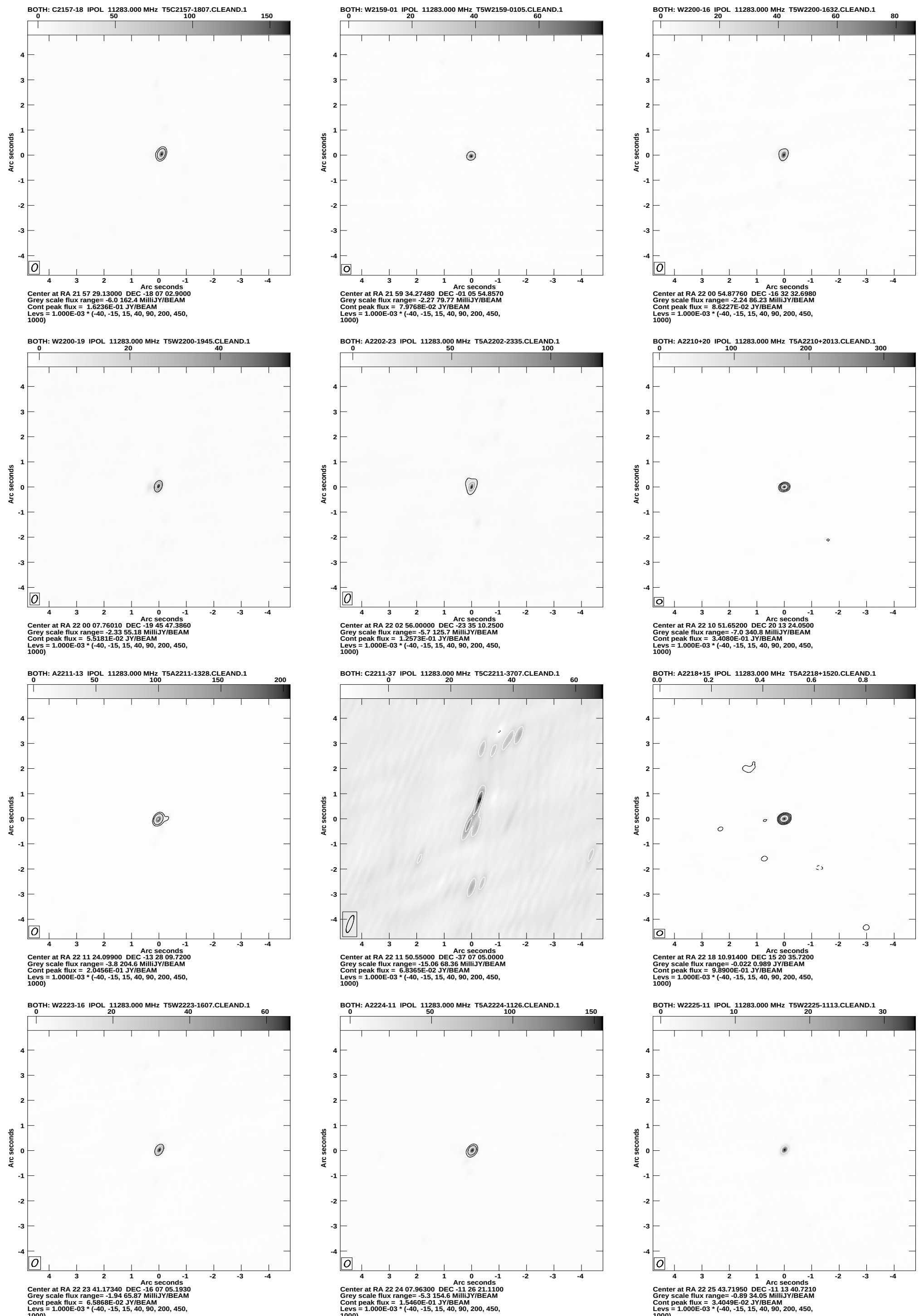

Figure 4. Images for alternative VLA reference sources, sorted in RA. (continued)

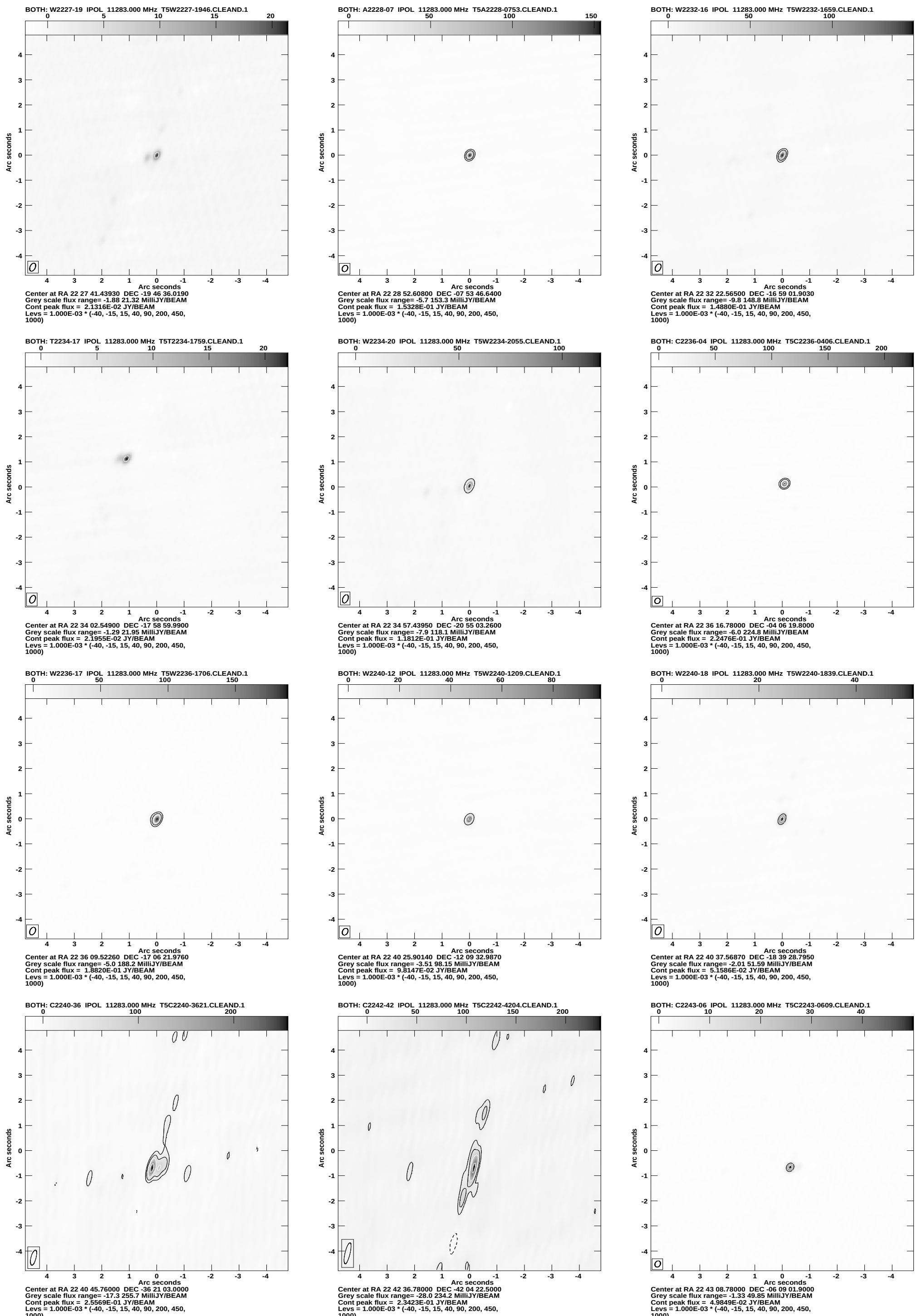

Figure 4. Images for alternative VLA reference sources, sorted in RA. (continued)

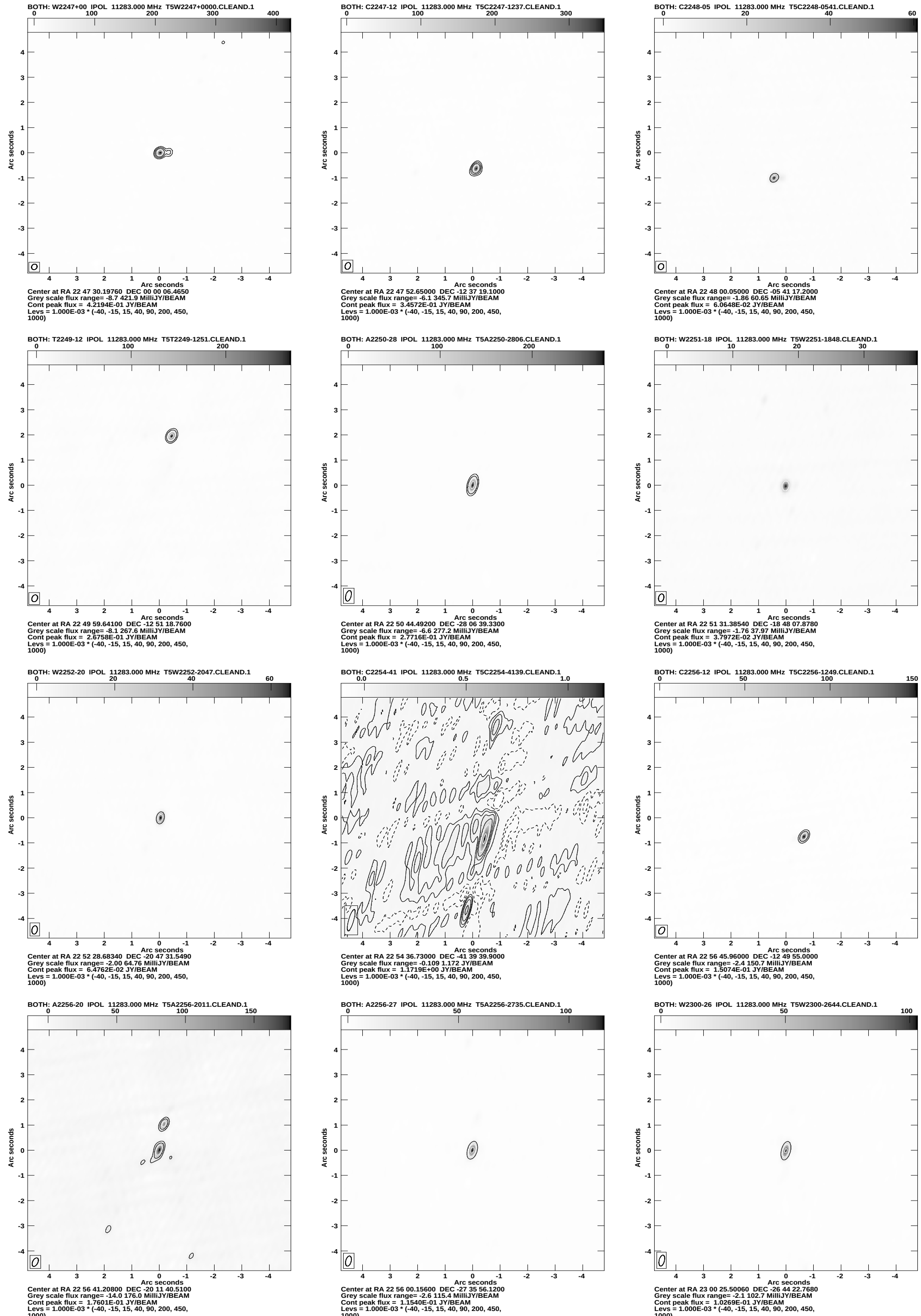

Figure 4. Images for alternative VLA reference sources, sorted in RA. (continued)

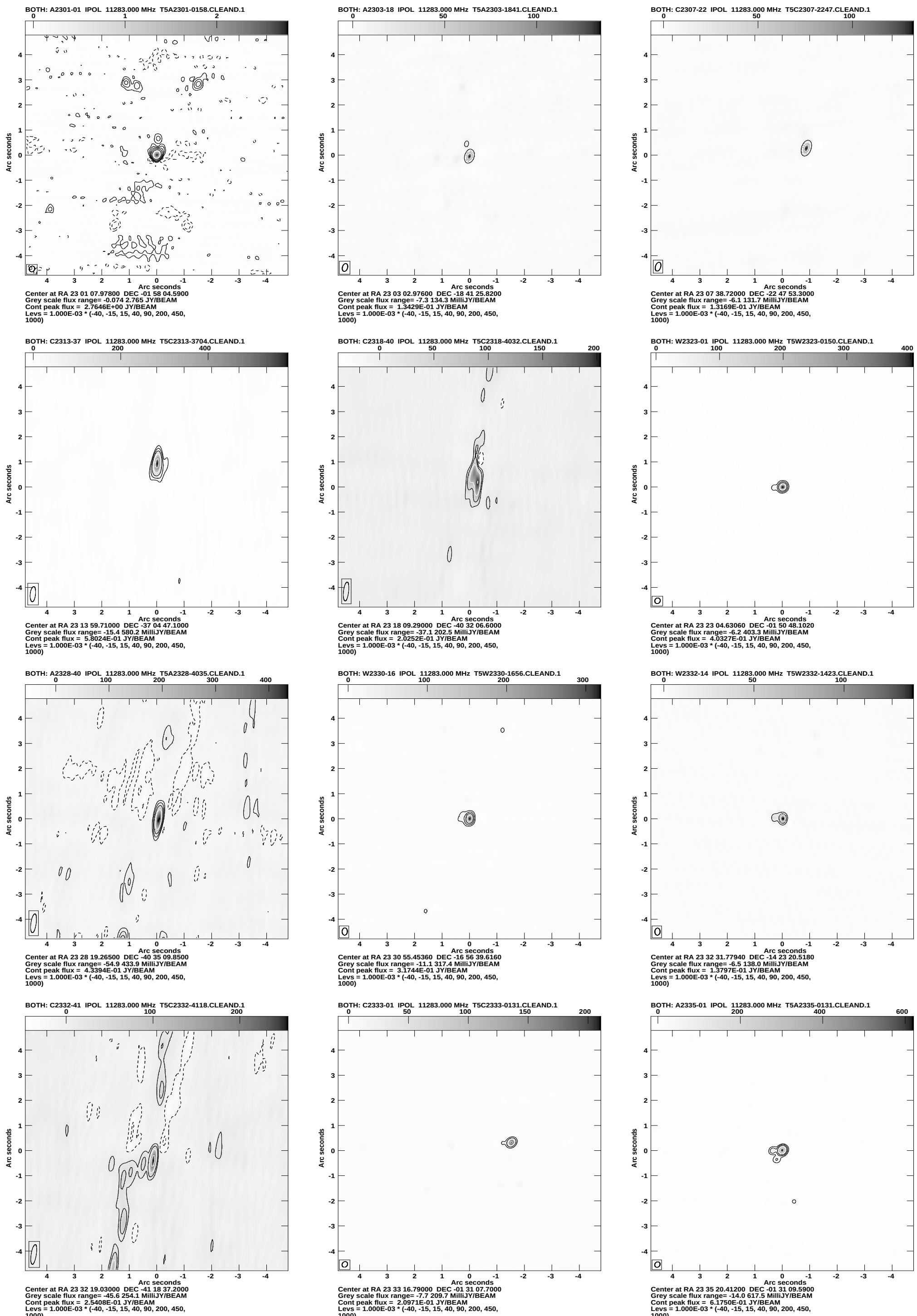

Figure 4. Images for alternative VLA reference sources, sorted in RA. (continued)

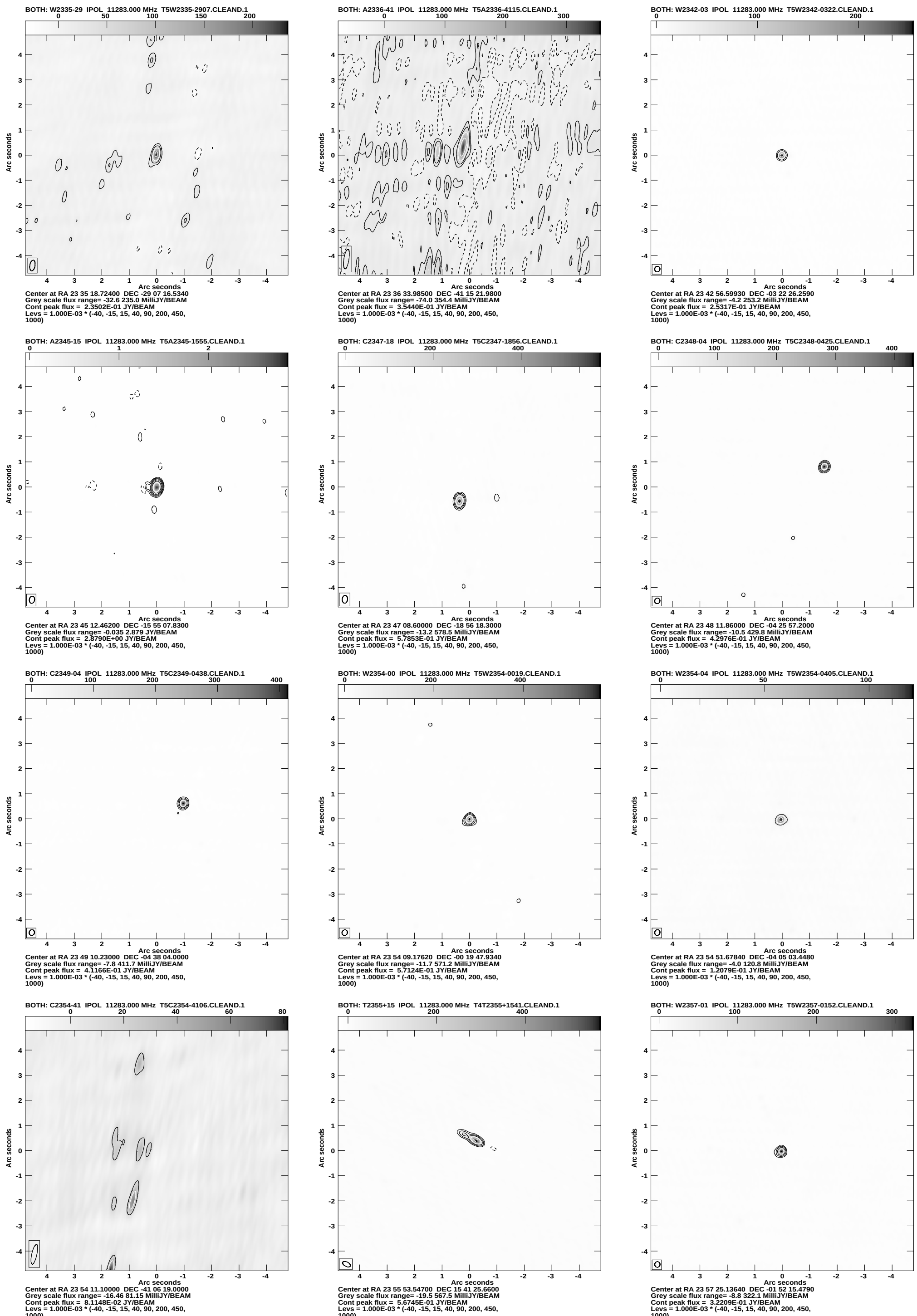

Figure 4. Images for alternative VLA reference sources, sorted in RA. (continued)

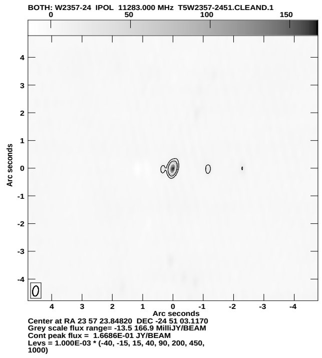

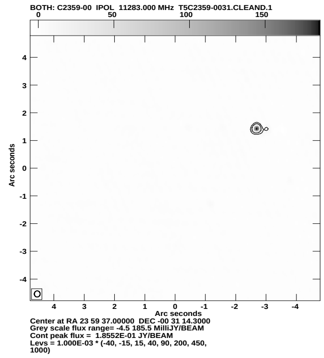

Figure 4. Images for alternative VLA reference sources, sorted in RA. (continued)